A Study of the Initial Interactions of Osteoblast-like Cells to Titanium and Zirconium Surfaces *In Vitro*

Zakiah Mohd Isa ***B.D.S., M.Sc.***

Thesis submitted for the degree of Doctor of Philosophy

Department of Prosthetic Dentistry

Eastman Dental Institute

University of London 1999

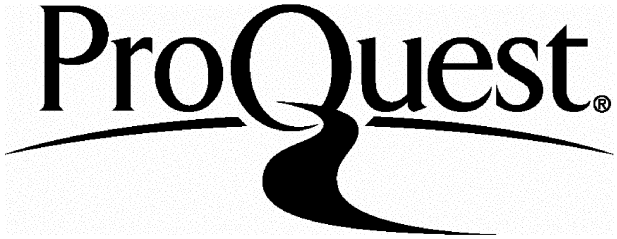

Abstract

Adhesion of cells to implant surfaces is a major factor in determining the pattern of events in osseointegration. Short-term *in vitro* studies have shown that bone cells react more favourably to rough substrate surfaces than to smooth ones. However, the findings are equivocal. It is not certain how cell-substrate interactions are affected by implant surface roughness, although integrins are thought to convey information about the substrate topography to the cells. This *in vitro* study investigated the effects of implant material composition and surface roughness on the early behaviour of three transformed human osteoblast-like cell lines, MG-63, HOS and U-2 OS, cultured on commercially pure titanium and zirconium substrates of different surface roughness. Surface roughness of the substrates was quantified using two techniques: a contact profilometer, and a non-contacting laser scanning profilometer. Cell attachment, proliferation and differentiation were studied using enzyme-linked immunosorbant assays, and immunofluorescence microscopy was used to detect integrin subunits and cytoskeletal arrangement 24 h after cellular attachment. The two instruments used to quantify surface roughness produced different results, as the basis of measurement of each system was different, and each method has its own measurement limitations. Biochemical assays used to measure cellular attachment and differentiation showed that there were no significant differences in the activity of cells grown on the different substrates. Immunofluorescence studies detected no marked variation in the integrin subunit expression and organisation of the cytoskeletal network of the cells. The experiments indicate that the cell lines may not discriminate between the surface chemistry and topography of the metals used in the study. A purely mechanistic theory of the cell-substrate interactions may not be sufficient to account for the variations in the reported behaviour of cells grown on different substrates.

Acknowledgements

I thank Professor John A. Hobkirk, Head, Department of Prosthetic Dentistry, and Dr Jonathan Bennett, lecturer, Department of Oral Pathology, Eastman Dental Institute for supervising this project.

I would also like to acknowledge the help I received, especially from:

Professor Alan Boyde, Hard Tissue Research Unit, Department of Anatomy and Developmental Biology, University College London.

Mrs. Nicola Mordan, Electron Microscopy Unit, Eastman Dental Institute.

Mr. Paul Darkins, Oral Pathology Department, Eastman Dental Institute.

I owe a debt of gratitude to Dr Peter Howell, Senior Lecturer, Prosthetics Department, Eastman Dental Institute and Hard Tissue Research Unit, Department of Anatomy and Developmental Biology, University College London for providing the confocal laser scanning micrographs in Figure 2.23, and especially for the time spent reading drafts of the manuscript. His interest and comments will always be appreciated.

I am most grateful to the University of Malaya, Kuala Lumpur for the scholarship and study leave awarded to me to undertake this work.

Finally, I thank my family for their constant prayers and support from across the seas while I was in London.

CONTENTS

LIST OF FIGURES

CHAPTER TWO

CHAPTER THREE

CHAPTER FOUR

LIST OF TABLES

1. Literature Review

1.1 Introduction

Dentists and scientists have for a long time been researching materials and techniques for providing predictable, efficient and effective methods of restoring a depleted dentition. Among the most versatile of these are osseointegrated implants. Since the first scientifically documented clinical successes of Brånemark and his co-workers in the edentulous milieu (Brånemark, 1983), applications of dental osseointegrated implants have progressed to use in the partially dentate (Sullivan, 1986; Wyatt and Zarb, 1998), prosthetic rehabilitation of oral and maxillo-facial defects (Parel *et al.*, 1986), and reconstruction of congenital defects in children and adolescents (Bergendal *et al.,* 1996). One-step surgical implant techniques are currently being used (Becker *et al.,* 1997; Buser *et al.,* 1998), besides the original Brånemark protocol of two-stage surgery for implant placement. Preliminary reports have also shown that placement of implants in irradiated jaws may give good results, even without adjunctive hyperbaric oxygen therapy to provide support in areas with compromised blood flow after irradiation (Jisander *et al.,* 1997; Keller, 1997; Niimi *et al.,* 1998; Nishimura *et al.,*1998). Osseointegration is also used in orthopaedic reconstruction of various parts of the human body (Brånemark, 1994).

1.1.1 Definition of osseointegration

Osseointegration was first described as a relationship where "bone tissue is in direct contact with the implant, without any intermediate connective tissue". It was later defined as a "direct structural and functional connection between ordered and living bone and the surface of a load carrying implant" (Brånemark, 1985). These definitions were based on retrospective radiographic and light microscopic observations, and implied that direct bone contact occurs around the entire implant. However, with current techniques of ultrastructural investigation, this interpretation appears to have been overestimated as 100% bone apposition is not necessarily obtained at the surface of the endosseous implant. Albrektsson and Johansson (1991) indicated that the proportion of direct bone-to-implant contact varies with the material and design of the implant, as well

as the state of the host bed, the surgical technique, and the time and conditions of loading. There is also varied morphology of bone opposing the implant, showing that osseointegration is a healing response consistent with the dynamic environment into which the prosthesis is inserted (Steflik *et al.,* 1997). Therefore, osseointegration is best defined as a "process whereby clinically asymptomatic rigid fixation of alloplastic materials is achieved, and maintained, in bone during functional loading" (Zarb and Albrektsson, 1991). Later, in 1994, Skalak and Brånemark proposed that osseointegration be considered as the sum total of the following definitions, obtained from the clinical, biological, biomechanical, and microscopical points of view:

a. a fixture is osseointegrated if there are no signs and symptoms under functional load.
b. at the light microscopic level, osseointegration is seen as a direct structural and functional connection of new bone to the fixture without the interposition of connective or fibrous tissue, and that this connection is capable of carrying normal physiological loads.
c. there should be no progressive movement between the fixture and surrounding bone under functional loading.
d. at the electron microscopic level, structures found within nanometres of most of the surface of the fixture should be identifiable as mineralised normal bone.

These definitions describe the end result of osseointegration, and while they are appropriate, the process of osseointegration itself is a lifelong activity of bone formation, adaptation to function and repair at the bone-implant interface. Cooper (1998) pointed out that there is therefore, still a need, to define the cellular and molecular events controlling bone formation and maintenance at this site so that the process of osseointegration is predictable, especially in areas where bone is deficient.

1.1.2 Criteria for the success of osseointegration

Osseointegration is a highly successful clinical protocol, although the success rates are influenced by many factors. These include implant system and the status of the bone at the implant site (Albrektsson *et al.,* 1986; Rϕynesdal *et al.*, 1998). Esposito *et*

al. (1998a) provided a comprehensive review of the many parameters which have been developed and used over the years to evaluate the success and failure of osseointegrated implants. Zarb and Albrektsson (1998) proposed that the following set of criteria is used to assess the outcome of implant supported prostheses. It highlights the essential clinical features of the successful osseointegration of implants to bone, and includes:

a. the lack or absence of signs of infection (either early on in the healing period, or later during function) attributable to the implants,
b. no pain, discomfort, or sensitivity around the implants,
c. no observable mobility (which is always a clear sign of failure) when tested clinically, and
d. the mean vertical bone loss is less than 0.2 mm annually following the first year of function, compared to baseline measurements made after abutment connection.

Wide-ranging and extensive data to support the success of osseointegrated implants is available for the Brånemark implant system (Albrektsson *et al.*, 1986; Albrektsson, 1988; Albrektsson *et al.*, 1988; Adell *et al.*, 1990; Albrektsson and Sennerby, 1991; Jemt, 1991). Other implant systems are relatively new, and adequate data is needed to form the basis for reliable statistics for a 10-year follow-up period to meet the minimum success criteria proposed by Albrektsson *et al.* (1986).

Esposito *et al.* (1998b) reviewed in detail the factors that can lead to implant failure. The reasons for the loss of implants after osseointegration has occurred may be multifactorial, with prosthetic factors (usually due to overload) and bacterial infection as the major causes. However, the reasons for the implant's failure to osseointegrate are still unknown, although excessive interfacial micromotion, rather than early loading *per se*, is acknowledged as one detrimental factor (Szmukler-Moncler *et al.*, 1998).

1.2 Factors which determine the success of osseointegration

Albrektsson *et al.* (1986) first referred to the six important factors which determine the success of osseointegration. These are: implant biocompatibility, design characteristics, implant surface characteristics, state of the host bed, surgical technique, and implant loading conditions. LeGeros and Craig (1993) categorised these factors into biomaterial, biomechanical and biologic determinants. In addition, patient motivation and oral hygiene procedures are also important considerations (Meffert *et al.*, 1992; Glantz, 1998a). These factors are interdependent and interrelated, and their recognition has led to the long-term success associated with osseointegrated implants.

1.2.1 Biomaterial factors

Dental implants are used in the oral cavity to improve the stability of a prosthesis. In order to be successful clinically, implant materials must satisfy two essential requirements:

a. they must not be toxic to the cells in the surrounding tissues, or undergo dissolution and cause systemic damage to the patient;
b. they must be able to form a stable bone-implant interface that is capable of carrying occlusal loads, and transferring or distributing stresses to the adjacent bone so that bone vitality is maintained over long periods (Hench and Wilson, 1993).

Three basic types of synthetic materials have been used for fabricating endosseous dental implants. These are metals and metal alloys, ceramics and carbons, and polymers (Williams, 1981; Lemons, 1990; Wataha, 1996).

Metals and metal alloys used for clinical and experimental implants have included titanium and titanium alloys, tantalum, stainless steel, cobalt-chromium alloys, gold alloys and zirconium alloys among others (Meenaghan *et al.*, 1979; Albrektsson and Hansson, 1986; Johansson *et al.*, 1990; Glantz, 1998b; Prigent *et al.*, 1998). These materials are selected based on their high corrosion resistance, strength, rigidity, ease of shaping and machining, and suitability for a wide range of sterilisation techniques.

Although the mechanisms that lead to osseointegration with titanium implants are not fully known, metals in general however, do not form an interfacial bond with bone. The implant is typically connected to bone via a micro-mechanical interlock using a variety of surface designs and textures that are used to promote bony in-growth and improve the interfacial attachment (Ellingsen, 1998).

Ceramics are generally hard materials with high compressive strengths. Carbon based materials are similar to ceramics, and due to their brittleness and low impact strengths, are not suitable for use in their bulk form in load-bearing applications. The choice of ceramics as implant materials is primarily due to efforts to develop materials based on crystalline structures which are bone-like and have similar physical properties to bone. Bioceramics may form two types of interfacial bond with bone: a bioactive ceramic is partially soluble, and forms bone via chemical reactions at the interface, while bioresorbable or biodegradable ceramics have a higher solubility, degrade gradually, and with time are replaced with bone (LeGeros *et al.*, 1991; Hench and Wilson, 1993).

Different chemical compositions of calcium phosphate ceramics (CPC), based on specific ratios of calcium and phosphorus are used clinically, both as a dense sintered material in non load-bearing areas, and as a plasma-sprayed coating for titanium implants (Pilliar *et al.,* 1991; Hayashi *et al.,* 1994). These hydroxyapatite (HA) coatings may contribute to more rapid osseointegration and greater amounts of bone-implant contact than is associated with uncoated titanium in the early stages of healing. However, HA coated implants are not seen as superior to titanium devices in the long-term because the difference does not appear to be clinically significant after 12 months of implantation (Zablotsky, 1992). In fact, bone contact with titanium may be more favourable in the long-term (Wheeler, 1996). This is attributed to interfacial problems related to the dissolution and weakening of the HA coatings, which have a tendency to become loose or dissociated from the central titanium implant (Ogiso *et al.,* 1998).

In comparison to metals and ceramics, polymers are weak, and generally flexible. They may however, be synthesised in a variety of compositions and fabricated

into many complex shapes and structures. They are mainly used as additives to give a beneficial secondary purpose, for example, as structural isolation for shock-absorption in load-bearing metallic implants (Mah, 1990).

1.2.1.1 Titanium and zirconium as implant materials

Two forms of titanium (Ti) are principally used for endosseous dental implants. They are commercially pure titanium (cpTi, at least 99.5% pure Ti) and a titanium alloy, titanium-aluminium-vanadium (Ti-6Al-4V). CpTi is available in four grades which vary in their oxygen content. Oxygen functions as a controlled strengthener in cpTi. As oxygen content increases, the strength of the metal increases and its ductility decreases (Brown, 1998). Nitrogen, carbon, hydrogen and iron are also present, but vary little between grades. Grade I cpTi is the purest and therefore the softest. Grade 4 cpTi has the most oxygen at 0.4% by weight, and is the material used for dental implants.

Ti-6Al-4V also contains low concentrations of nitrogen, carbon, hydrogen, iron and oxygen, but additionally approximately 6 per cent by weight aluminium and 4 per cent by weight vanadium. Besides reducing the melting and casting temperatures, alloying other metals with Ti also increases the strength of the alloy and decreases its density (Wataha, 1996). A stronger bone-implant interface may be achieved with cpTi than with Ti-6Al-4V, as greater removal torque forces were needed to loosen the interfacial connection between cpTi implants and the surrounding bone (Johansson *et al.,* 1998). This may indicate that cpTi is more favourable to bone cell differentiation than Ti-6Al-4V (Lincks *et al.*, 1998a). The impaired bone formation with the Ti alloy may be related to the release of aluminium ions, which can be detrimental to bone cell differentiation (Albrektsson and Johansson, 1991; LeGeros *et al.*, 1991; Thompson and Puleo, 1996).

Ti is the 'material of choice' in implant dentistry (Lautenschlager and Monaghan, 1993). Its excellent corrosion resistance is due to the surface which oxidises spontaneously upon contact with air or tissue fluids. This layer, normally approximately 2-5 nm thick is primarily TiO_2, but may contain TiO and Ti_2O_3 depending, partly on its method of preparation (Kasemo, 1983; Kasemo and Lausmaa, 1988). However, the

oxide layer is not uniform or constant. The type and thickness of the oxide layer also depend upon other factors such as roughness of the surface, and treatments to passivate or sterilise the surface (Meenaghan *et al.,* 1979; Swart *et al.*, 1992; Larsson *et al.*, 1994; Callen *et al.*, 1995; Larsson *et al.*, 1996*).* The oxide layer may undergo dissolution and allow a finite rate of diffusion of the oxide in the body (Lugowski *et al.,* 1991; Healy and Ducheyne, 1992; Smith *et al.,* 1997). However, there is little evidence that this has any clinical significance, and no case of local or systemic reaction to Ti has been reported (Steinemann, 1998).

As with all materials implanted in living tissues, Ti is not entirely inert and will elicit a response from the host tissue. Williams (1990) described a biocompatible material as one "which possesses the ability to perform with an appropriate host response in a specific application", and consequently, Stanford and Keller (1991) proposed that the term "osseointegration" reflects the results of a lack of a negative tissue response to Ti, rather than the presence of an advantageous one. This is because Ti does not stimulate or induce mineralised tissue formation at the bone-implant interface. Rahal *et al.* (1993) showed that Ti does not have the ability to induce osteogenesis from potential osteogenic precursor cells in mice marrow. Various studies have also shown that bone healing around machined Ti implants takes place by a gradual mineralisation process directed towards, but does not start, at the implant surface (Sennerby *et al.,* 1992; Yliheikkilä *et al.,* 1995; Larsson *et al.,* 1996).

A bioactive implant (i.e. an implant which bonds to bone) forms a hydroxycarbonate-apatite (HCA) layer on its surface when implanted (Hench and Wilson, 1993). Ti is a reactive material, and Hanawa (1991) found that it naturally forms calcium phosphate on its oxide layer in a neutral electrolyte solution simulating body fluids. The ratio of calcium and phosphate (Ca/P) in the Ca-P layer formed was 1.63, which is close to that of hydroxyapatite (1.67). He suggested that this layer may therefore present itself as a suitable surface for osseointegration. However, this Ca-P layer was very thin (less than 8 nm on the cpTi and Ti alloy plates studied). This may indicate that the layer was due to the transfer and adsorption of these elements from the tissue fluids, rather than a true apatite formation. In a similar investigation, Li and

Ducheyne (1997) showed that the Ca/P ratio formed was only 1.44. This is lower than HA, as Ca was deficient on the surface oxide. They termed the layer a quasi-biological apatite, formed as phosphate ions bind to the Ti hydroxide layer on the surface of cpTi in contact with aqueous solution.

Yan *et al.* (1997) investigated the effect of the Ca-P coating in a rat tibia model after 6, 10 and 25 weeks of implantation. At 25 weeks, the coated implants were found to adhere extensively to mature bone, without any intervening soft tissue. On the uncoated side, although apposition of bone was also observed in certain areas, in other areas fibrous tissue was found between the implant and new bone. It is not known whether the intimate bone-Ti implant contact found in the normal clinical situation is due to the effect of the Ca-P layer formed on the surface of the oxide layer, since at the time of implantation, this layer is not present on implant surfaces.

Zirconium (Zr) is in the same group (Group 4) as Ti in the periodic table. It is also covered by a stable oxide layer, which if damaged, is rapidly re-oxidised, and therefore has as excellent a resistance to corrosion in the biological environment as Ti (Kawahara, 1983). Table 1.1 compares some of the typical physical properties of Ti and Zr. The values are obtained from the technical data sheets provided by Goodfellow Metals Ltd., England.

Table 1.1 Physical properties of Ti and Zr

Physical property	**Ti**	**Zr**
Vickers Hardness No.	60	85-100
Tensile strength (MPa)	230-460	350-390
Yield strength (MPa)	140-250	250-310
Young's Modulus (GPa)	120.2	95

The potential of Zr as an implant material has been studied *in vivo* in rabbit tibia (Albrektsson *et al.*, 1985; Johansson *et al.*, 1994), and *in vitro* using fibroblast and osteoblast cultures (Steinemann, 1998). The results suggest that Zr is as biocompatible as Ti, as bone cell and tissue reactions to Zr and Ti do not differ significantly.

1.2.2 Biomechanical factors

When a superstructure and final restoration are built upon an implant, the whole structure is based on both biological tissue and mechanical components. Rangert *et al.* (1995) analysed data obtained from authors who reported failures in the literature due to fractured implants, and concluded that the fractures were caused by excessive bending overload on the implants. These excessive bending moments were basically a combination of different adverse loading conditions due to poor bone support, long cantilevers and broad bucco-lingual width of the teeth. Failures due to fractured implants may be prevented if these potential overload situations were identified before treatment (Rangert *et al.*, 1997).

The connection of the natural dentition to implants via a rigid attachment posed a theoretical concern that it may be hazardous to both implant and natural tooth survival (Sullivan, 1986). It is hypothesised that failure of either or both components might be due to the differences in the mobility of teeth and the deformation of the bone supporting the implant. Long-term studies had shown however, that there were no changes in implant or tooth failure rates where prostheses were supported by implants and natural teeth via a rigid connection (Van Steenberghe, 1989; Naert *et al.*, 1992). This suggests that the tooth and bone-implant components were able to undergo some deformation under functional load to compensate for the differences in their resiliency.

1.2.3 Biologic factors

The patient's medical status, type and quality of bone at the implant site, minimising tissue trauma at the time of surgery, prevention of infection, and good post-operative care are critical factors in the formation and maintenance of osseointegration (Albrektsson *et al.*, 1986; Weyant, 1994). Another factor which can affect the prognosis of oral implant treatment is smoking. Nicotine and other toxic materials absorbed into the blood stream through smoking have been proposed to cause adverse local and systemic effects which can affect the survival of the natural teeth (Krall *et al.*, 1997). Local effects which have been proposed are altered salivary flow and microbial growth, while some systemic effects which have been associated with smoking are

vasoconstriction, impaired wound healing after surgical treatment, and increased prevalence of bone loss.

Bain and Moy (1993) and Lindquist *et al.* (1997) showed that smoking may be directly related to the soft tissue changes and marginal bone loss around dental implants. As such, it should be considered a risk factor in implant therapy, separated from the other factors mentioned in a review article by Meffert *et al.* (1992), which are primarily related to the maintenance of the implant in general.

1.3 Cellular responses to surface properties of metallic implant materials

1.3.1 Introduction

To anticipate the cellular responses to an implanted biomaterial, it is necessary to understand the nature of the surface properties of the material at the interface. The surface of a material is not necessarily the same as the bulk material, as differences arise from the molecular arrangement, surface reactions and contamination (Ratner *et al.*, 1987; Ratner, 1994). The characteristics of metallic implant materials are governed by the properties of the metallic oxides, and not as much by the metal itself, as interactions on the molecular level between the implant surface and the tissues occur within a very short range, of the order of 1 nm or less (Kasemo and Lausmaa, 1988). This range may even be 20 times shorter than the oxide thickness on a metal implant, since the oxide layer thickens as it undergoes oxidation reactions in the body (Steinemann, 1998).

In vivo, the cell-surface interaction occurs indirectly via an adsorbed layer of proteins, and not directly with the surface itself (Brunette, 1988). The adsorption process occurs within seconds once the material is implanted, as a solid-liquid interface is immediately established. This creates a tendency for the molecules of the fluid around the implant (blood, serum, proteins and glycoproteins, which are components of the extracellular fluid) to be adsorbed onto the solid surface (Williams, 1990). The process is not uniform throughout the surface, and varies especially if the surfaces are of heterogeneous microstructure or composition. There is also competitive and specific

affinity adsorption of the various proteins present at the interface. Adhesive proteins like fibronectin (Fn) and vitronectin (Vn) are preferentially adsorbed, compared with other less surface active proteins, even though their concentrations may be higher. The nature of the protein layer also changes rapidly, as once adsorbed, proteins may undergo conformational change, and sequential adsorption or desorption of proteins takes place continually as layers are replaced or augmented.

The character of the adsorbed protein layer varies with the surface properties of the oxide layer, with the chemical, morphological and electrical surface features being important variables (Kasemo, 1983). These factors result in changes in the surface energy and therefore lead to variations in the amount and conformation of proteins adsorbed (Kasemo and Lausmaa, 1988). Surface characteristics of implant materials therefore affect the biological activity of cells at the interface by influencing the nature of the established protein layer on the material (Ratner, *et al.*, 1987; Bagambisa *et al.*, 1994). One of the surface properties that affects the adsorption isotherm of Fn to substrates is roughness (Francois *et al.*, 1997).

1.3.2 Surface topography of implants and cellular interactions

1.3.2.1 Definitions of surface topography and roughness

Surface topography describes the degree of roughness and orientation (the height, width and direction) of the surface of a material. Roughness describes the surface irregularities at a high resolution, resulting from the method of manufacture and/or other conditioning influences (BS 6741, 1987). Roughness average (R_a) is the internationally recognised term for describing surface roughness. It represents the average deviation of the surface to a centre reference line (BS 6741, 1987). Higher R_a values indicate rougher surfaces.

1.3.2.2 The effect of implant surface irregularity dimensions on cellular behaviour

The role of surface roughness of implant materials depends in part, on the different geometric dimensions of the implant surface irregularities, in relation to the size of cells and biomolecules involved at the interface (Kasemo and Lausmaa, 1988).

Rough or porous surfaces with irregularity dimensions which are greater than 100 μm may be advantageous from a mechanical point of view. This size of irregularity allows the bone to grow into them, leading to mechanical locking of the implant with bone. However, it is the surface irregularities which are above the nanometre range and below 20 μm (i.e. smaller or in the same magnitude as the sizes of cells and large biomolecules), which significantly influence the interface biology.

Considerable differences are seen in the adhesion, migration, and proliferation of different cells on dental implant surfaces of different surface topography (Brunette, 1988; Chehroudi *et al.*, 1989; Qu *et al.*, 1996). Fibroblasts attach in greater numbers and spread better on a smooth surface when compared to a rougher one (Könönen *et al.*, 1992; Cochran *et al.*, 1994; Niederauer *et al.*, 1994; Richards, 1996; Mustafa *et al.*, 1998). In contrast epithelial cells prefer rough surfaces (Niederauer *et al.*, 1994). Chehroudi *et al.* (1989) showed that the increased number of epithelial cells which attached to grooved Ti samples as opposed to smooth flat ones, was not merely a result of the greater surface area available for attachment with the rough surfaces, since a correction was made in the cell number to compensate for this difference.

Rough implant surfaces are also more favourable substrates for bone formation by osteoblasts (Chehroudi *et al.*, 1992). *In vitro* studies have shown that osteoblast-like (OB) cells adhere to and spread more readily on rough, sandblasted implant surfaces than on smooth ones (Bowers *et al.*, 1992; Groessner-Schreiber and Tuan, 1992; Keller *et al.*, 1994). These findings are corroborated by *in vivo* studies, which show increased levels of bone formation around implant surfaces with greater surface roughness (Carlsson *et al.*, 1988; Buser *et al.*, 1991; Wong *et al.*, 1995; Wennerberg *et al.*, 1996; Sullivan *et al.*, 1997). Bone-like tissues were formed on rough but not on smooth control surfaces, even though the oxide layers were of similar thickness (Chehroudi *et al.*, 1992).

In contrast, Larsson *et al.* (1994; 1996) showed that the nature of the oxide layer alone may be adequate to influence bone formation, regardless of implant surface roughness. They studied the response of rabbit tibia implanted with an electropolished

amorphous metal surface with a non-crystalline glassy oxide layer, and a polycrystalline metal surface with a deliberately thickened oxide layer produced by anodic oxidation. They found that the presence of the oxide layer was sufficient for bone formation to occur without any evidence of soft tissue encapsulation, even though the implants had relatively smooth surfaces. There may also have been a greater percentage of bone contact on implants with the thick, heterogeneous oxide layer, even though the difference was relatively small.

These *in vitro* and *in vivo* studies indicate that the micro-roughness of implant surfaces is an important variable in regulating cellular responses to the implant. Hence, it presents a potential aspect of the implant surface which could be modified in order to optimise the reactions of the different cells which interact with the implant at the interface (Boyan *et al.*, 1996; Kieswetter *et al.*, 1996a).

1.3.2.3 Micro-roughness dimensions of substrate surfaces and contact guidance

Substrate surface feature dimensions in the range of 1-10 μm have been shown to directly influence the orientation and migration of individual cells (Brunette, 1988; Chehroudi *et al.*, 1989; Meyle *et al.*, 1993; Meyle *et al.*, 1995). This phenomenon is known as contact guidance, and refers to the cell's response to its substrate topography. These responses include changes in cell shape, orientation, and polarity of movement (Clark *et al.*, 1987; 1990; Curtis and Wilkinson, 1998).

Contact guidance is dependent on cell type, and may be more important in normal cells than in transformed cells, where the shape response controls are progressively lost with increasingly transformed phenotypes (Plantefaber and Hynes, 1989). The loss in control over the shape response in transformed cells may be due to the altered expression of the cell surface receptors which modify cellular behaviour and phenotype, the integrins (Dedhar and Saulnier, 1990).

In order for contact guidance to occur, the surface morphology has to be the same size or smaller than the cells (Oakley and Brunette, 1993), or it would be "seen" as smooth, since the cells would not be able to sense the borders of the textural

morphology (Green *et al.*, 1994; Singhvi *et al.,* 1994). Cells not only bridge across smaller grooves, but they may also adapt to the grooves, or part of wider grooves, depending on the groove depths and cell types (Clark *et al.*, 1987; Abiko and Brunette, 1993; Curtis and Wilkinson, 1998). This implies that any orientational effect of the substrate on cells is related to the substrate's amplitude and textural or spatial dimensions.

Meyle *et al.* (1993) used parallel grooved substrates, which were 1 μm thick and 1 μm apart, to show that fibroblasts conformed to the contours of the underlying substrate morphology. Eisenbarth *et al.* (1996) prepared rough surfaces by grinding cpTi and Ti alloy substrates with silicon carbide papers, and showed that the majority of the oriented cells were found on substrates with the highest R_a value (i.e. 1.36 μm). While Oakley and Brunette (1993) showed that cells could align themselves inside a groove within 6 h after plating on the substrates, Meyle *et al.* (1993) and Eisenbarth *et al.* (1996) found that the influence of the surface was not effective immediately. The majority of the fibroblasts were found to align themselves with the substrate surface morphology only after more than two days of culture.

Green *et al.* (1994) analysed cell spreading on surfaces with a pit morphology, and on surfaces with pillars, where the pits and pillars were of equal dimensions. When placed on surfaces with pits, cells contacted the larger flat area, and were able to spread well with a small number of attachment points on the surface. However, when placed on surfaces with pillars, the cells contacted an area which was very much reduced, and therefore needed more points for attachment. This shows that cells behaved differently towards spacings and depths of grooved or rough surfaces (Clark *et al.*, 1990). As the R_a values of different configurations of a surface could be the same, this parameter alone is not sufficient to describe a substrate surface if cellular reactions to surface roughness are to be analysed. To eliminate the influence of chance or any other substrate feature on cellular behaviour, Curtis and Wilkinson (1998) stressed the importance of the quality of the prepared surfaces, and suggest that only reactions of cells to surfaces prepared by photolithography techniques or other high precision methods are to be considered useful.

1.3.2.4 OB cell proliferation and differentiation on metallic implants with different surface roughness

The proliferation and differentiation of OB cells may be affected by the surface roughness of the substrates on which they were grown. Ong *et al.* (1996) observed the orientation of rat bone marrow cells cultured on polished Ti and Ti ground to 600 grit after three, six, nine and twelve days. After the sixth day, cells on polished Ti were rounded, whereas cells on the ground Ti surfaces were elongated, and oriented in the direction of the grinding grooves. At this time, protein production by cells grown on the ground Ti surfaces was greater than that of cells grown on the polished surfaces. Ong *et al.* (1996) therefore suggested a possible influence of the substrate topography on cell orientation and protein synthesis. Groessner-Shcreiber and Tuan (1992) also showed the potential of substrates to modulate cell differentiation. Chick embryonic osteoblasts grown on rough and porous coated Ti surfaces were seen to have higher levels of alkaline phosphatase (AP) expression and calcium accumulation during a six to seven day culture period, compared to those grown on smooth surfaces.

Cells at different stages of maturity may also respond differently to the same surface (Boyan *et al.,* 1993; Boyan *et al.,* 1995; Schwartz *et al.,* 1996; Lincks *et al.,* 1998b; Lincks *et al.,* 1998c). These investigators showed the potential of rough surfaces to accelerate the maturation of two types of cells: non-transformed rat chondrocytes, and the MG-63 cell line. The chondrocytes were derived from two regions of the rat costochondral cartilage which were at two distinct stages of endochondral maturation *in vivo*; cells from the resting zone were relatively immature, while those from the growth zone were more mature. The use of MG-63 cells as a model for osteoblastic cell differentiation may be questionable. These cells are transformed cells, and there are doubts about their state of differentiation, although they are thought to be an immature OB cell line (Franceschi *et al.,* 1985). However, some osteosarcoma derived OB cell lines have retained the phenotypic properties associated with normal osteoblasts *in vivo* (Rodan and Noda, 1991), and therefore may be valuable osteoblastic models.

Boyan *et al.* (1995), Schwartz *et al.* (1996) and Lincks *et al.* (1998b) studied the behaviour of these cells when grown on Ti surfaces with five different surface

roughnesses. Their results show that when the MG-63 cells were grown on rougher surfaces, there were lower cell numbers, decreased rates of cellular proliferation, but increased AP specific activity when compared to cells grown on smoother Ti surfaces and the control polystyrene surface. However, the number of cells grown on Ti surfaces with intermediate roughness did not differ significantly from the controls. It was also reported that cell morphology varied as a function of roughness. Cells grown on the roughest Ti plasma-sprayed surfaces (R_a value of 6.81 μm) were rounded in appearance and had cytoplasmic extensions which spanned the distance between surface peaks, while those grown on smooth electropolished surfaces had a well spread, flattened morphology similar to that grown on control surfaces. Immature chondrocytes from the resting zone cartilage responded in the same manner as the MG-63 cells when they were cultured on the same surfaces.

The reduction in cell number and cell proliferation, together with the more osteoblast-like morphology, suggest that differentiation of these immature cells may be enhanced on the rougher surfaces. Lian and Stein (1992) observed that decreased proliferation of OB cells precedes the expression of the more differentiated phenotype in culture. The relatively weak proliferative response, in conjunction with an increased AP activity seen with the resting zone chondrocytes and MG-63 cells grown on the rougher surfaces, suggest that these cells were at a more advanced stage of differentiation than those cells which were grown on the smoother surfaces.

In contrast, although the attachment and proliferation of the more mature growth zone chondrocytes cultured on the roughest surfaces were significantly higher than those grown on tissue culture plastic, the AP activity was decreased. Boyan *et al.* (1995) suggested that the more mature cells may have remained longer in a proliferative state in culture conditions, and that the effect of rough surfaces may be more significant on immature and less differentiated cells.

Boyan *et al.* (1998) studied the effect of surface roughness in synergy with $1\alpha,25(OH)_2D_3$, on MG-63 cell synthesis of osteocalcin and production of the growth factors, latent transforming growth factor β (TGFβ) and prostaglandin E_2 (PGE_2). They

reported that surface roughness was able to regulate the osteocalcin expression, even without the addition of $1\alpha,25(OH)_2D_3$ in the culture medium, and that the effect of $1\alpha,25(OH)_2D_3$ on osteocalcin production was more marked on cells grown on rough surfaces than on smoother ones. Price *et al.* (1997) also found significant osteocalcin production in MG-63 cells grown on Bioglass and rough Ti and cobalt-chromium alloy, in the absence of $1\alpha,25(OH)_2D_3$. These results may have to be interpreted with caution as other researchers have found that the basal expression of osteocalcin in MG-63 cells was either very low (Lajeunesse *et al.*, 1990; Mahonen *et al.*, 1990), or totally dependent on the stimulation with $1\alpha,25(OH)_2D_3$ (Clover and Gowen, 1994).

$1\alpha,25(OH)_2D_3$ was also shown by Boyan *et al.* (1998) to increase the LTGFβ and PGE_2 production of cells grown on rough surfaces. Unlike its effect on osteocalcin production, $1\alpha,25(OH)_2D_3$ does not increase the production of LTGFβ and PGE_2 on cells grown on plastic and on the smoothest acid treated Ti surface, although the production of both factors on these surfaces was enhanced by surface roughness alone.

These results indicate the potential of rough surfaces to regulate differentiation of OB cells. The question that remains to be answered is what actually was meant by a rough surface? In order to analyse the results obtained by different investigators, the surface topography or roughness values have to be comparable. Presently, the surface topography of implant materials is mainly described using:

a. the R_a values (Bowers *et al.*, 1992; Keller *et al.*, 1994; Martin *et al.*, 1995; 1996; Wennerberg, 1996). This parameter does not describe the surface morphology and texture. Further characterisation of the surface morphology may or may not have been complemented by qualitative examination, for example, with scanning electron microscopy (SEM), to aid in relating the actual morphological dimensions of the surfaces to the cells of interest.
b. actual dimensions of the surface microtexture. However, this is only possible with high precision techniques like photolitography (Chehroudi *et al.*, 1989; Green *et al.*, 1994; den Braber *et al.*, 1998). Surface roughness measurements may or may not have been made, and this made it difficult to compare the results

obtained with results from other studies, where only surface roughness values of the materials studied were reported.

1.3.3 Surface roughness of commercial implants

Commercial implant systems vary with respect to material, design, surface topography and roughness (Wennerberg *et al.*, 1993). 3-D optical profilometer analysis of the surface topography of 13 implant systems showed the Nobelpharma implant to be the smoothest (R_a = 0.53 μm), and Osteoband, an HA-coated implant system (R_a = 2.94 μm), the roughest. Binon *et al.* (1992) used spectroscopic microanalytical techniques to show that the surfaces of four screw-type cpTi implants demonstrated varying degrees of contamination and oxide thickness, resulting from the manufacturing or cleaning processes.

Different cleaning and sterilisation treatments have been shown to affect bone cell attachment and phenotypic expression on implant surfaces *in vitro* (Swart *et al.*, 1992; Stanford *et al.*, 1994; Vezeau *et al.*, 1996). Preliminary (three weeks) studies of untreated and glow discharged tantalum implants inserted in various sites in primates (not confined to bony sites), showed that a biologically clean surface with high surface energies was associated with increased vascularity and significant differences in tissue response at the interface (Meenaghan *et al.*, 1979). However, it is not known how beneficial clinically these short-term effects would be, as Budd *et al.* (1991) found that any difference in the bone response to implant materials which had undergone different sterilising methods was not significant in the long-term.

The ideal roughness, morphology and texture of implant surfaces in long-term clinical function remain to be established. Even though the amount of bone formation at the bone-implant interface may be positively related to an increasing roughness of the implant surface, the roughness value is not infinite (Bowers *et al.*, 1992; Gomi and Davies, 1993). Wennerberg *et al.* (1996) suggested that there exists an upper and a lower limit of surface roughness for optimal bone response to implants. Their *in vivo* study showed superior bone fixation for implants blasted with 25 μm particles of Al_2O_3 or TiO_2, and 75 μm particles of Al_2O_3, when compared to smoother "as machined"

implants. The blasted surfaces had S_a (the 3-D roughness parameter equivalent to the 2-D R_a) values of 1-1.3 μm. Wennerberg *et al.* (1996) also showed that increasing the blasting particle sizes to 250 μm (S_a = 2.11 μm) did not further increase the short-term (four weeks) bone formation and attachment, and therefore concluded that an S_a of 1-1.5 μm may be the optimum roughness value for maximum bone-to-implant contact and retention.

However, as mentioned earlier, the R_a value alone, without any relation to the microtextural morphology and dimensions of the implant surface, may not be sufficient to explain cellular reactions to the implant. Hansson (1998) predicted mathematically an "ideal pit morphology" (with pit sizes ≥ 2–3 μm) which would produce the greatest shear strength at the bone-implant interface. This model also predicts that the shear strength would decrease if pits above a certain size, which is still to be established, are used. It is known that surfaces are not always consistent and predictable, and besides surface morphology, roughness values also depend on other factors, which will be discussed in the next chapter.

1.4 The bone-implant interface

1.4.1 Implant surface characteristics and healing of bone at the interface

To understand the process of osseointegration, it is necessary to understand the different processes and sequence that contribute to the healing of a fracture, as osseointegration is basically a wound healing process, rather than a developmental process where new bone is formed on the implant surface (Davies, 1998).

Fracture repair occurs in at least five discrete stages of healing. These stages follow the following sequence: formation of haematoma and inflammation, development of angiogenesis and formation of cartilage, cartilage calcification, cartilage removal and bone formation, and finally bone remodelling (Einhorn, 1998). The wound healing response can be outlined by following the expression of several important extracellular matrix (ECM) proteins, which are used as markers of the differentiation state of cells, callus development and bone formation (Einhorn, 1998).

The wound healing response after insertion of an endosseous implant follows this complicated, highly regulated cascade of events (Stanford and Keller, 1991; Schwartz and Boyan, 1994; Cooper, 1998). These involved: protein adsorption to the implant surface, recruitment of osteoblast precursor cells, cell attachment and differentiation of the undifferentiated mesenchymal cells into secretory osteoblasts, production of unmineralised matrix (osteoid) and finally, calcification of the ECM (O'Neal *et al.,* 1992; Schwartz and Boyan, 1994; Clokie and Warshawsky, 1995; Masuda *et al.,* 1997; Davies, 1998).

In all these events, the surface composition, topography, roughness and surface energy of implant materials have been shown to be inter-related factors which dictate the biological response. The role of these surface characteristics in the healing of bone around implants was reviewed by Kieswetter *et al.* (1996a).

1.4.2 Methods for studying the bone-implant interface

Earlier models for the assessment of bone responses to implants were *in vivo* studies resulting in static measurements of healed tissues (Albrektsson and Johansson, 1991). Retrieval analyses of healed tissues at the light microscopy levels do not provide definite descriptions of the bone-biomaterial interface, mainly due to the difficulty of sectioning and preserving an intact metal-tissue interface, and the resolution of the microscope. Ericson *et al.* (1991) pointed out that the nature of contact between implant, cells, organic and inorganic matrix should be interpreted at the ultrastructural level. However, obtaining suitable sections for transmission electron microscopic (TEM) investigation of the metal-tissue interface has not been easy. This has been limited by the lack of appropriate methodology to separate the implant from the tissues at the interface, which assures preservation of the delicate structures on the surface of the Ti oxide. Techniques which have been used to examine the interface include:

a. using a plastic or polycarbonate replica implant sputter coated with a thin layer of Ti (»50-200 nm) (Albrektsson and Hansson, 1986),
b. removing the metallic implant after it has been embedded in epoxy resin by electrochemical removal of the implant from the embedded sections (Bjursten *et al.*, 1990),

c. freeze-fracture techniques (Sennerby *et al.*, 1992; Clokie and Warshawsky, 1995).

The use of epoxy replica implants sputter coated with a layer of Ti made it possible for the interface of the Ti oxide and the tissue to be processed directly for ultrathin sections. The surface still resembled Ti implants since Ti oxide was the dominant molecular species (Chehroudi *et al.*, 1992).

In the electrodissolution technique, the bulk part of the metal was electrochemically removed, leaving the thin oxide surface of the implant (which is not dissolved) in the embedding medium (Bjursten *et al.*, 1990). This made it easier to section the samples. However, Sennerby *et al.* (1992) showed that this method can produce serious artefacts, including decalcification of the interface zone. This hindered reliable analysis of the interfacial tissue. Another argument against this technique is that if the implant is not smooth, then there would always be small areas of metal particles remaining in the embedding resin. This is a result of the eventual loss of electrical continuity as the metals are corroded (Richards *et al.*, 1995).

The implant can also be physically separated from the tissue in the embedding resin by freeze fracturing techniques. Rapid freezing in liquid nitrogen, followed by immediate immersion into boiling water caused fracture at the metal-tissue interface due to the difference in the coefficients of thermal expansion of the metal and polymer (Lowenberg *et al.*, 1991; Steflik *et al.*, 1992). Plunging directly into liquid nitrogen may, however, cause shattering of the embedding resin resulting in mechanical damage to the interface and cells (Richards *et al.*, 1995). This can be prevented by freezing the metal in the embedding resin slowly via convection through a block of metal or copper which is cooled in liquid nitrogen, before plunging the resin in boiling water. However, uncertainty may still exist, especially if some tissue retraction had occurred due to the differential shrinkage which occurs during freeze fracturing (Orr *et al.*, 1992).

Due to limitations in technique and sample preparation procedures for TEM examination, only selected areas are sectioned and analysed. A novel approach of

examining the adaptation of bone at the whole tissue-implant interface was presented by Boyde *et al.* (1998), using an SEM technique. This is done after sectioning the embedded bone with implant *in situ* using a fine diamond saw, whereby the metal device can then be removed from the bone without disrupting the delicate sheets of bone. Different thicknesses of tissue previously in contact with the metal was imaged by varying the accelerating voltage of the microscope to reveal the true 3-D area and the exact nature of the bone-metal contact. This allows the whole length of the area in contact with retrieved implants to be examined without any loss of sample.

1.4.3 Findings at the bone-Ti interface

Ericson *et al.* (1991) reported that next to metallic implants, cells were generally normal while inflammatory cells were absent or rare. Nevertheless, inflammatory responses should be examined at the earliest stages of osseous healing, rather than in healed tissues. Regarding mineralisation at the interface, most studies were able to identify a calcified matrix layer, produced by osteoblasts, adhering to Ti surfaces (Linder *et al.,* 1983; Lowenberg *et al.,* 1991; Orr *et al.,* 1992; Steflik *et al.,* 1994). Yliheikkilä *et al.* (1995) used bovine mandibular OB cells to investigate the interactions of mineralising osteoblast cultures with implant surfaces. They found that the mineralised matrix was always formed remote from the implant, several cell layers from the Ti alloy surface.

The main area of interest is, however, in identifying the components and assessing the morphology of the ECM directly adjacent to the interface. Two types of morphological arrangements have been found:

a. a clear zone, approximately 50 nm thick adjacent to the implant surface, which was characterised as an electron dense proteoglycan-rich layer, apparently without structured tissue (free of collagen fibres), or
b. direct contact between the collagenous ECM and the surface of the implant.

Using experimental implant systems comprising of metal-sputtered polycarbonate plugs and examination by TEM, the ultrastructure of the bone-Ti interface

was described as one in which morphologically distinguishable bone tissue (an ECM comprising mineralised collagen) was separated from the implant surface by a 20-50 nm zone of collagen-free ground substance (Albrektsson and Hansson, 1986). This layer was bordered by a second layer, 100-500 nm in thickness, which contained randomly distributed collagen fibres and occasional osteocytes. A third layer consisted of collagen fibres oriented in orderly bundles. Each of the layers showed some evidence of calcification, with fewer deposits in the zones closest to the metal.

Albrektsson and Hansson (1986) reported that the 20-50 nm "amorphous" zone contained a mixture of proteoglycans and glycosaminoglycans in unknown proportions. Other investigators reported the same interface morphology, except that the widths of the ground substance varied with the surface chemistry of the implant material (Linder *et al.,* 1983; Albrektsson *et al.*, 1985; Johansson *et al.*, 1990; Steflik *et al.*, 1992). Besides the 20-50 nm amorphous zone, other studies have also found a slender cell layer, and/or a poorly mineralised zone interposed between the newly formed bone and Ti (van Blitterswijk *et al.,* 1991; Nanci *et al.,* 1994).

Nanci *et al.* (1994) examined the bone-implant interface using polyclonal antibodies for non-collagenous bone and plasma proteins. The various antibodies used for the immunocytochemistry investigation were against osteopontin, osteocalcin, α_2HS-glycoprotein, albumin and Fn. They concluded that the concentration of osteopontin and α_2HS-glycoprotein, and the relative paucity of osteocalcin, albumin and Fn found in the electron dense layer was similar to the composition of cement lines, formed at the bone-HA interface, and at natural bone interfaces between old and new bone during wound healing (Davies, 1996).

To date, the nature and exact composition of this proteoglycan layer remain to be identified, as there have been few biochemical or molecular analyses of forming bone at implant surfaces (Klinger *et al.*, 1998). So far, it has been suggested to be either a layer abundant in proteoglycans, or a zone consisting primarily of osteopontin and not proteoglycans (Nanci *et al.*, 1994). However, the presence of one does not exclude the presence of the other, as both are major non-collagenous protein components of the

ECM, which are believed to be important in regulating bone function and turnover (Stanford and Keller, 1991; Klinger *et al.*, 1998).

In contrast to the above findings, Chehroudi *et al.* (1992) found direct contact between bone-like tissue and the surface of epoxy implants sputter coated with a layer of Ti oxide at the resolution of the TEM. However, in this study implants were placed subcutaneously in the parietal region of rats, and not directly into bone. Similar findings were also reported by Listgarten *et al.* (1992), using unloaded epoxy resin implants coated with Ti oxide. It is not clear whether the difference in the above findings could be related to the type of implants used, the area where implants were placed, whether the implants were loaded or not, or to the different methodologies and analytical techniques employed by the various investigators to examine the interfacial region.

1.5 In vitro studies of the bone-biomaterial interface

1.5.1 Introduction

To understand the differential tissue reactions which may be generated by implants at the bone-biomaterial interface, it is possible to avoid the difficulties associated with ultrastructural examination of retrieved implants by using *in vitro* models. Moreover, *in vivo* tests using animals are limited and costly (Natiella, 1988), and there is also an increasing moral pressure to reduce animal experimentation. *In vitro* systems, however, do not represent the systemic situation, and therefore caution must be exercised before extrapolating results directly to the clinical environment. Nevertheless, they enable the responses of individual cells to be evaluated to develop a concept of possible *in vivo* situations, before carrying out *in vivo* studies where necessary.

1.5.2 *In vitro* models for studying bone-biomaterial interactions

Among the practical advantages of using cell culture are:

a. cells of various origins, including human, may be used, as the primary determinant in selecting a tissue or cell line for study depends on the nature of the observations that is to be carried out,

b. various parameters can be chosen to gauge the specific cell responses and the results of various types of tests on the same material may be grouped together and analysed, and
c. tests are rapid, and experimental conditions may be standardised (Pizzoferrato *et al.*, 1985; Pizzoferrato *et al.*, 1994).

In cell-biomaterial research, *in vitro* systems were developed to deal with the assessment of different implant materials, with regard to:

a. implant material cytotoxicity and biocompatibility, and
b. growth and differentiation of specific cell types (derived from tissues which are normally in contact with the implant, such as bone and oral mucosa) when cultured in the presence of the material tested (Edgerton and Levine, 1993).

1.5.2.1 Cytotoxicity and biocompatibility assessment models

Earlier *in vitro* systems were basically processes of screening of biomaterials. Cells used were mostly macrophages and fibroblasts. Besides subjective assessment of morphology, markers of toxicity which were used were decrease in cell numbers, increase in release of lactate dehydrogenase and/or lysosomal enzymes by cells exposed to the test material, and detection of cell damage and death (Rae, 1986; Doillon and Cameron, 1990).

1.5.2.2 Assessment of tissue responses to orthopaedic and dental implants

Depending on the type of tissue response that needed to be examined, *in vitro* studies have used cells such as fibroblasts and epithelial cells (Hakkinen *et al.*, 1988; Keller *et al.*, 1989; Michaels *et al.*, 1991; Howlett *et al.*, 1994; Leung *et al.*, 1994; Niederauer *et al.*, 1994), as these cells are in contact with the implant *in vivo*. As it has been shown that bone cells may not respond in the same way as these cells to implant surfaces, and as bone formation is of great relevance in osseointegration, many research groups have used OB cells in studying cellular responses to dental and orthopaedic biomaterials (Harmand *et al.*, 1991; Puleo *et al.*, 1991; Swart *et al.*, 1992; Riccio *et al.*, 1994; Sinha *et al.*, 1994; Kornu *et al.*, 1996; Cooper *et al.*, 1998).

1.5.3 Osteoblasts

1.5.3.1 Osteoblast formation and origin

The osteoblast is the mature differentiated cell responsible for the formation and mineralisation of bone matrix. They are thought to arise from local undifferentiated mesenchymal progenitor cells in the stromal compartment of bone marrow, and are capable of differentiating into chondroblasts, myoblasts, fibroblasts and adipocytes. Friedenstein *et al.* (1987) showed this using bone marrow stromal cells which have the capacity to form bone when transplanted *in vivo* in diffusion chambers, and that all the tissues could arise from single clones or fibroblast colony-forming units (CFU-F). There were at least two distinct populations of the osteoprogenitor cells. One population was present in bone tissue and appeared capable of forming osteogenic tissue spontaneously. These cells are called determined osteogenic precursor cells (DOPCs). The other population was not necessarily present in bone tissue, and only formed bone in the presence of the inductive influence of bladder epithelium. These cells are called inducible osteogenic precursor cells (IOPCs).

For the osteoblast, there is an unknown number of stages in differentiation during which their proliferative potential decreases while their synthetic activity increases. However, this pathway is generally considered to proceed via an osteoprogenitor cell to the final osteocyte (Lian and Stein, 1992).

1.5.3.2 The osteoblast phenotype and markers of osteoblastic differentiation

The following are some markers by which the osteoblast phenotype may be recognised:

a. Alkaline phosphatase (AP) activity

AP is widely used as a marker of the osteoblast phenotype (Rodan and Noda, 1991). Differentiating osteoblasts *in vitro* express high levels of AP and type I collagen relatively early in the maturation sequence. AP is also expressed by pre-osteoblasts, osteocytes and osteosarcoma cells (Majeska and Rodan, 1982; Franceschi *et al.*, 1985). Although AP expression is not unique to bone, its level is relatively abundant in bone

and levels in differentiating cells are stimulated by Vitamin D_3 and hydrocortisone (Beresford *et al.*, 1994).

b. Synthesis of bone matrix proteins

The organic matrix of bone consists of approximately 90% type I collagen, and 10% non-collagenous proteins. These matrix proteins include osteocalcin (which at about 20%, is the most abundant non-collagenous protein in bone), matrix Gla protein, bone sialoprotein, osteopontin, osteonectin, fibronectin, thrombospondin, α_2HS-glycoprotein, tenascin, transforming growth factor β and fibroblast growth factors, and certain proteoglycans (e.g. decorin and biglycan) (Rodan and Noda, 1991; Stanford and Keller, 1991). So far, only osteocalcin is considered 'bone specific' as its expression is restricted to mineralised tissue cells including osteoblasts, odontoblasts and cementoblasts of teeth and those in hypertrophic chondrocytes. Osteocalcin expression is often associated with the onset of matrix mineralisation, and is therefore widely used as a phenotypic marker of bone formation. Although not uniquely expressed by osteoblasts, the high expression of osteopontin and bone sialoprotein in OB cells has made them useful markers of the osteoblastic phenotype, especially when used in conjunction with other markers (Hughes and Aubin, 1998a).

c. Hormone responsiveness

OB cells respond to a wide array of hormones, and some of these interactions are useful as markers of their phenotype. One of these is the binding of parathyroid hormone (PTH) to PTH receptors which results in cyclic AMP production (Auf'mkolk *et al.*, 1985). Another hormone which acts on the OB cells is $1\alpha,25(OH)_2D_3$. Vitamin D_3 enhances AP and osteocalcin productions in normal human OB cells and in human osteosarcoma cell lines (Auf'mkolk *et al.*, 1985; Beresford *et al.*, 1994; Clover and Gowen, 1994). In human marrow stromal cultures, glucocorticoids inhibit cell proliferation and increases AP synthesis (Beresford *et al.*, 1994).

d. Cell surface markers

Expression of at least some of the ECM proteins occur at different phases of the OB cell differentiation or maturation cascade (Lian and Stein, 1992). Polymerase chain

reaction and immunocytochemical data of bone matrix proteins synthesised by single colonies of rat foetal calvarial OB cells at different developmental stages show that bone matrix proteins follow a sequence of expression: Collagen I, AP, osteopontin, bone sialoprotein and osteocalcin (Liu *et al.*, 1994). Some of these proteins (e.g. Fn, bone sialoprotein and osteopontin) contain the amino acid sequence, Arginine-Glycine-Aspartate (RGD), which is the integrin-binding cell attachment motif (Pierschbacher and Ruoslahti, 1984). Little is known about the integrin expression in bone cells at progressive stages of the osteoblastic lineage. However, recent studies of the expression of integrin receptors of OB cells both *in vivo* and *in vitro*, suggest the possibility of qualitatively determining the osteoblast lineage by the integrins expressed during the different stages of osteoblastic differentiation (Moursi *et al.,* 1996; Alavi *et al.*, 1998). In particular, the $\alpha_5\beta_1$ integrin may be associated with the late stages of osteoblastic differentiation in primary OB cell cultures, and α_2 at a relatively earlier stage.

e. Induction of mineralisation and bone formation

The defining characteristic of the mature osteoblast is its ability to produce a mineralised bone matrix. Some osteoblastic culture systems can produce discrete, three-dimensionally organised mineralised matrices which are recognised as bone-like, when grown on implant materials (Davies *et al.*, 1991; Ripamonti, 1991; Chehroudi *et al.*, 1992; Ozawa and Kasugai, 1996). The formation of mineralised nodules *in vitro* is dependent upon the presence of serum, ascorbic acid, and β-glycerophosphate (Bellows *et al.,* 1986; Chung *et al.*, 1992), although Beresford *et al.* (1993) have shown that in the presence of the long-acting ascorbate analogue Asc-2-P, the formation and mineralisation of nodules in primary explant human bone cultures can occur in the absence of β-glycerophosphate. Mineralisation in culture has been characterised using various markers of bone formation, for example, nodule formation, positive staining for Ca and P, and positive staining for major non-collagenous proteins (Bellows *et al.*, 1986; Groessner-Schreiber and Tuan, 1992; Lian and Stein, 1992; Beresford *et al.*, 1993). However, "true bone" formation is viewed to have occurred, only if the Ca:P ratio of the nodules formed is similar to hydroxyapatite (Groessner-Schreiber and Tuan, 1992), or if the mineral density of the new bone falls between the normal range of

neonate and aged bone of the species from which the cells were derived (Gray *et al.*, 1996).

1.6 Integrins and OB cell-substrate interactions

1.6.1 Introduction

OB cells mainly use integrins for the majority of the initial cell attachment to various substrates *in vitro* (Stanford *et al.*, 1990; Gronowicz and McCarthy, 1996). Integrins were reported to be largely responsible for cell attachment to substrates, as RGD synthetic peptides competitively blocked cell attachment to the substrates by at least 50 to 60%, depending on the substrates and the integrin subunit tested (Gronowicz and McCarthy, 1996).

1.6.2 The Integrins

Integrins are a large family of transmembranous heterodimeric glycoproteins, present on the plasma membrane of almost all cells. They function as integrators, mediating the interactions between the cytoskeleton and the ECM, and can interact with a complex spectrum of ligands on cell surfaces and in the ECM (Hynes, 1987; Buck and Horwitz, 1987a; 1987b).

The association in discrete attachment sites, called focal adhesions, between the integrin subunit and the actin stress fibres of the cytoskeleton may be mediated or linked by several other proteins, including talin, vinculin and tensin (Burridge *et al.*, 1988). These proteins appear to have only structural functions. Other proteins, including the mitogen-activated protein kinase (MAP kinase) and the focal adhesion kinase (FAK) play an active part in the signalling pathway with the intracellular environment (Miyamoto *et al.*, 1995; Richardson and Parsons, 1995). The association of integrin receptors with the underlying cytoskeleton may explain their regulation of gene expression. By linking events at the cell surface to the cytoskeleton-signalling complex, integrins enable cells to modify their response to changes in the microenvironment of the plasma membrane which occurs both inside and outside the cells. These functions are termed "outside-in" and "inside-out" signalling, respectively (Hynes, 1992).

1.6.2.1 Structure of the integrin receptor

Each receptor is composed of an α and a β subunit joined noncovalently at amino-terminal domains to form the large globular extracellular head region, which binds to ligands. Each integrin subunit spans the plasma membrane with a long extracellular segment and a short intracellular domain.

Although integrins are αβ dimers, not all of the possible combinations of subunits exist. In addition, the range of dimers which can be formed depends on the particular α and β subunits. Presently, there are 15 known α subunits and eight β subunits, assembling into at least 22 different receptors (Akiyama, 1996; Guan, 1997). Each β subunit associates with one or more different α subunits. α_1, α_2, α_3 and α_5 can only form dimers with β_1. However, the α_v subunit can associate with multiple β subunits, i.e. β_1, β_3, β_5, β_6 and β_8 (Humphries, 1990). Most integrins have more than one adhesive ligand, and more than one integrin can bind to the same ligand. Changes in either the α or β subunit of integrin heterodimer alter their specificity for ligands (Juliano and Haskill, 1993). It appears that β_1 and β_3 integrins predominantly mediate cell-matrix interactions, with β_1 integrins binding to connective tissue proteins such as collagens, laminin and Fn, and β_3 integrins binding to vascular associated molecules such as fibrinogen, Vn and von Willebrand factor (Humphries, 1990).

1.6.2.2 The RGD sequence in ECM proteins

ECM proteins contain the amino acid sequence, RGD, which is recognised by integrins as their cell recognition/binding sites (Pierschbacher and Ruoslahti, 1984). In bone, there are several RGD-containing matrix proteins: collagen type I, thrombospondin, Fn, Vn, osteopontin and bone sialoprotein (Grzesik, 1997). Depending on their concentrations, and whether they are in solution or attached to a substrate, RGD synthetic peptides may mediate or inhibit adhesion of cells to the substrates (Sauk *et al.*, 1991; Grzesik and Robey, 1994). However, not all integrins recognise the RGD sequence, even though they bind to proteins which contain the RGD sequences (Grzesik and Robey, 1994; Ruoslahti, 1996).

1.6.2.3 Integrins and signal transduction

Integrins convey a series of signals after ligand binding or receptor clustering. Integrin mediated adhesion of cells to a variety of ECM molecules leads to a series of second messenger-type signalling pathways. These include enhanced tyrosine phosphorylation of specific proteins (Juliano and Haskill, 1993). One of these is a 125 kD protein. Based on its location at the focal contacts, this protein is termed "pp125 Focal Adhesion Kinase" ($pp125^{FAK}$). As integrins lack intrinsic catalytic activity, FAK is thought to be a candidate for a signalling molecule which is recruited by the integrins to trigger the generation of intracellular secondary messengers. Thus FAK may play a central role in signal transduction through integrins (Miyamoto *et al.*, 1995; Richardson and Parsons, 1995).

1.6.2.4 Regulation of the actin cytoskeleton

Cellular responses to extracellular physical and biochemical factors, include changes in cell shape and movement (Sinha *et al.*, 1994). These aspects of cell behaviour are governed principally by the actin cytoskeleton. Remodelling of the actin cytoskeleton therefore represents a key element of the response of many cells to extracellular stimuli. Actin is diffusely distributed in "rounded up" cells. However, in spreading cells it is organised in stress fibres across the cell (Burridge *et al.*, 1988; Hynes, 1992), and fixed at each end to the substrate in focal adhesion sites (Bagambisa *et al.*, 1994). This causes cell flattening on the substrate. Cell growth can be promoted by adhesion to the ECM only if it was followed by cell spreading, i.e. some degree of deformation of cell shape, and not just the occupancy of integrin receptors, is required to prevent apoptosis (Re *et al.*, 1994).

1.6.2.5 Integrin expression in human OB cells

The human OB cells are capable of producing a variety of integrin subunits. It was reported that high levels of α_1, α_3, α_5, β_1, and $\alpha_v\beta_5$ were found in OB cells from primary human bone explants (Hughes *et al.*, 1993; Clover and Gowen, 1994; Saito *et al.*, 1994). The expression of α_2, α_4, and β_3 (a minor OB cell integrin) subunits was relatively low, and no expression of α_6 was detected (Clover *et al.*, 1992; Clover and

Gowen; 1994; Gronthos *et al.*, 1997). Pistone *et al.* (1996) did not detect any α_2 in their OB cell cultures, and no α_5 and α_v subunits were observed on the OB cells which were cultured by Clover *et al.* (1992). Grzesik & Robey (1994) studied integrin expression within developing human long bone using immunohistochemical methods with a panel of anti-integrin antibodies. They found that bone cells *in vivo* and *in vitro* expressed α_4, $\alpha_5\beta_1$, α_v, $\alpha_v\beta_3$, and β_3/β_5 integrins. These integrins were expressed by all bone cells at different stages of maturation with quantitative, rather than qualitative variations. However, the α_4 subunit was expressed mainly by osteoblasts.

These results demonstrate that the integrin profiles of human bone cells may vary according to cell type, *in vivo* versus *in vitro* characteristics, and the method of detection used.

1.6.2.6 Integrin expression in human osteosarcoma cells

The integrin expression of cultured human bone cells is different when compared with transformed osteoblasts. The variations reported include increased expression, decreased expression or expression of integrins which are not normally present in that tissue type (Plantefaber and Hynes, 1989; Matsumoto *et al.*, 1995). These differences may be due to a number of reasons, among them the homogeneity/heterogeneity of the cell population, the process of malignant transformation, and changes due to long-term culture conditions (Albelda and Buck, 1990).

Dedhar and Saulnier (1990) reported that cultured HOS cells expressed relatively large amounts of the α_3 subunit, and smaller amounts of α_1, α_2, α_5 and α_6 subunits. This is in contrast to the results of Saito *et al.* (1994), who found strong expressions of α_1 and α_5 subunits in primary human bone cells. Clover and Gowen (1994) studied the integrin subunit profiles of MG-63 and HOS cell lines, compared to primary human OB cells. All three types of cells studied expressed α_3 and β_1 subunits in large quantities, with the osteosarcoma cell lines expressing higher levels of α_3 subunit than the normal human bone cells. The expression of other α subunits was dependent on

cell type, where α_4 and α_6 were only detected on the osteosarcoma cell lines. Both these subunits have been associated with highly invasive cells (Dedhar and Saulnier, 1990; Chen *et al.*, 1992), and could therefore reflect the metastatic potential of the osteosarcoma cells.

Vihinen *et al.* (1996) analysed the levels of collagen receptor integrins in eight human osteosarcoma cell lines, which included HOS, SaOS-2 and MG-63 cells. They reported that $\alpha_3\beta_1$ was the abundant receptor in all the cell lines. The α_1 subunit was also constantly seen, except in MG-63 cells. Even though the α_2 subunit is associated with the aggressive nature of osteosarcoma cells, no α_2 was seen in original HOS or SaOS-2 cells, except when they have undergone some transformation, either viral or chemical, or when they have been subcultured several times.

1.6.2.7 OB cell integrins and their ligands

Table 1.2 Summary of some OB cell integrins and their ligands

Integrin	Ligand	Reference
$\alpha_1\beta_1$	Collagens, Laminins	Clover *et al.*, 1992
$\alpha_2\beta_1$	Collagens, Laminins	Grzesik, 1997
$\alpha_3\beta_1$	Collagens, Laminins, Fn (minor)	Grzesik, 1997; Clover *et al.*, 1992
$\alpha_4\beta_1$	Fn	Grzesik and Robey, 1994
$\alpha_5\beta_1$	Fn (major)	Grzesik and Robey, 1994
$\alpha_v\beta_1$	Fn, Vn	Grzesik and Robey, 1994
$\alpha_v\beta_3$	Fn, Vn	Grzesik and Robey, 1994
$\alpha_v\beta_5$	Vn	Saito *et al.*, 1994

1.6.3 Cell attachment to substrates *in vitro*

Cells in culture form specialised types of contacts to substrates: focal adhesions, close contacts, extracellular matrix contacts (Chen and Singer, 1982), and point contacts (Tawil *et al.*, 1993).

Focal adhesions are characterised by a spacing of 10-20 nm between the cell membrane and substrate, and are frequently observed in early cell cultures. Focal

adhesions are considered to represent the strongest cell-substrate interactions in cultured cells, and are most prominent in adherent stationary cells. They can be identified using immunofluorescence, associated with:

a. actin microfilaments (Chen and Singer, 1982; Oakley and Brunette, 1993).
b. vinculin (Oakley and Brunette, 1993; Sinha *et al.,* 1994).
c. tyrosine phosphorylation. The increase in tyrosine phophorylation is specific for integrins since clustering of other cell surface proteins does not cause this effect (Juliano and Haskill, 1993).

Focal adhesions have been shown to appear within 20 minutes of cell-material interactions on favourable surfaces (Oakley and Brunette, 1993). They are initially located at cell peripheries, but at later times were also found within central areas of the cell, always closely related with the termination of actin microfilaments.

Close contacts have 30-50 nm spacing, and often occupy a larger linear dimension in section than the focal adhesions. ECM contacts are generally far removed from the substrate (>100 nm spacing), but are sporadically connected to the substrate by large and cable-like filamentous aggregates of Fn. They arise after 24 h or more of adhesion. Point contacts are closely apposed to the substrate (15 nm spacing), and like focal contacts, are also involved in the early stages of cell attachment and spreading (Tawil *et al.*, 1993). However, unlike the well-characterised focal contacts, where integrin binding to their ligands occurs, localisation of integrins in point contacts are ligand independent and are rarely co-distributed with actin or vinculin.

1.6.3.1 Fn and focal adhesions

Interactions between integrin receptors and Fn in focal adhesions are required for OB cell differentiation *in vitro*, since Fn antagonists added to the cultures of immature foetal calvarial OB cells inhibit their progressive differentiation (Moursi *et al.,* 1996; 1997). In stationary cells, Fn is predominantly organised in focal adhesions. As Fn arrangement in focal adhesions enhances cell attachment and proliferation (Schneider

and Burridge, 1994a), substrates which induce the organisation of Fn in focal adhesions are considered to be biocompatible (Groth and Altankov, 1996).

Schneider and Burridge (1994a) used immunofluorescence to examine the composition and organisation of focal adhesions developed by the OB cell line, MC3T3-E1, on glass and Ti discs under different conditions, i.e. either uncoated, or coated with Fn and serum. The cells were pre-incubated with cycloheximide prior to inoculation on the substrates to inhibit synthesis of endogenous matrix proteins. After 1 h and 4 h incubation periods, cells on uncoated glass and Ti attached, but did not spread. In addition, focal adhesions were not detected. However, when cells were plated on Fn and serum-coated discs, the cells spread well and developed focal adhesions which stained for vinculin, talin and β_1 integrins. Prominent stress fibres were seen to terminate at these focal adhesions. The focal adhesions also stained for phosphotyrosine indicating intracellular signalling associated with adhesion. Cells which were not treated with cycloheximide however, adhered and spread well on uncoated discs, and focal adhesions were detected, as with time, the cells were able to produce their own matrix proteins.

1.6.4 Variables affecting integrin expression of cells grown on substrates *in vitro*

Several studies have investigated the factors which affect integrin expression by cells cultured on different substrates. It was reported that differences were seen depending on the type of cells used, and the substrates on which the cells were grown (Hormia and Könönen, 1994; Sinha *et al.*, 1994; Dean *et al.*, 1995; Gronowicz and McCarthy, 1996; Sinha and Tuan, 1996).

1.6.4.1 Integrin expression is affected by both substrate composition and topography

Sinha and Tuan (1996) cultured primary human OB cells on Ti and cobalt-chromium (Co-Cr) discs, and control tissue culture polystyrene. They used immunohistochemistry to identify the integrins expressed. Significant differences in integrin expression were noted. These were tabulated as follows, where (+) indicates greater than 50% of cells cultured on a particular surface demonstrated positive staining.

Table 1.3 Summary of the integrin subunits expressed by primary human OB cells cultured on substrates of different surface roughness

Substrate	α_2	α_3	α_4	α_5	α_6	α_v	β_1	β_3
Polished Ti	+	+	+		+	+	+	+
Rough Ti	+		+			+	+	+
Polished Co-Cr	+		+			+	+	+
Rough Co-Cr	+		+			+	+	
Polystyrene	+		+		+	+	+	+

The results show that except for α_3 and α_5, all integrin subunits were expressed by cells grown on the control tissue culture polystyrene surface. Regarding the metal substrates, α_3 and α_6 subunits were only noted on cells cultured on polished Ti, while β_3 was detected on all surfaces, except on rough Co-Cr. α_5 was not detected on any of the metal surfaces. This suggests that the Fn receptor was not used by the cells to attach to the metals, and this may indicate that Fn may not be easily adsorbed on these surfaces. The suggestion that Fn was not used for the attachment of OB cells to metallic substrates is in agreement with the results of Schneider and Burridge (1994a), where it was shown that serum Vn was used for the adhesion of OB cells on Ti and glass. Only when plated on Fn coated surfaces, did the OB cells concentrate β_1 integrins within their focal adhesions, indicating the presence of the major Fn receptor, $\alpha_5\beta_1$.

By selective removal of serum Vn and Fn from the culture medium, Steele *et al.* (1992) showed that the initial attachment and spreading of fibroblasts and endothelial cells onto synthetic polymeric surfaces, such as tissue culture polystyrene, were also dependent upon the serum Vn component, and not on the Fn component. In another study, Howlett *et al.* (1994) showed that the attachment of human bone derived cells plated in medium during the first 90 minutes of culture was also primarily a result of adsorption of serum Vn onto the surface of tissue culture polystyrene, cpTi, stainless steel and alumina. Selective removal of Vn from the tissue culture medium resulted in 70% loss of cell adhesion and spreading on these materials, compared to only a reduction of <5% when Fn was depleted from the medium.

Sinha and Tuan (1996) also detected positive staining for α_2, α_4, α_v and β_1 on all the substrates, although previous studies on primary human bone integrin expression quoted earlier had found relatively low amounts of α_2 and no α_4. α_2 is a known collagen receptor, and this suggests that OB cells may bind to collagen through an integrin mediated interaction on the substrate where α_2 was expressed. This is true for all bone cells, since 90% of the protein expressed is collagen. However, α_3 was only seen on polished Ti and not on rough, and also not on Co-Cr regardless of the texture. This may reflect differences in the ECM ligand synthesis or serum protein ligand adsorption due to the different surface roughness, although the chemical composition of the substrates may be the same. Nevertheless, $\alpha_3\beta_1$ is a multifunctional receptor which can bind to Fn, collagen and laminin, and this study suggests that Fn may also be used by the OB cells to attach to polished Ti.

Sinha and Tuan (1996) also observed an association between integrin expression and cell morphology. They noted that OB cells on polished Ti surfaces were larger and more elongated, compared to cells on polished Co-Cr. Both α_3 and α_6 were expressed on polished Ti, but not on polished Co-Cr. They also noted that the cells on rough Ti were more rounded than those on rough Co-Cr. The only difference in integrin expression on these substrates was the absence of β_3 on rough Ti. The authors therefore suggested that α_3, α_6 and β_3 may play significant roles in the cell spreading process, since in an earlier experiment, Sinha *et al.* (1994) found that cytoskeletal organisation and stability were enhanced on Ti, compared to Co-Cr and PS.

The suggestion that cell shape may be related to integrin expression agrees with that of Chen *et al.* (1992), who found that integrin levels were up-regulated in cells which had been kept in suspension for some time (up to 24 h), before being allowed to adhere to substrates. However, if under adherent conditions the cells did not express a particular integrin subunit, then leaving the cells in suspension or in a rounded condition would not lead to induction of that subunit.

In another experiment, Gronowicz and McCarthy (1996) cultured SaOS-2 cells on discs made of 'Tivanium' (a Ti alloy), 'Zimaloy' (a Co-Cr alloy), 'plastic' and glass.

The metals were prepared similarly, i.e. both were sandblasted with 600 grit Al_2O_3, and then blasted with 100 mesh glass beads. The authors used Western blot analysis to identify and compare the integrins detected just prior to inoculation onto the substrates, and then 24 h after plating. The experiments were carried out in serum-free medium (SFM), and in some instances the cells were treated with cycloheximide to prevent synthesis of endogenous proteins. The integrins expressed are shown in Table 1.4. Changes in the integrin expression are indicated by arrows showing the magnitude of reduction or increased expression at the end of 24 h after cell inoculation.

Table 1.4 Summary of the integrin subunits expressed by SaOS-2 cells cultured in SFM on different substrates with similar surface topography

Substrate	α_1	α_2	α_5	α_v	β_1	β_5
Tivanium	↓		2.7×↑	1.7×↑	4.9×↑	↓
Zimaloy	↓		1.8×↑	1.7×↑	3.8×↑	↓
Plastic	2.5×↑	↑	2×↑	1.9×↑	9.5×↑	small ↑
Glass	↓		small ↑		6.4×↑	↓

The main finding in this study was that cells attached to the metals even when protein synthesis was inhibited. The authors concluded that protein synthesis was not needed for cell attachment, and that there was direct integrin binding to the metals, since RGD peptides in the medium inhibited cell attachment to Tivanium and Zimaloy by 28% and 40%, respectively. However, the mechanisms by which integrins may bind directly to the metals are unknown. When cells were pre-treated with polyclonal antibodies to Fn prior to inoculation on the discs, binding to Tivanium and Zimaloy was inhibited by 63% and 49%, respectively. However, when cells were pre-treated with antibody to the Vn receptor, no significant effect on cell adhesion to the metals was noted. Integrin expression after 24 h of attachment showed a great increase in the Fn receptor ($\alpha_5\beta_1$) but not in the Vn receptor ($\alpha_v\beta_3$ or $\alpha_v\beta_5$). This confirms the attachment inhibition results, which show that the majority of the OB cells in this study attached to metals via the Fn receptor, and not via the Vn receptor.

Hormia and Könönen (1994) showed that human gingival fibroblasts grown for

4 h on glass, smooth Ti or etched Ti surfaces expressed localised $\alpha_v\beta_3$ focal contacts, but only a diffuse $\alpha_v\beta_1$ distribution. Cells grown on rough sandblasted Ti expressed a diffuse distribution of both $\alpha_v\beta_3$ and $\alpha_v\beta_1$. Vinculin-containing focal contacts were seen in cells grown on glass and the smoother Ti, but not on the cells grown on sandblasted Ti surfaces. This finding suggests that fibroblasts bind to Vn through local focal contacts on smooth Ti, and bind to Fn through a diffused ECM contact association (Chen and Singer, 1982). However, as the study was carried out in complete medium, it is not certain if the attachment proteins were incorporated from the serum in the culture medium, or were cell derived, or both, as Fn and Vn are present in serum, and both promote cell adhesion (Fath *et al.*, 1989).

The results of the above studies indicate that different cultured cells use different integrins to attach to different substrates, and that the profile of integrin expression may be altered by both substrate composition and topography.

1.6.4.2 Different cell types exhibit different preferences for the same ECM molecules

Dean *et al.* (1995) used gingival cells (fibroblasts and epithelial cells) to determine if laminin and Fn could influence cell attachment to implant surfaces *in vitro*. They showed that coating of implant surfaces with Fn resulted in two to three times enhancement of gingival fibroblast binding on all the implant surfaces tested, with a lesser effect on epithelial cells. On the other hand, coating of the implant surfaces with laminin resulted in three to four times enhancement of gingival epithelial cell binding on all implant surfaces, with a lesser effect on the fibroblasts. The surface roughness of the substrates on which the proteins were laid down had little influence on the results.

1.6.4.3 Patterns of focal contact localisation differ with substrate material

By vinculin immunostaining, Sinha *et al.* (1994) showed that focal contact localisation was different on various substrates as a function of time, even though the number of cells forming focal contacts on the substrates was the same. On plastic surfaces, focal contacts were initially formed at the cell periphery but became completely redistributed throughout the cell by 12 h. However, on Ti and Co-Cr

substrates, redistribution of focal contacts was delayed until 24 h. The authors suggested that peripheral contact formation may be adequate to anchor the cells to metal substrates, while attachment to plastic required many focal contacts throughout the cell surface. These results suggest that cell adherence was stronger and more stable on metals than on plastic surfaces, and that stable adhesion occurs if enough bonds/attachment sites are formed.

1.7 Statement of problem

Therapy with osseointegrated implants is now an acceptable form of dental treatment and their use is widespread. The success of the technique is attributed to a strict observance of factors related to the selected biomaterial and host, and operative and clinical procedures (Albrektsson and Zarb, 1993). While the use of this form of treatment in ideal circumstances is well established, its success is poor in circumstances, with regards to host and clinical factors, which are not ideal. Yet patients with these characteristics are often those who could benefit most from successful treatment with implants (Ihara *et al.*, 1998).

Extending the potential of implant therapy so as to provide high and predictable success rates in areas where bone is lacking or of poor quality is the next challenge in implant dentistry. Bone grafting is an option in areas where there is insufficient bone to allow for implant anchorage, and the autogenous bone graft is recognised as the ideal bone substitute in implant indications (Gunne *et al.*, 1995; Widmark *et al.*, 1998). However, there are complications associated with harvesting autogenous bone grafts, including pain, scarring at the donor site, possible infection, and insufficient donor bone volume. In addition the overall implant procedure is less predictable and successful than in more conventional situations. Several other techniques and materials are currently available for bone grafting, however, they are also not without limitations and disadvantages (Tolman, 1995), and other clinical options have to be considered.

A review of the literature suggests that bone formation at the bone-implant interface may be enhanced or accelerated by one of two ways:

i. modifying the surface morphology and therefore the implant surface properties so that it is more favourable to bone cell adhesion and bone formation (Buser *et al.,* 1991; Bowers *et al.*, 1992; Gomi and Davies, 1993; Hayashi *et al.*, 1994; Martin *et al.*, 1995; Wong *et al.,* 1995; Boyan *et al.*, 1996; Kieswetter *et al.*, 1996b; Wennerberg *et al.*, 1996; Johansson *et al.*, 1998), or

ii. using external adjuncts/supplements, such as growth hormones and synthetic peptides to enhance the capacity of bone cells toward bone formation. The implant itself then either becomes an inert participant, or due to the presence of the surface adjuncts, is made attractive to and therefore interacts favourably with macromolecules which are responsible for events that determine wound healing and new bone formation (Boyan *et al.*, 1996; Dee *et al.*, 1996; Batzer *et al.*, 1998; Cooper, 1998; Dee *et al.*, 1998).

Application of synthetic adjuncts to implant surfaces requires research into methods of administration and other host related factors. It is also unknown how much more beneficial the effects of these adjuncts are to bone formation and maintenance in the long term, as the ultimate goal in implant therapy is the achievement and maintenance of bone around the implants. It is therefore necessary to understand and define the sequence of cellular events which occurs in osseointegration. If bone cell responses towards well-characterised implant surfaces are known, predictable and beneficial, then it may be more convenient to modify implant surface characteristics to elicit the desired cellular responses.

It has been shown that the majority of the initial attachment of bone cells to implant materials occur via integrins, which are not only attachment molecules but are also involved in signalling events after cell attachment. The attachment to implant materials, and the nature of the contact sites formed between cells and implant surfaces therefore influence subsequent tissue reactions to these surfaces. Since these responses may eventually affect the fate of intra-bony implants, it is important to understand the nature of the integrin expression and focal contact formation by osteoblasts interacting with different biomaterial surfaces.

The aim of this project was therefore to develop an understanding of the basic cellular reactions to implant surfaces with different surface properties, and to test the hypothesis that these properties influence the pattern of cellular behaviour during the period immediately following initial cell-substrate contact. The hypothesis was to be tested using a cell culture model so that the initial reaction of individual OB cells to the substrate surface could be examined.

Titanium is currently the "gold standard" implant material and zirconium has been shown to have potential for this role. They were therefore chosen as the substrates in this study. In order that differences in cellular reactions could be examined, two different surface features were chosen.

The main objectives of the study were:

1. To undertake a systematic evaluation of surface roughness variables on Ti and Zr discs used *in vitro*.
2. To study the effects of the substrate composition and surface roughness on the attachment and differentiation of OB cells *in vitro*.
3. To study the integrin expression and cytoskeletal development in early cell-substrate interactions, and to see if any difference in the integrin expression and pattern of distribution in the OB cells could be related to the different substrates on which the cells were grown.

In order to achieve the stated objectives, the study was carried out in three parts. In the first part of the study (Chapter 2), substrate preparation and analysis were carried out in order to characterise the surfaces used for the cell culture studies. A systematic evaluation of surface roughness was carried out using qualitative and quantitative techniques. Two types of profilometer systems commonly used to quantity surface roughness was evaluated to test whether surface roughness values obtained using the two different methods, are comparable.

The second part of the study (Chapter 3) involved growing OB cells on the characterised substrates to test if substrate composition and topography had any effect

on cell attachment and differentiation. As integrins have been shown to convey information about substrate topography to the cells, immunofluorescence study of the integrins which are ubiquitously expressed by OB cells was carried out (Chapter 4). This part of the study also involved staining the actin cytoskeleton, to see if the substrate topographies chosen in this study had any effect on cell spreading. The findings of the three parts of the study were then brought together in Chapter 5, where they were discussed and general conclusions made.

2. Preparation and Analysis of Substrate Surface Roughness

2.1 Introduction

The use of titanium (Ti) as a successful implant material with good clinical results is proven. Zirconium (Zr) has the potential to be as successful as Ti, as it also possesses the mechanical and corrosion resistance properties that make these metals ideal for application in the biological environment (Williams, 1981). The excellent corrosion resistance is due to their stable dioxide layer - titanium dioxide (TiO_2) and zirconium dioxide (ZrO_2). Although all of the reasons for the biocompatibility of Ti with bone are still not fully known, the oxide layer is considered as one of the major determinants (Kasemo and Lausmaa, 1988; Stanford and Keller, 1991). The mere presence of this layer has been shown to be sufficient for beneficial bone apposition, without any significant difference in the bone morphology and contact around implants (Larsson *et al.*, 1994).

Besides mechanical and chemical properties, physical properties like surface topography also influence the biological responses to the implant (Kasemo and Lausmaa, 1990). Varying levels of bone cell attachment, proliferation and differentiation have been related to the degree of implant surface roughness (Bowers *et al.*, 1992; Swart *et al.*, 1992; Hunter *et al.*, 1995; Martin *et al.*, 1996), and characterisation of the surface topography (both qualitatively and quantitatively) is therefore a critical procedure in the study of osseointegration and implant-tissue interactions.

2.1.1 Techniques for quantifying surface roughness

Many techniques for quantifying surface roughness exist, and these have been extensively reviewed by Wennerberg (1996). These techniques trace the surfaces of test materials by one of two ways: contact and non-contact methods, and embody both

collection of data on surface contour, and its presentation in a variety of ways thought to best indicate a particular characteristic.

The standard technique used for surface topography measurements is a direct method using stylus type devices (Stout, 1981). This makes use of the movement of a small diamond stylus as it traverses a path across the surface being measured at a constant velocity for a pre-determined length, recording the peaks and grooves which characterise the surface. A load is applied to the stylus so that it is always in contact with the surface. The vertical movements of the stylus are converted into an electrical signal by a transducer. After the necessary conversions this is amplified before being displayed as a profile line on a chart record. A variety of roughness parameters may then be computed from these profiles. These profiles are magnified to different extents in the horizontal and vertical axes, and therefore may not be similar to the original profile of the material (Stout, 1981). The apparent vertical extent of the surface irregularities is nearly always greater than their horizontal dimensions.

This technique of quantifying surfaces has its limitations. The stylus readings are influenced by the radius of the stylus tip, the pressure of the stylus tip on the surface, and the hardness of the material being examined. As a result, there is the potential to scratch soft surfaces. For reasons of strength, the shape of the stylus tip is either pyramidal or conical, and there is therefore, the possibility that the full depth of narrow and deep grooves is not recorded. This technique also suffers from a limitation common to all conventional linear tracing devices, i.e. they produce only 2-dimensional (2-D) surface profiles along a certain line or plane, and therefore the area examined is small. Surfaces are rarely uniform, and roughness may vary at different sites. Measurements made at different planes may therefore yield different results. Variations in measurements can reach up to 50% or more, even in machined surfaces (Thomas and Charlton, 1981). A technique which can analyse surface texture across a bigger surface area would therefore be more useful and relevant.

The non-contact methods include atomic force microscopes, scanning tunnelling microscopes, and optical devices (Wennerberg, 1996). The optical methods make use of

a laser beam or white light for illuminating the surface to be studied, and the surface characteristics are measured using a variety of optical principles based on interferometry, focus error detection, or confocal microscopy techniques (Stout *et al.*, 1993). Due to the superior location accuracy possible with an optical scanning profilometer, it is possible to make repeated parallel scans at known intervals, thus providing the potential for 3-D determination of surface characteristics. These methods make non-destructive measurements, and can detect small structures that could be filtered out with a mechanical stylus tip. Partly for this reason, when compared, there is a tendency for underestimation of the surface features with the contact stylus measurement and an overestimation with the optical scanning profilometers (Mattsson and Wågberg, 1993; Whitehead *et al.*, 1995; Wennerberg, 1996).

2.1.2 Definitions of surface topography and some surface roughness parameters

Topography refers to the external characteristics of a surface (Stout *et al.*, 1993). It is made up of features defined as roughness, waviness and form. However, it is only the roughness component which is analysed, as waviness and form are usually filtered or separated out from the recorded measurement data. Various parameters are used to quantify surface roughness (Stout, 1981). They characterise three basic aspects of the surface topography, i.e. height, spacing, and spatial or textural characteristics.

Height parameters measure the vertical variations (depths of grooves and pits), and they can be divided into two categories: a) height descriptions of a statistical nature which gives average values, i.e. parameters like R_a, R_q, and R_z, and b) extreme value height descriptors, like R_{max}, which depend on isolated occurrences. The spacing parameters measure the mean distance between surface peaks, and the parameters S and S_m are used to characterise the profile in a horizontal plane. Spatial parameters, like skewness and kurtosis indices, and the autocorrelation function, describe the variations of the surface based on multiple events (Stout, 1981). The use of vertical and horizontal parameters in combination may give an estimation of the surface shape of the materials studied. The fundamental surface roughness parameters are described by the following illustrations, reproduced from BS 6741, 1987 (Figures 2.1 to 2.5).

Roughness average (R_a) represents the average deviation of a surface profile from the mean reference line (m), within the sampling length, l (Figure 2.1). The mean line is defined so that equal areas of the profile lie above and below it.

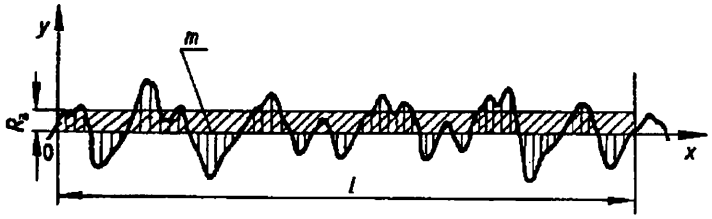

$$Ra = \frac{1}{l}\int_0^l |y(x)|\,dx$$

Figure 2.1 Graphic representation of R_a

R_q or root-mean-square roughness (RMS) is often used as an alternative to R_a. It gives larger numerical values than the equivalent R_a values, and is defined mathematically as:

$$Rq = \sqrt{\frac{1}{l}\int_0^l y^2(x)\,dx}$$

Due to the squaring procedure, it is more sensitive to extreme data values than R_a.

R_{max} is the true distance from the maximum peak height to the maximum valley depth throughout the whole sampling length. It may be of limited significance if used solely on its own, as the value may be affected by a scratch on the surface.

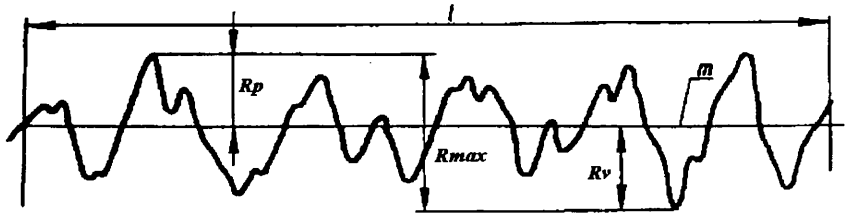

$Rmax = Rp + Rv$

Figure 2.2 Graphic representation of R_{max}.

R_z is defined as the mean of the maximum peak to valley height of five equal consecutive lengths, within the sampling length. As such it is less affected by extremes of the profile than R_{max}.

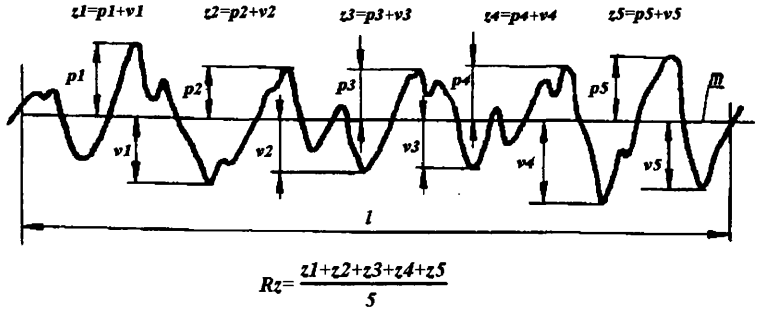

$$Rz = \frac{z1+z2+z3+z4+z5}{5}$$

Figure 2.3 Graphic representation of R_z.

S is the mean distance between the local peaks of the profile. By definition, a significant peak must have a valley between two peaks, and the lowest depth of the valley must be lower than the reference mean line of the surface. A peak that does not meet this criterion is called a local peak. To be counted in the scan, the height of the local peak, when measured from the nearest adjacent valley, must not be less than 10% of the value of the highest peak from the mean line (Stout, 1981).

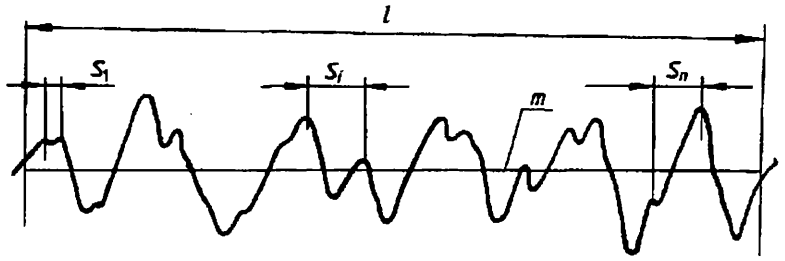

$$S = \frac{S_1 + S_2 + S_3 + \ldots + S_n}{n}$$

where n= number of local peaks of the profile over the sampling length

Figure 2.4 Graphic representation of S.

S_m is the mean distance between the true peaks counted in the scan.

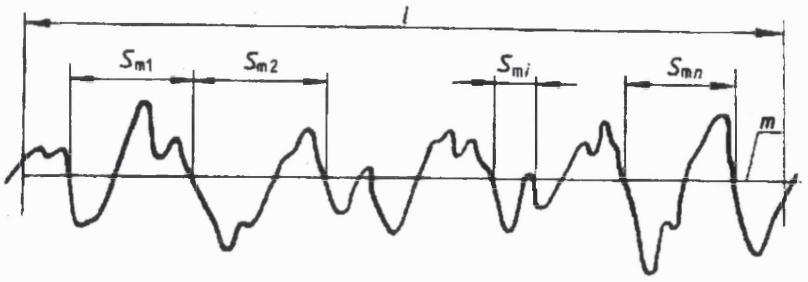

$$S_m = \frac{S_m1 + S_m2 + S_m3 + \ldots + S_mn}{n}$$

where n= number of spacings of the profile irregularities over the sampling length

Figure 2.5 Graphic representation of S_m.

The aim of this part of the investigation was to present a systematic approach to characterising surfaces to be used in the following cell culture studies. This was done using a laser scanning profilometer which provided the maximum potential range of data. Measurements were also made with the commonly used contact profilometer, to provide a comparison between the two techniques in their application, and with previous work in this field. The numerical values obtained for each surface roughness parameter analysed would be discussed in relation to the limitations of each technique used.

2.2 Materials and Methods

2.2.1 Surfaces analysed

The surfaces analysed were commercially pure Grade I titanium discs (cpTi), > 99.9% purity, and commercially pure zirconium discs (cpZr), > 99.8% purity. The discs were 15 mm in diameter and 1 mm thick, and were provided by Goodfellow Cambridge Ltd. (Cambridge Science Park, Cambridge, England).

2.2.1.1 Surface preparation and treatment

As received, the cpTi and cpZr discs had different surface finishes. The surface of the Ti was a normal rolled surface and was not blasted, although it had a blasted appearance. The Zr had been machined in a unilateral direction. Five trial surfaces were initially prepared for a pilot study to assess the baseline roughness values needed to compare the surfaces. The surfaces chosen were as follows:

1. Ti as received
2. Zr as received
3. Ti polished unidirectionally and serially using silicon carbide papers by hand until 1200 grit (approximate grain size of the final polishing particle was 15 μm)
4. Zr treated as Ti polished in (3) above, and
5. Zr blasted with 50 μm aluminium oxide (Al_2O_3) particles.

These surfaces were chosen for the following reasons: CpTi and cpZr discs were polished using the same grit of silicon carbide paper to provide surfaces with similar surface roughness, but with different surface chemistry. The "as received" Ti discs provided the rough surface required for the study.

Rougher surfaces were not used for two main reasons: a) Immunofluorescence microscopy was one of the techniques which would be used to assess the behaviour of bone cells grown on these surfaces, and it was anticipated that it would be difficult to view a very rough surface under a normal fluorescence microscope, and b) Ideally, in order to create a blasted surface without the surface contamination that would occur

with the commonly used Al_2O_3 particles, the Ti surface should be blasted with Ti oxide particles. However, the only available TiO_2 particles at the start of the study were less than 40 μm, and this would create a smoother surface than the cpTi as received. Therefore, no other rough surface was created for the Ti discs.

The Zr "as received" was machined smooth, but not polished. It was also initially proposed to blast some of the Zr discs with ZrO_2 particles to create rougher surfaces without any directional prominence to match that of the Ti as received. However, obtaining ZrO_2 particles to blast the discs proved difficult as well. The maximum particle size of ZrO_2 powder available was only 20 μm. This particle size was not markedly different from the silicon carbide particles (15 μm) that were used to create the smooth surfaces, and therefore would probably result in as smooth a surface as that of the polished Zr. Polishing Zr surfaces with rougher silicon carbide papers would only create deeper grooves, but with a similar appearance to the Zr surfaces which were polished with the finer 1200 grit papers. Even though the problem of surface contamination was mentioned, the 50 μm Al_2O_3 particles were eventually used to determine if a rough surface equivalent to that of the Ti "as received" could be created for the Zr surfaces.

After surface preparation, the discs were treated as follows: ultrasonically cleaned in a detergent (non-ammoniated General Purpose Cleaner Concentrate, L&R Manufacturing Co., Kearny, New Jersey, U.S.A.) for 30 minutes, degreasing with acetone (15 minutes), cleaning with 70% ethanol (15 minutes), and then passivating by immersing and agitating in 35% nitric acid for 30 minutes at room temperature. Acid passivation treatment was used to standardise the surface oxide thickness and composition (ASTM F86-91; Callen *et al.*, 1995). The discs were finally rinsed ultrasonically in distilled water (three 20-minute rinses). Cleaned discs were kept in 70% alcohol for storage before surface analysis was carried out.

2.2.2 Methods used to quantify surface roughness

Surface roughness was quantified using two techniques:

a. a 2-D contact stylus profilometer (Surftest 4, Mitutoyo Manufacturing Co. Ltd., Tokyo, Japan), and
b. a laser scanning profilometer, Proscan 1000 (Scantron Industrial Products Ltd., Taunton, England, U.K.).

2.2.2.1 Direction of measurements made

Before making any measurements, it was necessary to consider if the surface irregularities had any prominent lay pattern (anisotropic surfaces) or possess no dominating lay (isotropic surfaces). A surface lay is defined as the direction of the prevailing texture of the surface (BS 6741, 1987). Surfaces with highly noticeable directional properties give different roughness values, when measured along and across the lay (Stout *et al.*, 1993). Anisotropic surfaces should be measured perpendicular to the lay direction, where the contour of the irregularities is most pronounced (Wennerberg, 1996). In this study, Ti discs as received were not analysed in any particular direction because the surface is isotropic. This was verified by magnified images of the surface, which were projected onto a television (TV) monitor when measurements were made using the Proscan 1000 (see section 2.2.2.3.3). On the other hand, polished Ti and Zr discs showed the unilateral direction in which they had been ground, and therefore the surfaces were analysed in the direction perpendicular to that of the polishing procedure.

2.2.2.2 Measurement using the Surftest 4 contact profilometer

2.2.2.2.1 Basis of measurement using the Surftest 4

The Surftest 4 uses a conical diamond stylus with a tip radius of 5 μm to traverse across a surface, with a constant speed of 0.5 mm/s and a maximum downward force of 4 mN. As a surface is being measured, the stylus is displaced vertically by the surface irregularities. These displacements are converted into electric signals by the central processing unit of the apparatus, which, after the necessary conversions, are translated

into the selected parameters and displayed as a digital readout. The output can also be recorded as profile curves by the built-in plotter.

The Surftest 4 provides roughness measurements in four parameters: R_a, RMS, R_z and R_{max}. To minimise any effect of curvature or shape of the surfaces, a surface filter with a cut-off value of 0.8 mm was used. This is the standard cut-off used for R_a values over 0.1 μm and up to and including 2.0 μm, and for R_z values over 0.5 μm and up to and including 10 μm (BS 1134, 1990). The cut-off is equivalent to the sampling length (BS 6741, 1987), and this cut-off has a traversing or evaluation length of 4.8 mm, which includes five consecutive cut-offs as a standard. When a measurement is completed, the roughness values are stored in the system's memory. The parameter switch is then used to select the roughness value to be displayed. Values for all roughness parameters can be displayed sequentially as desired by resetting the parameter switch.

The system was calibrated before use to adjust the overall amplification. This was done by adjusting the gain of the electronic unit until the display showed an R_a value of 3.0 μm when a precision reference specimen was measured.

2.2.2.3 Measurement using the laser scanning profilometer (Proscan 1000)

2.2.2.3.1 Basis of measurement using the Proscan 1000

The Proscan 1000 is a PC controlled non-contact 3-D surface profiling and measuring system which employs a highly accurate laser displacement sensor to scan surfaces of objects held on a motorised x/y table. The laser beam used is a semiconductor laser with a wavelength of 780 nm. Objects are scanned as they are moved in the x and y directions under the fixed laser beam.

The system uses the laser triangulation principle to measure extremely fine vertical displacements on the contour of surfaces (Stout *et al.*, 1993). The laser spot is focused on the object to be measured, and the light from the laser is then reflected or scattered back into a fixed photo detector which receives a maximum signal when the

surface is at its focal point. When the object is moved, the height variations encountered along the surface are expressed as displacements of the spot on the photo detector since the start of the scan. The position of the spot on the detector is converted into an electric signal which is proportional to the height of each point on the scanned profile. By combining the three co-ordinates obtained from the height measured by the laser with the position of the sample in the x and y axes, a digitised colour coded 3-D image of the surface profile is produced. Dimensional measurements can then be easily made from these images using the software provided with the system. Hard copies are available through the IBM compatible personal computer with printer options, which is supplied with the unit.

2.2.2.3.2 The sensors

The resolution of the instrument depends on the sensor used. A sensor (KL131A) with a working distance of 10 mm, a measuring range of 400 ± 200 μm, a laser beam diameter of 12-35 μm, and a resolution of 0.02 μm was used in this study. The diameter of the laser beam is smallest when it is focused at the centre of the measuring range.

2.2.2.3.3 Measurement method using the Proscan 1000

Sensor KL131A was attached to the instrument and the flat metal disc to be analysed was positioned directly on the x/y table and stuck down using double sided tape. To ensure that the sample was in the correct measuring range of the sensor being used, the height of the laser beam from the specimen was adjusted by entering the READ menu in the controlling software. The separation of the sensor from the specimen was then adjusted by moving the sensor arm vertically until the value of the height reading displayed lies half-way between the FAR and NEAR warnings on the HEIGHT field. This was found to be approximately 200 μm. The sensor arm was then locked in that position.

The laser beam emitted from the sensor is detected after reflectance from surfaces being measured. The amount of light which is dispersed back to the detector depends on the reflectivity of the surfaces. To compensate for any variation a 'GAIN'

setting is used. Increasing the gain increases the sensitivity of the sensor to the returning laser light and also increases the power output of the laser. The gain is set in relation to the 'INTENSITY' reading given by the sensor for the specimen. This relates to the amount of laser light returning from the specimen. As the intensity varies across the surface of most specimens, a gain setting was chosen which was appropriate for the range of intensity values encountered. A high gain setting is used for dark surfaces which are not very reflective. For shiny reflective surfaces the intensity reading will approach 0 dB. The system automatically warns of any out of range reflectance since it would not be able to resolve the surface. These warnings appear automatically in the HEIGHT field. For this study, 'GAIN' was set at 0 dB.

During the measuring process, a camera was used to project magnified images of the laser beam and the disc being measured on to a TV monitor. The images were magnified 150 times, and this facilitated choosing areas and determining the direction of measurements to be made for anisotropic surfaces. The camera and TV monitor were however, options and not supplied as standard with the instrument.

The sensors provided with the Proscan 1000 have the facility to automatically take a series of measurements at any given point and record its average value as the result, thereby increasing the effective repeatability of the measurements. The averaging procedure is based on 2^n readings, where n = (0-15). The higher average values slow down the scan considerably. For this study, the average was set at 4 (2^2). This was decided upon after initial measurements made on the same area of one disc had shown that there was no difference in the roughness values obtained when the average was set at 4, 8, or 32 (data not shown).

2.2.2.3.4 Scanning an object

Once the 'HEIGHT', 'GAIN' and 'AVERAGE' settings were determined, the SCAN menu was selected and three further variables set. The 'START' position is the position of the laser beam on the object where measurements are to start. This may be set either manually, by moving the stage via the 'READ' menu, or by keying in the position of the x and y axes of the specimens on the measurement table in the 'START'

display. To reduce edge effects, random points close to the centre of the disc being measured were chosen as the 'START' positions for all scans.

The 'STEP SIZE' (or scanning interval) represents the actual distance the stage will move between taking measurements and was set for both the x and y axes. Each step represents a point of measurement which is made by the laser. The maximum step size allowed varies between the sensors. The minimum step size (for both the x and y axes) for KL131A is 1 μm, although there is an option for 0.1 μm with a different sensor. The maximum step size is 9.999 mm. The 'NUMBER OF STEPS' (or number of sampling points) is the total number of measurements taken in a single sampling line along each axis, and can be set to a maximum of 400 for this particular sensor. The total distance measured in both the x and y axes (i.e. the area scanned) is thus the 'STEP SIZE' multiplied by the 'NUMBER OF STEPS'. A small 'STEP SIZE' and a considerably large 'NUMBER OF STEPS' increase the degree of accuracy of the measurements made. However, high settings greatly reduce the speed of the scan.

Once these settings are determined, the system is ready to start scanning. Two types of scans are available. With 'FAST SCANNING', the machine takes measurements without stopping the stage. The scanning procedure is rapid, but the step size cannot be set below 5 μm. For smaller step sizes, 'NORMAL SCANNING' mode must be used, when the stage stops before taking each measurement. This is extremely slow. Depending on the step size and number of steps chosen, normal scanning can take more than two hours for a scan, compared to 7 to 8 minutes for fast scanning of the same area. For this study, 'FAST SCANNING' mode was used.

When a scan is completed, images of the scanned area are displayed in 3-D, plan and 2-D cross sections in four different display windows of the PC monitor (Figure 2.6). The 'AUTOLEVELLING' tool was then selected. This allows the software to find the best fit of the image to the arithmetic plane for analysis, and therefore the object for scanning does not require a high level of precise location on the x/y table. The scanning, levelling and analysis of measurements are fully automated, and values for the different surface roughness parameters are automatically calculated on selection from a

"UTILITIES" menu. As the discs were flat, no surface filter was used. The filter can be set at any value between 1 (the smallest) and 99 (the largest). This value determines the number of points on each side of an assigned centre scan point within a rectangle made up of 9 scan points, that the machine will take measurements from. The average of these values will be the final R_a of the centre scan point (Proscan 1000, User Manual).

The surface profile data calculated by the Proscan 1000 as the heights of scans (z-axis values) can be retrieved as ASCII files. These were subsequently imported into a spreadsheet software, Microsoft Excel for Windows 95, Version 7.0a (Microsoft Corporation) for graphical representation of the heights of the scans in 2-D, to complement the system's 2-D display.

The parameters chosen to characterise the surfaces using the Proscan 1000 were R_a, R_q, R_z, R_{max}, S, S_m and the real surface area (RSA) scanned. The RSA obtained from the scans enabled the percentage increase in surface area of rough surfaces to be determined, as the apparent surface area (APA) of the measured square can be calculated. This percentage increase in surface area made it possible to calculate a projected value for the real surface area of the whole disc being measured.

2.2.3 Pilot study

2.2.3.1 Obtaining baseline roughness values for the cpTi and cpZr surfaces

The five surfaces described in 2.2.1.1 were analysed using the Proscan 1000 to provide the baseline data for the roughness values of these different surfaces. At this stage of the study, an arbitrarily chosen area of 2.25 mm^2 (made up of 150 sampling points at 10 μm scanning intervals in both vertical and horizontal axes), was measured for each of these surfaces. Five discs were chosen at random per surface type, and three random areas on each of the chosen disc were scanned. This gave a total of 15 Proscan images per surface type, and from these images, the roughness values (mean and standard deviation) of a particular surface were obtained. The roughness parameters were measured in both the x and y axes, however, at this stage only the maximum values obtained from either axis were used. This gave a total of 15 values per roughness parameter for each surface type measured.

2.2.3.2 Determination of appropriate scanning variables for the Proscan 1000

Table 2.1 shows the roughness values for the surfaces measured in the pilot study. From these five surfaces, only Ti as received, polished Ti, and polished Zr were used for further analysis. To determine the appropriate scanning variables to be used for analysing the final substrates chosen for the following cell culture studies, the effects of using different scanning intervals and different number of sampling points for measuring the same area were also assessed. The scanning intervals used ranged from 1 μm, with 400 sampling points (the minimum step size and maximum number of steps available with the specific sensor used), to various combinations of different scanning intervals and number of sampling points to measure a scan distance of 1.5 mm in both the x and y axes. For all surfaces, measurements were made of the same area so that results were comparable.

From the results obtained (Figures 2.8-2.10), a decision was made to use a 5 μm scanning interval with 300 sampling points to measure the three final test surfaces. For each surface, five discs were randomly chosen to be measured, and for each disc, three areas were scanned. This gave a total of 15 Proscan 1000 images per surface type. From each Proscan image obtained, measurements were made at areas chosen by moving the x and y axis cursors to positions 0.3, 0.75 and 1.2 mm along each axis (see Figure 2.6). This meant that from each Proscan 1000 image, 6 values per roughness parameter were obtained. Therefore, the total number of values obtained per roughness parameter, for each substrate type, was 90 (i.e. 15×6 values, made up of 45 values in each x and y axis). This made it possible to calculate statistically if the mean roughness values of a particular parameter differ significantly between the two axes.

2.2.4 Scanning electron microscopy (SEM)

One arbitrarily chosen sample was selected from each group of the final test surfaces for qualitative examination with the SEM. Cleaned discs were mounted onto SEM aluminium stubs with carbon conducting cement before examination in a Cambridge 90B scanning electron microscope (Cambridge, U.K.) at 20 kV. The discs were examined at low and high power, and were photographed at these magnifications. Samples of Ti discs were also analysed by energy dispersive X-Ray analysis (EDAX) to check that the cleaning procedures had produced surfaces which were not contaminated (data not shown).

2.2.5 Confocal laser scanning microscopy

Ti as received and polished Ti were also examined by a confocal laser scanning microscope, Lasertec Reflection Confocal Microscope 1LM21 (Lasertec Corp., Wendell Road, London). Confocal microscopy is based on the principle of elimination of scattered or reflected light from planes which are out of focus, and only forms an image from a plane which is in focus. The final image is then built up by combining the in focus images, producing an optical tomogram of the sample. A significant advantage of the confocal microscope is its depth discrimination properties which enabled contours of the surface to be mapped, and these height gradations quantified. Specimens were examined with a 40× lens with a field width of 290 μm. Two kinds of images were made: "MAX" images and the "Z contrast" images (Figure 2.23). The "MAX" image is the in-focus image recorded while the microscope stage, driven by precision stepper motors, covers the sample through 256 steps with a height range of 6.85 μm for the polished samples, and 16.93 μm for the rough 'as received' discs. These ranges of movements are needed to cover the full range of focus of the samples studied. The "Z contrast" images show depth discrimination within a range of eight bands of grey scale, or they may be colour coded to represent the different depth ranges.

2.2.6 Statistical methods

Roughness values obtained were stored in a statistical package software, SPSS 7.5 for Windows (SPSS Inc., Chicago, U.S.A.). They were subjected to a normality test (the Kolmogorov-Smirnov statistic with a Lilliefors significance) and found to have a normal distribution. The mean values for all roughness parameters for each surface, made using the Proscan 1000 and Surftest 4, were obtained by dividing all the roughness values by the number of measurements made. Roughness values were tested by a one-way analysis of variance (ANOVA), and an unpaired Student's *t*-test was used to determine whether statistically significant differences existed in the mean roughness values between two substrates. Differences were considered significant at $P < 0.05$.

2.3 Results

The results are presented as a series of surface profiles obtained from the laser profilometer, Microsoft EXCEL graphs, figures and tables quantifying the surface roughness parameters, and SEM and confocal microscopy micrographs of the test surfaces used in the following cell culture studies.

2.3.1 Laser scanning profilometry images

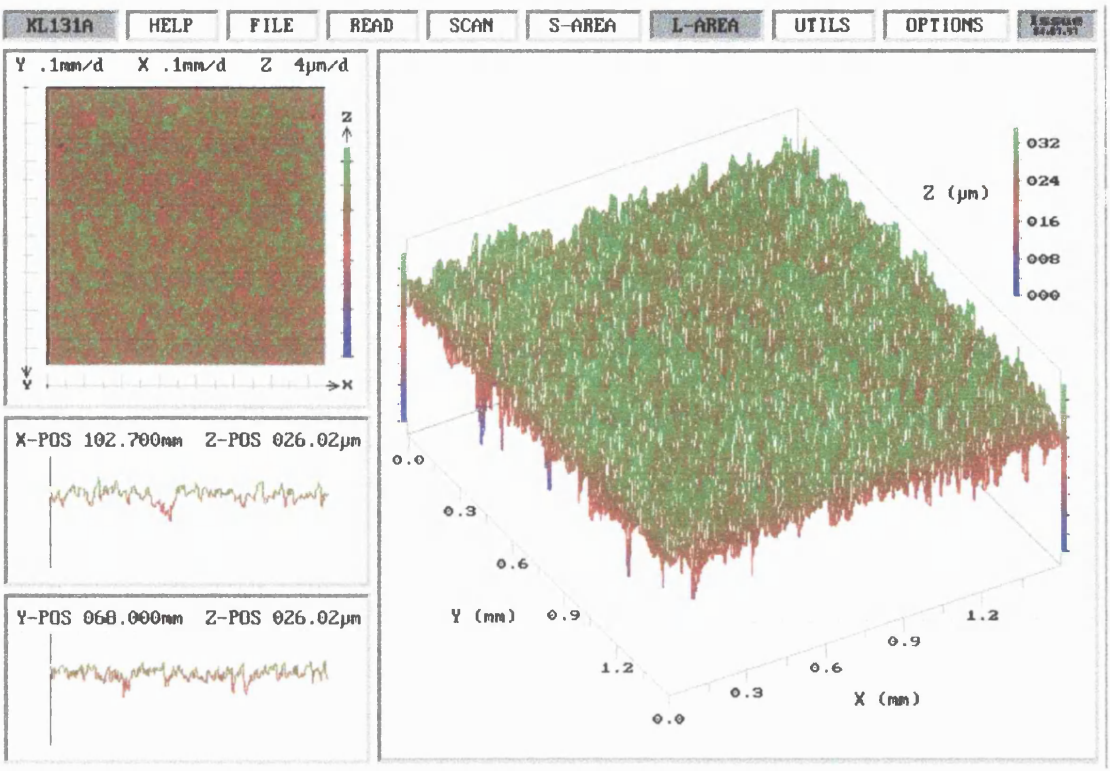

Figure 2.6 Information displayed by the Proscan 1000.

The Proscan 1000 displays information in four different windows (Figure 2.6). The largest window is a detailed scan in 3-D showing the x, y and z axes dimensions together with a coloured scale in the vertical axis. When a scan is completed, the vertical scale which represents the height dimensions of the scanned component, is automatically maximised by the system. However, there is an option to adjust the scaling after scanning so that different images scanned are proportional when comparing scans. The top left hand window is a plan view of the area scanned, with scales for x, y and z axes given at the top of the plan view. The height (z-axis) is shown in varying colour bands from blue (low values) to green (high values). The bottom two windows on the left show the cross section profile in 2-D for both the x and y axes. These two images are relative to the position of the cursor lines selected by the operator. Surface roughness values which were selected by entering the "UTILITIES" menu are displayed in these two windows (see section 2.2.2.3.4).

2.3.2 Roughness values for the surfaces used in the pilot study

Table 2.1 and Figure 2.7 show the mean roughness values for the surfaces used in the pilot study, obtained using the Proscan 1000.

Table 2.1 Roughness values for the surfaces used in the pilot study. Values are mean ± s.d. in μm. Measurements were made using 10 μm scanning intervals with 150 sampling points in both the x and y axes. Area measured = 2.25 mm^2. Number of roughness values per substrate = 15

Parameter	Ti as received	Polished Ti	Zr as received	Polished Zr	Zr blasted with Al_2O_3
R_a	1.84 ± 0.17	0.76 ± 0.06	0.90 ± 0.10	0.81 ± 0.05	1.23 ± 0.11
R_q	2.31 ± 0.21	0.95 ± 0.08	1.14 ± 0.13	1.01 ± 0.06	1.55 ± 0.15
R_z	9.08 ± 1.15	3.81 ± 0.45	4.58 ± 0.59	4.06 ± 0.27	6.38 ± 0.73
R_{max}	12.14 ± 1.61	4.99 ± 0.73	6.07 ± 0.91	5.08 ± 0.47	8.59 ± 1.36
S	54.67 ± 9.15	39.33 ± 5.94	41.33 ± 5.16	37.33 ± 10.33	40.67 ± 2.58
S_m	118.00 ± 22.10	70.67 ± 11.63	84.00 ± 16.39	72.00 ± 11.46	84.67 ± 11.25
RSA/mm^2	2.33	2.27	2.26	2.26	2.31
RSA/APA	1.04	1.01	1.00	1.00	1.03
% area increase	4	1	0.4	0.4	3

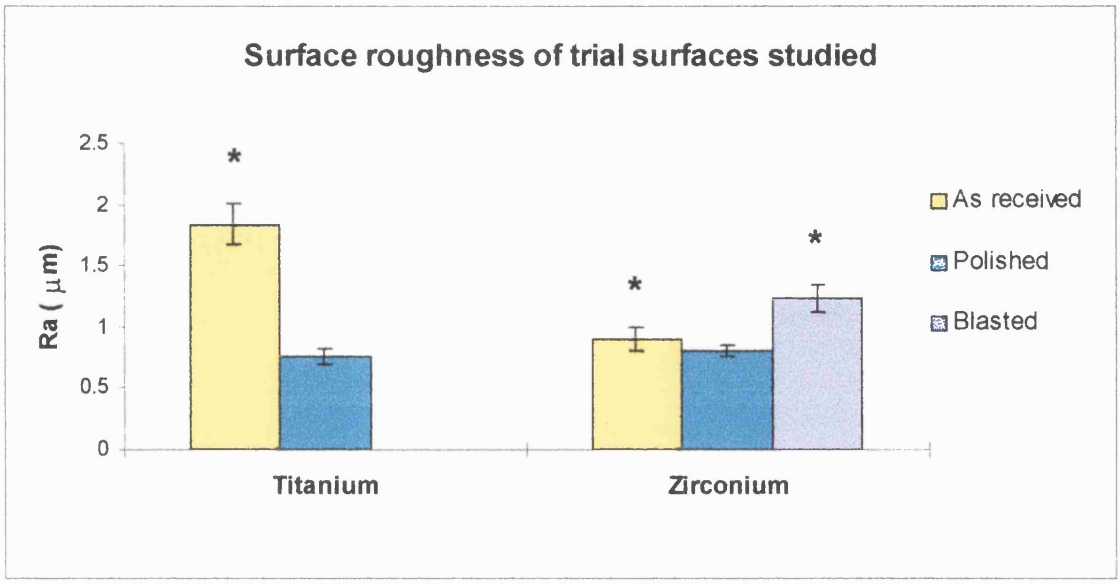

Figure 2.7 R_a values of the surfaces used in the pilot study. Values are mean ± s.d. in μm. *Significant difference ($P < 0.05$) between each surface and Zr polished.

Figure 2.7 shows the roughness values for the trial surfaces studied. Statistically, all the surfaces were significantly different from one another ($P < 0.05$). However, Ti and Zr polished to 1200 grit have approximately the same surface roughness ($P = 0.04$).

2.3.3 Effect of different scanning intervals on the roughness parameter values

Figures 2.8, 2.9 and 2.10 show the effect of varying the scanning interval between sampling points on the roughness parameter values of the surfaces studied. All measurements made were of the same area. The surface area scanned was 2.25 mm^2.

The results show that a large scanning interval between sampling points results in loss of detailed information. It is seen that the effect of varying the scanning interval on R_a is negligible. However, for R_z and the extreme value parameter, R_{max}, their mean value decreases as the scanning interval increases, i.e. height details are reduced. For the spacing parameters S and S_m, their mean value increases as the scanning interval increases, i.e. surface peaks are recorded as being further apart. It is therefore seen that increasing the scanning interval between sampling points for a certain assessment line or area, reduces the recorded height details, and increases the apparent distance between surface peaks.

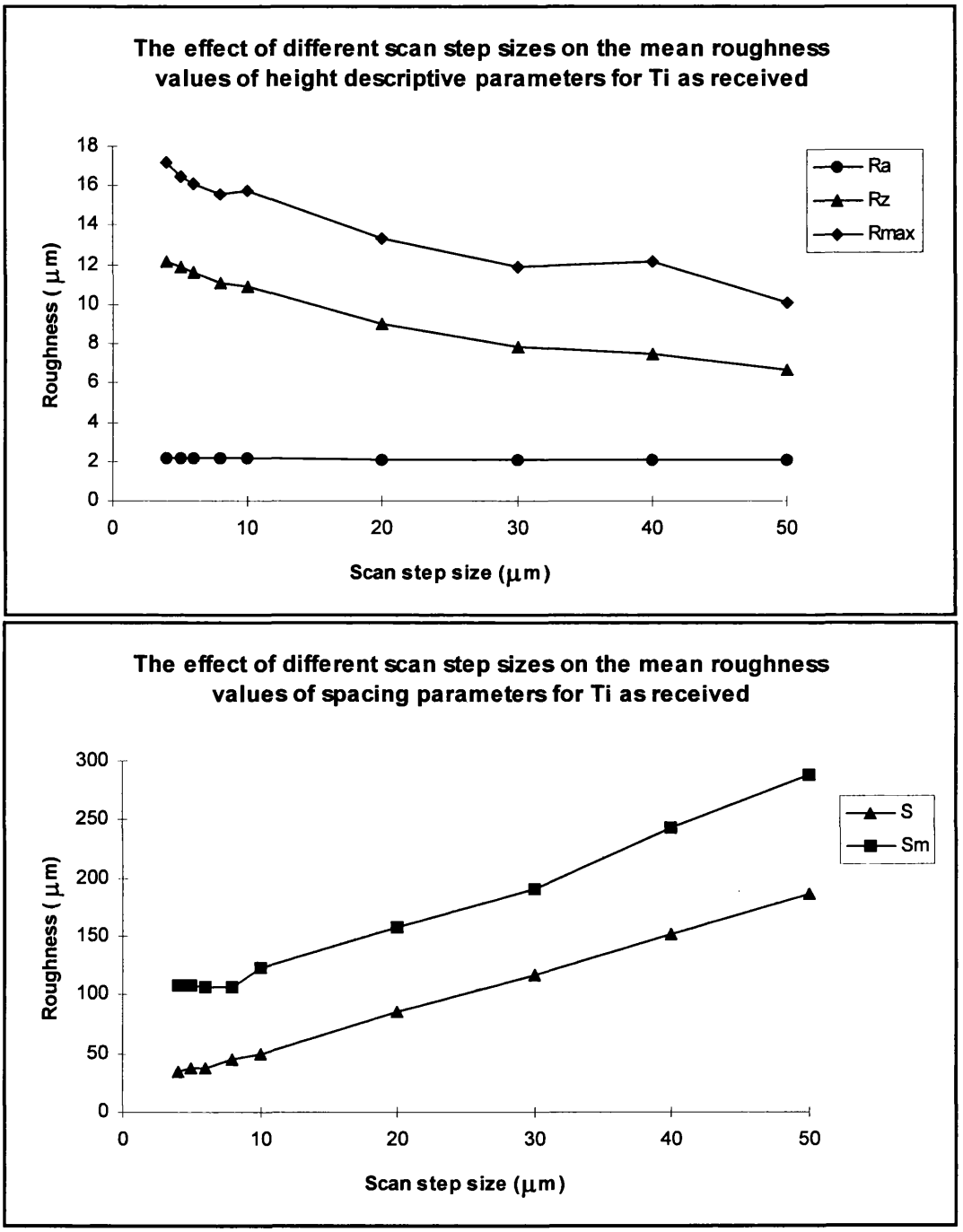

Figure 2.8 Variation in roughness parameter values with different scanning intervals for Ti as received.

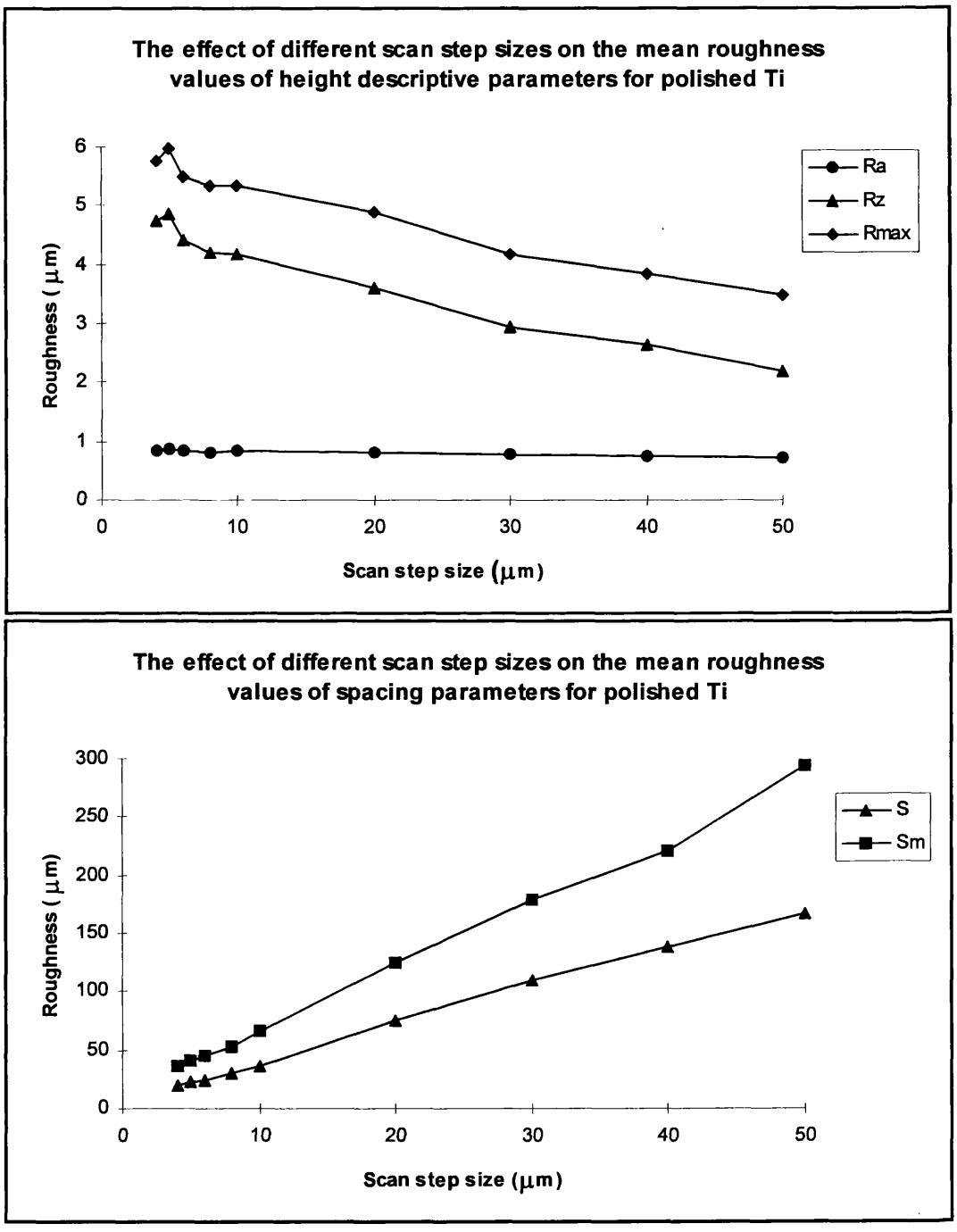

Figure 2.9 Variation in roughness parameter values with different scanning intervals for polished Ti.

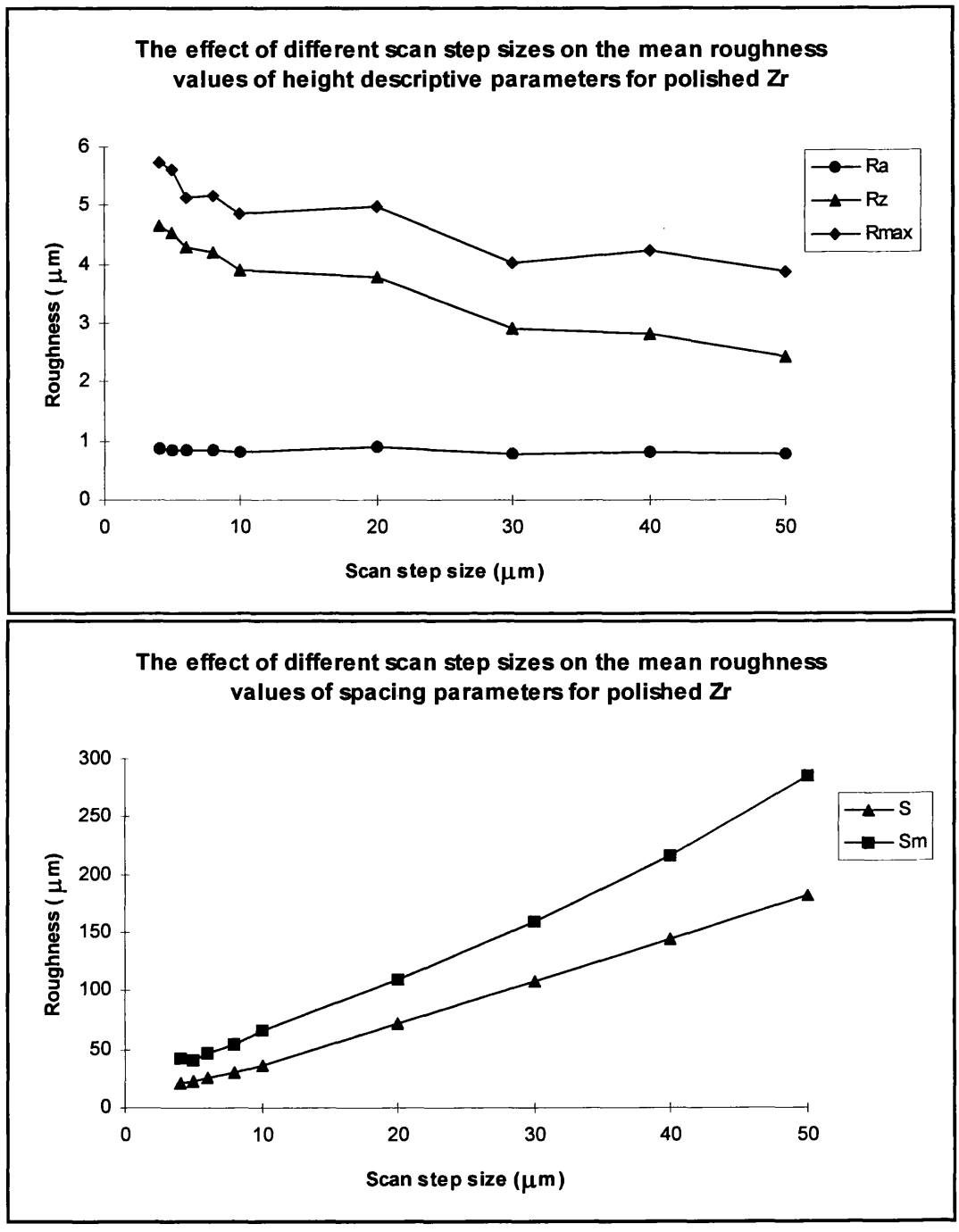

Figure 2.10 Variation in roughness parameter values with different scanning intervals for polished Zr.

2.3.3.1 Graphical representations of the profiles of the final surfaces studied

The detailed scans for the surfaces used in the cell culture studies are shown in Figure 2.11. A 1 μm scanning interval and the maximum number of sampling points (400) were used in this scanning procedure to show the maximum details that could be obtained with the Proscan 1000. The scans show that the surface of the Ti as received is markedly different from those of the polished Ti and Zr, as shown by the colours used to depict the height variations (z-axis scaling). The scan for Ti as received shows that the surface peaks were in the higher ranges (with the highest points shown in green), while the scans for both polished Ti and Zr show that the surface peaks were in the lower ranges (with the lowest range shown in blue).

Cross-sectional profiles of the three surfaces studied were compared over a 200 μm scan length in Figure 2.12. The graphical representations of all the substrates were obtained when a line of the scan, drawn from a series of z-axis height scans calculated by Proscan 1000, was retrieved as ASCII files into Microsoft Excel. The x and y axes have similar magnitudes so that the relationship between surface peak heights and spacings could be visualised easily, although it is kept in mind that the magnifications of the surface profile in both axes may not be similar, and therefore these profiles may not reflect the true profiles of the surfaces studied. It is seen that the heights of the peaks in the smooth polished Ti and Zr surfaces may be less than 5 μm, with peak spacings about the same distance, and showing regular surface profiles.

On the other hand, distances between the peaks of the rough "as received" Ti were not as regular as the smooth surfaces. Grooves may be approximately 30-40 μm deep, and peak spacings vary from 5-30 μm. This shows that the Ti as received had peaks which were much higher and further apart than the peaks in the smooth surfaces.

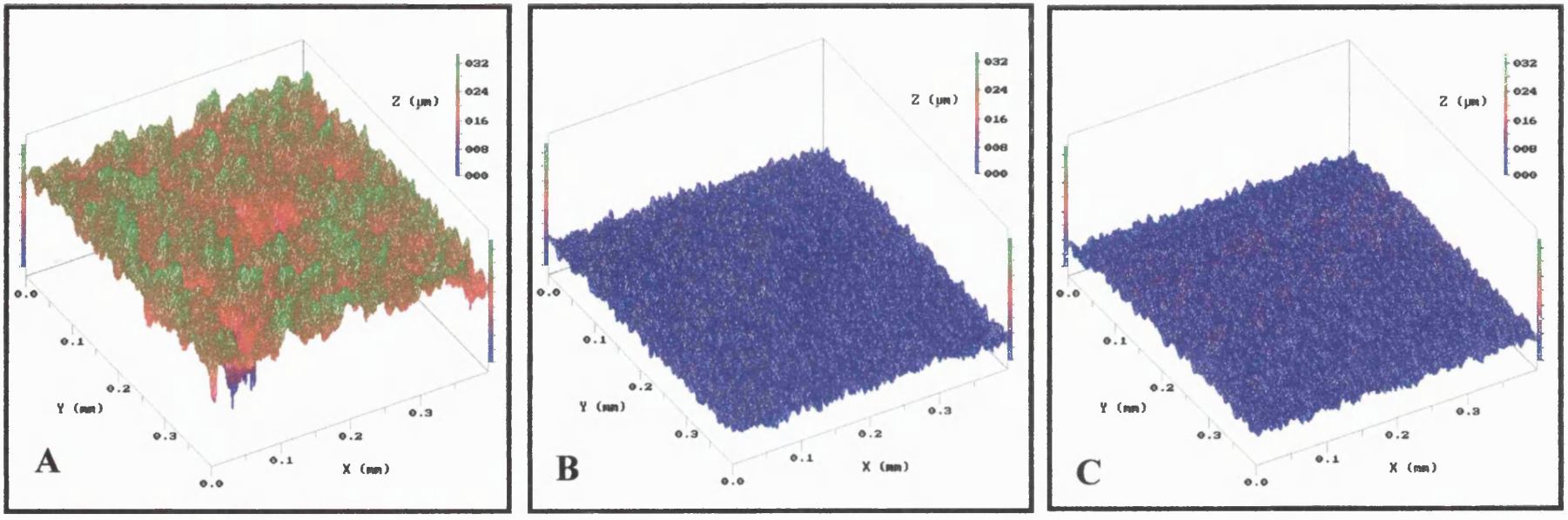

Figure 2.11 Proscan 1000 images comparing the 3-D profiles of the final surfaces studied. In order to show the maximum profile possible, all surfaces were measured at 1 µm scanning interval, with 400 sampling points. The z-axis scaling has been adjusted so that the images are proportional to each other. A: Ti as received, B: Ti polished to 1200 grit, C: Zr polished to 1200 grit.

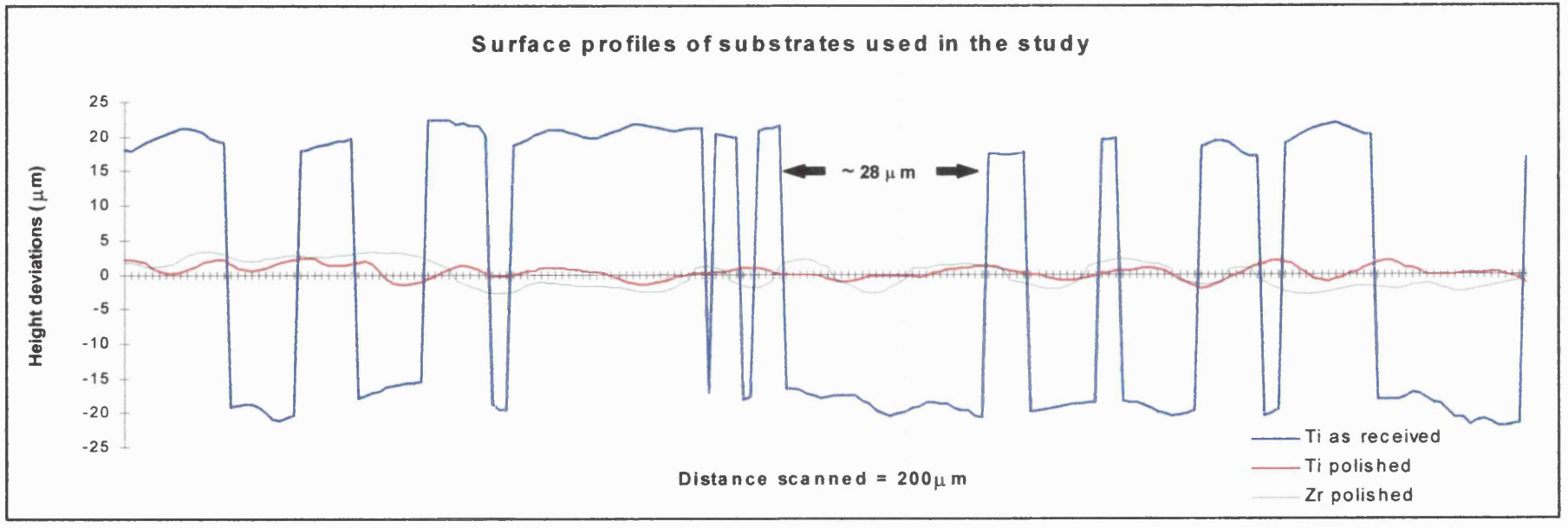

Figure 2.12 2-D graphical representations comparing the surface profiles of the final surfaces studied. The x and y axes have similar magnitudes. Each tick mark on the x-axis represents 1 μm.

2.3.3.2 The effect of scanning intervals on the visual representation of the surface profiles

The effect of the scanning distance on the 3-D and 2-D representations of the profiles of the surfaces studied is shown in Figures 2.13-2.18. Three combinations of different scanning intervals and different number of sampling points, making up a scanning distance of 1.5 mm in both x and y axes were assessed. It is seen from the 3-D Proscan 1000 images that increasing the scanning distance results in loss of vertical and horizontal surface details (Figures 2.13, 2.15 and 2.17).

The 2-D graphical representations of the 3-D images are shown in Figures 2.14, 2.16 and 2.18. The y-axis scale shows the departure of the surface peaks and valleys, calculated from a mean line by Microsoft Excel. It is seen that not only are the values for the amplitude parameters reduced, but the spacing parameter values are increased with the greater scanning distances.

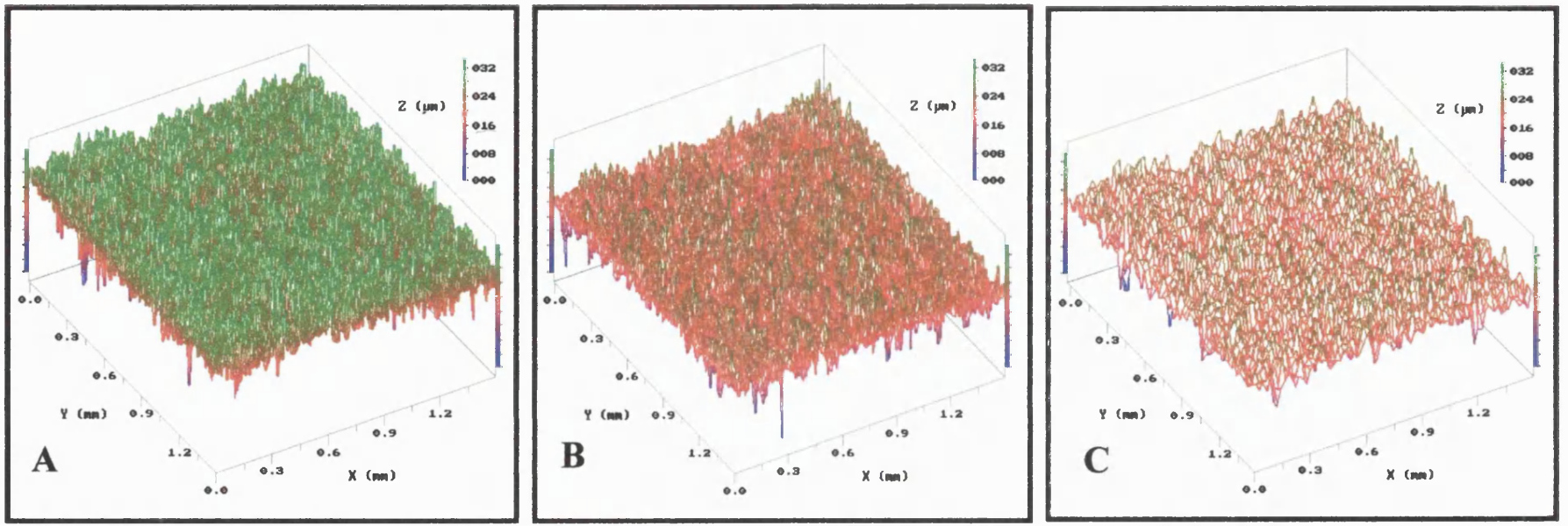

Figure 2.13 3-D Proscan 1000 images of Ti as received showing the reduction in vertical and horizontal detail as the scanning intervals are increased, while the number of sampling points are decreased. A: 6 µm scanning interval, 250 sampling points. B: 10 µm scanning interval, 150 sampling points. C: 20 µm scanning interval, 75 sampling points. Assessment area is 2.25 mm^2.

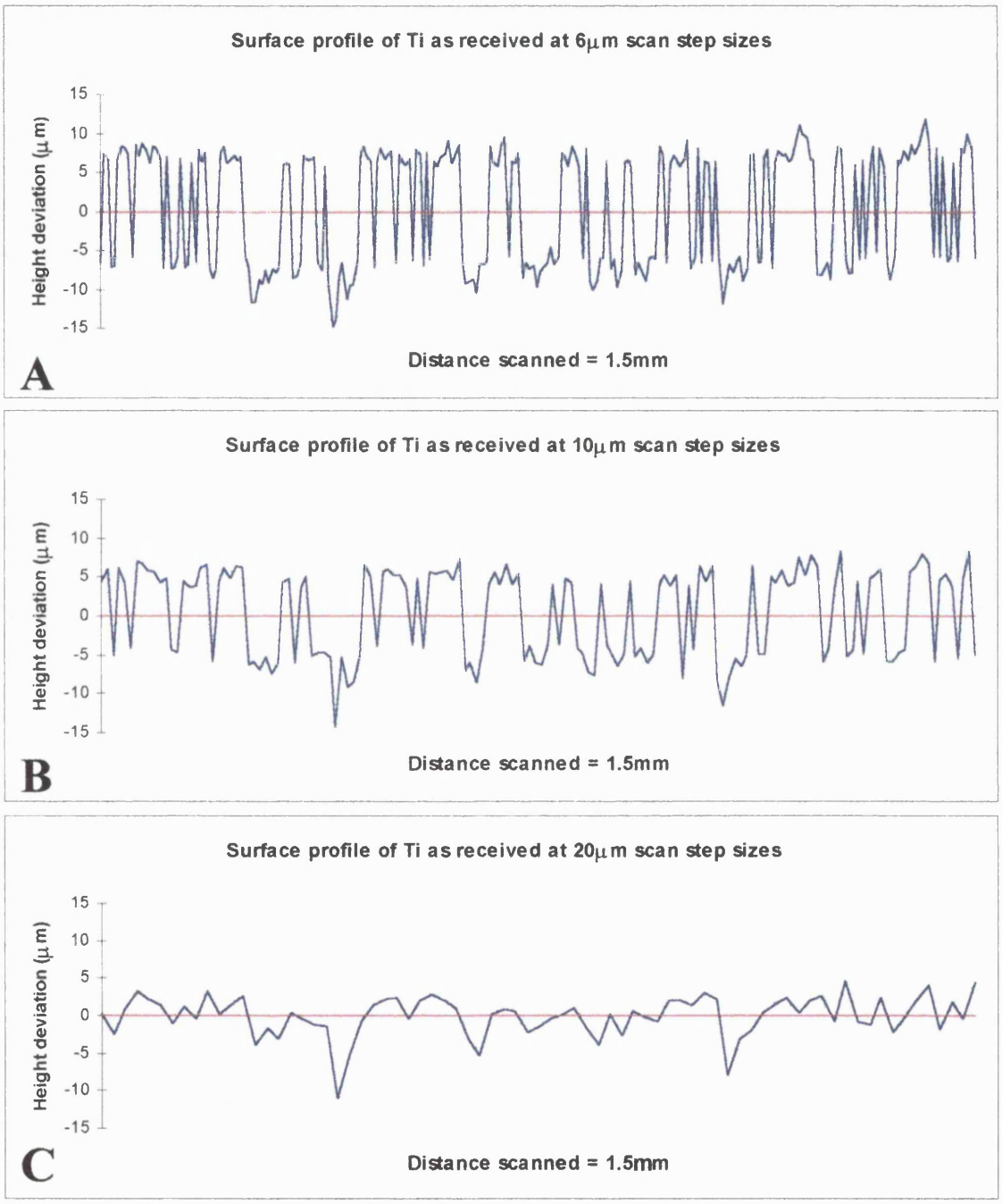

Figure 2.14 2-D graphical representations to compare the effect of different scanning intervals on the recorded surface profile of Ti as received. A: 6 μm scanning interval, 250 sampling points. B: 10 μm scanning interval, 150 sampling points. C: 20 μm scanning interval, 75 sampling points.

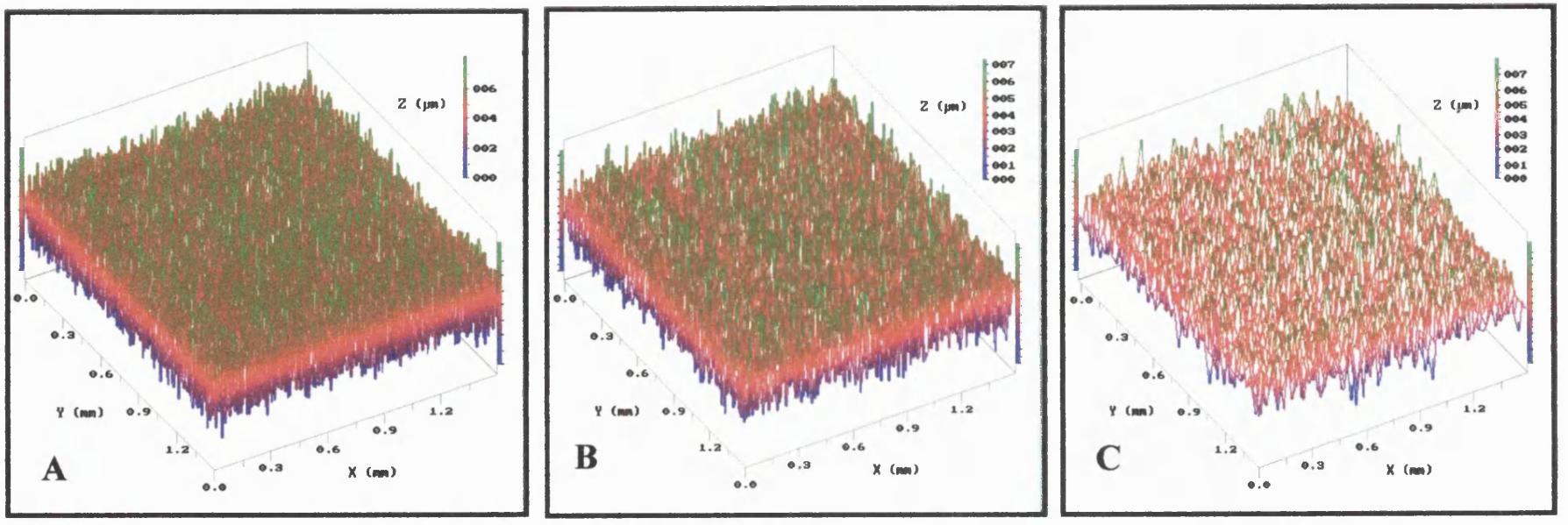

Figure 2.15 3-D Proscan 1000 images of polished Ti to show the reduction in vertical and horizontal detail as the scanning intervals are increased, while the number of sampling points are decreased. A: 6 µm scanning interval, 250 sampling points. B: 10 µm scanning interval, 150 sampling points. C: 20 µm scanning interval, 75 sampling points. Assessment area is 2.25 mm^2.

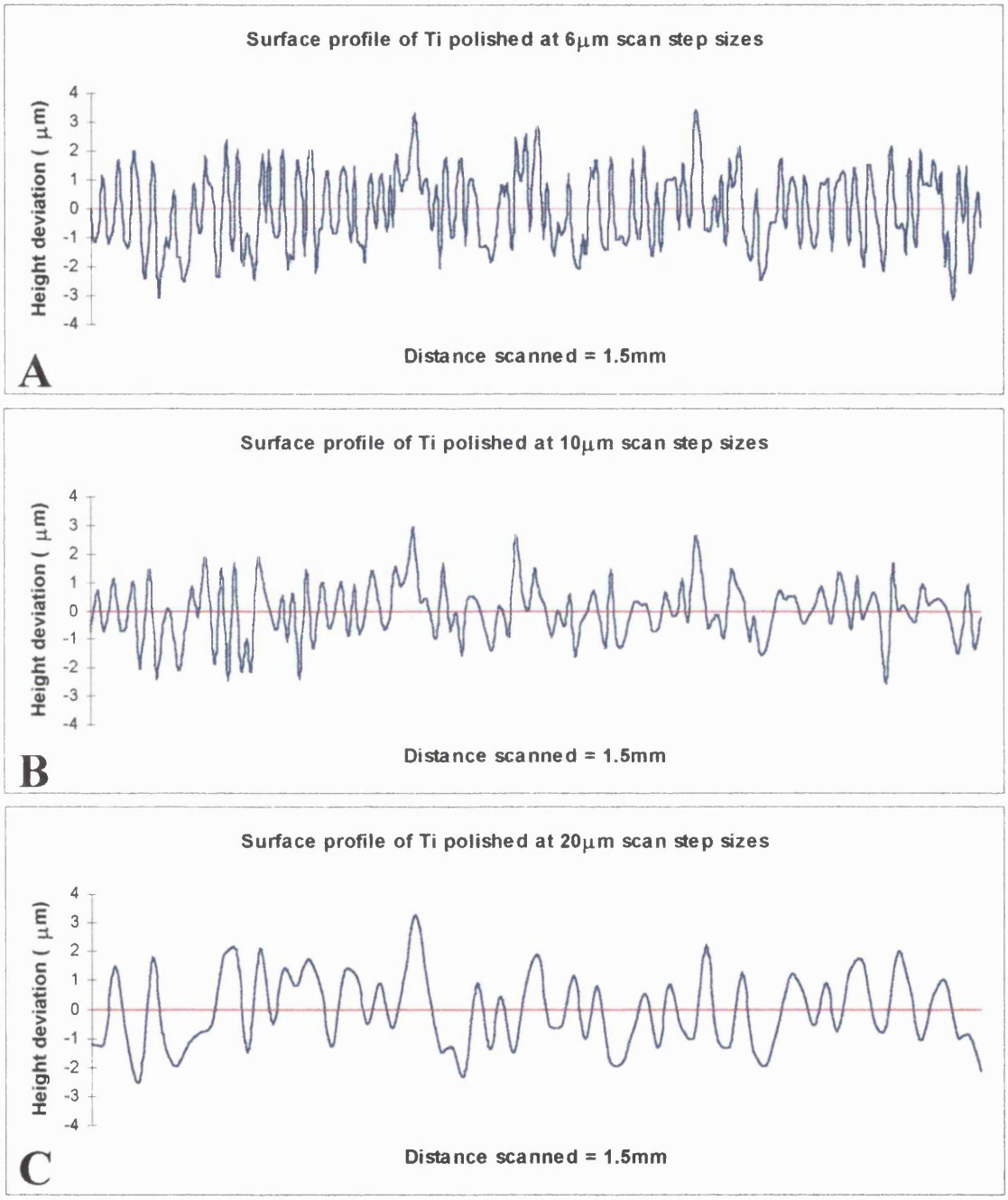

Figure 2.16 2-D graphical representations to compare the effect of different scanning intervals on the recorded surface profile of polished Ti. A: 6 μm scanning interval, 250 sampling points. B: 10 μm scanning interval, 150 sampling points. C: 20 μm scanning interval, 75 sampling points.

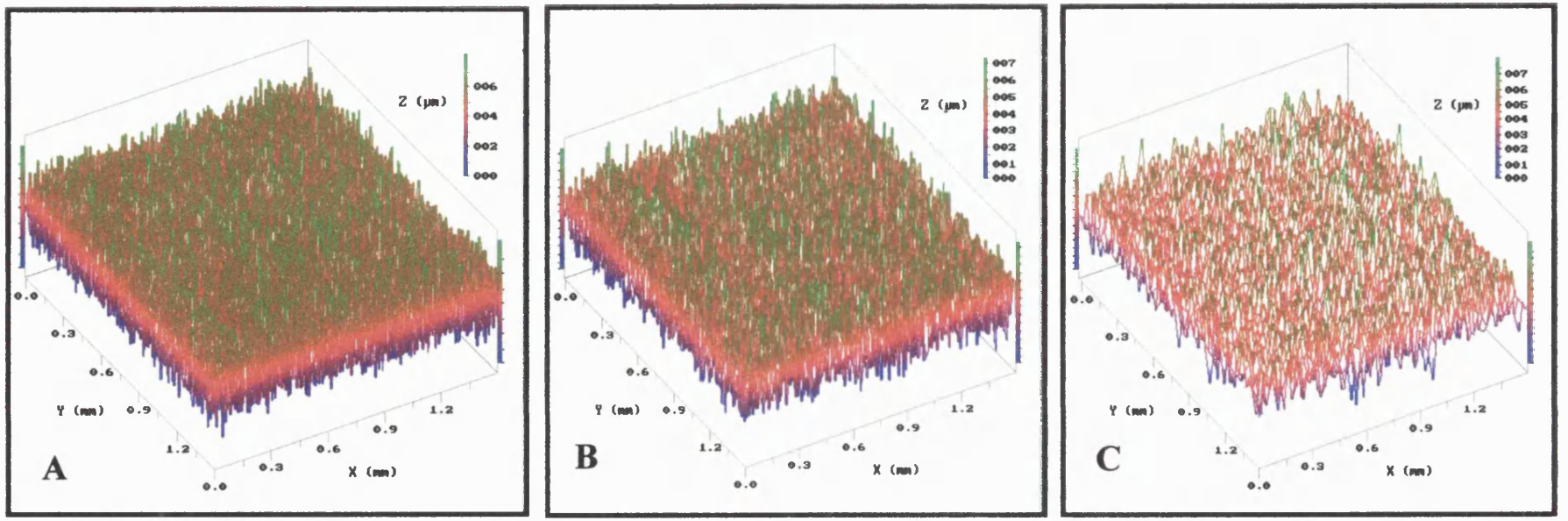

Figure 2.15 3-D Proscan 1000 images of polished Ti to show the reduction in vertical and horizontal detail as the scanning intervals are increased, while the number of sampling points are decreased. A: 6 µm scanning interval, 250 sampling points. B: 10 µm scanning interval, 150 sampling points. C: 20 µm scanning interval, 75 sampling points. Assessment area is 2.25 mm^2.

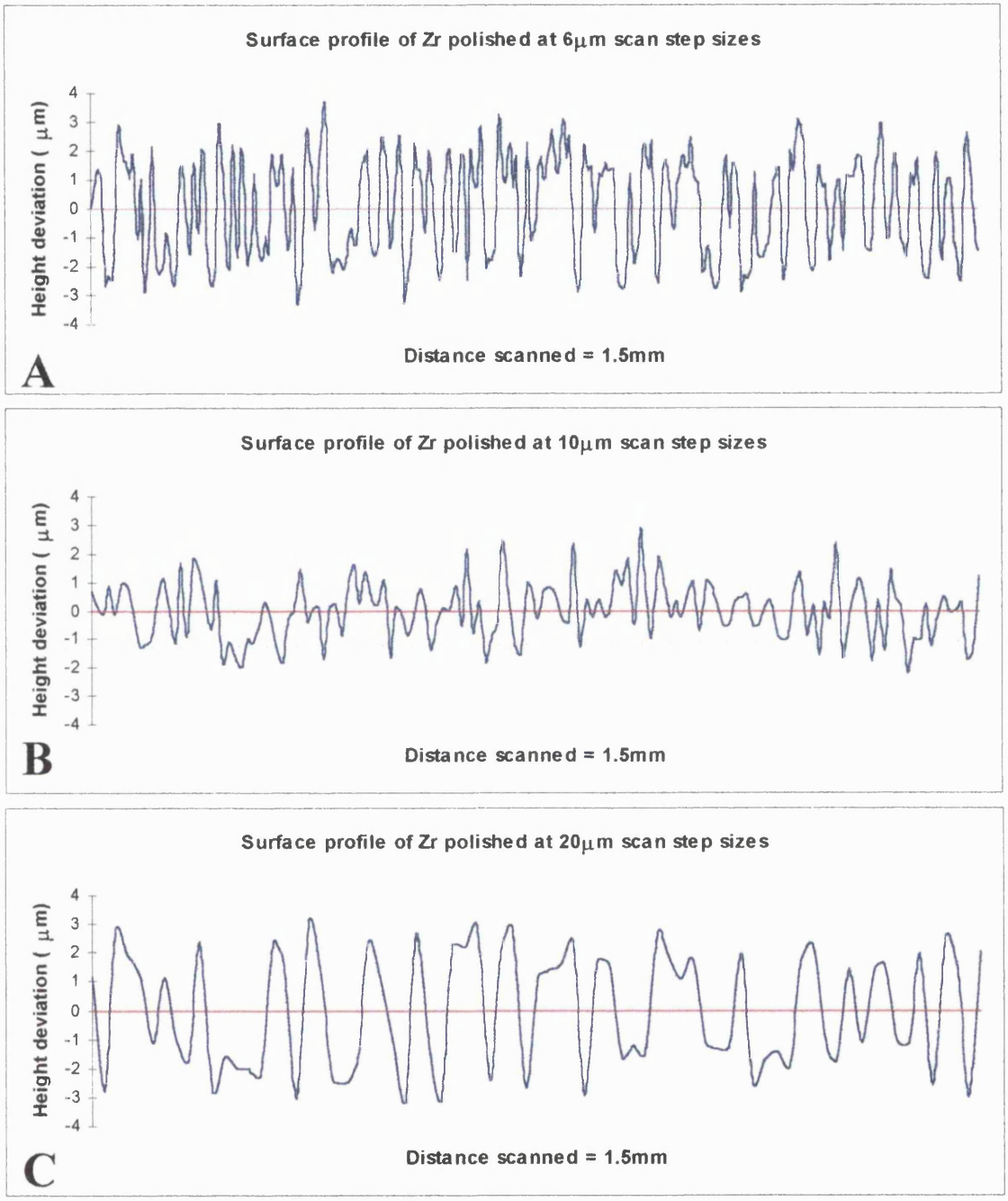

Figure 2.18 2-D graphical representations to compare the effect of different scanning intervals on the recorded surface profile of polished Zr. A: 6 μm scanning interval, 250 sampling points. B: 10 μm scanning interval, 150 sampling points. C: 20 μm scanning interval, 75 sampling points.

2.3.3.3 The effect of measuring roughness parameters across and along the surface lay for isotropic and anisotropic surfaces

Figures 2.19, 2.20, and 2.21 show the effect of measuring isotropic and anisotropic surfaces across and along the surface lay for Ti as received, polished Ti and polished Zr. For all surfaces, n = 45 in each x and y axis. Independent sample *t*-test was used to determine if means of roughness values made along the x and y axes for all substrates were significantly different ($P < 0.05$).

No particular direction was followed when choosing the areas to be scanned for Ti as received. When roughness measurements in the x- and y-axis were compared, only the S values were significantly different ($P = 0.001$), while the other parameters were similar when measured across and along the surface lay ($P > 0.05$) (Figure 2.19).

For polished Ti and Zr, roughness values were significantly different when made in the x and y-axis (Figures 2.20 and 2.21). The amplitude parameter values were greater when measurements were made along the x-axis (across the lay) ($P < 0.05$). For the spacing parameters, the mean distances between the peaks were significantly closer when measurements were made across the direction of the surface lay, than when measured along it ($P < 0.05$).

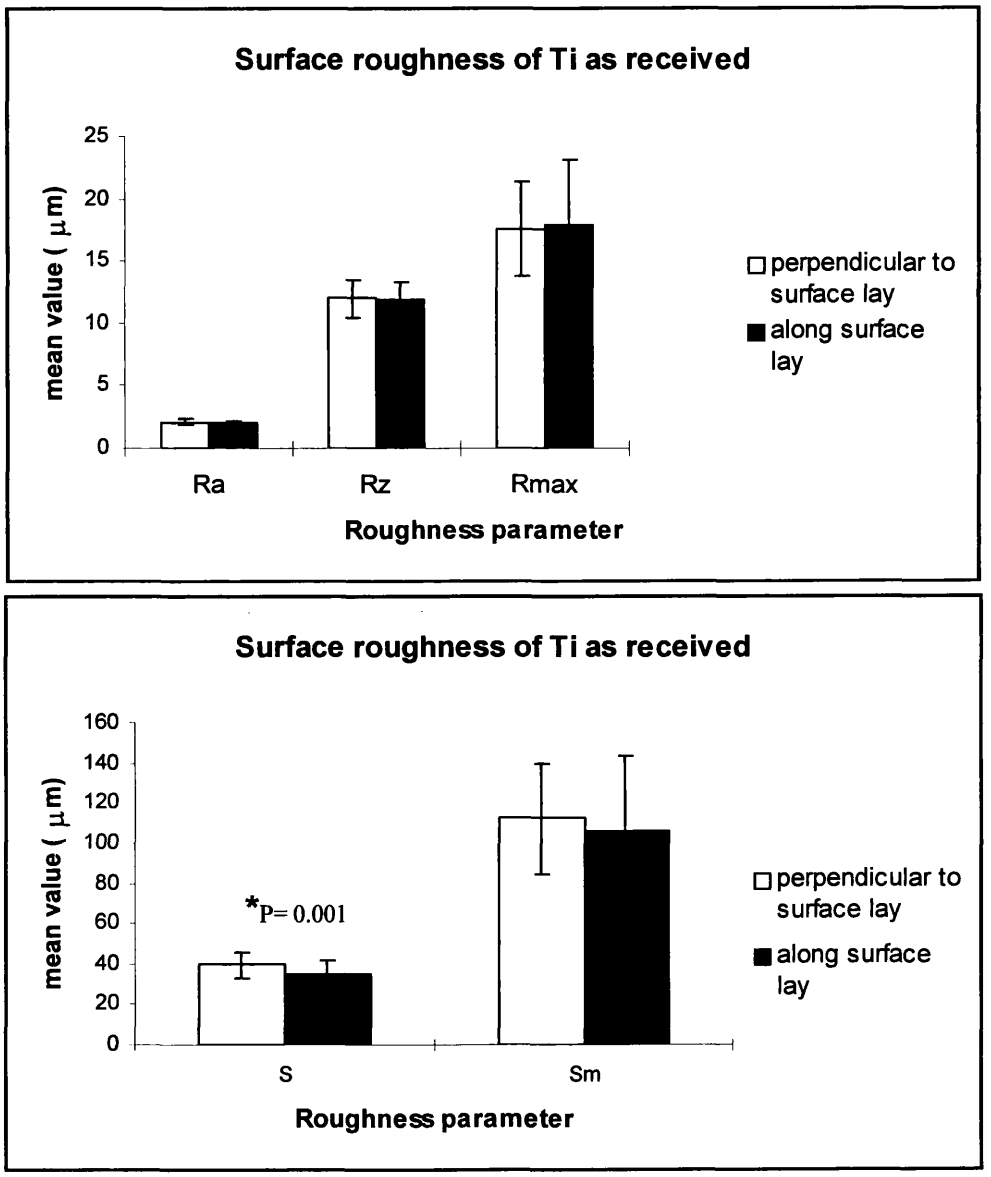

Figure 2.19 Surface roughness values of Ti as received. Measurements were made in two directions (x axis measurements were made perpendicular to surface lay, and y axis measurements were made along the surface lay). Values are mean ± s.d. in μm. Differences between means of each roughness parameter values were significant at $P < 0.05$. $n = 45$ for all roughness values along each axis.

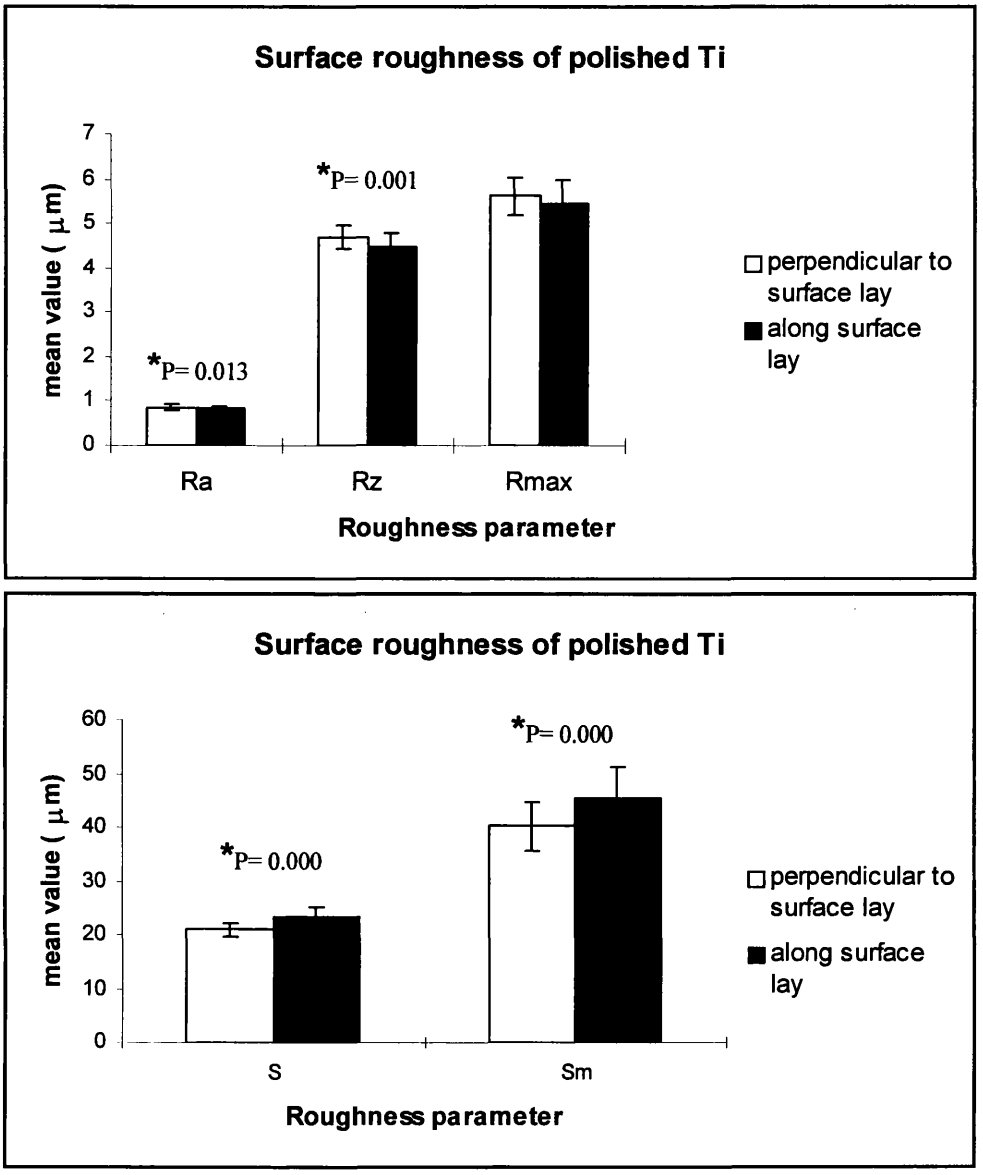

Figure 2.20 Surface roughness values of polished Ti. Measurements were made in two directions (x axis measurements were made perpendicular to surface lay, and y axis measurements were made along the surface lay). Values are mean ± s.d. in μm. Means of each roughness value were significantly different at $P < 0.05$. $n = 45$ for all roughness values along each axis.

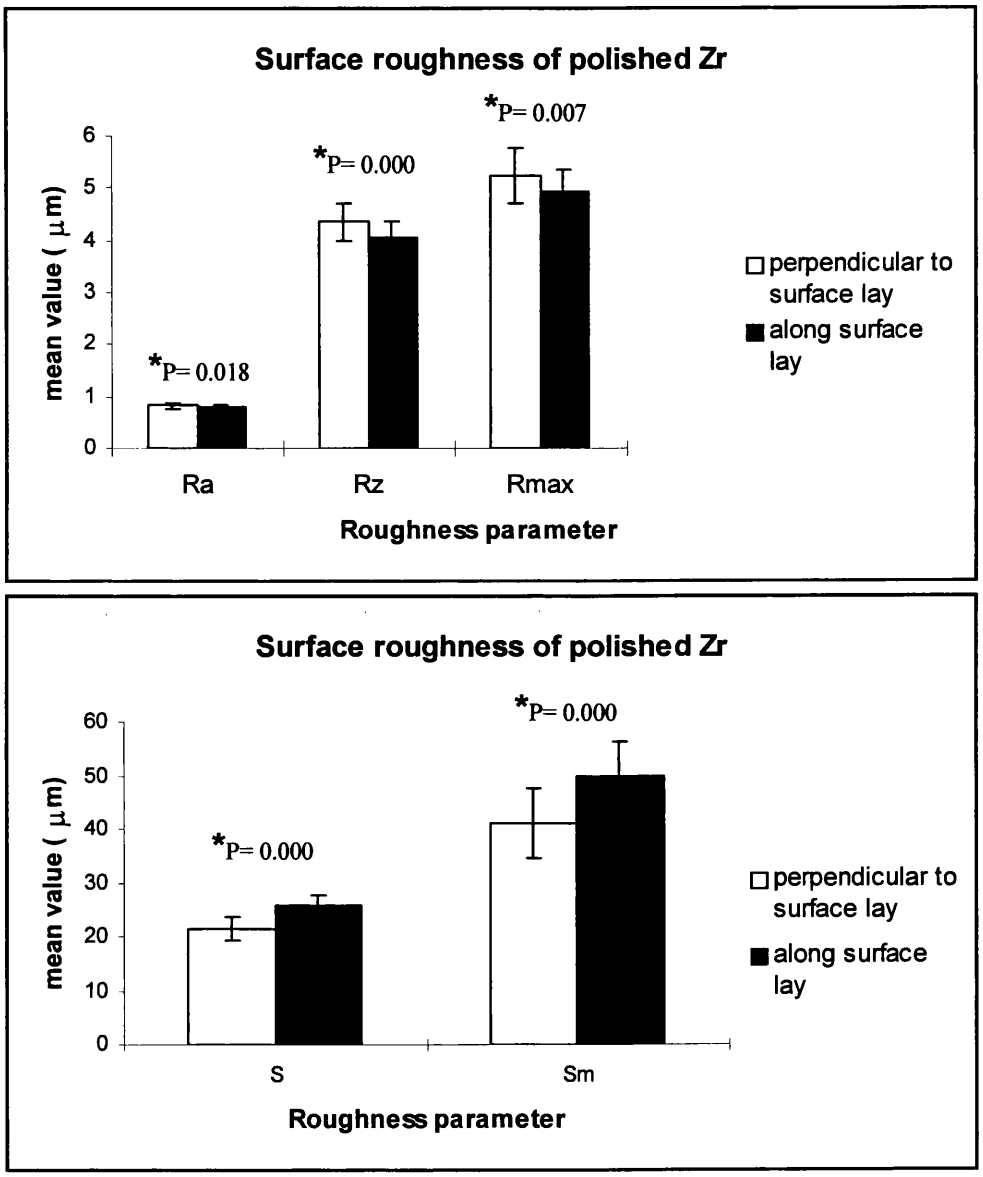

Figure 2.21 Surface roughness values of polished Zr. Measurements were made in two directions (x axis measurements were made perpendicular to surface lay, and y axis measurements were made along the surface lay). Values are mean ± s.d. in μm. Means of each roughness value were significantly different at $P < 0.05$. $n = 45$ for all roughness values along each axis.

2.3.4 Roughness values for the final substrates used in the cell culture studies

Decisions regarding the measurement variables and conditions to be used with the Proscan 1000 to analyse the final test surfaces were made after reviewing the results from Figures 2.8-2.10, Figures 2.13-2.18, and Figures 2.19-2.21. The following conditions were eventually used: 1) a 5 μm scanning interval with 300 sampling points to measure an assessment area of 2.25 mm^2, 2) roughness values obtained in both the x- and y-axis for Ti as received were averaged out, and 3) for the polished Ti and Zr surfaces, only values obtained when measurements were made across the surface lay were used.

Table 2.2 shows the roughness values of the three final test surfaces measured using the above conditions. The results show that Ti and Zr polished to 1200 grit are smoother than Ti as received because the height parameter values (R_a, R_z and R_{max}) are lower. While the distance between the adjacent local peaks (S) may be similar in all substrates, the mean value for the true peak spacing in Ti as received is twice that of the distances in the polished surfaces. This indicates a lower frequency of the deeper peaks and valleys in the rough Ti than in the smoother surfaces.

Table 2.2 Roughness values for the final test surfaces quantified using the Proscan 1000. Values are mean ± s.d. in μm. Measurements were made at 5 μm intervals for 300 sampling points. Area measured = 2.25 mm^2

Parameter	Ti as received	Polished Ti	Polished Zr
R_a	2.09 ± 0.20	0.86 ± 0.05	0.82 ± 0.07
R_q	2.69 ± 0.29	1.06 ± 0.06	1.00 ± 0.07
R_z	11.95 ± 1.42	4.68 ± 0.26	4.35 ± 0.37
R_{max}	17.69 ± 4.58	5.61 ± 0.41	5.23 ± 0.54
S	37.01 ± 6.94	20.96 ± 1.38	21.53 ± 2.26
S_m	109.07 ± 32.94	40.27 ± 4.56	41.00 ± 6.61
RSA/mm^2	2.55 ± 0.02	2.36 ± 0.01	2.34 ± 0.00
RSA/APA	1.13	1.05	1.04
% area increase	13	5	4

2.3.5 Comparison of the roughness values obtained using the Proscan 1000 and Surftest 4

Table 2.3 compares the roughness values of the final test surfaces, obtained using the different profilometer systems. It is seen that the values obtained using the Surftest 4 are very much lower than the values obtained using the Proscan 1000, especially for the smooth polished surfaces. Depending on the surface and the roughness parameter measured, the percentage difference in the roughness values obtained using the two different systems can vary from 30 to 400%.

Table 2.3 A comparison of the results from the Proscan 1000 and Surftest 4 on measurement of roughness of Ti as received, and polished Ti and Zr surfaces. Values are mean ± s.d. in μm

Surface	Parameter	Proscan 1000	Surftest 4	% difference
Ti as received	R_a	2.09 ± 0.20	1.47 ± 0.13	42
	R_q	2.69 ± 0.29	1.64 ± 0.14	64
	R_z	11.95 ± 1.42	9.13 ± 0.73	31
	R_{max}	17.69 ± 4.58	10.60 ± 1.15	67
Polished Ti	R_a	0.86 ± 0.05	0.26 ± 0.02	230
	R_q	1.06 ± 0.06	0.29 ± 0.02	266
	R_z	4.68 ± 0.26	1.79 ± 0.19	161
	R_{max}	5.61 ± 0.41	2.08 ± 0.36	170
Polished Zr	R_a	0.82 ± 0.07	0.17 ± 0.02	382
	R_q	1.00 ± 0.07	0.19 ± 0.02	426
	R_z	4.35 ± 0.37	1.34 ± 0.12	225
	R_{max}	5.23 ± 0.54	1.67 ± 0.29	213

2.3.6 SEM evaluation of the final test surfaces used in the cell culture studies

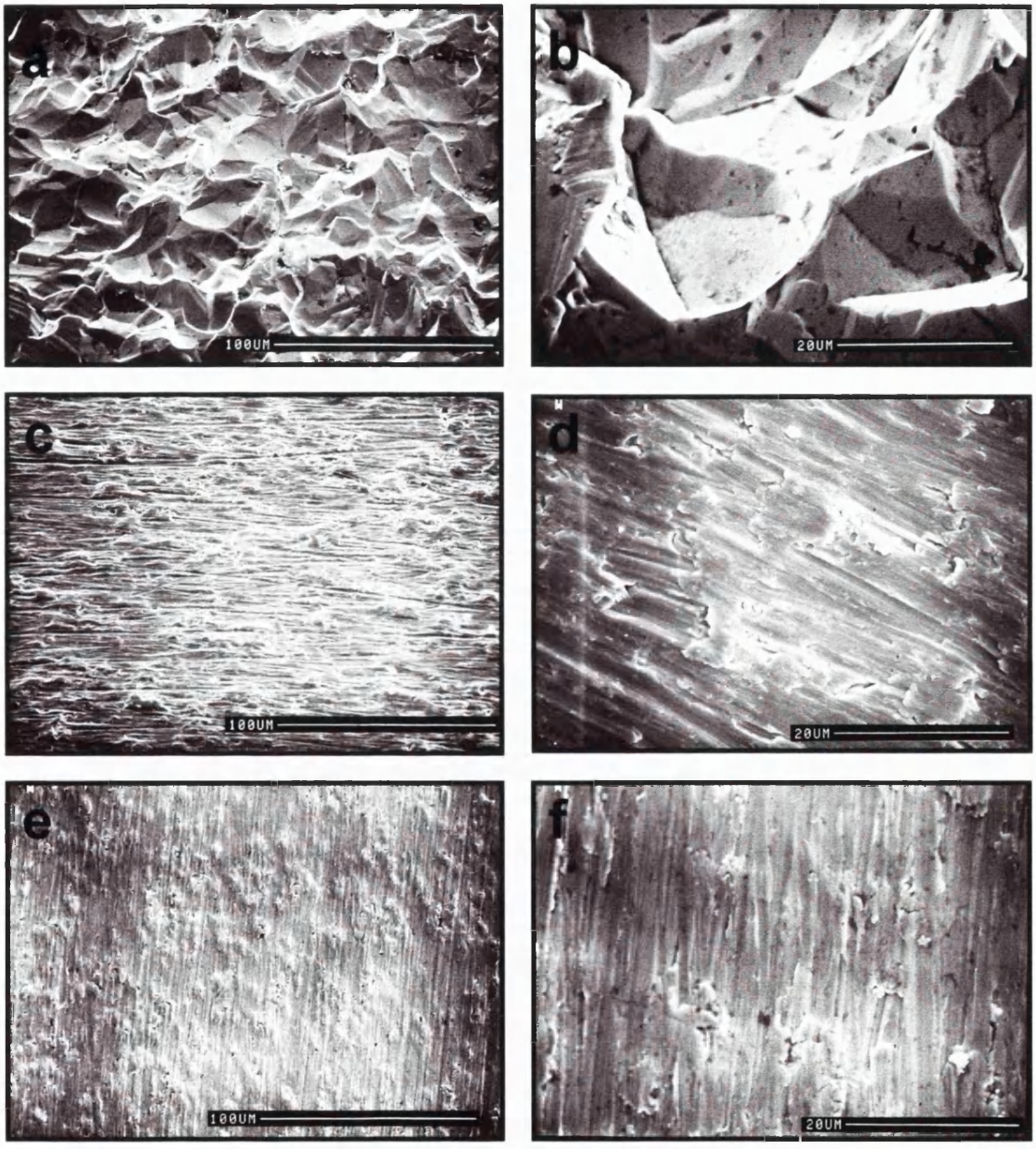

Figure 2.22 Scanning electron microscopy images of the final test surfaces used in the cell culture studies. (a) and (b): Ti as received, (c) and (d): Polished Ti, (e) and (f): Polished Zr. The polished Ti and Zr surfaces show a distinct directional prominence due to the grinding process using the same grade of silicon carbide papers. The micrographs for the 'as received' Ti show the morphological appearance of a rolled metallic surface with a regular topography.

2.3.7 Confocal laser scanning microscopy images of the cpTi surfaces

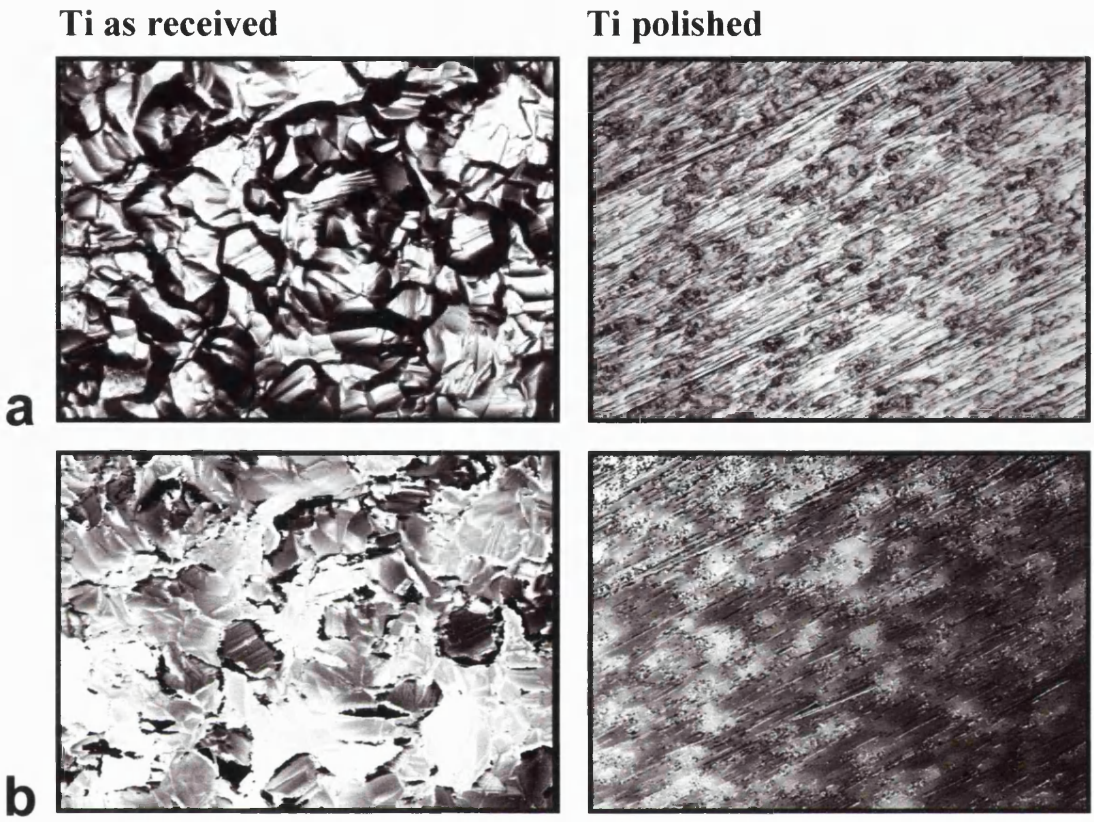

Figure 2.23 Confocal laser scanning micrographs of the Ti as received and polished Ti surfaces used in the cell culture studies. Two kinds of images were recorded for the same surface. (a): "MAX" image, which is the in-focus image. (b): "Z contrast" image showing depth discrimination within a range of eight bands of grey scale. The field width for all micrographs is 290 μm. Original magnification × 40.

2.4 DISCUSSION

2.4.1 Introduction

The current interest and emphasis on implant material roughness and bone cell reactions to the implant at the interface shows the need for a standardised technique to quantify implant material surface topography in order to be able to understand some of the cellular reactions to currently available implants, which vary in design, surface chemistry and topography. Non-destructive, high speed non-contact optical profilometers driven by computers are now being used besides the standard contact profilometer type instruments. These enabled more roughness parameters to be computed and 3-D profiles over a certain area could be made, in contrast to the 2-D line profiles obtained with conventional contact profilometers. However, since no internationally recognised standards for 3-D roughness parameters exist currently (Stout *et al.*, 1993), researchers have continually used the 2-D profilometers to assess surface roughness. As the measurement principles of these two techniques are different, it is essential to have an understanding of the results obtained from the use of these techniques so that tissue reactions to different implant surfaces could be analysed in relation to the limitations of the techniques used.

Ti has been used successfully in bone implants for several decades. Several reasons have been proposed for its success as an implant material. Of importance are the general considerations which are related to the design of the fixture, favourable host implant site, provision of optimal prosthodontic design, non loading or no excessive micromotion during healing, and general implant maintenance procedures to achieve ongoing osseointegration. More fundamentally the success of Ti and its alloys has been attributed to the material *per se*, and in particular its excellent corrosion resistance, and its so called biocompatibility when compared to other metals which have been used as implants. The oxide layer on Ti surfaces may also permit the formation of a Ca-P layer which has been observed *in vitro* (Hanawa, 1991; Li and Ducheyne, 1997; Yan *et al.*, 1997). This may serve as a favourable surface for integration of new bone with the implant.

Besides the chemical composition, properties related to the surface topography of an implant also play an important role in osseointegration. It is known that more rapid osseointegration and greater amounts of bone formation occur with implants coated with plasma-sprayed hydroxyapatite (HA) than with uncoated Ti, especially in the early stages of healing. This is thought to be due to the chemical bond which is formed with the HA of bone. However, plasma-sprayed Ti implants also tend to have rough surfaces which may be more favourable to bone formation than smooth uncoated Ti surfaces. Since surface roughness is one of the factors which play a dominant role with regard to the bone-tissue reactions at the interface, a detailed description of the morphological surface characteristics is a necessary precondition for the interpretation of these reactions.

2.4.2 Choice of substrates and substrate preparation

The main purpose of this whole investigation was to compare the responses of osteoblast-like (OB) cells grown on cpTi and cpZr surfaces of different topography and roughness. Both metals are known to be stable in the biological environment, and have been used as implant materials *in vivo*. Bone cells have been shown to attach, proliferate and differentiate to a greater extent on rough surfaces than on smooth ones, and therefore no effort was made to produce surfaces with a smooth mirror finish in this study. Substrates were only polished to 1200 grit, as surfaces with topographic features with the dimension of 2-5 μm, or with S_a (equivalent to the 2-D R_a) values of 1.5 μm had been associated with the highest tissue biocompatibility and bone formation (von Recum and van Kooten, 1995; Wennerberg *et al.*, 1996; Hansson, 1998).

The roughest surface studied was Ti as received, and initially it was decided to produce rough surfaces by blasting the cpTi and cpZr with oxide particles of the respective metals. This would be ideal as blasting the surface with the same metallic oxides would reduce surface contamination. However, it proved impossible to obtain the oxide particles in the sizes required. Despite varying the spray characteristics, the results of a pilot study (Table 2.1) show that it was impossible to produce similar rough surfaces for the Ti and Zr using the technology available with a particle blasting machine. Zr blasted with 50 μm particles of Al_2O_3 had an R_a value of 1.23 μm, which is

not very different from the 0.9 μm of the Zr as received, and still different from the R_a value of the rough "as received" Ti (1.84 μm). As the difference in the R_a values for Zr as received and Zr blasted with Al_2O_3 was not marked, these surfaces were not used in the cell culture studies. It was not known whether the subtle difference in the surface characteristics of the substrates which were not eventually used, would have had any significant effect on cellular behaviour, particularly as the Al_2O_3 may have contaminated the Zr surfaces.

Rougher silicon carbide papers were not used to produce rough surfaces, as the resultant profile would be similar to that of the smooth ones, but with deeper grooves. Moreover, Bowers *et al.* (1992) had shown that an irregular surface produced by sandblasting with 50 μm alumina oxide particles may be more conducive to cellular attachment than other rough surfaces produced by polishing/grinding or acid etching. Hence, only three surfaces which are markedly different (i.e. Ti as received, and polished Ti and Zr) were used in the following cell culture studies, and not the surfaces with intermediate grades of roughness. The R_a values of these surfaces were within the range of the R_a values of commercially available implants, i.e. between 0.53 and 2.94 μm (Wennerberg *et al.*, 1993). The surfaces chosen allowed reactions of cells grown on the same material with different surface roughness (Ti as received and Ti polished), and reactions of cells grown on two different materials with similar roughness (Ti and Zr polished to 1200 grit) to be compared.

2.4.3 Choice of instruments to quantify surface roughness of substrates

The contact profilometer is commonly used for quantifying surface topography of materials. The laser scanning profilometer offered greater accuracy, more variables for quantification of surface texture, and has been used in recent investigations of surface roughness (Wennerberg *et al.*, 1992; Whitehead *et al.*, 1995). Due to the on-site availability of the two instruments, both were used, and this made it possible to compare the roughness values obtained using the two measuring techniques.

2.4.4 Parameters chosen to quantify the surfaces

The commonly used R_a is a true amplitude parameter, giving the scale of the height distribution, but does not give any other information about the profile shape. Surfaces with the same R_a and S values can have different surface profiles and textures (Figure 2.24, reproduced from BS 1134, 1990). Therefore, in order to characterise the topography of a surface, more parameters are needed.

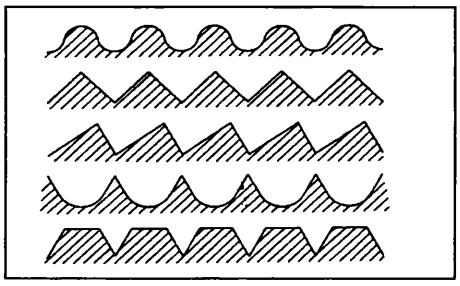

Figure 2.24 Surface profiles with the same R_a and spacing.

The parameters used in this study were height and spacing descriptors. Even used in combination they do not tell us anything about the shape of the profiles studied. More information on profile shape may be available with some instruments, where skewness and kurtosis indices can be obtained (Thomas, 1981). The skewness index is a measure of the symmetry of the profile about the mean line. A surface with high peaks has positive skewness, whereas a jagged, uneven surface tends to have a negative skew. A symmetrical height distribution, i.e. with as many peaks as valleys, has zero skewness. The kurtosis index (K) is a measure of the sharpness of the surface profile. A normal profile distribution has a K of 3. If $K<3$, the distribution has relatively few high peaks and low valleys. If $K>3$, the distribution has relatively many high peaks and low valleys.

Whitehead *et al.* (1995) used the R_{pm} parameter (which is the mean value of the levelling depths of five consecutive sampling lengths) obtained using both the contact stylus and optical profilometer to describe profile shape. Small R_{pm} values were reported to characterise a surface featuring wide peaks and narrow valleys, while greater R_{pm} values indicate a spiky, sharp ridge profile. The ratio R_{pm}:R_z was also used to characterise profile shape. A ratio higher than 0.5 indicates a sharp ridge profile, while a ratio smaller than 0.5 indicates a rounded profile.

As adequate information on surface texture may not be available with certain profilometers, the use of complementary qualitative techniques to characterise surfaces is important. Qualitative techniques like SEM and confocal microscopy have the advantage of high resolutions, and could provide information that would not be resolved even with the resolution of an optical scanning profilometer. In addition, the use of SEM with confocal or stereo photogrammetry facilities could also create 3-D contours with depth discrimination facilities. Data from stereo photogrammetry can be transferred into a PC and typical surface parameters like R_a, R_z and R_{max} could be computed (Stout *et al.*, 1993). Moreover, in studies like the present one, where cellular dimensions need to be associated to the topography of the substrates on which they were grown in order to understand their reactions to the substrates, the sole use of the R_a parameter is inadequate.

2.4.5 Factors which affect roughness values

Several studies have characterised the surfaces of implant materials in order to relate them to bone cell behaviour, either *in vivo* or *in vitro* (Bowers *et al.,* 1992; Gomi and Davies, 1993; Ungersböck and Rahn, 1994; Martin *et al.*, 1995; Wennerberg, 1996). Different surfaces and methods of surface preparation were used and different methods of characterising the surface topographies were utilised. However, even when using the same techniques, results may or may not be comparable. The results would depend on a number of factors, some of which are inherent material features and beyond the control of the operator, while others relate to the measurement instrument, measurement conditions and sampling procedures. The results of this study showed that the roughness parameter values obtained depended on the following factors:

a. material properties and surface preparation techniques
b. method of analysis of surface roughness
c. direction in which roughness measurements were made
d. scanning interval and size of the measured areas
e. use of surface filters.

2.4.5.1 Material properties and surface preparation techniques

Different materials have different physical properties and will not produce the same surface roughness even when prepared identically. Unless techniques are highly standardised and reproducible, there will always be variations in the surface topography between different sites in the same sample, and this inhomogeneous character of the surface occurs even in machined surfaces (Thomas and Charlton, 1981). This emphasises the importance of having adequate sampling sizes, as topography may vary greatly throughout a surface.

2.4.5.2 Method of analysis of surface roughness

One of the aims of this part of the study was to compare two common methods of measuring surface roughness. The two measuring methods used gave different results (Table 2.3), as has been previously shown by other workers (Whitehead *et al.,* 1995; Wennerberg *et al.*, 1996). One reason is that the stylus of the contact profilometer may not have been able to record the depths of narrower grooves, and therefore some of the information about the roughness of the surface being measured was lost. This is especially so with the smooth surfaces.

Figure 2.22 shows the surface topography of the final test surfaces studied as seen under the resolution of the SEM. On polished Ti and Zr surfaces, grooves due to the polishing procedures may be closer to each other than 5 μm. This may be verified by the profiles of the substrates seen in Figure 2.12. This suggests that the 5 μm radius of the stylus of the Surftest 4 was not able to register the full depth of the grooves, and therefore smoothed out the recorded profile. The radius of the stylus in contact profilometers therefore, is one limiting factor in its use to measure surface roughness.

The different results obtained using the two techniques may also be related to the different areas that were measured. As was mentioned earlier, the topography throughout a surface varies, and in this study, the areas measured were not relocated. The 2-D profilometer also measured along a line, and not across an area, like the optical profilometer. Subsequently only small sections were measured, even though the

evaluation length was 4.8 mm, while the laser profilometer measured across an area of 2.25 mm^2. However, Wennerberg (1996) had shown that even when the areas were relocated exactly by making indentations to make sure that the same area was measured each time by the two measuring instruments, the results still show higher values for the laser profilometer. Taking S_a and S_z values (3-D parameters considered as equivalent to the 2-D R_a and R_z values) from their results, these differences could be up to 36 and 156% respectively. The differences were however, more pronounced when smaller (half the area measured) and non-relocated areas were compared. The percentage differences for the S_a and S_z values went up to 100 and 163%, respectively. In this study the difference in the R_a and R_z values for Ti as received was 42 and 31%, respectively (Table 2.3). The percentage differences were more than doubled for the smoother Ti and Zr polished surfaces. The percentage differences in the R_a values of polished Ti and polished Zr were 230 and 380%, respectively, while for the R_z values, these differences were 160 and 225%.

Wennerberg (1996) also mentioned that optical profilometers have the tendency of creating spikes when surfaces with deep slopes were measured. This would increase the values of the roughness parameters measured. However, as this study only measured flat samples, in contrast to the screw-shaped implants that were measured by Wennerberg (1996), this problem was not encountered. Nevertheless, one of the limitations of measurement using laser technology is the spurious readings obtained when either the laser light is blocked from reaching a surface, or when the reflected light is blocked from reaching the photodetector, by an overhanging edge. This may not then reflect the true surface profile (apart from the different magnifications used in both axes when surface profiles were amplified). This may be the case with the rough "as received" Ti, as the crystals are complex and may not be regular (Figure 2.12 and Figures 2.22 and 2.23).

Differences in the roughness values obtained using these two techniques were also highlighted in another study, where the spark-erosion technique was used to create rough implant surfaces (Wennerberg *et al.*, 1997). The manufacturer of the spark-erosion technique claimed that the roughness created was related to the different degree

of current applied to the surfaces. Using a 3-D optical profilometer, Wennerberg *et al.* (1997) found that R_a values which were claimed by the manufacturer to be 2.7 μm and 7.8 μm, were only 2.5 μm and 2.7 μm, respectively. The differences in the values were attributed to the assumption that the manufacturer had measured flat samples using 2-D techniques, and therefore these values were different when 3-D measurement techniques were used.

Another method by which roughness could also be described, is by measuring the contact angle of the surfaces. Contact angle methods are used routinely in the characterisation of biomaterials to describe wettability or to estimate surface energy (Ratner *et al.*, 1987). For most surfaces, the contact angle θ, which describes the angle which a drop of fluid makes with the surface, varies with time or movement of the liquid front, a phenomenon known as hysteresis. Hysteresis is often a result of either surface heterogeneity or surface roughness, with heterogeneity usually causing much larger hysteresis effects than roughness, when roughness is less than 1 μm (Ratner *et al.*, 1987). In order to eliminate the effect of heterogeneity and relate contact angle measurements of surfaces to roughness, the roughness value of the surface measured has to be greater than 1 μm (Ratner *et al.*, 1987; Taylor *et al.*, 1998). The metal substrates used in this study had R_a values of 0.8 and 2 μm, and therefore the contact angle was not measured, as any change in contact angle would be related to the surface texture.

2.4.5.3 Directional prominence of surfaces and direction in which roughness measurements was made

Measurements of roughness of surfaces with a prominent direction should be made across the lay. Roughness measurements made across the lay will give greater values for the height parameters, and closer values for the spacing parameters (Figures 2.19-2.21). Hence, for both polished Ti and Zr, only roughness values in the x-axis (made across the surface lay) were used to quantify the surfaces. These results confirm the anisotropic nature of the polished Ti and Zr surfaces. These differences also illustrate the fact that some surfaces are fractal, i.e. the scales in the vertical and lateral directions are different, rather than similar (Stout *et al.*, 1993). Therefore, a change in

the surface topography due to wear or other processes would give rise to different fractal dimensions in different directions. However, the roughness values for the rough as received Ti surface were taken as the means of the total measurements made in both x and y directions, as the results in Figure 2.19 confirm its isotropic nature.

2.4.5.4 Scanning interval and size of the measured area

Parameter values are scale dependent: the values depend on the sampling area and the sampling interval (Wennerberg, 1996). From a statistical point of view, the size of the sampling area is important because it is directly related to the statistical reliability of the estimated parameters. The results obtained in this study indicate that a large sampling interval may miss important frequency components and give poor visual representation of the original topography of the surfaces measured (Figures 2.8, 2.9 and 2.10, and Figures 2.13, 2.15 and 2.17). These results show that scanning interval plays a key role in the quality of the surface roughness measurements made. Although it has little influence on the R_a values, the scanning interval is especially seen to have considerable effect on the spacing parameters and extreme value parameters, R_z and R_{max}. Therefore, an appropriate scanning interval and number of sampling points which will provide adequate information for both amplitude and spacing parameters must be determined before making roughness measurements.

Ideally, many sampling points with short lateral distances should be used, as smaller scanning intervals can resolve more lateral details. For instance, if the scanning interval is decreased, a single peak may be resolved into two separate peaks. However, a fine sampling interval may result in many redundant data points and greatly increase computing time, and therefore a compromise has to be reached in determining the choice of the measuring conditions to be used. In this study, the optimal scanning interval chosen was 5 μm, as this value was close to the smallest scanning interval of the instrument (i.e. 1 μm), and the amount of time taken to scan the surfaces at this scanning interval was still practical.

Most researchers using contact profilometers do not provide detailed information regarding the radius of the stylus tip, the scanning intervals, and the evaluation length

used to analyse the roughness of surfaces studied. It is therefore difficult to try and compare results of different investigators, as the reliability of measurements depends very much on these variables. Bowers *et al.* (1992) mentioned that they used a contact profilometer with a 1.5 μm radius diamond stylus to measure roughness along a 400 μm scan length during a 40 s scan. Three samples were measured for each group of substrates used in their cell culture studies. Among the surfaces which they analysed were cpTi polished to 600 grit and Ti blasted with 50 μm Al_2O_3 particles. The R_a value for the 600 grit Ti was reported as 0.14 ± 0.03 μm, while the sandblasted Ti had an R_a value of 0.87 ± 0.26 μm. Ungersbock and Rahn (1994) gave the R_a values for Ti blasted with Al_2O_3 particles (no particle size given) as 1.5 ± 0.2 μm. When compared, the results of the R_a values reported by Bowers *et al.* (1992) for the 600 grit Ti and the blasted Ti are 50% of the values reported by Ong *et al.* (1996) and Ungersbock and Rahn (1994). Ong *et al.* (1996) did not specify their evaluation length, but it was probably more than twice the evaluation length which was used by Bowers *et al.* (1992), whereas Ungersbock and Rahn (1994) clearly stated that their evaluation length was 1.3 mm with a cut-off of 0.25 mm.

In the present study, a cut-off (or sampling length) of 0.8 mm with an evaluation length of 4.8 mm was used for the contact stylus measurements. A small sampling length reduces the number of discrete height readings that can be made, and increases the variation between different sampling lengths. Increasing the cut-off value reduces the extent of this variation, and also increases the roughness value (Leitão and Hegdahl, 1981; Thomas and Charlton, 1981). It is therefore important that the evaluation length and cut-off values are specified when reporting surface roughness values.

The percentage increase in surface area for the trial surfaces and the test surfaces used in the cell culture studies are shown in Tables 2.1 and 2.2. For the trial surfaces, the surface area increase in Ti as received was only 4%, and the percentage increase in surface area for the smooth polished surfaces was less than 1%. This did not show a marked difference in surface area of the surfaces, even though it can be seen from the surface profiles (Figure 2.12) and the SEM micrographs (Figure 2.22) that they vary greatly in topography. These results were obtained using a 10 μm scanning distance with

150 sampling points, and they may be misleading as a more detailed information may have been lost by using the 10 μm scanning interval. The calculated area was therefore probably an underestimation of the effective surface area. However, when a 5 μm scanning interval with 300 sampling points was used to measure the same area, the percentage enlargement in the surface area increased to about 3 to 10 times, as more surface details were resolved (Table 2.2).

2.4.5.5 Use of surface filters

Filtering separates the different components of the topography according to the different frequency or wavelength. However, the use of surface filters has to be functionally justified (Stout *et al.*, 1993). Before comparisons were made of the roughness values obtained using the two instruments, the reference specimen for the Surftest 4 was analysed using the Proscan 1000. Using a 5 μm scanning interval with 300 sampling points, an R_a value of approximately 3.0 μm was obtained without using a surface filter. When a surface filter size of 1 was applied (see 2.2.2.3.4), this value was reduced to 1.70 μm. Therefore, a surface filter was not used when substrates were measured using the Proscan 1000.

2.4.6 Conclusions

This part of the study investigated systematically the variables that affect surface roughness values, and compared the relevance of two commonly used profilometer systems in characterising implant surfaces. The following conclusions were made:

1. The results of the measurements made using the contact surface profilometer and the laser scanning profilometer were different. These differences were basically due to: a). the different nature of methods of examination, i.e. one requires a pointer to track over material surfaces, while the other is a non contact, laser reflectivity technique, b). limiting factors inherent in the horizontal resolution of the two techniques used, i.e. one depends on the diameter of the diamond stylus used, and the other depends on the wavelength of the laser beam used, c). the different principles of profile image formation from which statistical measurements were computed, d). the size and character of the areas

measured, i.e. whether they were flat or curved surfaces. Generally, the contact profilometer gave smoother roughness values, while the laser scanning profilometer almost doubled these values. The choice of instrumentation used to characterise surface roughness may have important implications if an optimum roughness of an implant surface is to be predetermined for a desired tissue response.

2. For results using the same measurement technique to be comparable, details of scanning conditions and variables must be clearly stated. It is essential that the scanning interval and assessment length be quoted when roughness values are presented. For a certain assessment length, it is seen that increasing the scanning interval does not change the average height parameters significantly. However, values for extreme height and spacing parameters may be reduced markedly.
3. R_a is frequently used to quantify surface roughness. However, it is shown to be insensitive to significant measurement variables, and it should be used in combination with other parameters, like R_z, R_{max} and the spacing parameters. These parameters are more sensitive to measurement variables (Hall *et al.*, 1996). This is reflected by the large differences in these roughness parameter values when measurement conditions were varied.
4. SEM gives a good qualitative image of surfaces because of its high resolution, and should be used to supplement quantitative values of surface roughness. The confocal laser scanning microscope may be used as an alternative to other non-contact measurement techniques, as it enabled contour maps to be made of the surfaces being studied, and dimensional values can be given to these images.

This study has shown that each profilometer technique may be adequate in different situations, and that surface roughness of implant materials are best characterised by techniques which are able to complement each other in terms of making qualitative and quantitative measurements.

3. Adhesion and differentiation of osteoblast-like cells on metal substrates

3.1 Introduction

One of the requirements for a dental implant is a strong, intimate and stable adhesion to bone. There are many factors which are involved in determining the nature of the bone-implant interface, and among these are cellular responses to the implant. In order to ensure a close approximation of bone to implants, a knowledge of the responses of bone-forming cells to implants is essential. *In vitro* studies have shown that surface properties play an essential role in the response of osteoblast-like (OB) cells to dental implant materials. Besides reacting to material surface chemistry, OB cells are sensitive to differences in surface physical properties, particularly topography and roughness (Bowers *et al.*, 1992; Chehroudi *et al.*, 1992; Sinha *et al.*, 1994), and also to implant surface cleanliness and sterilisation techniques (Baier *et al.*, 1982; Doundoulakis, 1987; Swart *et al.*, 1992; Stanford *et al.*, 1994). Boyan *et al.* (1993) and Martin *et al.* (1995) have also suggested that cell responses may depend on their state of maturation, and that differentiation of immature OB cells may be enhanced or accelerated when the cells are cultured on rough surfaces.

3.1.1 Osteoblastic models used in bone-biomaterial studies *in vitro*

Rodan and Noda (1991) reviewed the models that are used to study osteoblastic gene expression *in vitro*. These include primary cultures, osteosarcoma derived cell lines, non-transformed cell lines, and experimentally immortalised cell lines. In implantology research, the use of primary cells, especially from the site where implants are to be inserted is ideal. Primary cultures allow better transferability of results obtained *in vitro* to osteoblasts *in vivo,* as they are likely to be more representative of the cells in the tissue from which they were derived, and if the cell culture conditions are appropriate, should express patterns of gene expression consistent with those found *in vivo* (Auf'mkolk *et al.*, 1985).

Primary cultures from bone tissues may be marrow, calvarial, or explant derived, isolated from mature or foetal bone donor sources, including humans (Davies, 1988; Doglioli and Scortecci, 1991; Puleo *et al.,* 1991; Bowers *et al.*, 1992; Chehroudi *et al.,* 1992; Groessner-Schreiber and Tuan, 1992; Swart *et al.,* 1992; Massas *et al.,* 1993; Howlett *et al.,* 1994; Keller *et al.,* 1994; Riccio *et al.*, 1994; Yliheikkilä *et al.,* 1995; De Santis *et al.*, 1996; Kornu *et al.,* 1996; Wilke *et al.*, 1998).

Bone tissues, primarily calvariae, from rat and rabbit are frequently used as a convenient source of bone cells. However, their use may have limitations in their relevance to adult human biology. Tomãs *et al.* (1997) compared the differences in the responses of rat, rabbit and human bone marrow cells to the corrosion products of a cobalt-chromium orthopaedic alloy and metal salts containing cobalt and chromium ions. Growth of human cells was inhibited when exposed to chromium ions, while there was no effect on the growth of rat and rabbit cells. Alkaline phosphatase (AP) activity of rat cultures was also much stronger than the activity of rabbit and human cultures. Although all cultures were able to form mineralised nodules, the nodules in rat cultures were bigger in size than the nodules in human and rabbit cultures.

Besides species variation, primary cultures are also not always available, difficult to establish, and are usually heterogeneous. Because of their ready availability, researchers have used human osteosarcoma derived cell lines, like the MG-63 and SaOS-2 cells (Martin *et al.,* 1995; Gronowicz and McCarthy, 1996; Price *et al.*, 1997). However, there are concerns about the predictability and differentiation state of these cells, and their phenotype may not reflect that of normal osteoblasts. This is a result of the deregulation of growth control which occurs in transformed cell lines, so that they may not follow the pattern of cell contact, proliferation and differentiation operative in normal cells (Lian and Stein, 1992). Malignant and transformed cells are also known to be less adhesive than normal cells, and the lost in anchorage-dependent growth control is one of the major characteristics of tumour cells (Plantefaber and Hynes, 1989).

MG-63 cells have some of the properties of normal human OB cells, as $1,25(OH)_2D_3$ also stimulates their AP and osteocalcin synthesis (Mahonen *et al.*, 1990;

Lajeunesse *et al.*, 1990; Clover and Gowen, 1994). Unlike MG-63 cells, the AP levels in HOS cells were not increased by $1,25(OH)_2D_3$, and no osteocalcin was detected in supernatants from HOS cells, even following treatment with $1,25(OH)_2D_3$ (Clover and Gowen, 1994). Like HOS cells, the U-2 OS cells also do not produce osteocalcin, with or without the addition of $1,25(OH)_2D_3$, and their basal AP level is also not significantly raised by treatment with $1,25(OH)_2D_3$ (Mahonen *et al.,* 1990).

The conditions for MG-63, HOS and U-2 OS cells to produce matrix which would mineralise in culture are not known (Hughes and Aubin, 1998b; Lincks *et al.*, 1998c), although other human osteosarcoma cell lines, like the HOS and SaOS-2 cells, have been reported to do so under appropriate culture conditions (Carvalho *et al.*, 1995; Ahmad *et al.*, 1998). Ahmad *et al.* (1998) observed mineralisation in SaOS-2 cells grown on metallic discs in culture supplemented with ascorbate, with or without 3 mM β-glycerophosphate. Mineralisation increased with time over a six week period and was based on the expression of the non-collagenous proteins, bone sialoprotein and osteocalcin, in addition to the presence of mineralised nodules. However, it was unclear if true calcification had occurred. Although calcification on the Ti alloy used was confined to the nodules formed, calcification on the cobalt-chromium alloy was diffuse across the surface of the discs. This may indicate dystrophic, rather than physiological calcification, as no microanalysis of the nodules formed was carried out to determine their precise mineral composition.

As an alternative to the use of human osteosarcoma cell lines, experimentally immortalised cell lines of human origin could be used. An example is the SV40 conditionally transformed adult osteoblastic cell line, HOB-02-C1 (Bodine *et al.*, 1996), which exhibits a transformed phenotype under specific culture conditions, but will revert to a normal phenotype when these conditions are modified. This would allow homogeneous cell populations to be maintained, and terminal differentiation of the cells could also be assessed on biomaterials, as the extracellular matrix (ECM) would mineralise in culture. A search of the literature did not reveal that such a cell line of human origin has been used in cell-biomaterial interaction studies.

The purpose of this part of the study was to compare the adhesion and differentiation of OB cells cultured on commercially pure titanium (cpTi) and zirconium (cpZr) surfaces with different roughnesses *in vitro.* Although there have been several studies reporting *in vitro* responses of different cells to various implant and orthopaedic materials, there have been no published reports of studies comparing the effects of material surface properties on the three human OB cell lines used in this study (MG-63, HOS and U-2 OS). Even though transformed cell lines may not be representative of normal cells, these cells are suitable as osteoblastic models for this study as two of the cell lines (MG-63 and HOS), exhibit some of the normal OB cell behaviour in culture, particularly their adhesion properties and integrin expression (Clover and Gowen, 1994). MG-63 cells have been used in previous investigations of cell-biomaterial reactions (Martin *et al.*, 1995; Price *et al.*, 1997), while HOS and U-2 OS cells have not been used in any published reports of this kind.

3.2 Materials and Methods

3.2.1 Cell culture

3.2.1.1 OB cell cultures

Human osteosarcoma derived OB cells were recovered from frozen stock. These cell lines were used because of their homogeneity and consistency, and because the same cell stock could be used continuously by passaging and keeping them frozen for use in repeated tests. Three cell lines were used to overcome concerns about the unpredictable behaviour of transformed cells, the possibility that the cells in each cell line may be in different states of maturation, and also to minimise the risks of results being artefacts of a particular cell line.

3.2.1.2 Substrates used for cell culture

The choice of substrate material and material surface preparation and analysis are discussed in Chapter 2. The substrates used for this part of the investigation were rough "as received" cpTi, and smooth, polished cpTi and cpZr surfaces. After surface preparation, the discs were cleaned as described in Chapter 2. Cleaned discs were kept

in 70% alcohol for storage. Before use for cell culture, they were air-dried in a tissue culture hood and sterilised by exposing to ultraviolet light for one hour on each side.

3.2.1.3 Culture medium

The medium used for cell culture and subsequent experiments was α-minimal essential medium (α-MEM) (GibcoBRL, Life Technologies, Paisley, Scotland), prepared in distilled water and supplemented with:

a. 1 µl/ml fungizone, from a 250 µg/ml stock solution (GibcoBRL, Scotland)
b. 1 µl/ml gentamicin, from a 100 mg/ml stock solution (GibcoBRL, Scotland)
c. 10% foetal calf serum (FCS) (Globepharm Ltd., Surrey, England), and
d. 2.2 g $NaHCO_3$ per litre of medium (Sigma Chemical Co., St. Louis, MO, U.S.A.).

3.2.1.4 Thawing cells from liquid nitrogen

Cells were recovered from cryostorage, thawed, and the cell suspension transferred to a centrifuge tube containing 5 ml of medium, and centrifuged at 1000 rpm at 4°C for 5 minutes. Cells were then cultured in 80 cm^2 tissue culture flasks (Nunc Brand Products, Nalge Nunc International, Denmark) in 15 ml medium supplemented with 10% FCS.

3.2.1.5 Cell maintenance and passage

Cell lines were maintained at 37°C in a humidified atmosphere of 95% air:5% CO_2 and passaged when confluent. The confluent monolayer was washed with phosphate buffered saline (PBS) and then incubated in 5 ml trypsin/EDTA solution (GibcoBRL, Life Technologies, Paisley, Scotland), until the cells were rounded up and the cell layer separated from the bottom of the flask (5-10 minutes at 37°C). After gentle agitation to ensure complete separation, the cell suspension was removed to a sterile universal container containing medium with 10% FCS to stop the trypsinisation reaction, and the flask rinsed with PBS to collect residual cells. This was then pooled with the cell suspension. The cells were pelleted by centrifugation at 1000 rpm for 5

minutes at 4°C. The supernatant was discarded, replaced with fresh medium, and the cell pellet dispersed by gentle agitation with a Pasteur pipette and resuspended in the medium. The cells were then either placed in two new flasks for further sub-culture, or used for experimentation.

3.2.1.6 Cell count

Before counting, the cell suspension was disaggregated in the medium by gentle agitation with a pipette, and then passed through a sterile nylon sieve with a 90 μm mesh size to ensure that there was no clumping of cells. A 20 μl aliquot was removed and the cell number in the suspension determined using a haemocytometer. At least two counts were taken for each cell population and a mean calculated. The cell suspension was then serially diluted with medium at the desired density for use in the various experiments.

3.2.2 OB cell responses to metallic substrates

3.2.2.1 Cell attachment to cpTi surfaces

The 15 mm diameter cpTi substrates fitted in the approximately 16 mm diameter wells of 24-well tissue culture plates (Nunc Brand Products, Nalge Nunc International, Denmark). Cells cultured directly in the tissue culture plastic wells were used as controls. Cells were seeded at a plating density of 7.5×10^4 cells/well in serum-free medium (SFM), and allowed to attach for 2 h and 24 h in an incubator under standard tissue culture conditions (37°C, 5% CO_2:95% air). This plating density resulted in a confluent monolayer of cells in the wells after 24 h. Triplicate wells were used for each test and control cultures. Cultures on the opaque metal substrates were indirectly monitored using phase contrast microscopy, by comparison with cultures grown in the plastic control wells. After incubation at the stated times, medium from all the wells were removed, washed gently once with 1 ml of PBS to remove any unattached cells, and the medium replaced with 400 μl SFM. The number of attached cells at the end of each incubation period was then estimated using the Cell Titre 96AQ ^{TM}(Pro Mega) MTS assay (Promega Corporation, Madison, WI, U.S.A.).

The manufacturer's protocol for the assessment of the number of cells in 96-well tissue culture plates was modified as the cells were grown on opaque metal surfaces in 24-well tissue culture plates. Reagents for the Cell Titre 96AQ assay were prepared just before use according to the manufacturer's instructions. Briefly, 2 ml MTS solution and 100 µl PMS solution (or 20:1 part MTS:PMS solution) were mixed. Then 80 µl of the MTS/PMS solution was added to each well containing the 400 µl fresh medium. The 24-well plates were then incubated at 37°C in 5% CO_2 for 4 h in the dark. Wells with SFM alone (without cells) were also incubated with the MTS/PMS solution to serve as background controls. After 4 h, 100 µl aliquots of the dye-containing medium was aspirated from each test well, and these aliquots were transferred to a minimum of 2 wells in a 96-well tissue culture plate (Nunc Brand Products, Nalge Nunc International, Denmark). The mean values of the absorbances from these 96-wells were calculated to give the absorbance of each test well. Absorbance was measured using an enzyme-linked immunosorbant assay (ELISA) plate reader (Reader 340 ATTC, SLT Labinstruments, Salzburg, Austria) at 492 nm.

To construct a standard curve for each experiment carried out, cells were plated in SFM directly in the 24-well plates at different concentrations ranging from 1×10^4 to 2×10^5 cells/well for each incubation period. Metabolic activity of the cells was reflected by the increase in the optical density (OD) of wells containing increasing cell concentrations over the range of cell densities examined. These standard curves were used to convert all absorbance values from the test wells into cell numbers. The average number of cells attached to the cpTi substrates for all cell lines at both incubation periods was determined after triplicate experiments were carried out.

3.2.2.2 Acridine orange staining of cells on cpTi surfaces

In order to verify that cells were attached to the metals at the end of each incubation period, and to qualitatively confirm the results of the MTS assay, some cells were stained with acridine orange.

Wells were washed once with 1 ml PBS to remove unattached cells. Attached cells were fixed in absolute alcohol for 30 minutes. They were then passed through

descending grades of alcohol (70% and 50%) into distilled water, rinsed in 1% acetic acid for a few seconds, and in two 1-minute changes of distilled water. Cells were then stained with diluted acridine orange solution (0.01% aqueous acridine orange in pH 6.0 phosphate buffer) for 3 minutes, rinsed in pH 6.0 buffer for 1 minute, and in 0.1 M calcium chloride solution for ½-1 minute, followed by a final rinse in pH 6 phosphate buffer solution. CpTi discs with labelled cells were then removed from the wells and attached to glass slides using cyanoacrylate cement, coverslipped with a drop of Apathy's mountant (Raymond Lamb, London, U.K.), and examined with a fluorescence microscope equipped with epifluorescence (Zeiss Axioskop, Germany) with ×20 and ×40 objective lenses.

It was difficult to view cells on the surface of the rough as received Ti using the fluorescence microscope, due to the background fluorescence from the surface and the different depths of focus created by the rough surface of the metal. This made accurate counting of cells stained with acridine orange impossible. However, it was possible to use this technique to make a qualitative assessment of the number of adherent cells present. Quantitative data on the number of cells adherent to each surface was provided by the MTS assay.

3.2.2.3 Scanning electron microscopic (SEM) examination of cellular morphology

To observe the morphology of cells on the substrates after 2 h and 24 h of attachment, some cells grown on the cpTi substrates were prepared for SEM. At the end of the incubation period, cells were fixed in 1 ml of 3% glutaraldehyde in 0.1 M cacodylate buffer at 4°C, and post-fixed in a 1% osmium tetraoxide solution for 2 h at 4°C. Dehydration was achieved by successive rinses in graded concentrations of alcohol (50%, 70%, 90%, 100%), followed by three 10-minute changes of 100% acetone, before being processed through a critical point drier, Balzer CPD 020 (Balzers Union, U.K.). Specimens were mounted on aluminium stubs using carbon conducting cement, and sputter coated with gold-palladium (Polaron E5000, Bio-Rad, U.K.). The samples were then examined at 15 kV in a Cambridge 90B scanning electron microscope (Cambridge, U.K.).

3.2.2.4 Cell proliferation

Cell proliferation on cpTi, cpZr, and tissue culture control surfaces was assessed using a microplate immunoassay to detect incorporation of 5-bromo-2'-deoxy-uridine (BrdU) into cellular DNA (Boehringer Mannheim GmbH, Germany). 5×10^4 cells per well were seeded onto the various surfaces and allowed to equilibrate for 24 h in medium plus 10% FCS. At this time, cells in the tissue culture plastic wells were about 75% confluent. Cells in all wells were then washed twice with PBS to remove unattached cells, the medium replaced with 400 µl fresh medium, and the cells incubated for another 20 h. The manufacturer's protocol on assessing cell proliferation was then followed, using materials from the assay kit. 40 µl of BrdU labelling solution was added per well, and cells incubated for a further 4 h at 37°C. At the end of that time, medium was carefully removed and wells washed twice with PBS. Attached cells were fixed with 0.5 M ethanol/HCl for 30 minutes at -20°C. The incorporation of BrdU into DNA of the cells was detected using a mouse monoclonal antibody to BrdU, and the binding of the antibody was quantified using a standard immunoperoxidase technique. 100 µl of the coloured product from each well was then transferred to 96 well plates and the absorbances read at 405 nm. Wells containing pure peroxidase were used as blanks to compensate for any background absorbancy.

3.2.2.5 Assessment of cellular differentiation

To assess the effects of the substrates on OB cell differentiation, cells grown on the various substrates were examined for AP expression, synthesis of osteocalcin and mineralisation in culture when supplemented with 10 mM β-glycerophosphate and 50 µg/ml Asc-2P, a long-acting ascorbate analogue (Wako Chemicals GmbH, Neuss, Germany).

3.2.2.5.1 Total alkaline phosphatase (AP) activity in the cell layers

The cell lines were first tested on control tissue culture plastic to confirm that they had AP activity, and that this activity was enhanced when $1,25(OH)_2D_3$ (Vit D_3) and hydrocortisone (HC) were added to the tissue culture medium. Later, the cell lines

were cultured on the metallic substrates, in medium plus 10% FCS, to test if substrate surface roughness alone had any effect on the AP activity.

3.2.2.5.1.1 The effect of Vitamin D_3 and hydrocortisone on the AP activity of the three OB cell lines

$1,25(OH)_2D_3$ (Calbiochem, La Jolla, CA, U.S.A.) was solubilised in ethanol, and stored as a stock solution (10^{-4} M) in gaseous nitrogen. Just before use, the stock preparation was diluted 1:10 (v/v) with α-MEM, and 1 µl of this working solution was used for every 1 ml medium used in culturing the cells. Two culture conditions were used: a). Medium +10% FCS, and supplemented throughout the culture period with 10^{-8} M Vit D_3 and 10^{-7} M HC (positive control wells), and b). medium +10% FCS alone. As Vit D_3 is light sensitive, care was taken to maintain supplemented cultures in the dark.

For each culture condition, 1×10^4, 4×10^4 and 1×10^5 cells/well were plated in quadruplicate wells. At the end of 24 h, wells with 1×10^5 cells/well were already confluent. Medium was changed for all the wells, and the cells were cultured for 72 h with another medium change after 48 h. At the end of 4 days in culture, medium in all wells was replaced with 500 µl SFM, and cells were left for a further 24 h. Wells were then washed twice with PBS, and attached cells were lysed with 200 µl of cell lysis buffer per well. The buffer was made up of 50 mM Tris (pH = 7.5), containing 0.9% NaCl and 0.1% Triton X-100 in distilled water.

The cells were then freeze-thawed twice (freeze at -70°C, and thaw at 37°C) to aid cell breakdown and release of AP. To ensure the detachment and breakdown of cells, they were scraped off the top of the discs and the bottom of the wells with an appropriate tool. Cell lysates with the same cell concentration and condition were then pooled in 2 ml eppendorfs, and centrifuged at 2000 rpm for 30 minutes before being analysed for AP activity.

To standardise the amount of protein present in the cell lysates, total cell layer protein in the pooled lysates was assessed using the Biocinchoninic acid (BCA) protein

assay (Pierce Chemicals, Rockford, Illinois, U.S.A.). 10 µl of the cell lysates, test blank (PBS only), and test standards (2 mg/ml BSA diluted in PBS to various concentrations ranging from 20 µg/ml to 1280 µg/ml) were placed in triplicate wells of a 96-well tissue culture plate. 200 µl of the BCA working reagent was then added to each well. One side of the plate was gently tapped to mix the samples and to start the reaction, and to ensure absence of air bubbles. The plate was then incubated at 37°C for 30 minutes, at the end of which the absorbance was read at 550 nm using a microplate reader. The concentration of protein present in the cell lysates was determined by reference to the standard curve, obtained using known concentrations of the test standards.

AP activity in the cell lysates was assessed as follows. In each well of a 96 well plate, 50 µl Tris buffer (pH 9), 50 µl $MgCl_2$, 50 µl stock substrate solution (p-nitrophenyl phosphate, p-npp (Code 104-40, Sigma), prepared by dissolving 40 mg of p-npp in 10 ml of distilled water) and 50 µl cell lysates (diluted in PBS to compensate for differences in the protein concentrations) were mixed. The samples were then incubated for 30 minutes at 37°C. At the end of 30 minutes the reaction was stopped by adding 50 µl of 2 M NaOH to each well. The amount of p-nitrophenol released was determined using a microplate reader at 405 nm. The results from the test samples were compared to a standard curve which was obtained by diluting appropriate volumes of p-nitrophenol standard, 10 µmol/ml (Code 104-1, Sigma), in 0.02 N NaOH. The standards used ranged from 0.005-0.1 µmol/ml, and AP activity was expressed as µmol p-nitrophenol released/mg protein/min. Experiments to assess the effects of Vit D_3 and HC on the AP activity of the three cell lines were repeated three times.

3.2.2.5.1.2 AP activity of OB cells grown on metallic substrates

MG-63, HOS and U-2 OS cells were seeded into 24-well plates containing the various metal substrates (Ti as received, polished Ti, and polished Zr) at a density of 4×10^4 cells/well. The cells were grown in medium plus 10% FCS, without the addition of Vit D_3 and HC. Cells reached confluence in 48 h. Confluent cells were washed twice in PBS, and the medium in all wells replaced with 1 ml fresh medium. The cultures were then incubated for a further 48 h. At this time, the medium in all wells was replaced with 500 µl SFM and left overnight, after which the cell layers were lysed and

assessed for AP activity as described above.

3.2.2.5.2 Osteocalcin

Cultures on plastic substrates were grown in two conditions: a). Medium supplemented throughout the culture period with 10^{-8} M 1,25$(OH)_2$Vitamin D_3 and 10^{-7} M HC (positive control wells), and b). medium plus 10% FCS alone. Cultures on all metal substrates were grown in medium plus 10% FCS only. 1×10^4 cells/well were plated into triplicate wells for each substrate type. At the end of 48 h, medium was changed for all the wells, and they were then left for another five days, with medium changes every 48 h. At the end of seven days in culture, medium in all wells was replaced with 500 µl SFM and left overnight. The following day, supernatants were collected and stored at -70°C, until assayed.

Osteocalcin released into the medium was determined by a specific enzyme immunoassay, the Novocalcin assay (Metra Biosystems UK Ltd., Great Haseley, Oxford, U.K.). The Novocalcin assay is a competitive ELISA system which measures newly synthesised intact osteocalcin. 25 µl of osteocalcin standards or samples were added to 125 µl of anti-osteocalcin antibody in osteocalcin coated strips/wells provided with the kit, and incubated for 2 h at room temperature. The strips were then washed three times with 300 µl of wash buffer. 150 µl of reconstituted enzyme conjugate was then added and the samples incubated for 1 h. The wells were then washed three times with 300 µl of wash buffer. 150 µl of working substrate solution was then added to each well, and incubated for 30 minutes. 50 µl of 3 N NaOH was finally added to each well to stop the reaction, and the absorbance read at 405 nm using a microplate reader. The concentration of osteocalcin present was determined by reference to a standard curve, which was calculated from known osteocalcin standards. The results were expressed as amount of osteocalcin liberated in ng/ml supernatant, and were not corrected for protein content.

3.2.2.5.3 Mineralisation in culture

To test if the cells can produce matrix which would mineralise when cultured on the metal substrates, OB cells were cultured for 10-14 days. 5×10^4 cells per well were seeded in medium +10% FCS in 6-well plates containing the metal substrates. After 24 h, the wells were washed once with PBS to remove unattached cells, and the medium was changed to a supplemented medium, containing 50 μg/ml Asc-2P and 10 mM β-glycerophosphate. Medium was changed every two days and the cells surrounding the metal substrates in the 6-well plates were routinely examined with phase contrast microscopy. After 10-14 days (when cell layers were seen to detach from the substrates), cells were immediately fixed in 2.5% glutaraldehyde for SEM-EDAX analysis. Cultures were not able to be left longer than 14 days in culture.

3.2.2.5.3.1 X-ray microanalysis

The ability of the cells to produce calcified deposits was assessed by analysis of the surface of the substrates on which cells were grown using the energy dispersive x-ray analysis (EDAX). The samples for EDAX were prepared as for SEM, however, they were not post-fixed in osmium tetraoxide. Fixed samples were studied with a scanning electron microscope (JEOL 820). The EDAX system is a Kevex Sigma Gold equipped with a super quantum detector x-ray analyser. Single spot analysis was performed on selected areas of the substrate surface where MG-63 and U-2 OS cells were cultured at an accelerating voltage of 10 kV. The scans were obtained by analysing the spots for about 1000 sec per area. For scans of material on cpTi substrates, the quantification programme of the machine was able to normalise the results by extracting the Ti peaks from the Ca and P peaks, so that the results obtained were the actual concentrations of the elements Ca and P (in atomic %) present on each spot scanned. However, it was unable to do this with the Zr peaks for materials on the cpZr surfaces, without interfering with the results of the other peaks. As our interest was in the Ca to P ratio as an index of hydroxyapatite formation, no calculation was made to correct for the presence of the Zr peaks in the scans of the other elements.

3.2.3 Statistical analysis

Cell attachment data were subjected to normal probability plots, and found to have a normal distribution. Data are expressed as the mean number of attached cells ± s.d. of three experiments, and analysed by the analysis of variance (ANOVA). The Student's *t*-test was then used to determine if differences in mean number of cells attached on two different substrates were statistically significant at $P < 0.05$. In all figures for the cell attachment results, the error bars reflect the standard deviation for the data series.

For cell proliferation, AP and osteocalcin assay results, non-parametric tests were used, and the results are presented graphically as box and whisker plots. The box contains the interquartile range which comprises 50% of the values, with the whiskers extending from the box to the highest and lowest values obtained, and the median shown by a line across the box. Markers (*) show outlying values. The Mann Whitney U-test was used to test if the median values between two substrates were significantly different at $P < 0.05$.

3.3 RESULTS

3.3.1 Cell morphology at 2 h and 24 h attachment on cpTi surfaces as revealed by acridine orange staining

Acridine orange staining verified that there were cells attached to the metals at both times tested. All cell lines showed the same morphological appearance and this is illustrated by using the HOS cells. Figure 3.1 shows the representative morphology of the cells at 2 h of attachment. Although some cells had begun to spread, the majority of cells were still rounded. Some cells were seen in clumps, especially cells on the rough surfaces.

Figure 3.2 shows that by 24 h, almost all cells had spread. Clumping of cells was also seen. Only micrographs of cells cultured on smooth surfaces are illustrated due to the high level of background fluorescence encountered on the rough surfaces.

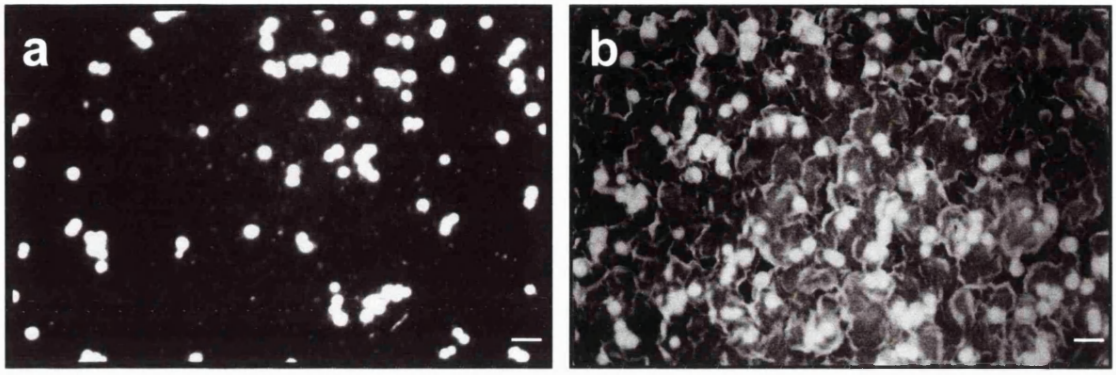

Figure 3.1 The morphological appearance of HOS cells on polished Ti (a) and Ti as received (b) at 2 h attachment. They are shown as representative illustrations for the behaviour of all the cell lines tested at 2 h. At this time, cells were still rounded on both surfaces. Original magnification × 200. Bars denote 10 μm.

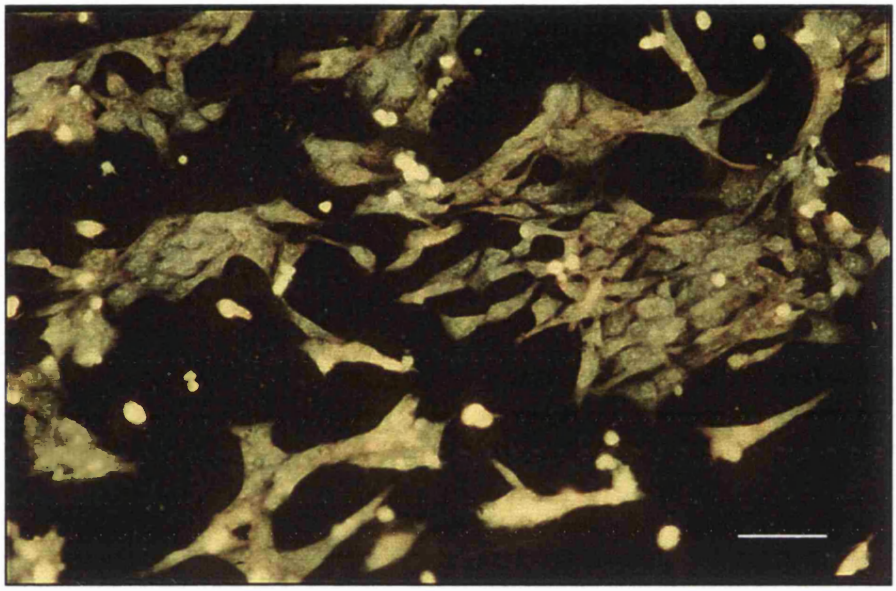

Figure 3.2 Morphology of HOS cells on polished Ti at 24 h attachment. The cells are spread in all directions. Some cells are in clusters. Acridine orange stain, original magnification × 400. Bar denotes 10 μm.

3.3.2 SEM evaluation of typical OB cell morphology at 2 h and 24 h attachment on cpTi surfaces

At 2 h, the majority of cells cultured on rough and polished Ti had begun to spread and extended processes or filopodia which contacted the substrates via discrete focal points at the base of the cells (Figures 3.3a and 3.3b). Cells spread better on the polished Ti (Figure 3.3a), as it is seen that OB cells on the rough "as received" surface (Figure 3.3b) are more spherical, and have more surface blebs, providing them with a rougher texture than cells on polished Ti. On both surfaces, cells did not spread in any particular direction.

On the polished Ti surface, the cell bodies seemed to spread and conform to the underlying smooth surface, although spread cells did not show any inclination to align along the surface grooves. On the rough surface, although the cell bodies lay in the grooves of the rough surface, once spread, they were able to bridge across the depressions and did not appear to intimately conform to the concavities (Figure 3.3b). Figure 3.3b also shows that the width of the concavities of the rough Ti surface is about 1-1½ times the diameter of the cells, and just about the same height as the cell bodies. At 24 h, surface blebs were no longer seen, and this indicates that the cells on both surfaces were well spread (Figures 3.4a and 3.4b). At this time also, cells on both surfaces were confluent (Figures 3.5a and 3.5b).

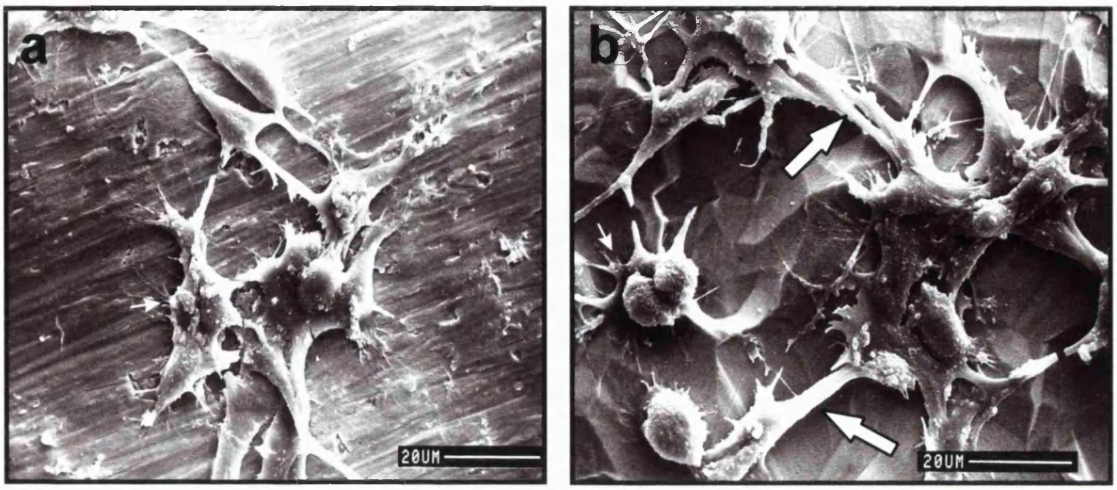

Figure 3.3 SEM of HOS cells at 2 h attachment on polished Ti (a) and Ti as received (b). Note the clear difference in the topography of the substrate surfaces. Cells on both surfaces exhibit surface blebs and cell processes. However, surface blebs are more prominent on cells grown on the rough surface. Small arrowheads show discrete points of attachment of cells to the substrates, while arrows show the bridging of spreading cells across the peaks of the rough Ti surface (Original magnification × 1000).

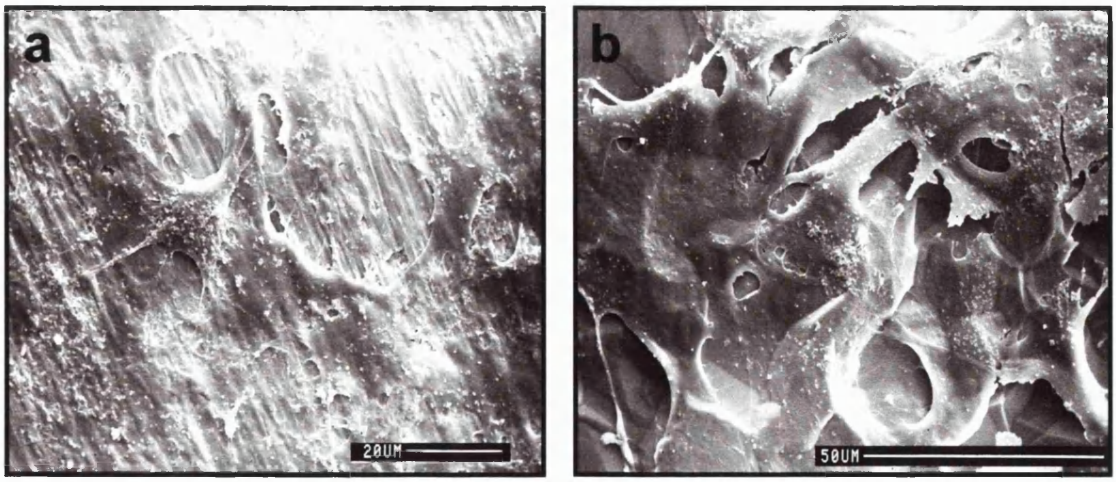

Figure 3.4 SEM of HOS cells at 24 h attachment on polished Ti (a) and Ti as received (b) under high power (original magnification × 1000). At this time, cells are flattened and well spread. Cell surfaces are smoother than at 2 h, and no surface blebs are seen on the OB cells on either surface. The cell periphery is not as readily seen on the polished surface as it is on the rough Ti surface.

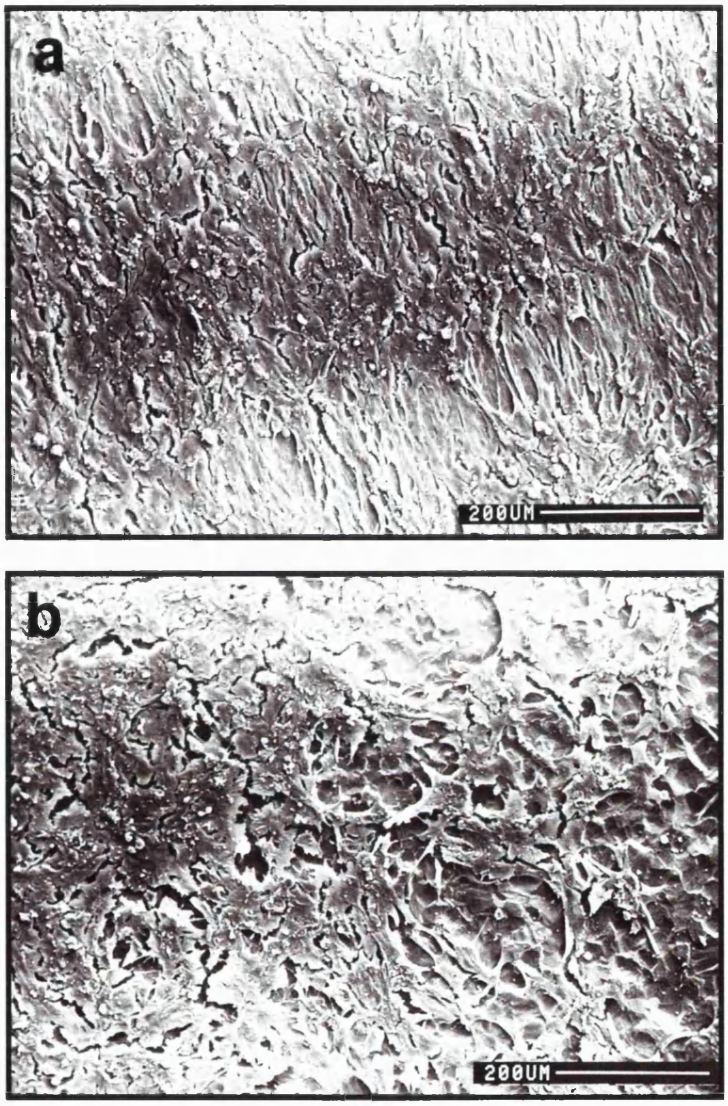

Figure 3.5 SEM showing a confluent layer of HOS cells covering polished Ti (a) and Ti as received (b) at 24 h attachment in serum-free medium (original magnification × 120). By 24 h, all cells were completely spread. The SEM evaluation at this resolution suggests that cells on polished Ti may have aligned themselves along the grooves which resulted from the polishing procedure, while cells on the rough surface tend to spread in all directions.

3.3.3 Cell attachment on cpTi surfaces

The results of the cell attachment assays in serum-free medium are presented in Figure 3.6. Although the bar charts may suggest that there were more cells attached to the polished Ti than to rough "as received" Ti at 2 h, and more cells attached to rough Ti than to polished Ti at 24 h for all cell lines, these differences were not statistically significant ($P > 0.05$). When the number of attached cells on metal substrates was compared to the number of attached cells on tissue culture control plastic, there was no statistically significant difference between the MG-63 and U-2 OS cell lines. However, there were significantly more HOS cells attached to the control plastic than to either the rough "as received" cpTi or the polished cpTi substrates, both after 2 h and 24 h attachment ($P = 0.004$). At 2 h, the 95% confidence limit for the difference in the mean number of cells attached to Ti rough and the control plastic, and for polished Ti and the control plastic for HOS cells were 9.4×10^3 to 4.8×10^4 cells, and 6.8×10^3 to 4.0×10^4 cells, respectively. At 24 h, the 95% confidence limit for the difference in the mean number of cells attached to Ti rough and the control plastic, and for polished Ti and the control plastic for HOS cells were 7.9×10^3 to 6.3×10^4 cells, and 3.6×10^4 to 6.9×10^4 cells, respectively. When cell attachment on the same substrates was compared, no difference was found in the attachment of the different cell lines to the same substrates.

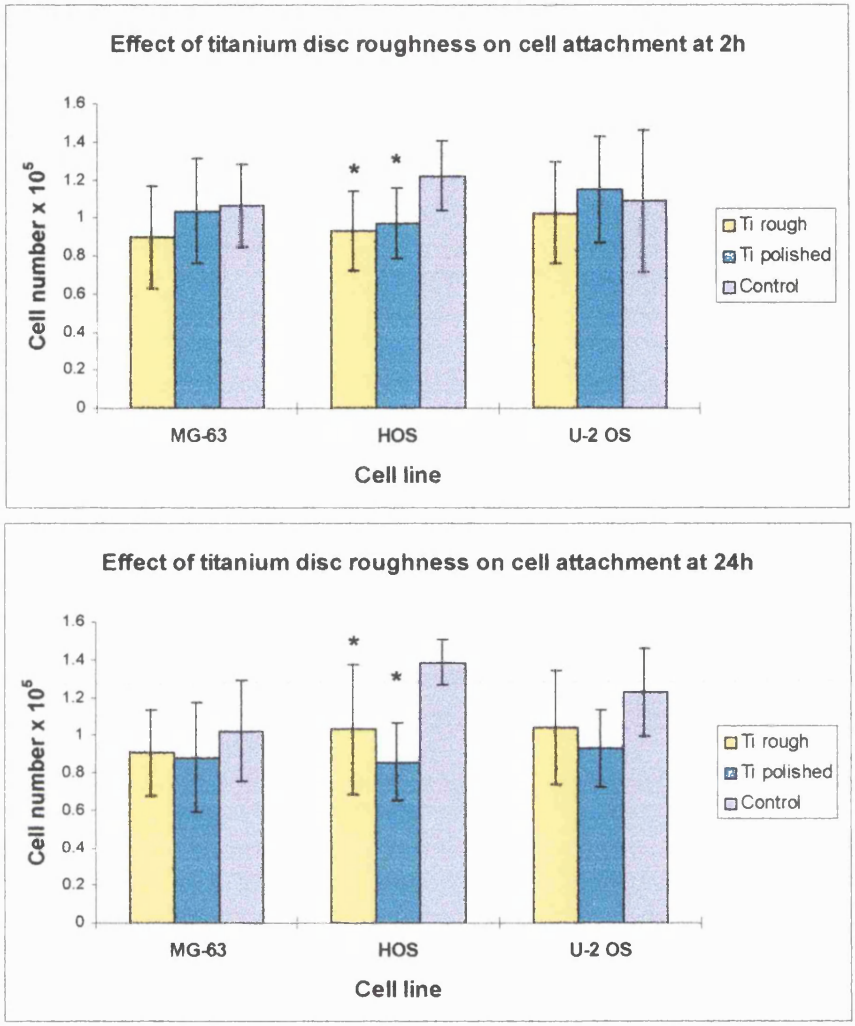

Figure 3.6 Bar charts showing the relative number of cells (mean ± s.d.) attached to cpTi substrates and control tissue culture plastic. Data are mean results from three replicate experiments. At 2 h and 24 h, 60-90% of cells plated had attached, but there was no significant difference ($P > 0.05$, titanium discs vs. control plastic) in the number of cells adherent to either the rough "as received" or polished Ti surfaces for MG-63 and U2-OS cell lines. However, at both times, there were more HOS cells attached to the tissue culture plastic control wells than to both cpTi surfaces (*$P < 0.01$). When the three cell lines were compared, no significant difference in cell attachment to similar substrates was detected.

3.3.4 Cell proliferation

As shown in Figures 3.7-3.9, at 48 h after plating on the substrates, cells appeared to proliferate better on metals than on plastic for all cell lines. Although there was one different result for the U-2 OS cell line, where cell proliferation on Ti polished was lower than on the tissue culture control plastic surface, this was an isolated result. In general the results clearly show that cells proliferate better on metals than on tissue culture plastic. However, the proliferation rate of cells on the different metallic surfaces were variable and not consistent.

3.3.5 AP activity

Figure 3.10 shows that addition of Vit D_3 and HC to the medium enhances the AP activity of all the cell lines, and especially for the MG-63 cell line, where the AP activity was enhanced by more than 50%. On the other hand, surface chemistry and roughness of the substrates alone had no such effect on the AP activity of all the cell lines (Figures 3.11-3.13). Each experiment showed a consistent trend to demonstrate that there was no difference in the AP activity of cells grown on the different substrates.

3.3.6 Osteocalcin production

Figure 3.14 shows the effect of the substrates on osteocalcin production of the cell lines used in this study. Vit D_3 and HC in the medium were not seen to have any stimulatory effect on the osteocalcin production of these cell lines. For HOS cells, there was no difference in the osteocalcin production of the cells grown on all the different substrates. For MG-63 cells, osteocalcin production of cells grown on the rough as received Ti was significantly higher than those of the cells grown on the other substrates, while for the U-2 OS cells, the osteocalcin production of the cells grown on polished Zr surfaces was significantly higher than those of the cells grown on the other substrates.

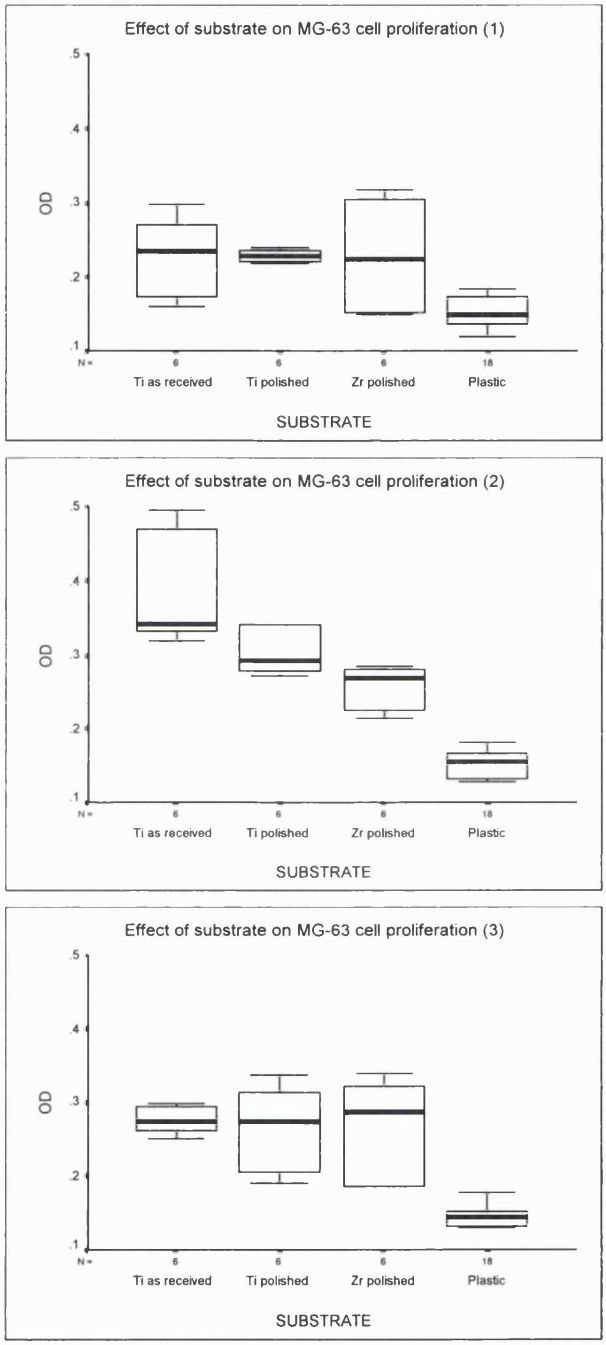

Figure 3.7 Effect of substrate on MG-63 cell proliferation 48 h after cell inoculation. Generally, cells proliferated better on all metals than on tissue culture plastic ($P < 0.02$). In all three experiments, the cell proliferation rate on the control plastic was similar. However, cell proliferation on the metallic substrates was not. The results of experiments 1 and 3 show that there was no significant difference in the cell proliferation rate on the metallic substrates. In experiment 2, there was increased cell proliferation on both Ti substrates compared to Zr ($P = 0.01$ for Ti as received vs. polished Zr, and $P = 0.04$ for polished Ti vs. polished Zr), but there was no significant difference in the cell proliferation activity between the two Ti substrates.

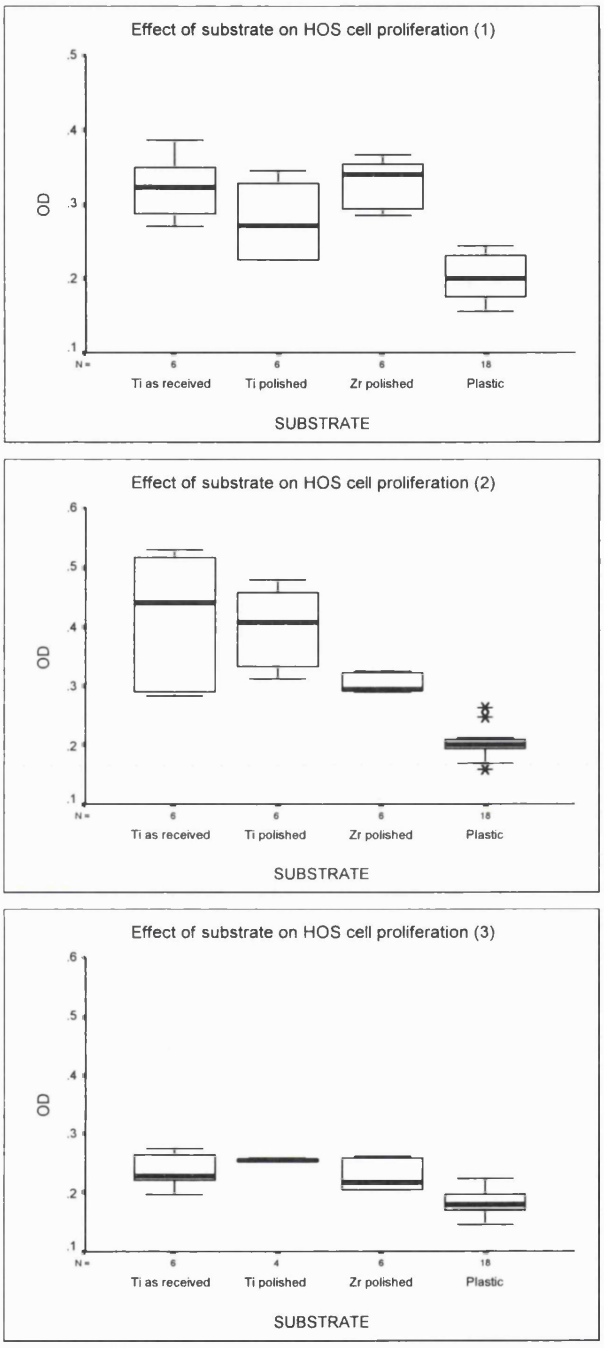

Figure 3.8 Effect of substrate on HOS cell proliferation 48 h after cell inoculation. The proliferation rate of cells on all metals was significantly higher than that on tissue culture plastic ($P < 0.02$). Although cell proliferation on the plastic was similar, cell proliferation on the metallic substrates was variable. In experiments 1 and 3, there was no significant difference in the cell proliferation rate on all the metallic substrates. In the second experiment, there was increased cell proliferation on Ti polished when compared to that on polished Zr ($P = 0.01$), although there was no significant difference in the cell proliferation between Ti as received and Zr. There was also no significant difference in the cell proliferation rate on either Ti substrate.

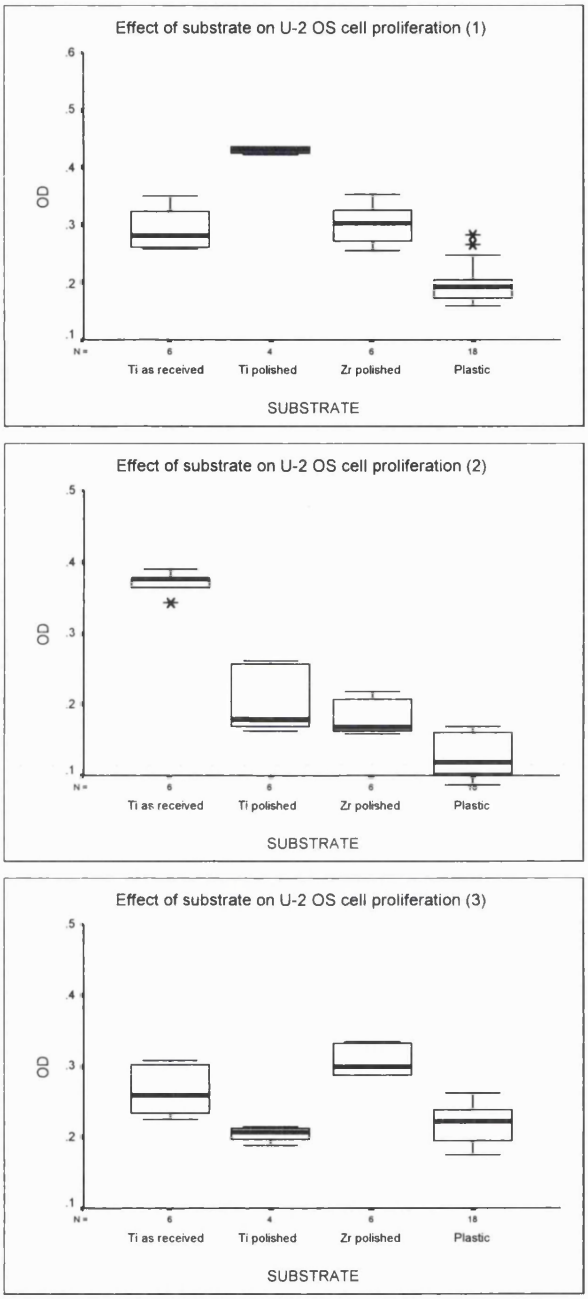

Figure 3.9 Effect of substrate on U2-OS cell proliferation 48 h after cell inoculation. Cell proliferation on all substrates was variable. In the first two experiments, cells proliferated better on the metals than on plastic ($P < 0.02$), In the first experiment, cell proliferation was highest on Ti polished compared to Ti as received and Zr ($P < 0.01$), with no significant difference in the cell proliferation rate between Ti as received and Zr. In the second experiment, cell proliferation on Ti as received was significantly different from the cell proliferation on Ti polished and Zr ($P = 0.01$), with no significant difference in cell proliferation on Ti polished and Zr. In the third experiment, although cells proliferated better on Ti as received and on Zr than on plastic ($P < 0.01$), there was no difference between the proliferation rate of cells grown on plastic and polished Ti.

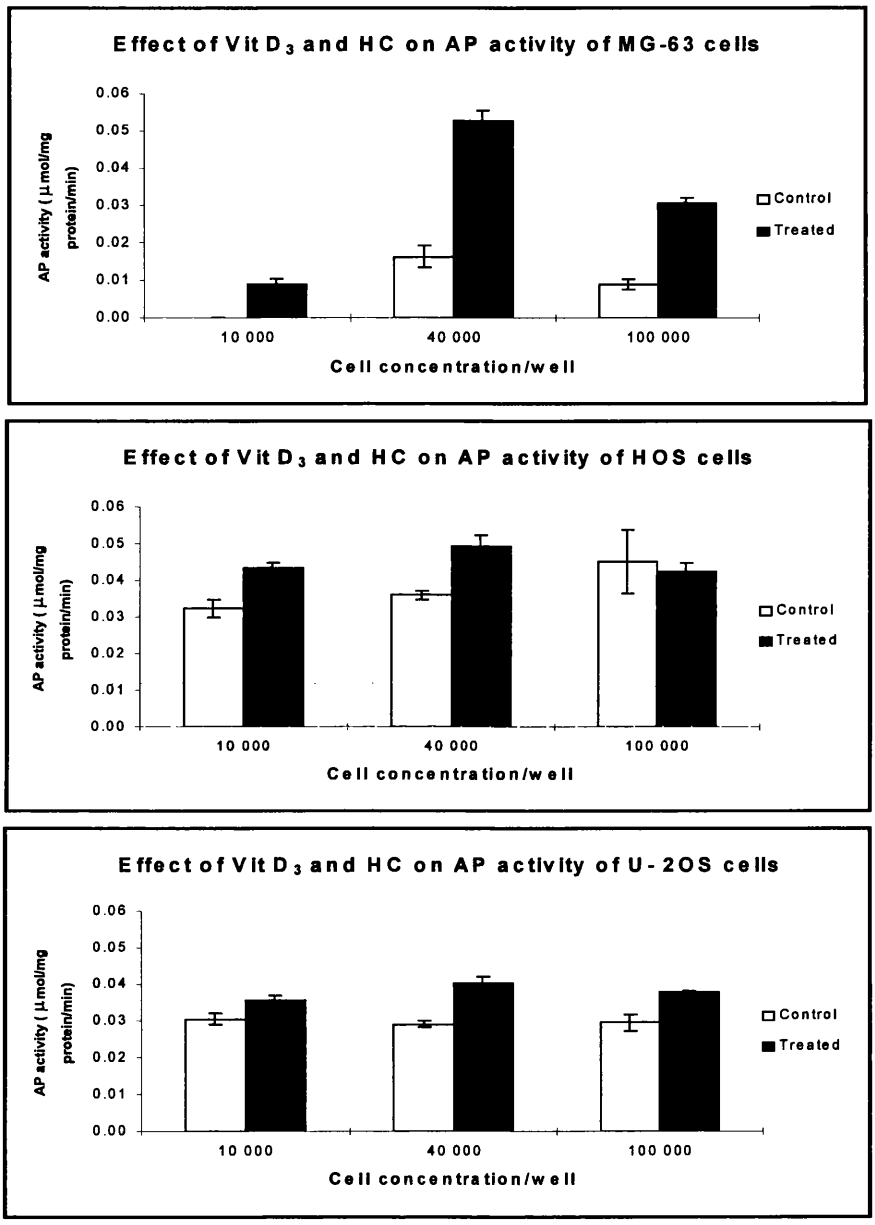

Figure 3.10 The effect of Vit D_3 and HC on the AP activity of the cell lines cultured on tissue culture plastic. Various cell concentrations were cultured for 5 days in the absence (control cultures) and in the presence of 10^{-8} M Vit D_3 and 10^{-7} M HC (treated cultures). Data are expressed as mean ± s.d. (n=3) from one representative experiment. It is seen that the addition of Vit D_3 and HC to the medium enhances the AP activity. This was most marked in the MG-63 cells.

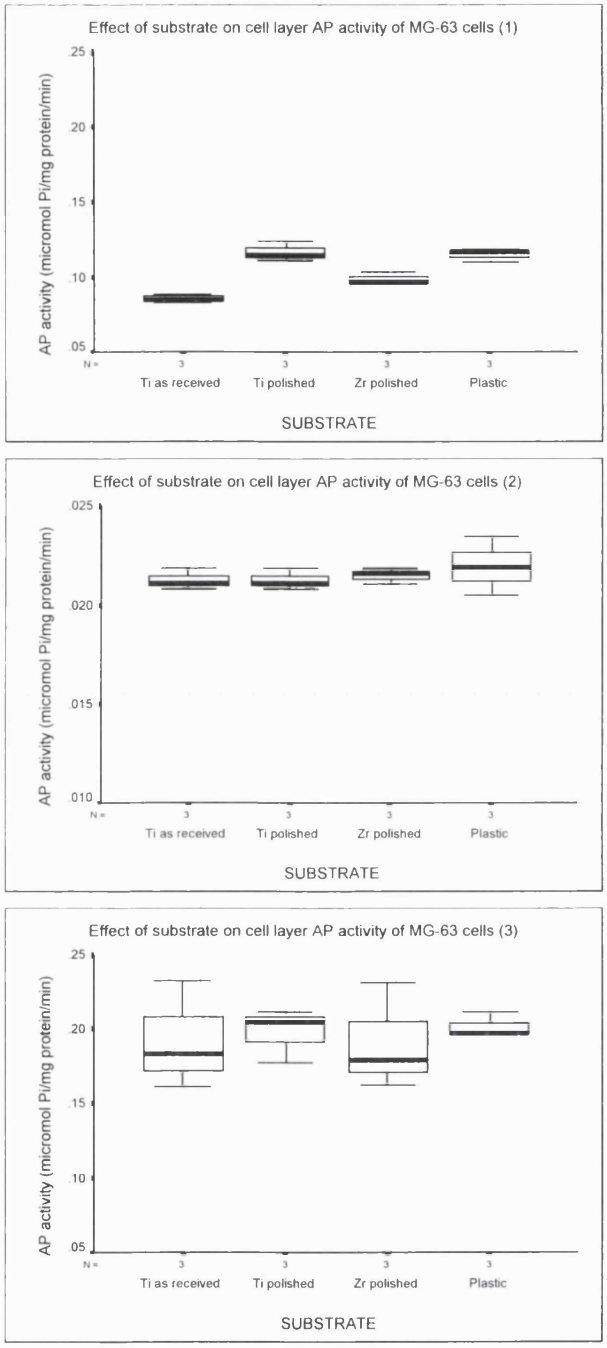

Figure 3.11 Effect of substrate surface on AP activity in MG-63 cells cultured for 5 days in medium supplemented with 10% FCS. Three experiments were carried. The substrate surface had no effect on AP activity as the differences between the median values were not significantly different ($P > 0.05$).

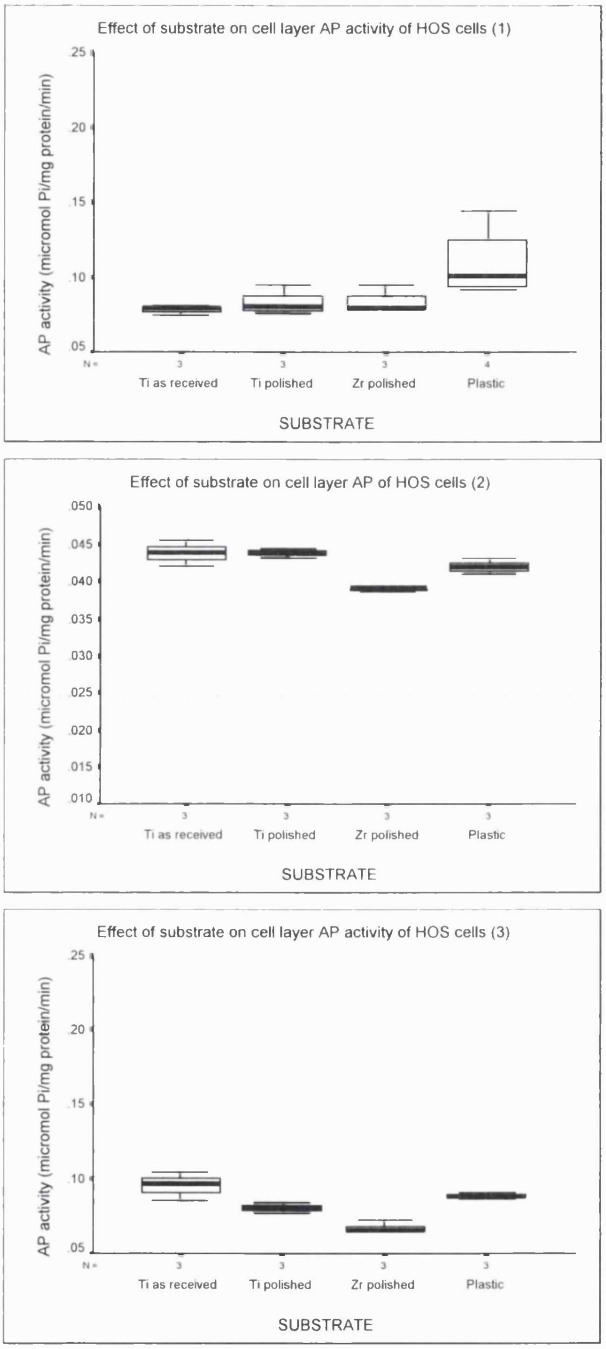

Figure 3.12 Effect of substrate surface on AP activity in HOS cells cultured for 5 days in medium supplemented with 10% FCS. Three experiments were carried out. The substrate surface had no effect on AP activity as the differences between the median values were not significantly different ($P > 0.05$).

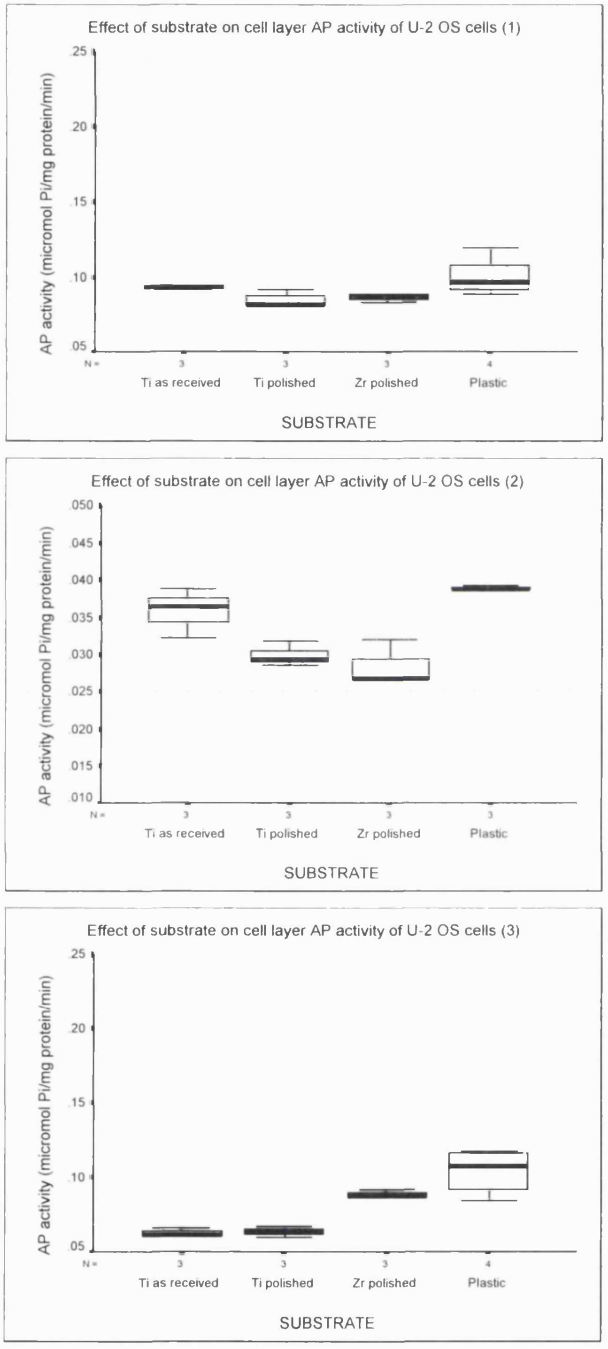

Figure 3.13 Effect of substrate surface on AP activity in U-2 OS cells cultured for 5 days in medium supplemented with 10% FCS. Three experiments were carried out. The substrate surface had no effect on the AP activity as the differences between the median values were not significantly different ($P > 0.05$).

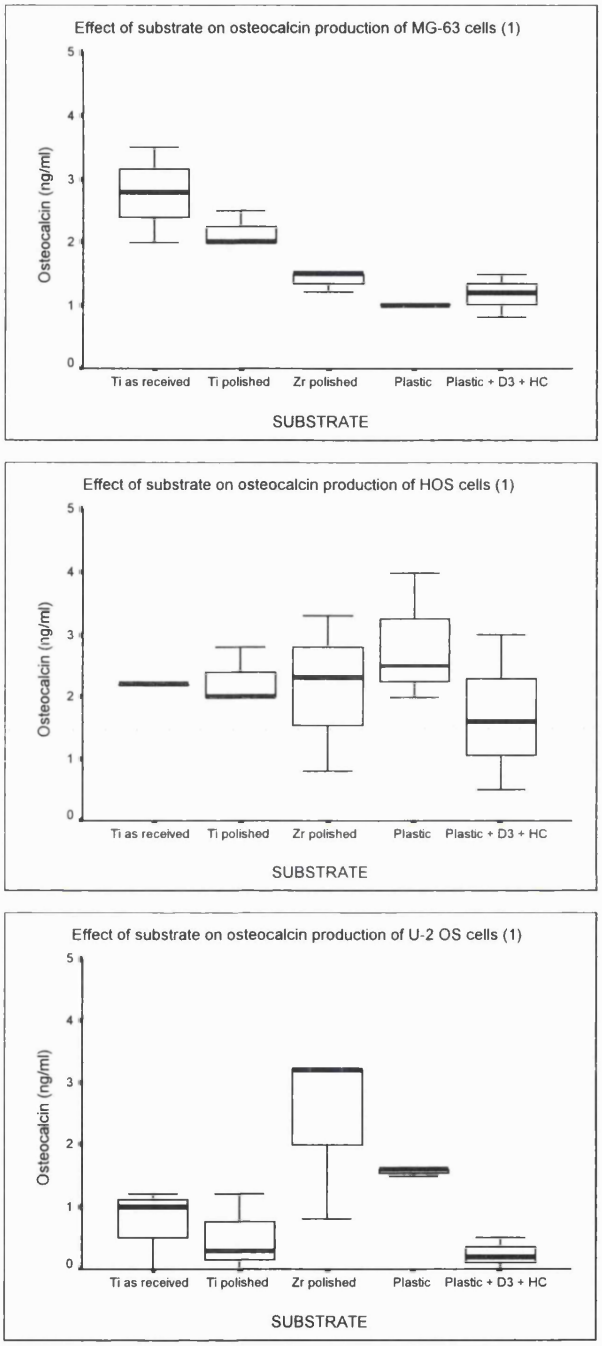

Figure 3.14 Effect of substrate surface on osteocalcin production of OB cell lines. Vit D_3 and HC did not significantly increase the osteocalcin production of cells grown on tissue culture control plastic surfaces. For MG-63 cell lines, the osteocalcin production of cells grown on rough cpTi substrates was significantly higher than those grown all the other substrates ($P < 0.01$). No difference was seen in the osteocalcin production by HOS cells grown on all substrates, while for the U-2 OS cell line, the osteocalcin production of cells grown on polished Zr surfaces was significantly higher than those of cells grown on the other surfaces ($P < 0.02$).

3.3.7 Matrix mineralisation

Figures 3.15-3.18 show the appearance of cells (MG-63, HOS and U-2 OS cells at different magnifications of the SEM) cultured on the different substrates for 10-14 days. The areas examined were of intact cell layers, away from the areas where the cells had detached from the substrates. A compact cell layer was formed, and multilayering was present.

3.3.7.1 SEM evaluation

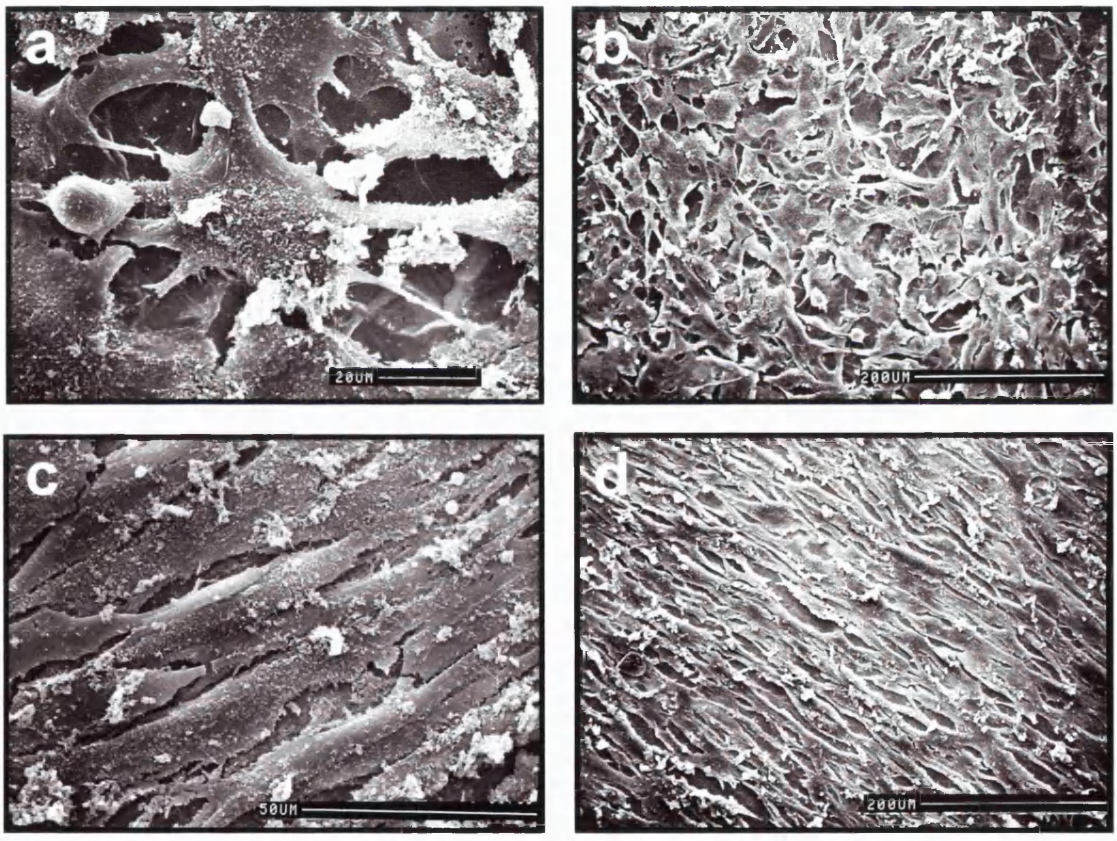

Figure 3.15 Scanning electron microscopy of MG-63 cells grown for 2 weeks on Ti as received (a and b) and polished Ti (c and d). Cells on both surfaces showed similar adaptation and spreading on the substrates. On Ti as received, cells grew in a multilayer but did not have a clear orientation. Cells are seen to bridge the concavities of the rough Ti. On polished Ti, elongated cells were aligned along the grooves created by the polishing procedures.

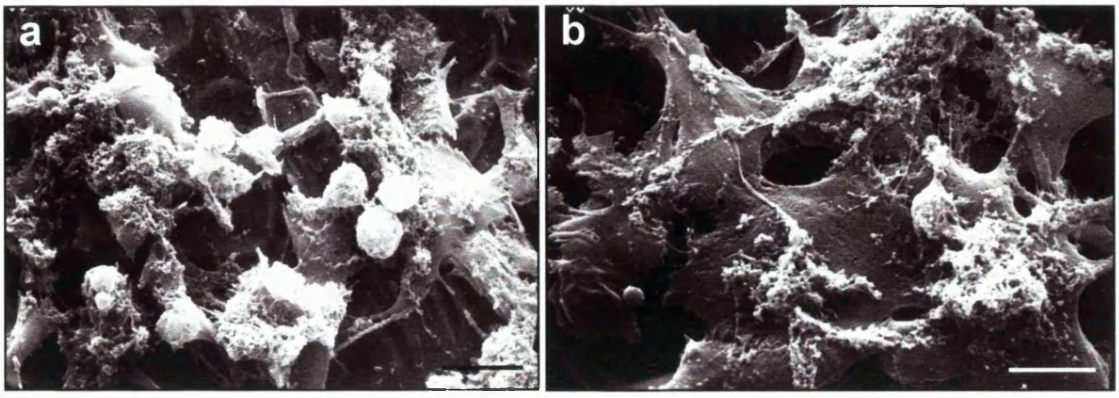

Figure 3.16 High power SEM micrographs showing U2-OS cells on rough as received Ti at 10 days of culture. Globular deposits of shrunken cells are seen on top of the cell layer. In a: bar denotes 10 μm, and in b: bar denotes 5 μm.

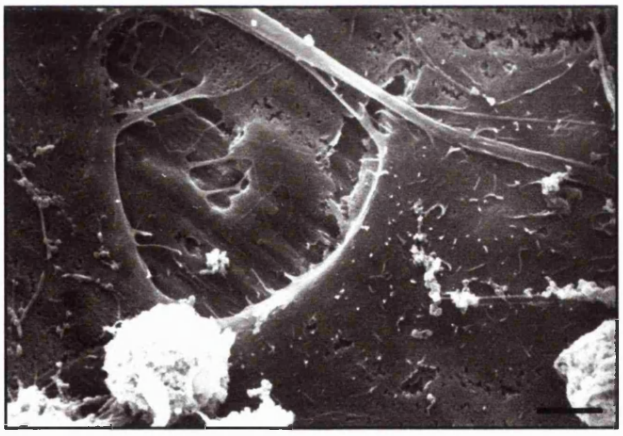

Figure 3.17 SEM showing multilayering of U2-OS cells on polished Zr at 10 days of culture. No collagen fibres could be identified. Round shaped shrunken cells can be seen on top of the cell layer. Bar denotes 2 μm.

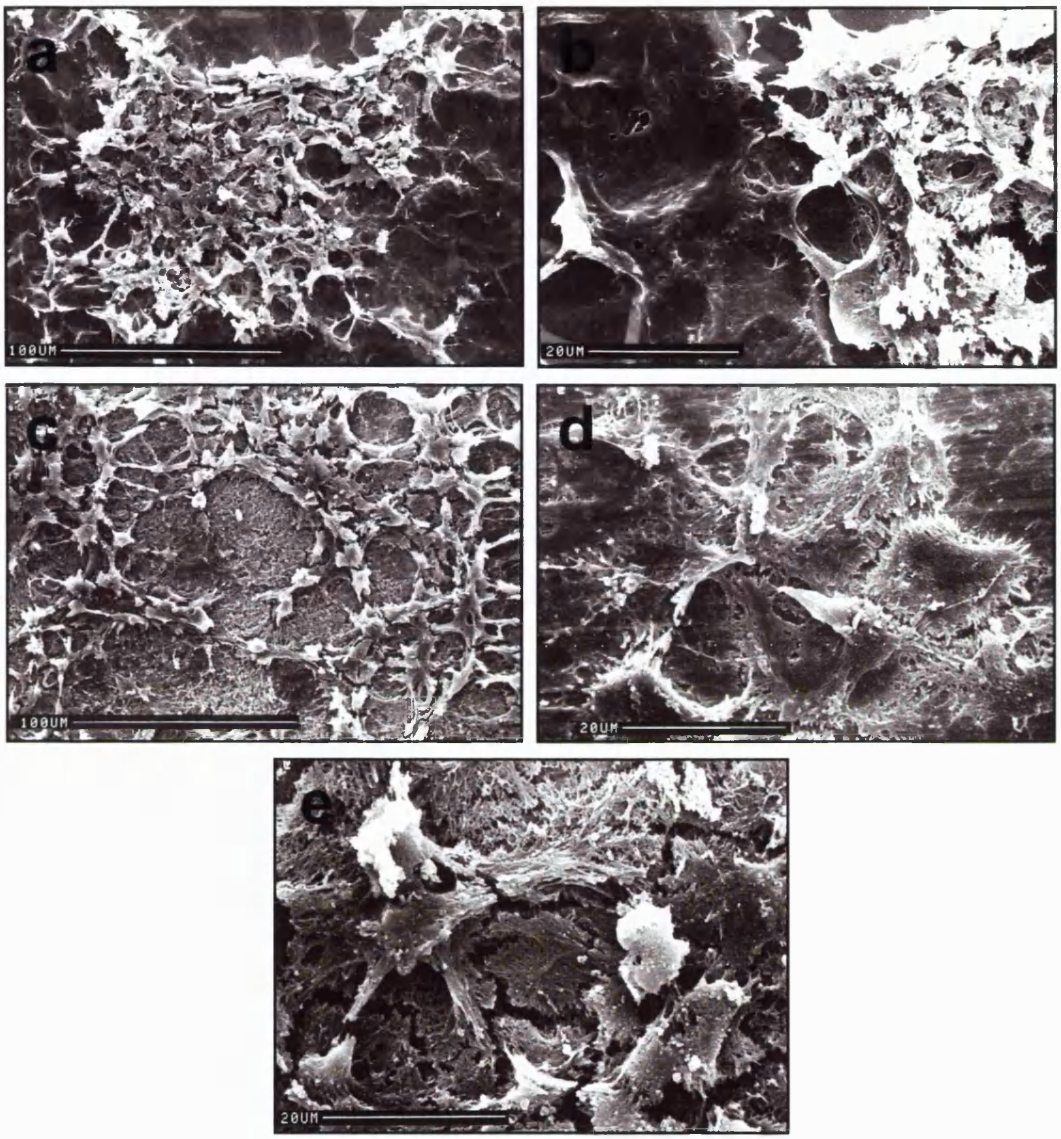

Figure 3.18 SEM of HOS cells at 10-14 days in culture. The surfaces are (a) and (b): Ti as received, (c) and (d): polished Ti, (e): polished Zr. The micrographs show multilayering of cells, but no evidence of mineralisation. Breaks (cracks) in the cell layer are drying artefacts incurred during specimen preparation procedures.

3.3.7.2 Results of EDAX line scans

Table 3.1 lists the calcium and phosphate concentrations of MG-63 and U-2 OS cell lines after 10-14 days in culture. The results show that the Ca/P ratios were very low, and not the same as apatite. This may indicate dystrophic calcification.

Table 3.1 Point analyses of the Ca and P content present on substrate surfaces where cells were cultured for 10 to 14 days in medium supplemented with Asc-2P and 10 mM β-glycerophosphate. The areas scanned for mineral content were the adherent cell surfaces and the adjacent metal surface (uncovered by cells). Values are mean ± s.d. The Ca/P ratios of the areas scanned for both cell lines show that they were distinctly lower than apatite

Cell line	Substrate	Area scanned	Ca (Atomic %)	P (Atomic %)	Ca/P
MG-63	Ti as received	Cell surface	8.15 ± 0.66	14.73 ± 5.62	0.55
	Ti as received	metal surface	10.07 ± 0.74	18.40 ± 0.63	0.12
	Polished Ti	Cell surface	9.97 ± 4.99	23.34 ± 5.50	0.43
	Polished Ti	metal surface	3.02 ± 0.06	24.54 ± 4.08	0.12
	Polished Zr	Cell surface	2.65 ± 2.53	12.45 ± 5.42	0.21
	Polished Zr	metal surface	3.85 ± 1.56	10.73 ± 4.79	0.36
U-2 OS	Ti as received	Cell surface	8.74 ± 0.54	15.87 ± 0.49	0.55
	Ti as received	metal surface	8.51 ± 3.87	12.61 ± 1.66	0.67
	Polished Ti	Cell surface	6.93 ± 0.34	31.79 ± 1.36	0.22
	Polished Ti	metal surface	6.66 ± 1.05	32.98 ± 5.06	0.20
	Polished Zr	Cell surface	4.10 ± 0.11	11.21 ± 0.37	0.37
	Polished Zr	metal surface	3.00 ± 0.85	9.54 ± 0.83	0.31

3.4 DISCUSSION

Surface topography of biomaterials plays an essential role in the initial attachment of OB cells to dental implants. Cell adhesion is a prerequisite for further cellular functions, such as spreading, proliferation and other biosynthetic activity. This research evaluated the responses of three human OB cell lines to cpTi and cpZr which were prepared to provide three different surfaces, i.e. rough and regular (Ti as received), and smooth and regular (Ti and Zr polished unilaterally to 1200 grit). Ti was used because it is well established as an implant material, and Zr should be comparable to Ti as they belong to the same group in the periodic table of elements.

At the initial stage of this investigation, the attachment of the three cell lines to cpTi surfaces was compared. Cell attachment to the cpTi surfaces was examined in serum-free medium to negate the effect of attachment proteins present in serum. It has been shown that cells can attach in serum-free medium, and that they may do so much more rapidly to substrates in the absence of serum, or in low concentrations of serum than in higher serum conditions (Taylor, 1961). This initial adhesion from the suspension is largely due to physico-chemical forces (Van der Waals and electrostatic interactions) acting between the cell surface, the substratum and the intervening medium. This type of interaction is sometimes referred to as non-specific adhesion (von Recum and van Kooten, 1995). As the surface is rapidly covered by proteins or serum in the medium (2 to 5 nm layer forms within the first minute of contact), a second reaction, the reaction between the cell surface receptors and their ligands occurs (Brunette, 1988). This specific integrin-ligand interaction is much stronger than the non-specific reaction and is observed as focal contact formation, which may occur as early as 20 minutes after cell inoculation on favourable substrates (Oakley and Brunette, 1993). After this, cell spreading occurs rapidly.

Cells are also able to spread in serum-free medium. The initial spreading of cells grown on glass substrates in serum-free medium is said to be a passive process due to the forces that exist between the substrate and the culture medium (Revel and Wolken,

1973), even though Knox (1984) found that there was no spreading at all in BHK (baby hamster kidney) cells even after 24 h in the complete absence of serum.

The OB cells used in this study adhered to Ti in serum-free medium, and they were also able to spread after 24 h (Figures 3.4 and 3.5). It was reported that OB cells spread and develop focal adhesions only when grown on serum pre-coated glass and plastic surfaces (Burridge *et al.,* 1988). When cultured on non-pre-coated or BSA pre-coated materials they failed to spread, even though they attached to the substrates. This behaviour was also seen in OB cells grown on Ti surfaces (Schneider and Burridge, 1994a). The present study however, shows that not only do the OB cells adhere to the metals in serum-free medium, but that they also spread very well. This may be explained by the ability of OB cells to synthesise and secrete their own matrix proteins, within the time that they were allowed to attach to the substrates, i.e. within the two hour attachment period used in this investigation (Steele *et al.*, 1992). Fibronectin (Fn) production by cells cultured in serum-free medium may even be more abundant than in cells cultured in complete medium (Abiko and Brunette, 1993).

The present study focused on comparison of adhesion to different substrates and did not compare serum-free medium to complete medium. Nevertheless, coating of implants by matrix proteins present in the serum or by those secreted by the OB cells may be an important event in facilitating cell attachment to the implant surface. Kornu *et al.* (1996) reported that OB cells were able to adhere to Ti in 2 h, as effectively in serum-free medium as in complete medium. However, they noted that the number of cells attached in serum-free medium was only half that attached in complete medium. Serum in the medium contains the attachment proteins, Fn and Vitronectin (Vn). Howlett *et al.* (1994) found that the attachment of bone-derived cells during the first 90 minutes of attachment was increased two-fold on tissue culture plastic (TCP) when cultured in medium containing 10% foetal bovine serum (FBS). When Fn and Vn were depleted from the serum, either singly or both at the same time, only Vn depletion reduced cell attachment to the plastic surface. Attachment of bone cells to TCP in culture depleted of serum Fn was the same as when intact FBS was used, and that only

when Fn was precoated onto TCP was the attachment at least equal to that as when Vn was present in the medium and adsorbed onto the surface.

Gronowicz and McCarthy (1996) showed that when SaOS-2 cells were treated with cycloheximide to prevent endogenous protein synthesis for at least 24 h before plating on to metallic substrates, and in addition cultured in the presence of cycloheximide throughout the incubation period, the cells still attached and spread. They also reported that even at 24 h of attachment, the number of cells which attached to metallic substrates was not affected by the presence of serum in the medium, as much as it would affect the attachment of cells to glass substrates. Only cells grown on glass in serum-free medium condition did not spread, although they attached to the substrates. Spreading of cells at 24 h was shown by immunostaining of actin stress fibres. They concluded that binding and spreading of cells to metallic substrates was partly due to direct integrin binding, and that serum was only required for the long-term integrity of the cells in culture. The survival times of cultures in serum-free medium vary greatly between cell types and on different substrates, however, cells which attached and spread in serum-free medium would eventually round up and become detached after several hours (Taylor, 1961).

Coating of substrates with serum, Fn, and other attachment proteins has been shown to reduce the time required for cells to develop focal adhesions and spread (Schneider and Burridge, 1994b). Cells adhere and spread better, and stress fibres are more prominent on Ti coated with Fn than on uncoated Ti surfaces. Stress fibres developed in cultured cells due to the tight adhesions that these cells make on their substrates at the focal adhesion sites.

Contrary to the finding of Kornu *et al.* (1996), Okamoto *et al.* (1998) found that the quantity of human OB cells attaching to hydroxyapatite (HA) and Ti was not affected by serum components. The time course of adhesion of the OB cells to serum-pre-coated or non pre-coated substrates (attachment assay was done in serum-free medium) was also similar. Nevertheless, they agreed that serum was needed for cells to spread. With serum pre-coating of substrates, OB cells adhered tightly and closely to

both Ti and HA, and they spread in all directions. With non precoating of the substrates, OB cells adhered loosely without spreading. When RGD peptides were incorporated in the medium, spreading of cells on serum pre-coated HA was inhibited, while the spreading of cells on Ti was not. This suggests that tight adhesion and spreading of OB cells on HA were dominated by RGD peptides, while those on Ti might be mediated by factors other than RGD peptides, and therefore not solely integrin related.

Different cells attach in varying amounts to various biomaterials. Fibroblasts and OB cells respond differently in cell attachment assays to Ti (Hunter *et al.*, 1995). Human OB cell adherence was seen to be greater on Ti than on cobalt-chromium (Sinha *et al.,* 1994), but rat calvarial OB cell adherence was greater on cobalt chromium than on Ti (Puleo *et al.,* 1991). Malignant or transformed cells are also known to be less adhesive than normal cells.

Variations in the number of cells attached to different substrate surfaces reported in different studies may also be due to the different methods of assessment of cell attachment. These may involve direct counting of the attached cells after detaching them from the substrates using a number of techniques. The cells may then be counted directly using a haemocytometer, or a Coulter counter, or indirectly by counting unattached cells and then subtracting this value from the number inoculated on the substrates (Bowers *et al.*, 1992), or by employing radioactive techniques to label cells that are subsequently detached and counted in a scintillation counter. The use of the MTS assay was appropriate for this study as cells did not have to be detached from the opaque substrates (Miller and McDevitt, 1991; Hussain *et al.*, 1993). It was shown that cells adhered firmly to rough titanium, and once attached, could not be easily retrieved by a single trypsin treatment (Martin *et al.*, 1995; Price *et al.*, 1997).

Several theories have been put forward on how surface topography affects cell responses, even though the exact mechanisms are still unclear (den Braber *et al.*, 1998). These are based on several individual studies which tested separate hypotheses. Two of the reasons given for the greater attachment of OB cells to rougher implant surfaces were the improved surface energy and wettability, and the greater surface area available

for cell attachment (Niederauer *et al.*, 1994). Another theory was that even though the greater surface area was not available for cells to adhere to (as in grooves which are narrower than the dimensions of the cells), it is still available for the adsorption of attachment proteins like Fn, which would then lead to tighter cell adhesion to the substrates (Schneider and Burridge, 1994b).

One difficulty encountered with the use of the MTS assay was the background absorbance that always occurred at the end of the incubation period when the culture medium (containing phenol red) was incubated with the MTS reagents, even in cell-free wells. Therefore, it was always necessary to prepare a triplicate set of control wells (without cells) containing the same volume of culture medium and reagents as the experimental wells, to allow for this.

It was initially thought that there would be differences in cellular adhesion on the cpTi substrates used in this study. However, the preliminary results show that this was not the case. There was no relationship between surface roughness and cell adhesion noted. However, the attachment and subsequent spreading of all cell lines on the materials used indicates the biocompatibility of the metals to OB cells. As adhesion is only a short term biologic response, further assessment of the longer term responses of the OB cells was carried out. This involved assessing cell proliferation and differentiation, which would indicate a direct influence of the substratum on cellular activity.

In the present study, cellular proliferation was measured using a modification of the BrdU microplate assay. This assay measures freshly synthesised DNA, and therefore indicated cell division on substrates. A finding was despite the similar number of cells attached to the different substrates initially, proliferation of all OB cell lines was better on metals than on plastic. Most types of cultured cells will proliferate only when they are in contact with, and spread on a solid surface. Normal cells grow until the solid surface is completely covered by a cellular monolayer, and then stop proliferating. In transformed cells, cell-contact and proliferation may be unrelated. This loss of anchorage-dependent growth control is one of the major characteristics of tumour cells

(Plantefaber and Hynes, 1989). Folkman and Moscona (1978) showed that by accurately controlling the amount of cell spreading on a substrate (i.e. by modulating cell morphology between flat and spherical), a small change in spreading has a large effect on the extent of DNA synthesis. OB cells have been shown to grow faster on titanium alloy than on tissue culture plastic (Puleo *et al.*, 1991). However, after 5 days, the rate of growth was the same.

Prigent *et al.* (1998) also noted no difference in the proliferation rate of cells grown on different metals of different surface roughness. They used flow cytometry to study cell proliferation on various substrates polished to a smooth mirror-finish, and showed that within the same cell line, there was no difference in the proliferation rates (studied by examining the distribution of cells at the various cell cycles) of epithelial cells and fibroblasts cultured on plastic, titanium and titanium-tantalum surfaces. The only difference was the different proliferation rates of the different cell lines, when compared to each other. Their finding implies that with the cells used, surface composition and roughness may not be that relevant to cell proliferation. On the other hand, Hunter *et al.* (1995) showed that even when different substrates were highly polished to the same smooth surface, primary rat fibroblasts showed different proliferation on the different material surfaces, while a rat OB cell line (UMR 106.01) did not. These results show that responses to material composition and roughness may also be cell specific.

The work of one research group (Martin *et al.*, 1995; 1996 and Boyan *et al.*, 1998) with MG-63 cells shows that substrate surface roughness alone was capable of regulating OB cell proliferation, differentiation and matrix production *in vitro*. Surface roughness of a material is usually described by referring to the R_a value. In the present study, the R_a value for the rough as received Ti was 2.09 μm. Boyan *et al.* (1998) used rougher cpTi substrates, with the R_a values of 3.68 μm, 3.90 μm and the roughest, which was Ti plasma-sprayed, had an R_a value of 6.81 μm. The smoother polished Ti and Zr surfaces used in the present study (R_a values of 0.84 μm and 0.80 μm, respectively) were similar to their smoother as machined Ti (R_a value of 0.87 μm). Therefore, the Ti as received used in the present study may be considered smooth when compared to the

rough Ti used by this research group, and it would be expected that the results of the present study would be similar to the results of their smooth Ti, where the cell attachment and differentiation of MG-63 cells on the smooth substrates and substrates with intermediate roughness did not differ from those of cells cultured on the smooth tissue culture control plastic.

In order for cells to be sensitive to the difference in substrate morphology or roughness, the dimensions of the surface texture have to be related to the cell size. Nishimura and Kawai (1998) studied the response of OB cells grown on cpTi surfaces prepared by etching the surfaces with different acids. Even though the roughest surface had an R_{max} value of 19.5 μm, the pore size of the rough irregularities produced by acid etching was only approximately 3 μm. The R_{max} of the smoothest irregular surface prepared by etching in hydrochloric acid was 4.8 μm, with the pore size approximately 0.1-0.5 μm. These pore sizes were too small for the cells to grow into, and initial attachment results (up to a period of 8 h) show no difference in the number of cells attached to the different surfaces. Differences were however seen when cell proliferation was considered. Cell proliferation and AP activity were higher on the roughest surfaces. The range of R_{max} values used by Nishimura and Kawai (1998) was similar to the ones used in this study (R_{max} for Ti rough was 17.69 μm, and R_{max} for polished Ti and Zr were 5.61 μm and 5.32 μm, respectively), although no differences in the cell proliferation and differentiation were seen in all the cell lines grown on the metallic surfaces used.

Substrate surface morphology may also affect the cell differentiation by influencing cell shape and direction of spreading (Ong *et al.*, 1996). Oakley and Brunette (1993) showed that fibroblasts were able to align and adapt within grooves which are about the same size or smaller than themselves. They were also able to straddle grooves which were 3 μm high, and continue to spread as on smooth surfaces. When grooves presented themselves as barriers to spreading, or cells run out of space to spread, proliferation of cells is stopped and they were "forced" to differentiate. These cells are then arrested in the G_1 phase of the cell cycle, where the cells undergo a time of high metabolic activity and continue on to the maturation stage. If this concept is

extended to the roughness profiles of the surfaces used by Martin *et al.* (1995, 1996) and Boyan *et al.* (1998) it would also partly explain the low proliferation and high metabolic rates of the cells grown on the rougher implants, as the cells were "buried" in deep depressions. Cells attach to the underlying substrates through focal adhesions, which are sites of binding of integrins to their ligands, and sites for the assembly of cytoskeletal proteins and actin microfilaments. These sites mobilise the cells to the substrates so that cell tension can be resisted as the cells begin to spread (Burridge *et al.,* 1988). Cytoskeletal organisation and changes in cell shape which follow integrin engagement, may lead to bending of microfilaments at the attachment sites as they adapt to rough surfaces which act as barriers to cell spreading, and thus may influence subsequent cell-substrate interactions (Re *et al.*, 1994).

Figures 3.3 and 3.4 show the morphology of HOS cells at 2 h and 24 h of attachment in relation to the morphology of the underlying substrates. On the rough surface, rounded cells appear to be slightly smaller than the depressions or valleys. When focal adhesions are formed, they appear to attach to the sides of the depressions, and although initially seemed to be 'restrained' within the depressions, they were able to stretch and span across the peaks of the rough surfaces. The rough cpTi surface used in this study was therefore not a barrier to cell spreading.

Although the proliferation assay results (Figures 3.7-3.9) show that cells proliferated better on the metals than on plastic, the AP and osteocalcin expressions were similar on all substrates, indicating that the metals are as favourable as tissue culture plastic for the proliferation and differentiation of OB cells, and that the surface roughness used in this study was not effective in promoting cellular differentiation.

The results of this study show that cells grown on the metal substrates have retained their bioactivity, and were able to adhere and proliferate on the surfaces used. Biochemical analyses show that both cpTi and cpZr are suitable surfaces for cell proliferation and maintenance of the osteoblastic phenotype. An attempt was made to produce mineralised matrix when cells were cultured on the substrates in the presence of 50 μg/ml Asc-2P and 10 mM β-glycerophosphate. Although the exact conditions for

these cell lines to mineralise are not known, the culture condition used in this study is the standard condition used in most mineralisation experiments (Beresford *et al.*, 1993; Dee *et al.*, 1996). However, it proved impossible to retain the cells for longer than 10-14 days in culture, as the cell layers detached from the culture surfaces at that time. This happened on all substrates, including the tissue culture plastic, and occurred in all the cell lines used. Cells were therefore fixed for examination by SEM and mineral composition at the time that the cell layers were seen to begin detaching from the culture surfaces. Based on SEM observations and EDAX line scan results, it seemed that true calcification was not present, even though multilayering of cells was observed during the culture period. The results in Table 3.1 show that the Ca/P ratio was very low, and therefore was not apatite.

3.5 Conclusions

1. Both the Ti and Zr surfaces used in the study were suitable substrates for cell adhesion, proliferation and differentiation, and therefore suggest these materials are equally biocompatible for use as implant materials.
2. There was evidence in this study that the substrate topography was capable of regulating cellular orientation, although this study differs from other studies as the degree of surface roughness used did not show any evidence of being able to regulate cellular differentiation.
3. The OB cells were able to bridge across the rough surface used in this study, and then spread as well as on the smooth surfaces. The cells on the rough and smooth surfaces seemed to be able to proliferate equally. These cells were therefore likely to be at the same state of differentiation, and it is the combined presence of other factors which may play a more important role in governing the expression of OB cells cultured on surfaces with different textures.
4. The cell lines used were not able to produce a mineralised matrix when cultured on the substrates. This may be due to the choice of cells as the osteoblastic model, and the conditions which have not been specified for these cell lines to mineralise in culture.

4. Integrin Expression of Osteoblast-like Cells Attached to Metallic Implant Materials

4.1 Introduction

The ultimate goal in studying cellular responses to substrate topography is to use the information to promote increased bone formation at bone-implant interfaces. It has been shown that osteoblast-like (OB) cells are sensitive to differences in implant material surface roughness and chemistry (Bowers *et al.*, 1992; Sinha *et al.*, 1994). The information about substrate surface topography and chemistry are thought to be relayed to the cells partly by the major family of cell surface adhesion receptors, the integrins, and differences in the integrin expression and distribution must be determined to some extent by the substrate surface (Sinha and Tuan, 1996). Several studies have investigated the factors which affect integrin expression of cells grown on different substrates *in vitro*. It was reported that differences in integrin expression and distribution were seen depending on the type of cells used and the substrates on which the cells were grown (Hormia and Könönen, 1994; Sinha *et al.*, 1994; Dean *et al.*, 1995), and that integrin expression was affected by both substrate composition and topography (Sinha and Tuan, 1996). It is also hypothesised that the cytoskeleton network may be induced to orient itself to follow the directional prominence of the substrates on which the cells were grown, as one of the consequences of the cues transferred following integrin binding to their ligands on the substrates with directional prominence (den Braber *et al.*, 1998). Orientation of cells to the substrate topography has been shown to affect the state of differentiation of the cells (Ong *et al.*, 1996).

The aim of the final part of this investigation was to carry out a pilot study evaluating the pattern of integrin expression and organisation of the actin cytoskeleton of OB cells grown on substrates with different surface composition and roughness, in order to determine whether the integrin expression and organisation of the cytoskeletal component depend upon the underlying surface. The influence of the substrate composition and topography may be seen as i) differences in integrin expression, ii)

alteration in the distribution pattern of the integrin subunits expressed, or iii) differences in the organisation and prominence of actin stress fibres.

In order to analyse the effect of different substrates on integrin expression *in vitro*, cells were stained with monoclonal antibodies to selected integrins which are regarded as characteristic of the osteoblastic phenotype. Three α integrin subunits, α_2, α_3, and α_5, and the β_1 subunit were chosen for study. These integrins are ubiquitously expressed by OB cells, and are important for their attachment and differentiation (Hughes *et al.*, 1993; Clover *et al.*, 1994; Saito *et al.*, 1994; Gronthos *et al.*, 1997). The β_1 integrin in combination with the α subunits are primarily responsible for the adhesion of bone cells to specific extracellular matrix (ECM) protein components, which act as their ligands (Table 1.2). In addition to binding to the ECM proteins, integrins link the matrix to the actin cytoskeleton of the cell at the focal adhesion sites (Buck and Horwitz, 1987a; 1987b).

The cell lines used in this study were the human osteosarcoma cell lines, MG-63, HOS and U-2 OS. Even though MG-63 and HOS cell lines may not display characteristics identical to those observed in normal human OB cells in terms of cellular proliferation and differentiation, they can be used as models to study cell adhesion and integrin expression as they have been shown to express the integrin subunits also expressed by primary human OB cells in culture (Clover and Gowen, 1994). Integrin expression in the U-2 OS cell line has not been previously studied. However, they may be expected to express these OB cell integrins (Dedhar and Saulnier, 1990; Vihinen *et al.*, 1996).

Changes in integrin expression and the distribution pattern of integrins expressed may be responsible for the differential responses seen in OB cells cultured on substrates with different surface roughnesses (Sinha and Tuan, 1996). The orientation of the cytoskeleton has been related to cell adhesion and spreading (Groth and Altankov, 1996), and therefore may reflect the biocompatibility of the substrates on which the cells were grown. For these reasons, the expression and organisation of the integrins and the

actin network of the OB cells grown on various substrates used in this investigation were studied.

4.2 Materials and Methods

4.2.1 Substrates

The choice of substrate material and material surface preparation and analysis are discussed in Chapter 2. Before use for cell culture, they were air-dried in a tissue culture hood and sterilised by exposing to ultraviolet light for one hour on each side (described earlier in Chapter 3). The substrates used for this part of the investigation were rough "as received" cpTi, and smooth, polished cpTi and cpZr surfaces.

4.2.2 Cell culture

To see if the integrin subunits chosen were study were expressed by MG-63, HOS and U-2 OS cells, they were first tested on glass slides. 7.5×10^3 cells/well were grown in 8-well chamber glass slides (Nunc, Inc., Naperville, IL, U.S.A.) and left to attach for 24 h until almost, but not fully confluent, in α-MEM supplemented with 10% FCS under standard tissue culture conditions. These served as the control cultures. To test which integrin subunits were expressed when the OB cells were grown on the metallic substrates, 4×10^4 cells were grown on the substrates placed in 24-well tissue culture plastic. The cells were left to attach for 24 h in α-MEM supplemented with 10% FCS. To view the development of actin stress fibres, cells were grown as above (on glass slides and on metals) for two incubation periods, 1 h and 24 h.

4.2.3 Immunohistochemistry

4.2.3.1 Determination of integrin subunits expressed by OB cell lines grown on different substrates

For immunofluorescence staining to detect integrin subunits expressed, after the 24 h incubation period, cells on glass slides and metal substrates were washed three times with PBS and were then fixed in 4% paraformaldehyde for 10 minutes at room temperature. After washing three times in PBS, the cells were left to block in 5% FCS in PBS for 1 h at room temperature.

For immunolocalisation of α_2, α_3 and α_5 integrin subunits, the cells were permeabilised in 0.1% Triton X 100 in PBS for 10 minutes at room temperature before blocking. However, this step was not carried out for detection of the β_1 subunit. The blocking serum was discarded, and wells were incubated with primary antibody for 1 h at room temperature. Primary antibodies were diluted in 1% BSA/PBS as shown in Table 4.1. The primary antibodies were omitted from wells assigned as negative control wells, and replaced by 1% BSA/PBS. Wells were washed three times in PBS (three 5-minute rinses), then incubated with the secondary antibody (FITC-Conjugated Rabbit Anti-mouse Immunoglobulins, Dako, Denmark) in the dilutions shown in Table 4.1, for 1 h at room temperature. The cells were finally rinsed in PBS (three 5-minute rinses). Specimens on glass slides were coverslipped in an aqueous mountant, glycerol in PBS (Sigma Diagnostics, St. Louis, MO, U.S.A.) and examined using a fluorescent microscope with ×40 objective lens (Zeiss Axioskop, Germany). The specimens were photographed using an Agfachrome RSX 200 professional film (Agfa, Germany).

The cells grown on metal substrates were treated differently from those grown on glass. After the final rinse with PBS, the labelled metal discs were dehydrated by two 10-minute immersions in absolute alcohol, followed by two 10-minute immersions in xylene. The discs were then glued on glass slides using a tiny drop of cyanoacrylate adhesive, and cover-slipped with a thin layer of DPX mountant (Histological Equipment Ltd., West Bridgford, Nottingham, U.K.). The mountant was allowed to dry and harden. Once hardened, the labelled specimens were examined using a Zeiss microscope

equipped with epifluorescence. Specimens were viewed using ×100 objective lens under oil immersion (numerical aperture of 1.25).

Initially an attempt was made to photograph the specimens on metal substrates using the Agfachrome RSX 200 professional film. However, due to the rough surface, light used for viewing the immunofluorescent label was reflected off the discs as backscatter causing it to fade almost immediately. Specimens photographed using this film were unsatisfactory. To overcome this problem extensive preliminary investigations were carried out. Finally, neutral density filters were used to cut down on the incident light in combination with a new very fast black and white professional film, Kodak Tmax p3200 ASA (Eastman Kodak Company, Rochester, New York, U.S.A.). The author would like to acknowledge the expert help and advice of Professor Alan Boyde, Department of Anatomy and Developmental Biology, University College London in developing this technique. Because of the time required for development it was only possible to apply this technique to later experiments. Immunohistochemistry for each substrate was carried out at least twice for each cell line.

Table 4.1 Primary monoclonal antibodies used against various integrin subunits tested in this study and their dilutions

Primary antibody	Dilution	Source	Secondary antibody dilution
β_1 (CD29)	1:50	Southern Biotechnology	1:200
α_2 (HAS 4)	supernatant, used as neat	Gift of Prof. M. Horton, UCL	1:100
α_2 (HAS 6)	1:50	Gift of Prof. M. Horton, UCL	1:100
α_3 (CD 29c)	1:50	Serotec	1:100
α_5 (CD 29e)	1:20	Serotec	1:50

4.2.3.2 Cytoskeletal organisation

To visualise actin filaments, 7.5×10^3 cells/well were grown in 8-well chamber glass slides, or 4×10^4 cells/well were cultured in 24-well plates containing the metal discs and left to attach for 24 h on glass, and 1 h and 24 h on metals. Cells were then fixed with 4% paraformaldehyde for 10 minutes at room temperature. They were then treated with acetone following the protocol of Bagambisa *et al.* (1994). This consisted of treating the cells for 2 minutes to a 1:1 solution of acetone and water at -20°C, followed by 5 minutes in cold acetone, another 2 minutes in a 1:1 solution of acetone and water at -20°C, final rinsing in PBS at room temperature. Actin was stained with 1 μg/ml rhodamine phalloidin (Sigma) for 1 h at 37°C. After three 5-minute rinses in PBS, samples on glass slides were coverslipped in aqueous mountant, while the samples on metal discs were dehydrated in alcohol and xylene, before viewing using an epifluorescence microscope. Specimens on glass and metal substrates were photographed using the Kodak Tmax p3200 speed black and white professional film as described in 4.2.3.1.

4.3 Results

The pattern of expression of the different integrin subunits for samples grown on glass slides was viewed at ×400 magnification, while samples grown on metal substrates were viewed under oil immersion. Distribution of integrins expressed was difficult to follow on the rough cpTi surfaces due to the varying depths of focus created by the rough surfaces. The integrins on smooth surfaces were in one plane of focus and could thus be easily visualised. An attempt was made to quantify the integrins expressed using image analysis techniques. However, it was difficult to analyse integrin expression on the rough surfaces, and it was only possible to assess the integrin expression qualitatively.

4.3.1.1 Integrin expression of cell lines grown on different substrates

When grown on glass slides, all integrin subunits tested were expressed by each cell line. β_1 integrin subunits were expressed in focal granularities. The U-2 OS cell line had the strongest expression among all the cell lines tested (Figure 4.1b). When grown on metals, β_1 integrin was expressed focally, especially in areas of cell-cell contact (Figure 4.1, c-j). When examined under oil immersion, the β_1 integrin subunits were expressed as streak-like or dot-like patches distributed throughout the cells, especially at the cell periphery (Figure 4.2). This pattern of β_1 integrin expression was shown by all the cell lines grown on the metal substrates.

α_3 integrin subunits were expressed by all cell lines grown on glass substrates. They were expressed as small punctate granularities, which are smaller than the streaks and dot-like structures seen with the β_1 integrins, throughout the cytoplasm. The expression of the α_3 subunit was similar for all the cell lines grown on the different substrates (Figure 4.3a-c, and Figure 4.4).

In contrast to the expressions of the β_1 and the α_3 integrin subunits, the α_2 and α_5 subunits were diffusely expressed throughout the cytoplasm. They were very difficult to view on glass, however on metals, the pattern of expression was clearly diffuse. No distinct or clearly formed dot-like structures (showing grouping of integrin subunits) were seen. This is illustrated by micrographs of the α_5 integrins subunits grown on glass substrates (Figure 4.3, d-f), and the representative samples of MG-63 and U-2 OS cells grown on the polished cpTi and cpZr substrates (Figure 4.5). No α_2 expression was seen when HOS cells were grown on all metal substrates, although the α_2 was expressed when these cells were grown on glass substrates.

The general description of the integrin subunits expressed above are summarised in Table 4.2.

Table 4.2 Summary of the integrin subunits expressed when OB cells were cultured on the various substrates used in this study. Results are expressed qualitatively, as no practical way was found to assess the amount of integrins expressed on the metallic substrates, especially those on rough "as received" Ti. To qualitatively describe the nature of the staining detected, the following descriptions were used: (FG) indicates granular focal expression, (PG) indicates punctate granularities, (D) indicates diffuse expression, and (-) indicates no detected staining

Cell line	**Substrate**	α_2	α_3	α_5	β_1
MG-63	Glass	D	PG	D	FG
	Rough Ti	D	PG	D	FG
	Polished Ti	D	PG	D	FG
	Polished Zr	D	PG	D	FG
HOS	Glass	D	PG	D	FG
	Rough Ti	-	PG	D	FG
	Polished Ti	-	PG	D	FG
	Polished Zr	-	PG	D	FG
U-2 OS	Glass	D	PG	D	FG
	Rough Ti	D	PG	D	FG
	Polished Ti	D	PG	D	FG
	Polished Zr	D	PG	D	FG

Figure 4.1 Immunofluorescent detection of the β_1 integrin subunit expression in three human osteosarcoma cell lines grown on different substrates at 24 h attachment.

When grown on glass slides, the β_1 integrin subunits were identified and expressed as focal granularities (FG) at the cell peripheries (arrows in a and b) of MG-63 and U-2 OS cells. HOS cells grown on glass slides also showed the same pattern of β_1 integrin expression (not shown). When grown on metals, the same pattern of distribution of the β_1 integrin subunit was seen in all cell lines grown on the different metal substrates. On all the metal surfaces, where cells were in contact, β_1 integrins appear to be confined to the cell-cell contacts.

The following micrographs of cell lines grown on various substrates, show the pattern of β_1 integrin expression as described above.

(a). MG-63 cells on glass slide, (b). U-2 OS cells on glass slide.
(c). HOS cells on Ti as received, (d). HOS cells on polished Ti, (e). HOS cells on polished Zr.
(f). U-2 OS cells on polished Ti, (g). U-2 OS cells on polished Zr. U-2 OS cells on Ti as received not shown.
(h). MG-63 cells on Ti as received, (i). MG-63 cells on polished Ti, (j). MG-63 cells on polished Zr.
(k). Negative control of β_1 integrin (primary antibody omitted) of U-2 OS cells on polished Zr. No detectable levels of immunofluorescence seen.
(l). Negative control of β_1 integrin (primary antibody omitted) of HOS cells on Ti as received.
All micrographs are original magnification ×400. Bar in l denotes 10 μm, for micrographs a-l.

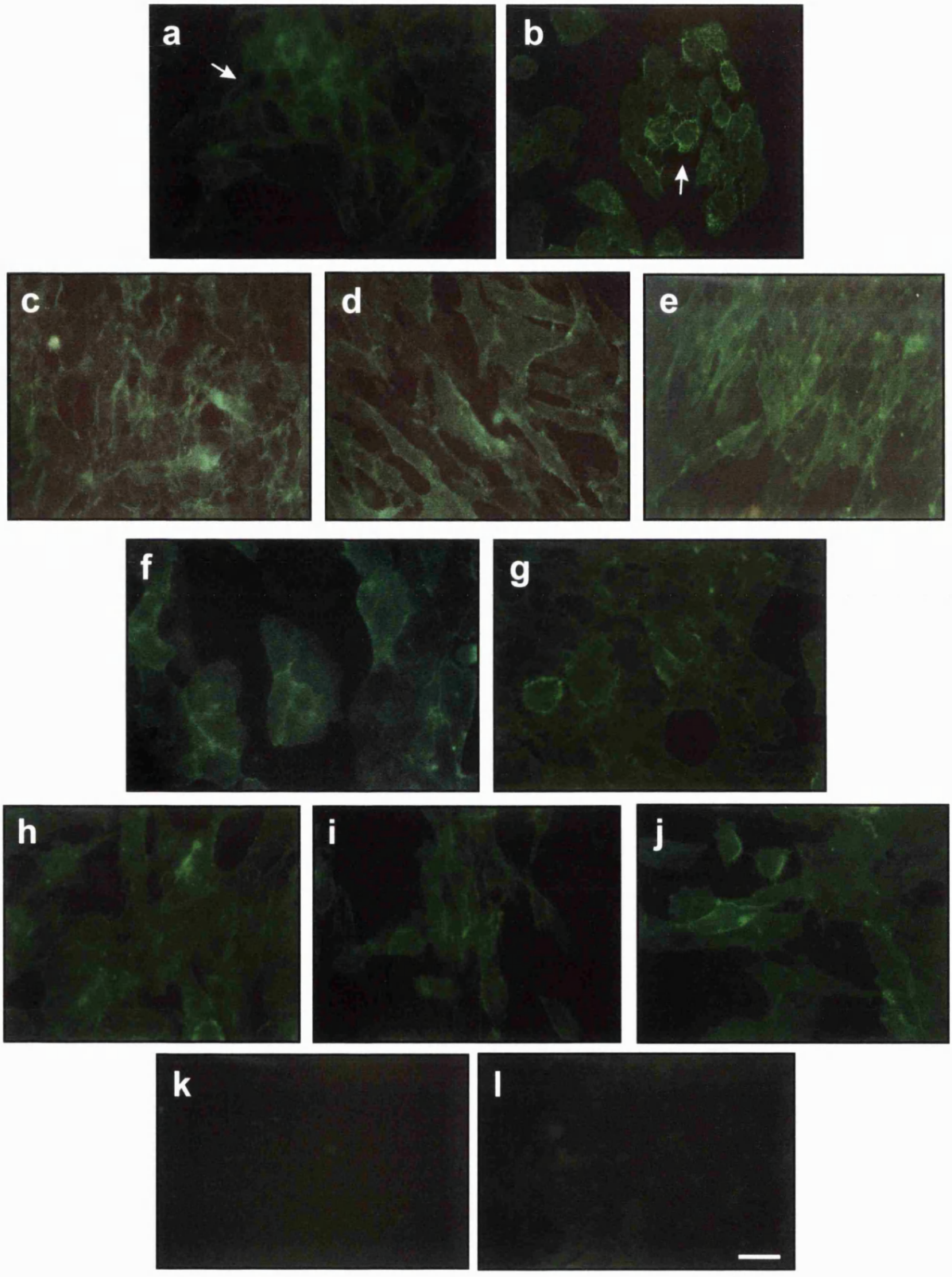
a
b
c
d
e
f
g
h
i
j
k
l

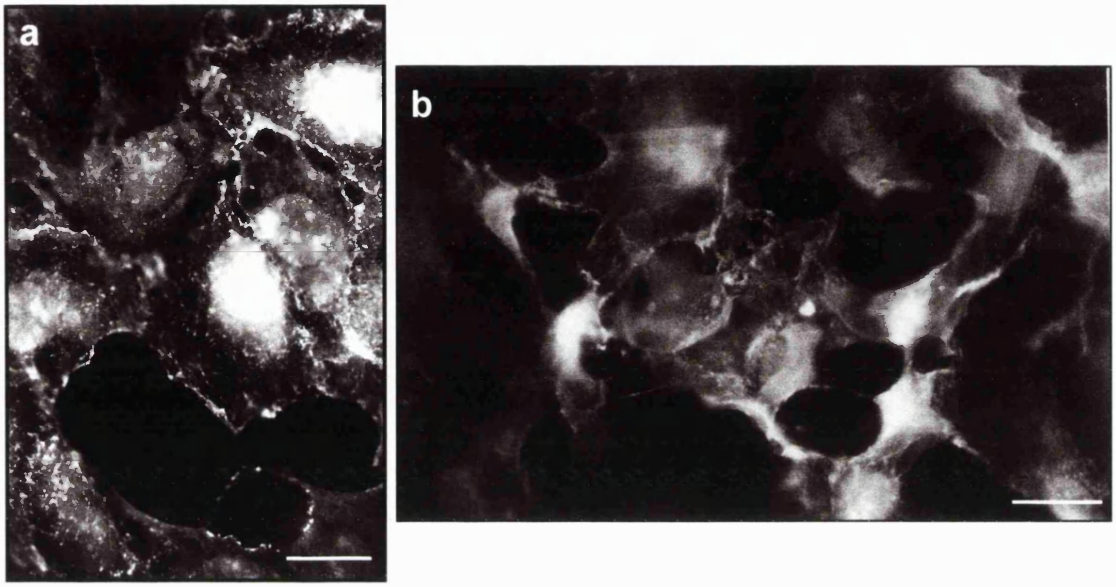

Figure 4.2 Indirect immunofluorescence micrographs of β_1 integrin expressed by U-2 OS cells cultured for 24 h in medium containing 10% FCS on (a): polished Zr, (b): Ti as received. The high power micrographs show that the integrins were typically distributed throughout the cell surface and cell periphery in clear focal granularities. In (b), details are only seen for small areas at a time due to the rough surface being at different depths of focus of the microscope used. Original magnification × 1000 (under oil immersion). Bars denote 5 μm.

Figure 4.3 Morphological appearance of the α_3 and α_5 integrin subunits expressed by three human osteosarcoma cell lines on glass substrates.

In contrast to the β_1 integrin expression, α_3 integrin subunits of all cell lines used grown on glass slides were expressed as small punctate granularities (PG) throughout the cell surface and at the cell periphery (arrows). α_2 and α_5 integrins were expressed diffusely throughout the cytoplasm. No areas of focal localisation of integrin subunits were seen.

The following micrographs of cell lines grown on glass substrates show the pattern of α_2 and α_5 integrin expression as described above.
(a), (b) and (c) show the α_3 integrin subunit expression by MG-63, HOS and U-2 OS cells, respectively.
(d), (e) and (f) show the α_5 integrin subunit expression by MG-63, HOS, and U-2 OS cells, respectively.

All micrographs shown were original magnification ×400. Bar in c = 10 μm, for a-c. Bar in f = 10 μm, for d-f.

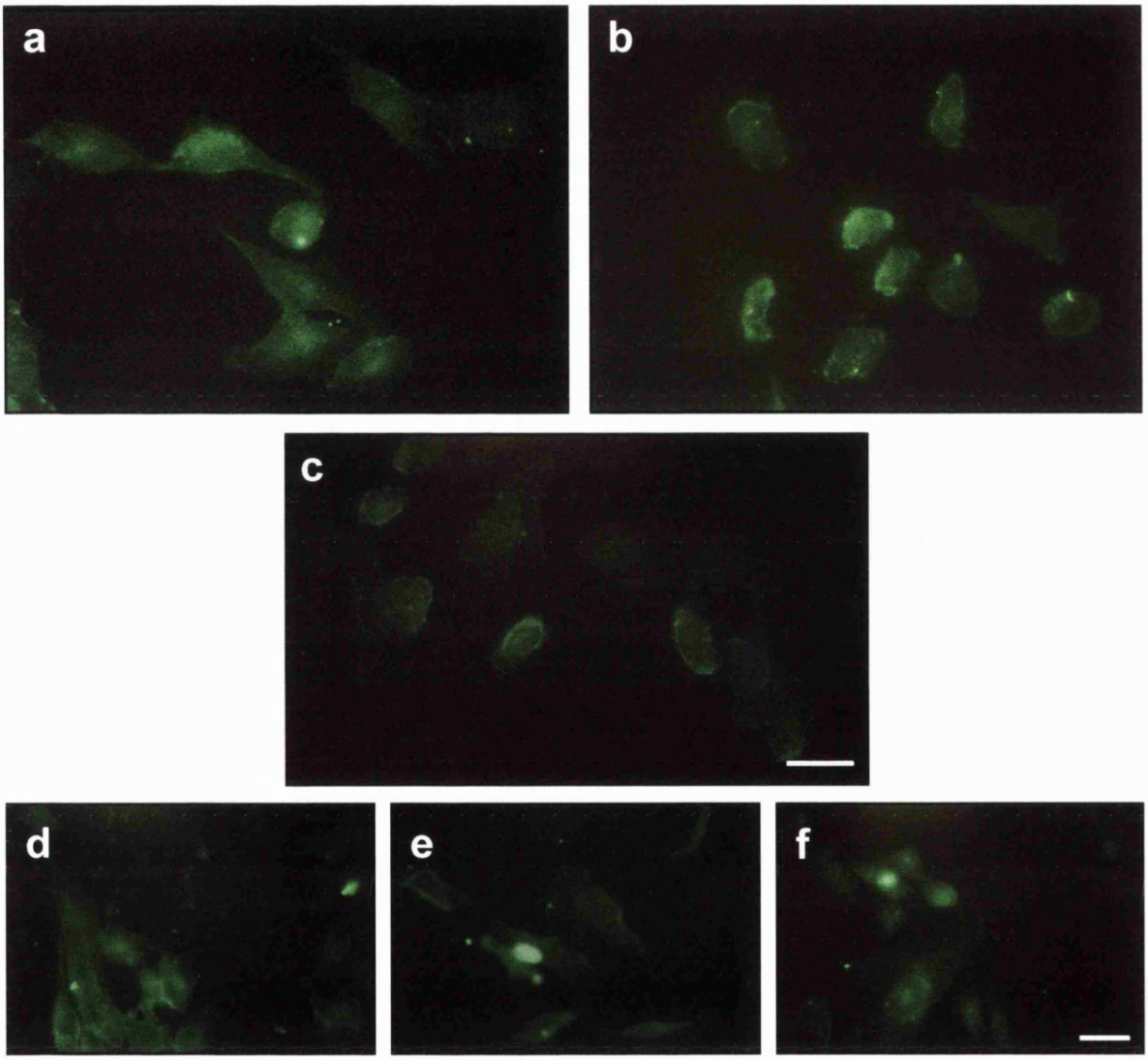
a
b
c
d
e
f

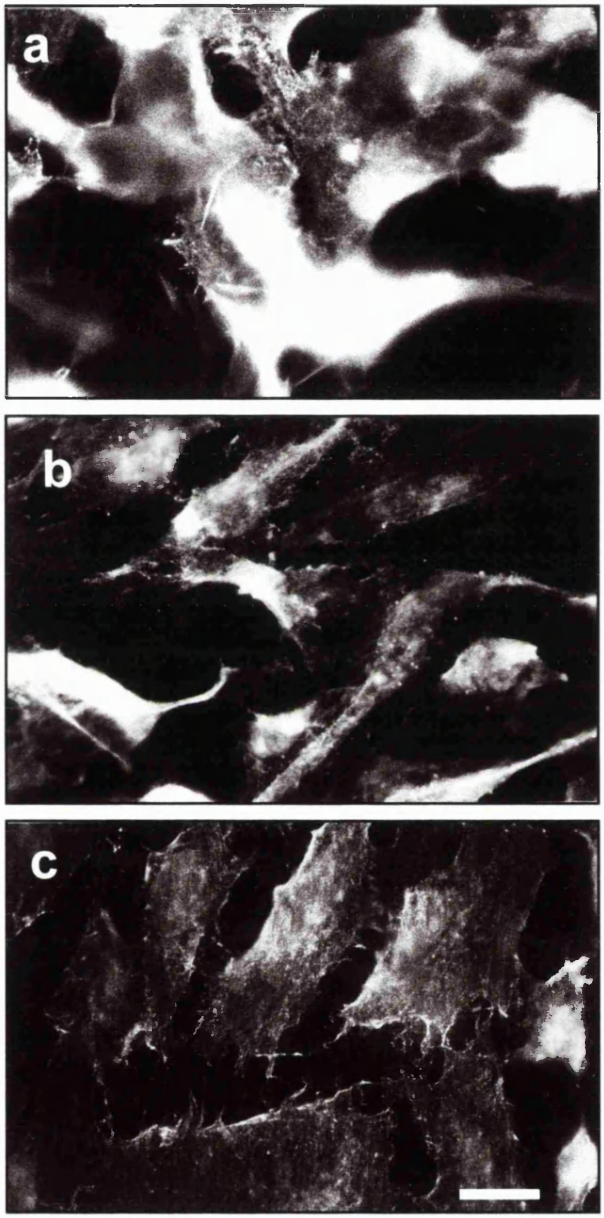

Figure 4.4 When grown on metal substrates, all cell lines expressed the α_3 integrin subunit as small punctate granularities (PG). This type of integrin expression is illustrated using HOS cells grown on (a): Ti as received, (b): Polished Ti, (c): Polished Zr. Original magnification × 1000. Bar in c denotes 5 μm, for a-c.

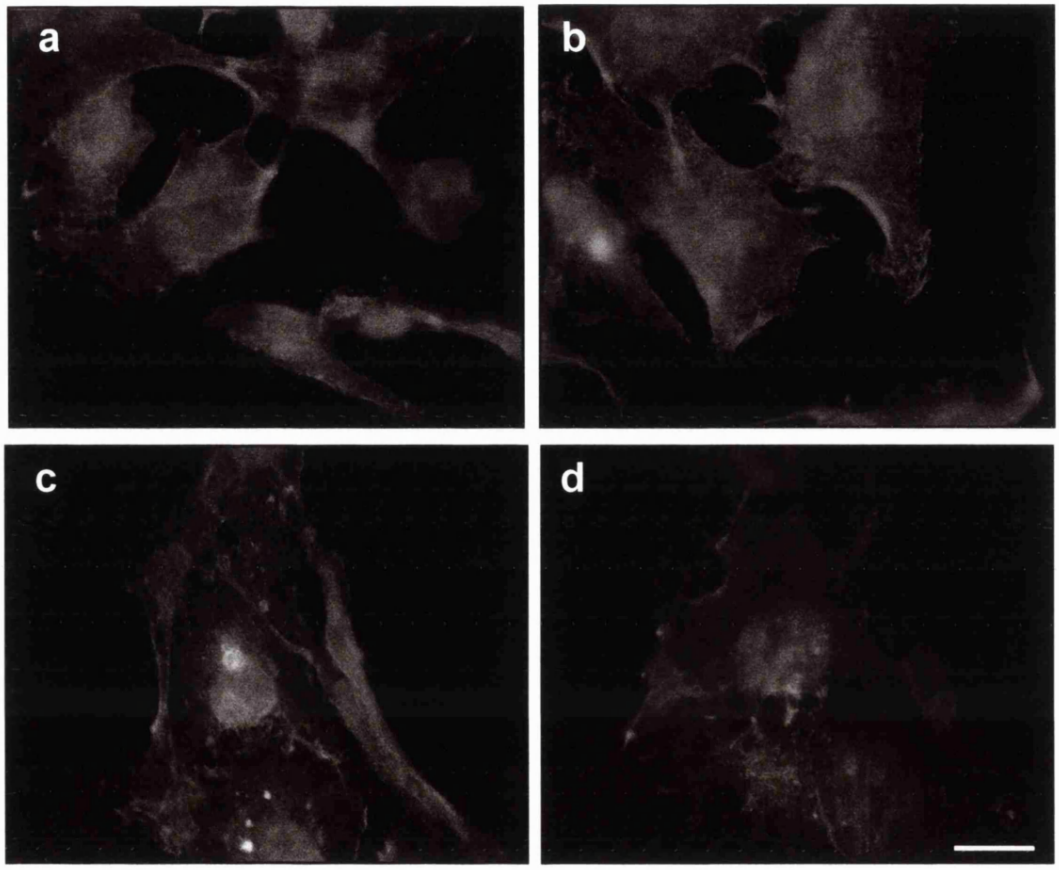

Figure 4.5 Expression of the α_2 integrin subunit by MG-63 and U-2 OS cell lines cultured on metal substrates. a: MG-63 cells on polished Ti, (b). MG-63 cells on polished Zr, (c). U-2 OS cells on polished Ti, (d). U-2 OS cells on polished Zr. Both cell lines expressed the integrins in a diffuse pattern throughout the cytoplasm. Integrin expression on rough as received Ti is not shown. However, it demonstrated the same diffuse expression. There was no apparent staining when HOS cells were cultured on metallic substrates (not shown). Original magnification ×1000. Bar in d denotes 5 μm, for a-d.

4.3.1.2 Actin cytoskeleton organisation and cell spreading

The state of spreading of the OB cells which attached to the substrates could be visualised by actin staining with rhodamine-phalloidin. Figure 4.6 shows MG-63 cells attached for 1 h in medium + 10% FCS on metals. During the initial stages of spreading, stress fibres are not yet developed. Microtubules were seen as patches/streaks on the cell surface.

As the cells are flattened on the surfaces, the actin fibres were spread over the substrates. Normal spreading is seen both on glass and metal substrates. These were shown using representative samples of MG-63 and U-2 OS cells grown on glass slides (Figure 4.7), and all the cell lines used grown on representative metal substrates (Figure 4.8).

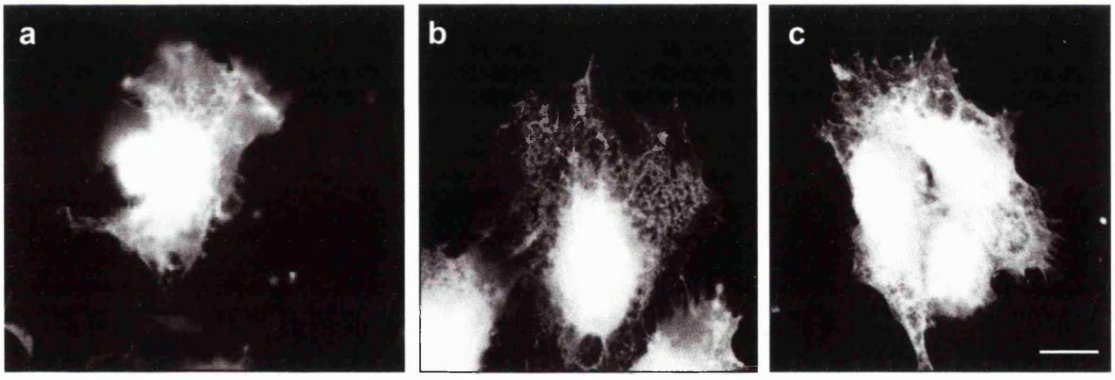

Figure 4.6 Fluorescent staining of actin filaments in MG-63 cells after 1 h attachment. Rhodamine conjugated phalloidin staining shows diffuse actin distribution in the cytoplasm. No stress fibres are seen in cells adherent to (a): rough Ti; (b): polished Ti; (c): polished Zr. The cells extended their cytoplasmic processes randomly in various directions. Original magnification × 1000. Bar in c denotes 5 μm, for a-c.

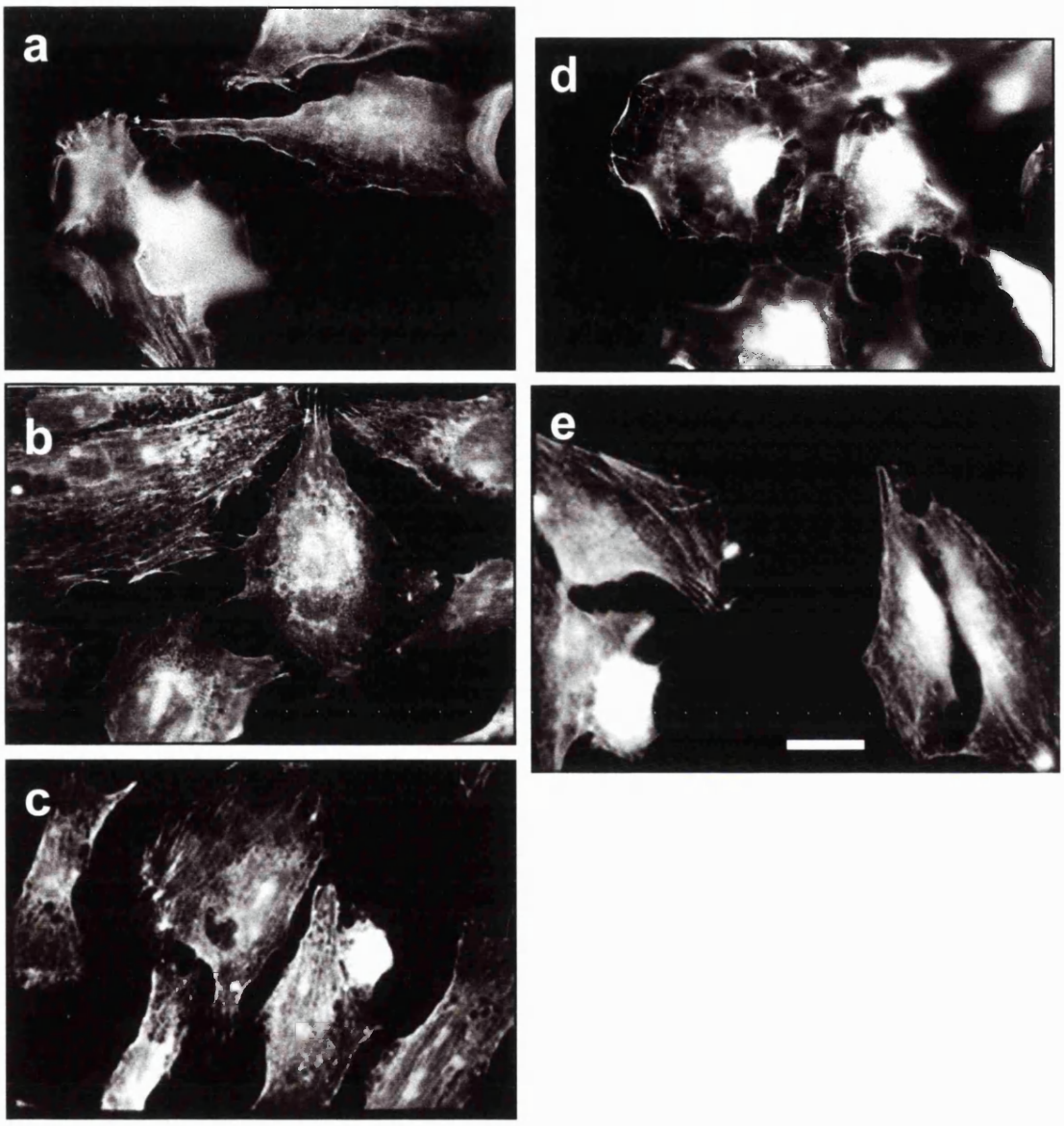

Figure 4.8 Morphology of the actin stress fibres of the cytoskeleton in OB cells after 24 h attachment on metallic substrates. The stress fibres were stained with rhodamine conjugated phalloidin. The micrographs show (a). HOS cells on Ti as received, (b). HOS cells on polished Ti, (c). HOS cells on polished Zr, (d). U-2 OS cells on Ti as received, (e). MG-63 cells on polished Zr. Although cells are spread, the stress fibres are not as well developed and prominent as those seen in cells grown on glass slides (Figure 4.7). Original magnification × 1000. Bar in e denotes 5 μm, for a-e.

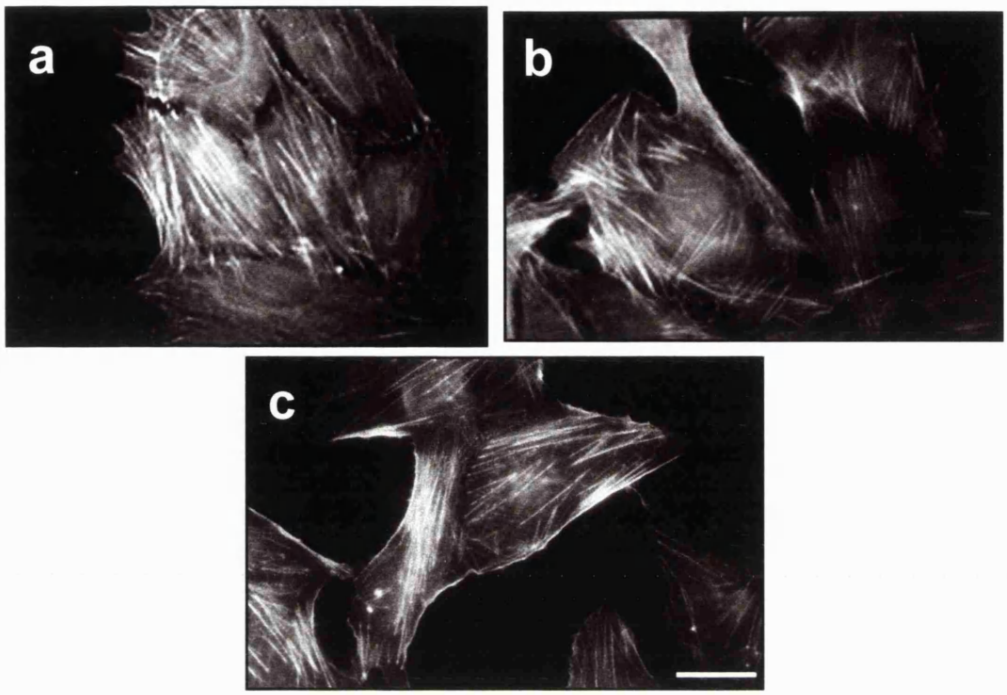

Figure 4.7 Morphology of the actin stress fibres of the cytoskeleton in cells grown on glass slides revealed using rhodamine conjugated phalloidin. Stress fibres are seen after 24 h attachment in MG-63 cells (a and b), and U-2 OS cells (c). By 24 h, the cells have spread extensively and developed prominent stress fibres. Some fibres are still radially oriented. Original magnification × 1000. Bar in c denotes 5 μm, for a-c.

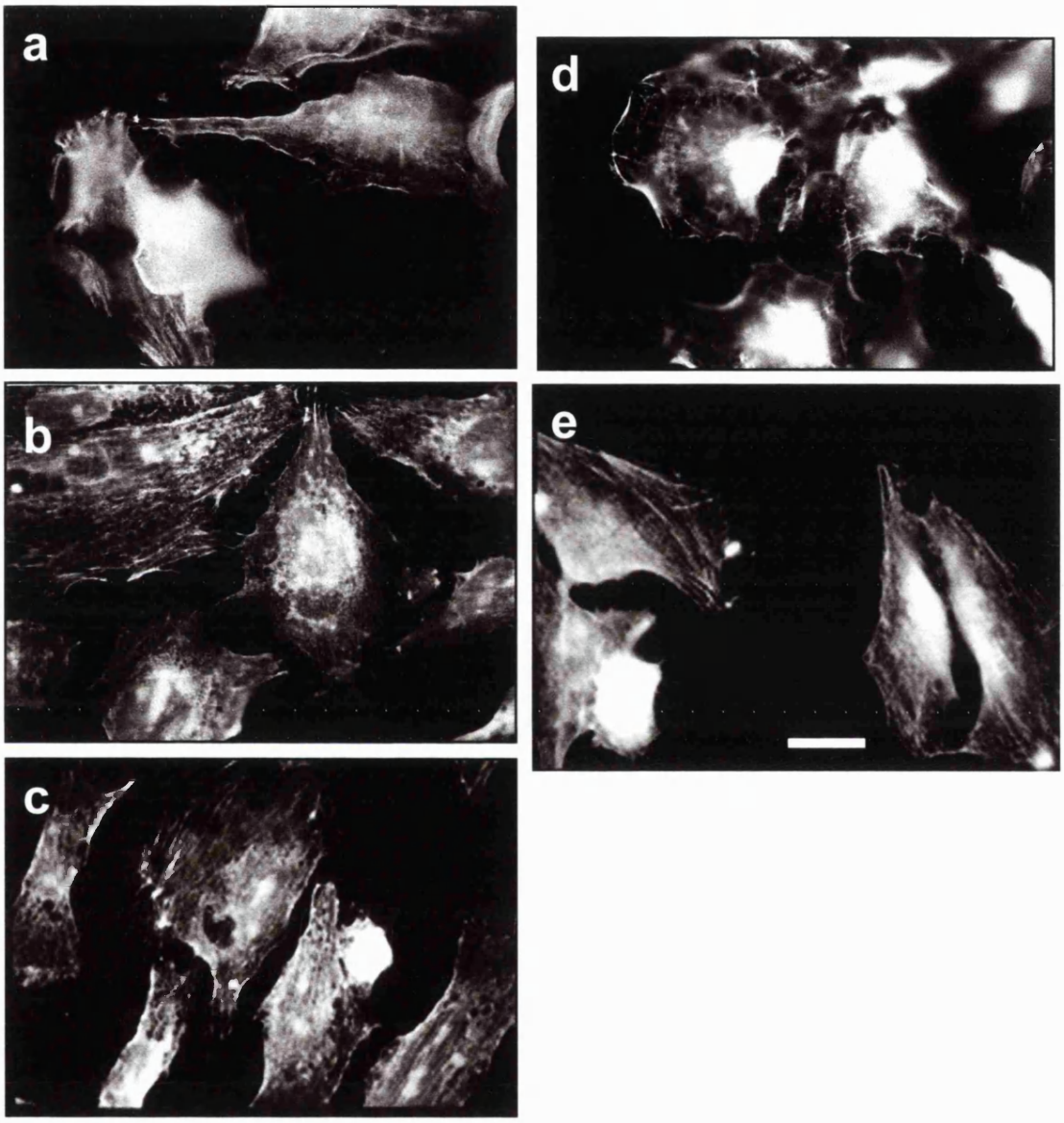

Figure 4.8 Morphology of the actin stress fibres of the cytoskeleton in OB cells after 24 h attachment on metallic substrates. The stress fibres were stained with rhodamine conjugated phalloidin. The micrographs show (a). HOS cells on Ti as received, (b). HOS cells on polished Ti, (c). HOS cells on polished Zr, (d). U-2 OS cells on Ti as received, (e). MG-63 cells on polished Zr. Although cells are spread, the stress fibres are not as well developed and prominent those seen in cells grown on glass slides (Figure 4.7). Original magnification × 1000. Bar in e denotes 5 μm, for a-e.

4.4 Discussion

Physicochemical properties of a biomaterial determine the adsorption of proteins that will influence the cellular reactions subsequent to cell attachment. Cell attachment is not only due to the ability of cells to bind directly to material surfaces, but also to reactions which occur as the material surface becomes conditioned by the culture medium and serum. Generally *in vivo*, cells do not bind directly to the material surface but rather to the extracellular glycoproteins adsorbed onto the surfaces (Brunette, 1988). Surface roughness is an important feature that may affect the adsorption of proteins as a result of the differences in the surface energy and surface wettability of materials with different surface roughnesses. This initial interaction produces a layer of macromolecules which may then modify the behaviour of cells on the substrates (Martin *et al.*, 1995).

Integrins are cell attachment molecules present on the plasma membrane of almost all cells. In culture, distinct integrins bind to their specific extracellular matrix ligands to form focal contacts, which are specialised adhesions to the underlying substrate (Buck and Horwitz, 1987a; Hynes, 1987). OB cells mainly use integrins for the majority of the initial cell attachment to various substrates *in vitro* (Stanford *et al.*, 1990; Gronowicz and McCarthy, 1996), and form focal contacts on a variety of substrates (Puleo and Bizios, 1992). Cellular interactions with their substrates and the extracellular matrix at the attachment sites are believed to generate specific signals that determine the cellular reaction to the extracellular environment.

Integrin mediated signalling depends both on binding specific extra-cellular matrix ligands including Vn, Fn and collagen type I and the establishment of a functional relationship with the cytoskeleton. As most OB integrins show the β_1 subunit, it follows that it is the α subunit which generally confers the ECM substrate specificity (Albelda and Buck, 1990). Unattached cells have a diffuse distribution of integrins on their surface. In the presence of an ECM ligand, specific integrin heterodimers become organised to form characteristic focal adhesions (Burridge *et al.*, 1988). These have a role in signalling events subsequent to cell attachment (Hynes, 1992). In addition to

specific integrin heterodimers, focal adhesions also comprise an array of cytoplasmic proteins such as vinculin, talin and α-actinin (Buck and Horwitz, 1987a; Hynes, 1987), which connect the cytoplasmic domains of the integrin heterodimer to actin stress fibres.

Even if there is no ECM ligand available for integrin binding, point contacts may form. These structures, first described in astrocytes or cardiac fibroblasts *in vitro* (Tawil *et al*, 1993), are small (90-200 nm) punctate regions of the cell closely apposed (15 nm) to the substrate. Integrins may also be expressed as point contacts when cells are motile or in the early stages of spreading when focal adhesions become disrupted and redistributed throughout the cytoplasm (Chen and Singer, 1982).

In this study, β_1 integrins were localised in structures resembling focal adhesions, whilst the α_2, α_3 and α_5 integrins had a diffuse or slightly granular staining pattern suggestive of point contacts. Because the latter do not localise to focal adhesion-like structures, the evidence presented here suggests that the β_1 integrin is not forming $\alpha_2\beta_1$, $\alpha_3\beta_1$ or $\alpha_5\beta_1$ heterodimers. Nevertheless, there are several studies indicating that osteoblasts or their precursors (Hughes *et al.*, 1993; Clover and Gowen, 1994; Saito *et al.*, 1994), or cells derived from osteoblast cell lines (Dedhar and Saulnier, 1990; Clover and Gowen, 1994) do express these integrin types. Several cell attachment studies have grown cells on coated substrates to determine whether particular proteins can function as ligands for cell attachment (Schneider and Burridge, 1994a; Gronowicz and McCarthy, 1996; Sinha and Tuan, 1996). Short term adhesion studies (2 h) where substrates were coated with ECM proteins, have shown that these proteins increase cellular attachment in a dose-dependent manner and that at the optimal concentration of ECM protein coating, 90-100% of cells attached to all matrices, compared to 20-40% in uncoated wells (Clover and Gowen, 1994).

There is evidence that MG-63 cells express the α_2, α_3 and α_5 subunits (Clover *et al.*, 1992). These results are confirmed by unpublished work from our laboratory (Alavi, A. L., Ph.D. Thesis, University of London - in preparation). Furthermore, functional studies using a murine calvarial model, have established a role for the $\alpha_3\beta_1$ and $\alpha_5\beta_1$ integrins in osteoblast differentiation. Taken together it is rather surprising that none of

the α subunits studied appeared to localise to the structures resembling focal adhesions. The reasons for this are unclear but may reflect differences in antibody binding properties between studies.

The major difficulty encountered in this investigation was viewing and photographing the fluorescence on the metal substrates. The reason for this was related to the property of the surfaces being examined. As the metal substrates were opaque, epifluorescence microscopy was used, and light reflected off the specimens caused rapid fading of the immunofluorescence. The problem of fading of fluorescence was minimised by using neutral density filters to reduce the incident light, and very fast black and white film to photograph the specimens. It was more difficult to view the integrin labelling on the rough Ti as light was scattered and reflected at different planes, and so only small areas were in focus at a time. In several cases there were apparent nuclear staining, even with the omission of the primary antibodies. For this reason, it was considered an artefact of the indirect immunofluorescence technique on the metal substrates (Sinha and Tuan, 1996).

In this pilot study cells were cultured in medium supplemented with 10% FCS. Serum contains a heterogeneous mixture of proteins including Fn and Vn which are known to coat implant surfaces and promote the attachment of anchorage dependent cells (Clover and Gowen, 1994; Howlett *et al.*, 1994; Schneider and Burridge, 1994a; Gronowicz and McCarthy, 1996; Sinha and Tuan, 1996). Because of this it is important to emphasise that the current study looked at the distribution of a small number of integrin heterodimers on the cell surface and did not provide functional data on their role in binding to specific ECM ligands. This area, together with studies involving double staining to co-localise specific integrin subunits, actin filaments or proteins known to be associated with focal adhesions such as focal adhesion kinase (FAK) may be developed further in the future.

The integrin receptors for Vn are $\alpha_v\beta_1$, $\alpha_v\beta_3$ and $\alpha_v\beta_5$ (Wayner, *et al.*, 1991; Hynes, 1992), although the major Vn receptor is $\alpha_v\beta_3$. In the context of bone, $\alpha_v\beta_3$ has been established as the major osteoclast integrin, but its expression as an osteoblast

integrin is controversial (Horton and Davies, 1989; Nesbitt *et al.*, 1993; Grzesik and Robey, 1994; Sinha and Tuan, 1996).

Fath *et al.* (1989) showed that when endothelial cells are grown in the presence of serum in the culture medium, while both the Vn and Fn receptors may be concentrated in focal contacts initially, with time, the Fn receptor, tends to be cleared away and become redistributed away from the focal contacts. This happens at approximately 6 h in culture, where some focal contacts contain only the Vn receptor or the Fn receptor, while occasionally some cells exhibited focal contacts containing both the receptors. However, by 12 h in culture, most cells contain focal contacts expressing only the Vn receptor. This means that in a mature focal contact, only Vn is accumulated and is not cleared from the focal contact, and therefore Vn is suggested to be more important than Fn for the formation of focal contacts.

The results of this study seemed to show that there was no difference in integrin expression between the cell lines or the different substrates. Only the β_1 integrin localised to the focal contact-like structures whilst the α_2, α_3, and α_5 were not. The $\alpha_3\beta_1$ and $\alpha_5\beta_1$ heterodimers are important in the formation of bone-like tissue *in vitro.* The α_5 subunit is a feature of more mature osteoblasts but there may be a down regulation of α_3 expression as cultures mature. This suggests that the $\alpha_3\beta_1$ heterodimer may be a feature of earlier osteoblasts (Moursi *et al.*, 1997). It is thus possible that the presence of the point granularities when staining for α_3 may reflect a mechanism by which cells make their initial response to the surface of the material, with α_5 binding becoming more important following subsequent adhesion to its specific matrix ligand. In this regard it is also relevant that the levels of expression of Fn mRNA and its subsequent synthesis are high during the early stages of osteoblast differentiation (Stein *et al.*, 1990), and both the $\alpha_3\beta_1$ and $\alpha_5\beta_1$ heterodimers are Fn binding integrins.

To examine more closely the sites of adhesion of the cells to the substrates, actin myofibrils were studied. Stress fibres formed after 24 h in culture, and the sites of attachment of the stress fibres to the substrates could be seen (Figures 4.7 and 4.8). Sinha *et al.* (1994) described three types of cytoskeletal (cell) morphologies observed in

OB cells cultured on Ti and cobalt-chromium alloys. These are related to the different stages in the cell spreading process after attachment and are described as: Type I, where cells are small and displayed only faint staining and no discernible actin filament formation. This morphology was seen with cells that were cultured for 3 h. Type II cells showed cortical filaments below the cell membrane with some radially oriented filaments. This morphology was seen with cells that were cultured for 6 h. Type III cells had distinct well-formed actin filaments that were parallel to one another and the long axis of the cell. At this stage, the cytoskeleton is most organised and is seen in cells cultured for at least 12 to 24 h.

Gronowicz and McCarthy (1996) studied the spreading of SaOS-2 cells on metal substrates and on glass in serum-free medium. They showed that most cells cultured on the metals had spread and developed stress fibres 24 h after plating on the substrates, while only 20% of cells on glass had spread. Spreading of cells on substrates indicates good attachment. In the present study, staining of the actin filaments on the cells grown on metallic substrates were carried out after 1 h and 24 h attachment. The results show that cells are able to spread on the metals used. However, cell spreading may not be as efficient as on the smooth control glass slide. This is seen when Figures 4.7 and 4.8 were compared, where it is seen that the actin stress fibres of cells grown on the control glass slides were more prominent than those seen on the polished Ti and Zr substrates. Actin filaments were also formed on the rough Ti substrate, and cell spreading was also not impaired by the substrate surface roughness used in the study. The formation of the actin stress fibres shows that the substrates used in the study, regardless of substrate roughness, are favourable substrates for cell attachment and cell spreading.

In general, this study did not show clearly that the profile of integrin expression was altered as a function of the substrate topography and chemistry. Nevertheless, some variations were seen in the distribution of the integrins expressed on glass and on metal substrates, although no differences were seen in the integrin expression of cells cultured on metals with different surface roughness and chemistry (Ti rough as opposed to polished Ti and Zr substrates).

4.5 Conclusions

1. OB cells may use different integrins to attach to different substrates.
2. Differences in integrin expression may be related to the cell types, and to the degree and type of substrate surface roughness and chemistry.
3. Integrins expressed and utilised by cells to attach to different substrates may reflect the differentiation state of the cells used.
4. A purely mechanistic theory of substrate surface roughness alone may not be sufficient to account for the variations in integrin expression and distribution that have been associated with OB cells grown on different substrates.

5. GENERAL DISCUSSIONS AND SUGGESTIONS FOR FUTURE WORK

5.1 Introduction

Osseointegration is a clinical observation at the end of a combination of various factors which influence this process, from patient selection to post-operative care, and reflects the events which occur systemically when a patient receives this form of treatment. With the high success rates which have been achieved with osseointegrated implants, we expect the following outcomes:

a. The adhesion of implant materials to hard and soft tissues should be optimised.
b. The union between bone and the implant material should enable the transferring of functional loads from the implant to bone.
c. New bone should form and regenerate as a normal wound healing process, and the properties of normal bone should be largely restored.
d. The changes should occur as rapidly as possible, with maximum bone formation along the entire length of the implant (Skalak and Brånemark, 1994; Cooper, 1998; Zarb and Albrektsson, 1998).

In order for all these expectations to be fulfilled, we need to understand the basis of bone formation at the bone-implant interface. Bone can only be formed by the bone-forming cells, the osteoblasts, and therefore it is essential that initial cellular adhesion to the implant surface is understood, as cellular adhesion to a substrate is necessary for further cellular responses.

This study was carried out in three parts to highlight the importance of characterising surfaces and using the appropriate culture conditions to illustrate cellular reactions to implant materials. In Chapter 2, the topic of surface roughness was introduced, and a systematic method of quantifying surface roughness of implant materials was presented. Variables that would affect the results of surface roughness measurements using the commonly available contact profilometer, and a laser scanning

profilometer were discussed. Both techniques have their limitations, and provide only quantitative information about substrate topography. As such, they would have to be complemented with qualitative examination using scanning electron microscopy, or confocal laser scanning microscopy, in order that the relationship of the cells to the substrate topography could be visualised.

Chapter 3 considers experiments to investigate cellular differentiation and its relationship to substrate topography. The results in this part of the investigation showed that the substrate topography used did not have any significant effect on the differentiation of the cells grown on smooth or rough surfaces. Chapter 4 examines the possible effects of substrate topography on individual cells, rather than a collective effect, as was considered in Chapter 3, where the biochemical assay results would represent the activity of all cells present on the substrates.

Information about substrate topography is thought to be conveyed to the cells via integrins, which are responsible for the majority of the initial attachment of osteoblast-like cells to their substrates. For this reason, the integrin expression and the arrangement of the actin stress fibres of cells which attached to the substrates were studied.

Integrins have been shown to localise at focal adhesions, which are not only attachment sites, but are also cytoskeleton-signalling complexes which enable cells to modify their responses to the environment both inside and outside the cells (Hynes, 1992). Culturing cells on different substrates can affect cell growth and differentiation, as different signals may be generated in response to binding to different substrate and ECM components. One of the cellular responses to these signals may be manifested as changes in cell shape (Ben-Ze'ev, 1986). Changes in cell shape are important in determining cellular metabolism, which further regulates cell growth and differentiation. All these initial interactions are the results of integrin binding to their specific ligands adsorbed on to the substrates on which the cells were attached.

OB cells have been shown to form focal adhesions when cultured on various biomaterials (Puleo and Bizios, 1992; Schneider and Burridge, 1994a; 1994b). In an

attempt to study and explain their role in osseointegration, cpTi surfaces were coated with fibronectin (Fn), and cellular reactions to coated and uncoated surfaces were studied (Schneider and Burridge, 1994b). When adhesions are strong and the substrate inflexible, the microfilaments align into bundles stretching between the points of tight adhesion. Contraction against strong adhesions may also recruit additional microfilaments to the stress fibre and therefore contribute to the prominence of these structures. Cells grown on less adhesive substrates have been observed to adopt a more rounded morphology which lack stress fibres. However, the addition of the adhesive protein Fn, restores cells to the normal morphology where stress fibres are seen (Schneider and Burridge, 1994a).

This indicates that stress fibres and focal contacts are related to the substrate adhesiveness, and therefore to the surface energy and physical properties of the substrates. Focal contacts are characteristics of cells which are not motile, well spread and in a proliferative state (Burridge *et al.*, 1988). Increasing the adhesiveness of the cell-substrate contacts by adding Fn, resulted in closer and increased area of cell contact (corresponding to the increased number and distribution of the focal contacts) to the surface (Schneider and Burridge, 1994b). Cell adhesion is therefore essential for biomaterials to integrate with host tissues, and tighter cell adhesion may possibly result in more bone-implant contact.

Francois *et al.* (1997) measured the amount of Fn adsorbed by cpTi coverslips which had undergone different surface treatments. As these surfaces had different surface areas due to their different roughnesses, the authors also corrected the surface areas by roughness so that the amounts of Fn adsorbed by the different surfaces could be normalized. They found that when the adsorption of Fn was not corrected by surface area, the protein adsorption was highest on the roughest sandblasted surfaces, followed by a similar amount of adsorption on both the smoother control poly(methylmethacrylate) (PMMA) coverslips and the mirror polished cpTi, and the least adsorption on the acid treated cpTi, with intermediate roughness. However, when the surface area correction was made, Fn adsorption to the rough sandblasted and acid treated cpTi discs was only 50% of that occurring on smooth mirror-polished Ti or

PMMA. This is further evidence that different types of roughness of Ti surfaces may affect Fn adsorption and cell adhesion, and therefore is critical in determining further cellular reactions.

5.2 Experimental Approach

There have been many approaches taken to study cell-biomaterial interactions in the field of dental and orthopaedic implantology. The approach chosen is determined by the ultimate goals of the investigations, which may include:

a. identification of cytotoxic, biocompatible or potentially bioactive implant materials
b. identification of the physical and chemical properties of the materials which affect cellular reactions, and the mechanisms by which the materials exert these effects
c. identification of the mechanisms by which cells react to these biomaterials
d. evaluation and establishing factors (either physical, chemical or biological) which may modify the situation towards stimulatory or more favourable cellular reaction, for example, increased and more rapid bone formation around the implants
e. predicting events that may occur in *in vivo* situations, as a result of the presence of the device within the biological environment.

Animal models have always been used to predict potential *in vivo* situations, although it is recognised that there are metabolic differences between humans and different animal species. Financial and logistical considerations, and moral pressures to reduce animal experimentation have also led to the increasing role that *in vitro* cell culture studies have played in cell-biomaterial interaction studies.

In vitro tissue culture studies include organ culture and cell culture. In organ culture, a small fragment of tissue or whole embryonic organ is explanted to retain tissue architecture, while in cell culture, the tissue is dispersed mechanically or enzymatically, or by spontaneous migration of particular cells from an explant are

propagated as an attached monolayer of cells in tissue culture flasks (Freshney, 1994). Organ culture maintains the different cell-cell relationships *in vitro*, and therefore is closer to the *in vivo* situation than cell culture techniques. Different tissues can be maintained using a variety of methods (Lasnitzki, 1994), however, they cannot be cultivated indefinitely *in vitro.* In cases where longer periods of cultivation are needed, a combined *in vitro-in vivo* procedure may be used, where tissues are implanted into a suitable host such as diffusion chambers (Gundle *et al.*, 1995) and the chorioallantoic membrane of developing chick eggs, in which a blood supply to the tissue in culture was rapidly established (Leung, 1998).

This project set out to study the initial interactions of OB cells to material surfaces. An *in vitro* cell culture model was therefore appropriate, as *in vivo* and organ cultures would be heterogenous. The choice of cell lines was made after considering the relevant parameters and ultimate aim of the experiments, i.e. to study whether the substrate surface roughness used in the study affects the initial interaction of bone cells to the surfaces. Human osteosarcoma cell lines were chosen in these experiments as they are homogeneous cultures, and identical to each other. They are also easily obtained and handled, and experiments can be standardised. Primary OB cells do not possess these properties, and results may vary as the osteoblast lineage and state of differentiation may be inconsistent.

The behaviour of MG-63 and HOS cells has been compared with normal human OB cells (Clover and Gowen, 1994) and it was found that their adhesive properties, initial differentiation, and integrin expression are the same, and these are the basis of this study. It is not known whether these cell lines are able to produce mineralised matrix in culture, and the conditions for terminal differentiation of these cells into bone, have not been defined (Lincks *et al.*, 1998c). Although in this study, cultures were grown on the substrates in an attempt to see if the matrix could mineralise, failure to produce mineralised cultures was not related to the suitability of the surfaces as implant materials, but rather to the limitations inherent in these cell lines. It is also acknowledged that transformed and tumour cells normally have no contact with

implants *in situ*, and therefore normal human cells should be used in the next phase of the experiments.

However, it is also realised that even the use of primary cells in an *in vitro* situation could never be extrapolated to the *in vivo* situation, where systemic factors have a controlling influence. Davies *et al.* (1991) summarised the limitations of *in vitro* situations as: the absence of biomechanical forces, cellular reactions occur in the absence of the complex interplay of the inflammatory response, neovascularization, platelet interactions, and the role of stromal stem cells, rather than differentiated cells, and other cell types in the complex *in vivo* environment. In *vitro* situations therefore, at best, represent only the interactions of certain cells during specific phases of the host-biomaterial interactions, and may even then, reflect only the assumed situations. These reasons therefore merit the use of cell lines as initial approaches in the experiments.

5.3 The relationship of substrate surface roughness to OB cell attachment, differentiation and bone formation

The interaction of cells with implants is determined by physical and chemical factors, one of the most important being implant surface topography (Brunette, 1988). *In vitro* studies have demonstrated that the surface structure of implants affects bone cell growth and differentiation patterns (Bowers *et al.*, 1992; Ong *et al.*, 1996; Martin *et.*, 1995; Boyan *et al.*, 1998), and ultimate bone formation (Wennerberg, 1996).

In studies relating cell reactions to implant surfaces, roughness was indicated by surface roughness parameter values, textural dimensions and pore sizes of the roughness irregularities of the surface, or qualifying surfaces with SEM micrographs. For maximum bone formation and greater removal torque forces, rough surfaces with isotropic and evenly spaced indentations, as produced by blasting surfaces with 25 or 75 μm particles of TiO_2 or Al_2O_3 (numerically characterised with R_a or S_a values of around 1.5 μm, maximum peak to valley height R_{max} or S_t values of 20-26 μm, and surface peak distance S or S_{ax} values of 10-17 μm) appear to be optimal (Wennerberg, 1996). She also suggested that rougher surfaces (as shown by blasting surfaces with 250 μm

particles, numerically described as having S_a values of about 2 μm, S_t values of 37 μm, and surface peak distance S or S_{cx} values of 13-20 μm) may have no further advantage to the bone formation as the optimal roughness value may have been exceeded, or that increased roughness have resulted in ionic leakage from the implants which was detrimental to apatite and bone formation. No qualitative examinations of the surfaces used were made, and as this was an *in vivo* study, no comparison of the OB cells to the pit sizes of the roughness irregularities could be made. However, it may be assumed that the pit diameter was less than 10 μm, as the irregular pit diameters would always be less than the values quantifying the horizontal peak spacings.

Hansson (1998) used a mathematical model (quoted in Norton, 1998), to show that the interfacial shear strength is built upon two key features of the pits in rough surfaces: pit density and pit effectivity. He showed that greatest shear strength of the implant is produced by spherical pits, packed as closely together as possible, and having a pit diameter of ≥ 2–3 μm. The dimension calculated by Hansson is much smaller than the dimensions of the irregularities used by Wennerberg (1996), although he quoted the same R_a value of 1.5 μm as the roughness value of his ideal surface.

Although *in vitro* work with OB cells has indicated that the number of cells attached may be related to increased surface roughness of Ti substrates (Bowers *et al.*, 1992), the surfaces used may be considered smooth, with R_a values of about 0.2 μm. Swart *et al.* (1992) and Stanford *et al.* (1994), working within this range of surface roughness also showed that it is not surface roughness *per se* which affects OB cell attachment to the surfaces.

The *in vitro* work of Martin *et al.* (1995) and Boyan *et al.* (1998) showed that surface roughness may have the ability to enhance maturation of immature OB cells and increase alkaline phosphatase (AP) activity and matrix protein synthesis. Although working with transformed cells they showed that the most AP activity was produced by cells growing on the roughest plasma sprayed cpTi surface, with R_a value of 6.8 μm and R_{max} of about 40 μm. These studies did not use spatial parameters to characterise their

surfaces. However, SEM examination showed that the pits on the rough surface were about 20 μm in diameter.

Titanium plasma-sprayed implants are produced by spraying at high temperatures and at a very high velocity, partially molten particles of Ti powder, with a particle size of 50 to 100 μm (Lemons and Dietsh-Misch, 1999). This process produces porous or rough Ti surfaces, as shown by the roughness values obtained by Martin *et al.* (1995) and Boyan *et al.* (1998). However, the surface roughness was quantified using a contact profilometer, and therefore these results may be smoothed out, and R_a and R_{max} values may be higher if quantified using an optical profilometer, as was done by Wennerberg (1996). Enhancement of MG-63 cell differentiation may then be due to the pit size, which was very deep in relation to the cell size. Cells may have been "buried" in the pits, and therefore forced to differentiate rather than spread and proliferate. Terminal differentiation to mineralisation was not pursued, as conditions to promote mineralisation were not known in this cell line.

Cooper *et al.* (1999) however, working with primary foetal bovine mandibular OB cells managed to culture these cells to the mineralisation stage on machined cpTi surfaces ($R_a = 0.8$ μm), Ti surfaces grit-blasted ($R_a \approx 4$ μm), and Ti plasma sprayed with TiO_2 particles ($R_a \approx 5$ μm). It was difficult to grow cultures on the rough Ti plasma sprayed surfaces as the cells on this surface displayed a tendency to spontaneously contract or reflect after around 5 days in culture. Nevertheless, when successfully cultured to 14 days, mineralisation (qualitatively assessed by Von Kossa staining and osteocalcin and bone sialoprotein staining) was found to be less than that which was found on the machined cpTi and grit blasted cpTi surfaces. This may be further evidence that there is an upper limit to the surface roughness of implant surfaces for favourable bone formation.

Vercaigne *et al.* (1998) however, maintained the view that the relationship between surface roughness and bone formation is still inconclusive, as they found no difference in bone formation when plasma sprayed Ti alloy implants (R_a value ranging from 4.7-40 μm) were inserted in goats for up to three months. They however, found

that although there were areas of direct bone contact along the bone-implant interface, some areas of the implant were only contacted by fibrous tissue. They concluded that the very rough coatings may have lead to increased ionic leakage which interfered with bone formation, and that certainly very rough surfaces are not favourable for optimal bone-implant contact, other than for mechanical interlocking.

In the present study, the roughness of Ti as received falls in between the surfaces described by Wennerberg (1996) as optimal, and the plasma-sprayed Ti surface shown by Martin *et al.* (1995) and Boyan *et al.* (1998) as being able to regulate bone matrix protein expression by "forcing" immature cells to skip the proliferation stage and go straight into differentiation (Boyan *et al.*, 1998). Ti as received had an R_a value of about 2 μm, R_{max} 18 μm, and S value of 37 μm. With these values, the cells were able to distinguish it as a rough surface, and still be able to bridge across the grooves (Figures 3.3b and 3.4b). The similar cellular responses to cell attachment, spreading and alkaline phosphatase activity may be due to the fact that once the cells were able to attach and spread without any limiting factors, they were able to continue into the differentiation stage equally, and the effect of the surface roughness on the cell lines used was not seen.

The above examples show that, regardless of the R_a value, it is the relationship of the cells to the surface pits and topography that matters, and it is the extreme height parameters and spatial parameters that are critical in determining cellular responses. These are the roughness parameters that should be quoted by research workers in this field, and not the commonly used R_a value. Besides that, a qualitative examination of the surfaces studied is also essential in order to fully characterise the surfaces. The results of bone cell attachment, differentiation and bone formation have always been equivocal. The results of this study have added to our knowledge but left the question of an optimal surface roughness still unanswered.

5.4 *Integrin expression and organisation of actin stress fibres of OB cells grown on metallic substrates*

The presence or absence of integrin subunits expressed by cells grown on substrates was solely based on immunofluorescence results, a technique which is non-quantitative. It was initially decided to quantify the integrins expressed using image analysis techniques, but the limitation in using a normal fluorescence microscope in examining rough surfaces ruled out this possibility. When expressed, there were no difference in the integrin expression and distribution of a specific integrin receptor for all cell lines grown on different substrates.

In this study the cells were seeded in medium containing 10% FCS, and only the β_1 integrins were distributed as focal contacts, while other integrin subunits were either distributed in punctate granularities or diffusely distributed throughout the cell surface (Table 4.2). Since focal contacts represent the sites for strongest cell-substrate adhesion, our results suggest that the surfaces were able to support cell adhesion. Both Fn and Vn are needed for cell attachment, and these adhesive proteins are present in the serum used in culturing these cells.

The organisation of the stress fibres showed that cell spreading was not inhibited on the metal substrates, regardless of the surface roughness. Cells used in the study may need more than 24 h to orient their stress fibres to indicate the direction of their spreading. This is shown in Figure 4.7, where actin stress fibres in MG-63 and U-2 OS cells grown on smooth glass slides are oriented radially. Figure 4.8 shows OB cells on polished Ti and polished Zr are beginning to orient themselves to the substrate morphology as shown by the direction of the stress fibres in relation to the long axes of the cells.

5.5 Conclusions and the relevance of the study to the understanding of cell-biomaterial interactions

It is clear that the metals and surface roughness of substrates used in this study support OB cell attachment, proliferation and early differentiation as shown by the SEM micrographs and results of the ELISA assays. However, ELISA techniques are not sufficiently sensitive to detect changes at the individual cell level, as they measure the response of the whole population of vital cells attached to the substrates.

Therefore immunofluorescence studies were carried out to gauge the early responses of the individual cells. In this study, integrin expression was affected by the type of cells used, and also by the substrates on which the cells were grown. This was shown by the lack of α_2 expression by HOS cells when grown on metal substrates, although the integrin subunit was expressed when HOS cells were grown on glass slides. This indicates that the same cells may use different integrins to attach to different substrates. However, this was only shown by the HOS cell line, and not by the MG-63 and U-2 OS cell lines. One criticism of this study was that no validition of the results was done by coating substrates with ligands for the specific integrin tested. Coating of substrates with ECM proteins which are ligands for the integrins tested would also serve as positive controls for the experiments.

Formation of actin stress fibres on all substrates showed that cell spreading was not limited by the rough surface of the cpTi as received, and that the cells spread equally well on the polished metal substrates as on the rough ones. However, as actin stress fibres are not as prominent as those seen on cells grown on glass substrates (Figures 4.7 and 4.8), it may be concluded that the cells were able to sense differences in the culture surfaces, and that the cells do respond to the substrate morphology. This is further supported by SEM micrographs (Figures 3.5 and 3.15) which show the cells aligning themselves along the grooves of the polished Ti surface, but spreading in all directions on the rough as-received Ti surface. However, this study did not show that the difference in the alignment of the cells on the rough and polished surfaces altered the differentiation of the cells, as shown by the similar biochemical assay results.

The mechanism controlling the cell-substrate interactions in relation to substrate surface roughness and morphology are still not understood. However, it is clear that:

a. the depth and width of grooves, and their periodicity influence the behaviour of bone cells,
b. integrins may be responsible for transferring information about the substrate morphology to the intracellular components. This investigation has justified that further work is needed to ascertain the precise role of integrins in cell attachment to biomaterials of different surface morphology and roughness.

The ultimate goal in studying response of cells to substrate topography is to use the information to promote tissue regeneration and to increase the amount of bone formation at bone-implant interfaces. In this study substrate surface roughness has been evaluated and it has been shown that cells are able to immediately distinguish between substrate morphology, as shown by the spreading pattern of the cells on the substrates used. However, differences were not noted in the integrin expression and biochemical assay results. These may be due to the degree of substrate surface roughness used, as they may be too similar for subtle differences to be detected by biochemical assays. Nevertheless these results should have been validated using other appropriate tests to confirm the results obtained.

This aim of this study was to document the effect of substrate surface roughness on cellular reactions. The hypothesis tested was that surface roughness regulates the bone cell reaction to the surfaces. This study has shown that the substrates used played a role in the cellular response, and that the cell culture model provides an important early step for such studies.

However, it is acknowledged that variations in the results of cell-substrate interactions of different roughnesses depend on the cell types used, time in culture, different materials and methods of preparation of surfaces, different morphological dimensions and roughness of substrates used, different methods of quantifying surface roughness, and finally to the different assays, techniques, and reagents used to

Ti as received 2	1.96	2.43	10.81	13.37	32.00	74.00	2.544
	2.32	3.29	15.92	35.62	52.00	251.00	2.544
	1.93	2.39	9.93	13.73	31.00	104.00	2.544
	2.07	2.64	11.13	13.78	29.00	84.00	2.541
	2.01	2.53	11.23	14.20	29.00	89.00	2.541
	2.02	2.62	11.68	17.32	35.00	87.00	2.541
	1.79	2.23	10.17	12.16	29.00	66.00	2.534
	1.75	2.32	11.37	16.77	35.00	97.00	2.534
	1.77	2.32	11.01	16.70	33.00	95.00	2.534
Ti as received 3	2.41	3.05	13.34	20.63	36.00	129.00	2.578
	2.20	2.98	12.99	22.19	41.00	108.00	2.578
	2.20	3.05	13.71	26.18	42.00	214.00	2.578
	2.28	2.98	13.90	25.53	43.00	117.00	2.581
	2.38	3.02	13.65	20.45	40.00	103.00	2.581
	2.07	2.78	12.63	21.94	39.00	93.00	2.581
	2.23	2.81	12.69	18.97	30.00	108.00	2.590
	2.35	2.90	12.13	15.58	32.00	98.00	2.590
	2.28	2.97	12.64	20.09	31.00	126.00	2.590
Ti as received 4	1.84	2.35	11.65	14.92	33.00	100.00	2.539
	2.26	2.93	12.86	19.58	42.00	139.00	2.539
	1.90	2.40	10.63	14.54	30.00	77.00	2.539
	2.09	2.62	11.56	15.41	33.00	88.00	2.561
	2.09	2.58	10.54	13.28	28.00	87.00	2.561
	2.55	3.05	12.66	16.80	33.00	98.00	2.561
	2.25	2.83	12.73	16.16	35.00	131.00	2.543
	2.22	2.95	12.53	21.15	38.00	176.00	2.543
	2.24	3.44	14.78	36.33	66.00	200.00	2.543
Ti as received 5	2.13	2.90	13.79	22.08	43.00	118.00	2.551
	2.08	2.66	11.01	16.79	33.00	77.00	2.551
	2.15	2.92	12.82	20.18	40.00	120.00	2.551
	1.71	2.17	9.18	12.08	27.00	88.00	2.546
	1.98	2.58	13.16	19.52	36.00	98.00	2.546
	1.84	2.32	10.17	12.23	27.00	72.00	2.546
	2.33	3.20	12.75	20.78	36.00	84.00	2.562
	2.36	2.94	12.67	16.20	30.00	94.00	2.562
	2.01	2.56	10.43	16.07	32.00	108.00	2.562
Polished Ti 1	0.73	0.94	4.54	5.27	21.00	49.00	2.349
	0.75	0.91	3.82	4.56	24.00	38.00	2.349
	0.76	0.95	4.11	4.98	23.00	43.00	2.349
	0.82	0.99	4.12	5.48	20.00	34.00	2.351
	0.79	0.96	4.05	4.58	21.00	35.00	2.351
	0.82	1.01	4.15	5.58	22.00	41.00	2.351
	0.67	0.85	3.98	4.25	22.00	37.00	2.354
	0.73	0.90	3.91	4.38	21.00	35.00	2.354
	0.78	0.95	4.17	5.08	23.00	40.00	2.354
Polished Ti 2	0.77	0.95	4.56	6.20	24.00	47.00	2.361
	0.81	1.01	4.30	4.95	21.00	47.00	2.361
	0.83	1.02	4.61	5.43	21.00	49.00	2.361
	0.84	1.03	4.29	5.20	22.00	36.00	2.366
	0.79	1.00	4.70	5.49	22.00	41.00	2.366

References

ABIKO, Y., and BRUNETTE, D. M. (1993). Immunohistochemical investigation of tracks left by the migration of fibroblasts on titanium surfaces. *Cells Mater* **3**, 161-170.

ADELL, R., ERIKSSON, B., LEKHOLM, U., BRÅNEMARK, P-I., and JEMT, T. (1990). A long-term follow-up study of osseointegrated implants in the treatment of the totally edentulous jaws. *Int J Oral Maxillofac Implants* **5**, 347-359.

AHMAD, M., MCCARTHY, M., and GRONOWICZ, G. (1998). An in vitro model for mineralization of human osteoblast-like cells on implant materials. *Biomaterials* **20**, 211-220.

AKIYAMA, S. K. (1996). Integrins in cell adhesion and signalling. *Hum Cell* **9**, 181-186.

ALAVI, A. L., WALSH, S., BERESFORD, J. N., and BENNETT, J. H. (1998). Integrin expression in a mandibular explant model of osteoblast differentiation. *In "Biological mechanisms of tooth eruption, resorption and replacement by implants".* (Z. Davidovitch, and J. Mah, Eds.), pp. 361-367, Harvard Society for the Advancement of Orthodontics, Boston, Massachusetts.

ALBELDA, S. M., and BUCK, C. A. (1990). Integrins and other cell adhesion molecules. *FASEB J* **4**, 2868-2880.

ALBREKTSSON, T. (1988). A multi-center report on osseointegrated oral implants. *J Prosthet Dent* **60**, 75-84.

ALBREKTSSON, T., DAHL, E., ENBOM, L., ENGEVALL, S., ENGQUIST, B., ERIKKSSON, A. R., FELDMANN, G., FREIBERG, N., GLANTZ, P. O., KJELLMAN, O., KRISTERSSON, L., KVINT, S., KONDELL, P. A., PALMQUIST, J., WERNDAHL, L., and ASTRAND, P. (1988). Osseointegrated oral implants - A Swedish multicentre study of 8139 consecutively inserted Nobelpharma implants. *J Periodontol* **59**, 287-296.

ALBREKTSSON, T., and HANSSON, H. A. (1986). An ultra-structural characterization of the interface between bone and sputtered titanium or stainless steel surfaces. *Biomaterials* **7**, 201-205.

ALBREKTSSON, T., HANSSON, H. A., and IVARSSON, B. (1985). Interface analysis of titanium and zirconium bone implants. *Biomaterials* **6**, 97-101.

ALBREKTSSON, T., and JOHANSSON, C. (1991). Quantified bone tissue reactions to various metallic materials with reference to the so-called osseointegration concept. *In*: "The bone-biomaterial interface" (J. E. Davies, Ed.), pp. 357-363, University of Toronto Press, Toronto.

ALBREKTSSON, T., and SENNERBY, L. (1991). State of the art in oral implants. *J Clin Periodontol* **18**, 474-481.

ALBREKTSSON, T., and ZARB, G. A. (1993). Current interpretations of the osseointegrated response: Clinical significance. *Int J Prosthodont* **6**, 95-105.

ALBREKTSSON, T., ZARB, G., WORTHINGTON, P., and ERIKSSON, A. R. (1986). The long-term efficacy of currently used dental implants: A review and proposed criteria of success. *Int J Oral Maxillofac Implants* **1**, 11-25.

AMERICAN SOCIETY FOR TESTING AND MATERIALS, NO. F86-91, VOL.13.01. Standard practice for surface preparation and marking of metallic surgical implants.

AUF' MKOLK, B., HAUSCHKA, P. V., and SCHWARTZ, E. R. (1985). Characterization of human bone cells in culture. *Calcif Tissue Int* **37**, 228-235.

BAGAMBISA, F. B., KAPPERT, H. F., and SCHILLI, W. (1994). Cellular and molecular biological events at the implant interface. *J Cranio Maxillofac Surg* **22**, 12-17.

BAIER, R. E., MEYER, A. E., AKERS, C. K., NATIELLA, J. R., MEENAGHAN, M., and CARTER J. M. (1982). Degradative effects of conventional steam sterilization on biomaterial surfaces. *Biomaterials* **3**, 241-245.

BAIN, C. A., and MOY, P. K. (1993). The association between the failure of dental implants and cigarette smoking. *Int J Oral Maxillofac Implants* **8**, 609-615.

BATZER, R., LIU, Y., COCHRAN, D. L., SZMUCKLER-MONCLER, S., DEAN, D. D., BOYAN, B. D., and SCHWARTZ, Z. (1998). Prostaglandins mediate the effects of titanium surface roughness on MG63 osteoblast-like cells and alter cell responsiveness to 1α,25-$(OH)_2D_3$. *J Biomed Mater Res* **41**, 489-496.

BECKER, W., BECKER, B. E., ISRAELSON, H., LUCCHINI, J. P., HANDELSMAN, M., AMMONS, W., ROSENBERG, E., ROSE, L., TUCKER, L. M., and LEKHOLM, U. (1997). One-step surgical placement of Brånemark implants: A prospective multicentre clinical study. *Int J Oral Maxillofac Implants* **12**; 454-462.

BELLOWS, C. G., AUBIN, J. E., HEERSCHE, J. N. M., and ANTOSZ, M. E. (1986). Mineralised bone nodules formed in vitro from enzymatically released rat calvaria cell populations. *Calcif Tissue Int* **38**, 143-154.

BEN-ZE'EV, A. (1986). Regulation of cytoskeletal protein synthesis in normal and cancer cells. *Cancer Rev* **4**, 91-116.

BERESFORD, J. N., GRAVES, S. E., and SMOOTHY, C. A. (1993). Formation of mineralized nodules by bone derived cells in vitro: A model of bone formation? *Am J Med Genet* **45**, 163-178.

BERESFORD, J. N., JOYNER, C. J., DEVLIN, C., and TRIFFIT, J. T. (1994). The effects of dexamethasone and 1,25-dihydroxyvitamin D_3 on osteogenic differentiation of human marrow stromal cells *in vitro*. *Arch Oral Biol* **39**, 941-947.

BERGENDAL, B., BERGENDAL, T., HALLONSTEN, A. L., KOCH, G., KUROL, J., and KVINT, S. (1996). A multidisciplinary approach to oral rehabilitation with osseointegrated implants in children and adolescents with multiple aplasia. *Euro J Orthod* **18**, 119-129.

BINON, P. P., WEIR, D. J., and MARSHALL, S. J. (1992). Surface analysis of an original Brånemark implant and three related cones. *Int J Oral Maxillofac Implants* **7**, 168-174.

BJURSTEN, L. M., EMANUELSSON, L., ERICSON, L. E., THOMSEN, P., LAUSMAA, J., MATTSSON, L., ROLANDER, U., and KASEMO, B. (1990). Method for ultrastructural studies of the intact tissue-metal interface. *Biomaterials* **11**, 596-601.

BODINE, P. V. N., TRAILSMITH, M., and KOMM, B. S. (1996). Development and characterization of a conditionally transformed adult human osteoblastic cell line. *J Bone Miner Res* **11**, 806-819.

BOWERS, K. T., KELLER, J. C., RANDOLPH, B. A., WICK, D. G., and MICHAELS, C. M. (1992). Optimization of surface micromorphology for enhanced osteoblast responses in vitro. *Int J Oral Maxillofac Implants* **7**, 302-310.

BOYAN, B. D., BATZER, R., KIESWETTER, K., LIU, Y., COCHRAN, D. L., SZMUCKLER-MONCLER, S., DEAN, D. D., and SCHWARTZ, Z. (1998). Titanium surface roughness alters responsiveness of MG63 osteoblast-like cells to 1α,25-$(OH)_2D_3$. *J Biomed Mater Res* **39**, 77-85.

BOYAN, B. D., HUMMERT, T. W., KIESWETTER, K., SCHRAUB, D., DEAN, D. D., and SCHWARTZ, Z. (1995). Effect of titanium surface characteristics on chondrocytes and osteoblasts *in vitro*. *Cells Mater* **5**, 323-335.

BOYAN, B. D., SCHWARTZ, Z., and HAMBLETON, J. C. (1993). Response of bone and cartilage cells to biomaterials *in vivo* and *in vitro*. *J Oral Implantol* **19**, 116-122.

BOYAN, B. D., HUMMERT, T. W., DEAN, D. D., and SCHWARTZ, Z. (1996). Role of material surfaces in regulating bone and cartilage cell response. *Biomaterials* **17**, 137-146.

BOYDE, A., WOLFE, L. A., HOWELL, P. G. T., WONG, K., JONES, S. J., and GREENBERG, G. L. (1998). Efficient microscopy to survey bone healing around dental implants. *J Dent Res* 77 (Special issue B) 838, Abstr. 1653.

BRÅNEMARK, P-I. (1985). Introduction to osseointegration. *In*: "Tissue-Integrated Prostheses." (P. I. Brånemark, G. A. Zarb, and T. Albrektsson, Eds.), pp. 11-76, Quintessence Publishing Co. Inc., Chicago.

BRÅNEMARK, P. I. (1983). Osseointegration and its experimental background. *J Prosthet Dent* **50**, 399-410.

BRÅNEMARK, P. I. (1994). Osseointegration: Biotechnological perspective and clinical modality. *In*: "Osseointegration in skeletal reconstruction and joint replacement" (P-I. Brånemark, B. L. Rydevik, and R. Skalak, Eds.), pp. 1-24, Quintessence Publishing Co. Inc., Chicago.

BRITISH STANDARD 6741 (1987). British standard glossary of surface roughness terms Part 1: Surface and its parameters.

BRITISH STANDARD 1134 (1990). British standard glossary of surface roughness terms Part II: Determination of surface roughness.

BROWN, D. (1998). All you wanted to know about titanium, but were afraid to ask. *Br Dent J* **182**, 393-394.

BRUNETTE, D. M. (1988). The effects of implant surface topography on the behaviour of cells (Review). *Int J Oral Maxillofac Implants* **3**, 231-246.

BUCK, C. A., and HORWITZ, A. F. (1987a). Cell surface receptors for extracellular matrix molecules. *Ann Rev Cell Biol* **3**, 179-205.

BUCK, C. A., and HORWITZ, A. F. (1987b). Integrin, a transmembrane glycoprotein complex mediating cell-substratum adhesion. *J Cell Sci* Suppl **8**, 231-250.

BUDD, T. W., BIELAT, K. L., MEENAGHAN, M. A., and SCHAAF, N. G. (1991). Microscopic observations of the bone/implant interface of surface-treated titanium implants. *Int J Oral Maxillofac Implants* **6**, 253-258.

BURRIDGE, K., FATH, K., KELLY, T., NUCKOLLS, G., and TURNER, C. (1988). Focal adhesions: Transmembrane junctions between the extracellular matrix and the cytoskeleton. *Ann Rev Cell Biol* **4**, 487-525.

BUSER, D., SCHENK, R. K., STEINEMANN, S., FIORELLINI, J. P., FOX, C. H., and STICH, H. (1991). Influence of surface characteristics on bone integration of titanium implants. A histomorphometric study in miniature pigs. *J Biomed Mater Res* **25**, 889-902.

BUSER, D., BELSER, U. C., and LANG, N. P. (1998). The original one-stage dental implant system and its clinical application. *Periodontology 2000* **17**, 106-118.

CALLEN, B. W., LOWENBERG, B. F., LUGOWSKI, S., SODHI, R. N. S., and DAVIES, J. E. (1995). Nitric acid passivation of Ti6Al4V reduces thickness of surface oxide layer and increases trace element release. *J Biomed Mater Res* **29**, 279-290.

CARLSSON, L., RÖSTLUND, T., ALBREKTSSON, B., and ALBREKTSSON, T. (1988). Removal torques for polished and rough titanium implants. *Int J Oral Maxillofac Implants* **3**, 21-24.

CARVALHO, R. S., SCOTT, J. E., and YEN, E. H. K. (1995). The effects of mechanical stimulation on the distribution of β_1 integrin and expression of β_1-integrin mRNA in TE-85 human osteosarcoma cells. *Arch Oral Biol* **40**, 257-264.

CHEHROUDI, B., GOULD, T. R., and BRUNETTE, D. M. (1989). Effects of a grooved titanium-coated implant surface on epithelial cell behaviour *in vitro* and *in vivo*. *J Biomed Mater Res* **23**, 1067-1085.

CHEHROUDI, B., RATKAY, J., and BRUNETTE, D. M. (1992). The role of implant surface geometry on mineralization *in vivo* and *in vitro*: A transmission and scanning electron microscopic study. *Cells Mater* **2**, 89-104.

CHEN, W. T., and SINGER, S. J. (1982). Immunoelectron microscopic studies of the sites of cell-substratum and cell-cell contacts in cultured fibroblasts. *J Cell Biol* **95**, 205-222.

CHEN, D., MAGNUSON, V., HILL, S., ARNAUD, C., STEFFENSEN, B., and KLEBE, R. J. (1992). Regulation of integrin gene expression by substrate adherence. *J Biol Chem* **267**, 23502-23506.

CHUNG, C. H., GOLUB, E. E., FORBES, E., TOKUOKA, T., and SHAPIRO, I. M. (1992). Mechanism of action of β-glycerophosphate on bone cell mineralization. *Calcif Tissue Int* **51**, 305-311.

CLARK, P., CONNOLLY, P., CURTIS, A. S. G., DOW, J. A. T., and WILKINSON, C. D. W. (1987). Topographical control of cell behaviour. I. Simple step cues. *Development* **99**, 439-448.

CLARK, P., CONNOLLY, P., CURTIS, A. S. G., DOW, J. A. T., and WILKINSON, C. D. W. (1990). Topographical control of cell behaviour. II. multiple grooved substrata. *Development* **108**, 635-644.

CLOKIE, C. M. L., and WARSHAWSKY, H. (1995). Morphologic and radioautographic studies of bone formation in relation to titanium implants using the rat tibia as a model. *Int J Oral Maxillofac Implants* **10**, 155-165.

CLOVER, J., DODDS, R. A., and GOWEN, M. (1992). Integrin subunit expression by human osteoblasts and osteoclasts *in situ* and in culture. *J Cell Sci* **103**, 267-271.

CLOVER, J., and GOWEN, M. (1994). Are MG-63 and HOS TE85 human osteosarcoma cell lines representative models of the osteoblastic phenotype? *Bone* **15**, 585-591.

COCHRAN, D. L., SIMPSON, J., WEBER, H. P., and BUSER, D. (1994). Attachment and growth of periodontal cells on smooth and rough titanium. *Int J Oral Maxillofac Implants* **9**, 289-297.

COOPER, L. F. (1998). Biologic determinants of bone formation for osseointegration: Clues for future clinical improvements. *J Prosthet Dent* **80**, 439-449.

COOPER, L. F., MASUDA, T., WHITSON, S. W., YLIHEIKKILÄ, P., and FELTON, D. A. (1999). Formation of mineralizing osteoblast cultures on machined, titanium oxide grit-blasted, and plasma-sprayed titanium surface. *Int J Oral Maxillofac Implants* **14**, 37-47.

COOPER, L. F., MASUDA, T., YLIHEIKKILÄ, P. K., and FELTON, D. A. (1998). Generalizations regarding the process and phenomenon of osseointegration. Part II. In vitro studies. *Int J Oral Maxillofac Implants* **13**, 163-174.

CURTIS, A. S. G., and WILKINSON, C. D. W. (1998). Reactions of cells to topography. *J Biomater Sci Polym Ed* **9**, 1313-1329.

DAVIES, J. E. (1988). *In vitro* assessment of bone biocompatibility. *Int Endod J* **21**, 178-187.

DAVIES, J. E. (1996). *In vitro* modelling of the bone/implant interface. *Anat Rec* **245**, 426-445.

DAVIES, J. E. (1998). Mechanisms of endosseous integration. *Int J Prosthodont* **11**, 391-401.

DAVIES, J. E., OTTENSMEYER, P., SHEN, X., HASHIMOTO, M., and PEEL., S. A. F. (1991). Early extracellular matrix synthesis by bone cells. *In*: "The bone-biomaterial interface" (J. E. Davies, Ed.), pp. 214-228, University of Toronto Press, Toronto.

DEAN, J. W., CULBERTSON, K. C., and D'ANGELO, A. M. (1995). Fibronectin and laminin enhance gingival cell attachment to dental implant surfaces in vitro. *Int J Oral Maxillofac Implants* **10**, 721-728.

DEDHAR, S., and SAULNIER, R. (1990). Alterations in integrin receptor expression on chemically transformed human cells: Specific enhancement of laminin and collagen receptor complexes. *J Cell Biol* **110**, 481-489.

DEN BRABER, E. T., DE RUIJTER, J. E., GINSEL, L. A., VON RECUM, A. F., and JANSEN, J. A. (1998). Orientation of ECM protein deposition, fibroblast cytoskeleton, and attachment complex components on silicone microgrooved surfaces. *J Biomed Mater Res* **40**, 291-300.

DE SANTIS, D., GUERRIERO, C., NOCINI, P. F., UNGERSBÖCK, A., RICHARDS, G., GOTTE, P., and ARMATO, U. (1996). Adult human bone cells from jaw bones cultured on plasma-sprayed or polished surfaces of titanium or hydroxylapatite discs. *J Mater Sci Mater Med* **7**, 21-28.

DEE, K. C., ANDERSEN, T. T., and BIZIOS, R. (1998). Design and function of novel osteoblast-adhesive peptides for chemical modification of biomaterials. *J Biomed Mater Res* **40**, 371-377.

DEE, K. C., RUEGER, D. C., ANDERSEN T. T., and BIZIOS, R. (1996). Conditions which promote mineralization at the bone-implant interface: A model *in vitro* study. *Biomaterials* **17**, 209-215.

DOGLIOLI, P., and SCORTECCI, G. (1991). Characterization of endosteal osteoblasts isolated from human maxilla and mandible: An experimental system for biocompatibility tests. *Cytotechnology.* **7**, 39-48.

DOILLON, C. J., and CAMERON, K. (1990). New approaches for biocompatibility testing using cell culture. *Int J Artif Organs* **13**, 517-520.

DOUNDOULAKIS, J. H. (1987). Surface analysis of titanium after sterilization: Role in implant-tissue interface and bioadhesion. *J Prosthet Dent* **58**, 471-478.

EDGERTON, M., and LEVINE, M. J. (1993). Biocompatibility: Its future in prosthodontic research (Review). *J Prosthet Dent* **69**, 406-415.

EINHORN, T. A. (1998). The cell and molecular biology of fracture healing. *Clin Orthop* **355S**, S7-S21.

EISENBARTH, E., MEYLE, J., NACHTIGALL, W., and BREME, J. (1996). Influence of the surface structure of titanium materials on the adhesion of fibroblasts. *Biomaterials* **17**, 1399-1403.

ELLINGSEN, J. E. (1998). Surface configurations of dental implants. *Periodontology 2000* **17**, 36-46.

ERICSON, L. E., JOHANSSON, B. R., ROSENGREN, A., SENNERBY, L., and THOMSEN, P. (1991). Ultrastructural investigation and analysis of the interface of retrieved metal implants. *In* "The Bone Biomaterial Interface" (J. E. Davies, Ed.), pp. 425-437, University of Toronto Press, Toronto.

ESPOSITO, M., HIRSCH, J. -M., LEKHOLM, U., and THOMSEN, P. (1998a). Biological factors contributing to failures of osseointegrated oral implants (I). Success criteria and epidemiology. *Eur J Oral Sci* **106**, 527-551.

ESPOSITO, M., HIRSCH, J. -M., LEKHOLM, U., and THOMSEN, P. (1998b). Biological factors contributing to failures of osseointegrated oral implants (II). Etiopathogenesis. *Eur J Oral Sci* **106**, 721-764.

FATH, K. R., EDGELL, C. S., and BURRIDGE, K. (1989). The distribution of distinct integrins in focal contacts is determined by the substratum composition. *J Cell Sci* **92**, 67-75.

FOLKMAN, J., and MOSCONA, A. (1978). Role of cell shape in growth control. *Nature* **273**, 345-349.

FRANCESCHI, R. T., JAMES, W. M., and ZERLAUTH, G. (1985). 1α,25-dihydroxyvitamin D_3 specific regulation of growth, morphology, and fibronectin in a human osteosarcoma cell line. *J Cell Physiol* **123**, 401-409.

FRANCOIS, P., VAUDAUX, P., TABORELLI, M., TONETTI, M., LEW, D. P., and DESCOUTS, P. (1997). Influence of surface treatments developed for oral implants on the physical and biological properties of titanium. (II). Adsorption isotherms and biological activity of immobilized fibronectin. *Clin Oral Implants Res* **8**, 217-225.

FRESHNEY, R. I. (1994). Introduction to basic principles. *In*: "Animal cell culture: A practical approach" (R. I. Freshney, Ed.), pp. 1-14, Oxford University Press, Oxford.

FRIEDENSTEIN, A. J., CHAILAKHYAN, R. K., and GERASIMOV, U. V. (1987). Bone marrow osteogenic stem cells: *In vitro* cultivation and transplantation in diffusion chambers. *Cell Tissue Kinet* **20**, 263-272.

GLANTZ, P. -O. (1998a). Biomaterial considerations for the optimised therapy for the edentulous predicament. *J Prosthet Dent* **79**, 90-92.

GLANTZ, P. -O. (1998b). The choice of alloplastic materials for oral implants: Does it really matter? *Int J Prosthodont* **11**, 402-407.

GOMI, K., and DAVIES, J. E. (1993). Guided bone tissue elaboration by osteogenic cells *in vitro*. *J Biomed Mater Res* **27**, 429-431.

GRAY, C., BOYDE, A., and JONES, S. J. (1996). Topographically induced bone formation in vitro: Implications for bone implants and bone grafts. *Bone* **18**, 115-123.

GREEN, A. M., JANSEN, J. A., VAN DER WAERDEN, J. P. C. M., and VON RECUM, A. F. (1994). Fibroblast response to microtextured silicone surfaces: Texture orientation into or out of the surface. *J Biomed Mater Res* **28**, 647-653.

GROESSNER-SCHREIBER, B., and TUAN, R. S. (1992). Enhanced extracellular matrix production and mineralization by osteoblasts cultured on titanium surfaces *in vitro*. *J Cell Sci* **101**, 209-217.

GRONOWICZ, G., and MCCARTHY, M. B. (1996). Response of human osteoblasts to implant materials: Integrin-mediated adhesion. *J Orthop Res* **14**, 878-887.

GRONTHOS, S., STEWART, K., GRAVES, S. E., HAY, S., and SIMMONS, P. J. (1997). Integrin expression and function on human osteoblast-like cells. *J Bone Miner Res* **12**, 1189-1197.

GROTH, T., and ALTANKOV, G. (1996). Studies on cell-biomaterial interaction: Role of tyrosine phosphorylation during fibroblast spreading on surfaces varying in wettability. *Biomaterials* **17**, 1227-1234.

GRZESIK, W. J. (1997). Integrins and bone - Cell adhesion and beyond. *Archivum Immunologiae et Therapiae Experimentalis* **45**, 271-275.

GRZESIK, W. J., and ROBEY, P. G. (1994). Bone matrix RGD glycoproteins: Immunolocalization and interaction with human primary osteoblastic bone cells in vitro. *J Bone Miner Res* **9**, 487-496.

GUAN, J.-L. (1997). Role of focal adhesion kinase in integrin signalling. *Int J Biochem Cell Biol* **29**, 1085-1096.

GUNDLE, R., JOYNER, C. J., and TRIFFITT, J. T. (1995). Human bone tissue formation in diffusion chamber culture in vivo by bone-derived cells and marrow stromal fibroblastic cells. *Bone* **16**, 597-601.

GUNNE, J., NYSTRÖM, E., and KAHNBERG, K. (1995). Bone grafts and implants in the treatment of the severely resorbed maxillae: A 3-year follow up of the prosthetic restoration. *Int J Prosthodont* **8**, 38-45.

HAKKINEN, L., YLIURPO, A., HEINO, J., and LARJAVA, H. (1988). Attachment and spreading of human gingival fibroblasts on potentially bioactive glasses in vitro. *J Biomed Mater Res* **22**, 1043-1059.

HALL, R. M., UNSWORTH, A., SINEY, P., and WROBLEWSKI, B. M. (1996). The surface topography of retrieved femoral heads. *J Mater Sci Mater Med* 7, 739-744.

HANAWA, T (1991). Titanium and its oxide film: A substrate for formation of apatite. *In*: "The bone-biomaterial interface" (J. E. Davies, Ed.), pp. 49-61, University of Toronto Press, Toronto.

HANSSON, S. (1998). Dental implants - why choose a rough surface? Astra Tech Insight **1**, 5.

HARMAND, M. F., BORDENAVE, L., BARIELLE, A., NAJI, A., JEANDOT, R., ROUAIS, F., and DUCASSOU, D. (1991). *In vitro* evaluation of an epoxy resin's cytocompatibility using cell lines and human differentiated cells. *J Biomater Sci Polym Ed* **2**, 67-79.

HAYASHI, K., INADOME, T., TSUMURA, H., NAKASHIMA, Y., and SUGIOKA, Y. (1994). Effect of surface roughness of hydroxyapatite-coated titanium on the bone-implant interface shear strength. *Biomaterials* **15**, 1187-1191.

HEALY, K. E., and DUCHEYNE, P. (1992). The mechanism of passive dissolution of titanium in a model physiological environment. *J Biomed Mater Res* **26**, 319-338.

HENCH, L. L., and WILSON, J. (1993). Introduction. *In*: "An introduction to bioceramics - Advanced Series in Ceramics, vol. 1" (L. L. Hench, and J. Wilson, Eds.), pp. 1-24, World Scientific, Singapore.

HORMIA, M., and KÖNÖNEN, M. (1994). Immunolocalization of fibronectin and vitronectin receptors in human gingival fibroblasts spreading on titanium surfaces. *J Periodontol Res* **29**, 146-152.

HORTON, M. A., and DAVIES, J. (1989). Perspectives: Adhesion receptors in bone. *J Bone Miner Res* **4**, 803-808.

HOWLETT, C. R., EVANS, M. D., WALSH, W. R., JOHNSON, G., and STEELE, J. G. (1994). Mechanism of initial attachment of cells derived from human bone to commonly used prosthetic materials during cell culture. *Biomaterials* **15**, 213-222.

HUGHES, D. E., SALTER, D. M., DEDHAR, S., and SIMPSON, R. (1993). Integrin expression in human bone. *J Bone Miner Res* **8**, 527-533.

HUGHES, F. J., and AUBIN, E. (1998a). The osteoblast lineage and osteoblastic differentiation. *In* "Methods in bone biology" (T. R. Arnett and B. Henderson, Eds.), pp.2-11, Chapman and Hall, London.

HUGHES, F. J., and AUBIN, E. (1998b). Properties of established cell lines. *In* "Methods in bone biology" (T. R. Arnett and B. Henderson, Eds.), pp.29-34, Chapman and Hall, London.

HUMPHRIES, M. J. (1990). The molecular basis and specificity of integrin-ligand interactions. *J Cell Sci* **97**, 585-592.

HUNTER, A., ARCHER, C. W., WALKER, P. S., and BLUNN, G. W. (1995). Attachment and proliferation of osteoblasts and fibroblasts on biomaterials for orthopaedic use. *Biomaterials* **16**, 287-295.

HUSSAIN, R. F., NOURI, A. M. E., and OLIVER, R. T. D. (1993). A new approach for measurement of cytotoxicity using colorimetric assay. *J Immunol Methods* **160**, 89-96.

HYNES, R. O. (1987). Integrins: A family of cell surface receptors. *Cell* **48**, 549-554.

HYNES, R. O. (1992). Integrins: Versatility, modulation, and signaling in cell adhesion. (Review). *Cell* **69**, 11-25.

IHARA, K., GOTO, M., MIYAHARA, A., TOYOTA, J., and KATSUKI, T. (1998). Multicentre experience with maxillary prostheses supported by Brånemark implants: A clinical report. *Int J Oral Maxillofac Implants* **13**, 531-538.

JEMT, T. (1991). Failures and complications in 391 consecutively inserted fixed prostheses supported by Brånemark implants in edentulous jaws: A study of treatment from the time of prosthesis placement to the first annual checkup. *Int J Oral Maxillofac Implants* **6**, 270-275.

JISANDER, S., GRENTHE, B., and ALBERIUS, P. (1997). Dental implant survival in the irradiated jaw: A preliminary report. *Int J Oral Maxillofac Implants* **12**, 643-648.

JOHANSSON, C. B., HAN, C. H., WENNERBERG, A., and ALBREKTSSON, T. (1998). A quantitative comparison of machined commercially pure titanium and titanium-aluminium-vanadium implants in rabbit bone. *Int J Oral Maxillofac Implants* **13**, 315-321.

JOHANSSON, C. B., HANSSON, H. A., and ALBREKTSSON, T. (1990). Qualitative interfacial study between bone and tantalum, niobium or commercially pure titanium. *Biomaterials* **11**, 277-280.

JOHANSSON, C. B., WENNERBERG, A., and ALBREKTSSON, T. (1994). Quantitative comparison of screw-shaped commercially pure titanium and zirconium implants in rabbit tibia. *J Mater Sci Mater Med* **5**, 340-344.

JULIANO, R. L., and HASKILL, S. (1993). Signal transduction from the extracellular matrix (Review). *J Cell Biol* **120**, 577-585.

KASEMO, B. (1983). Biocompatibility of titanium implants: Surface science aspects. *J Prosthet Dent* **49**, 832-837.

KASEMO, B., and LAUSMAA, J. (1988). Biomaterial and implant surfaces: A surface science approach. *Int J Oral Maxillofac Implants* **3**, 247-259.

KAWAHARA, H. (1983). Cellular responses to implant materials: Biological, physical and chemical factors. *Int Dent J* **33**, 350-375.

KELLER, E. E. (1997). Placement of dental implants in the irradiated mandible: A protocol without adjunctive hyperbaric oxygen. *J Oral Maxillofac Surg* **55**, 972-980.

KELLER, J. C., DOUGHERTY, W. J., GROTENDORST, G. R., and WIGHTMAN, J. P. (1989). *In vitro* cell attachment to characterized cp titanium surfaces. *J Adhesion* **28**, 115-133.

KELLER, J. C., STANFORD, C. M., WIGHTMAN, J. P., DRAUGHN, R. A., and ZAHARIAS, R. (1994). Characterizations of titanium implant surfaces. III. *J Biomed Mater Res* **28**, 939-946.

KIESWETTER, K., SCHWARTZ, Z., DEAN, D. D., and BOYAN, B. D. (1996a). The role of implant surface characteristics in the healing of bone (Review). *Crit Rev Oral Biol Med* **7**, 329-345.

KIESWETTER, K., SCHWARTZ, Z., HUMMERT, T. W., COCHRAN, D. L., SIMPSON, J., DEAN, D. D., and BOYAN, B. D. (1996b). Surface roughness modulates the local production of growth factors and cytokines by osteoblast-like MG-63 cells. *J Biomed Mater Res* **32**, 55-63.

KLINGER, M. M., RAHEMTULLA, F., PRINCE, C. W., LUCAS, L. C., and LEMONS, J. E. (1998). Proteoglycans at the bone-implant interface. *Crit Rev Oral Biol Med* **9**, 449-463.

KNOX, P. (1984). Kinetics of cell spreading in the presence of different concentrations of serum or fibronectin-depleted serum. *J Cell Sci* **71**, 51-59.

KÖNÖNEN, M., HORMIA, M., KIVILAHTI, J., HAUTANIEMI, J., and THESLEFF, I. (1992). Effect of surface processing on the attachment, orientation, and proliferation of human gingival fibroblasts on titanium. *J Biomed Mater Res* **26**, 1325-1341.

KORNU, R., MALONEY, W. J., KELLY, M. A., and LANE SMITH, R. (1996). Osteoblast adhesion to orthopaedic implant Alloys: Effects of cell adhesion molecules and diamond-like carbon coating. *J Orthop Res* **14**, 871-877.

KRALL, E. A., DAWSON-HUGHES, B., GARVEY, A. J., and GARCIA, R. I. (1997). Smoking, smoking cessation, and tooth loss. *J Dent Res* **76**, 1653-1659.

LAJEUNESSE, D., FRONDOZA, C., SCHOFFIELD, B., and SACKTOR, B. (1990). Osteocalcin secretion by the human osteosarcoma cell line MG-63. *J Bone Miner Res* **5**, 915-922.

LARSSON, C., THOMSEN, P., LAUSMAA, J., RODAHL, M., KASEMO, B., and ERICSON, L. E. (1994). Bone response to surface modified titanium implants: Studies on electropolished implants with different oxide thicknesses and morphology. *Biomaterials* **15**, 1062-1074.

LARSSON, C., THOMSEN, P., ARONSSON, B. -O., RODAHL, M., LAUSMAA, J., KASEMO, B., and ERICSON, L. E. (1996). Bone response to surface-modified titanium implants: Studies on the early tissue response to machined and electropolished implants with different oxide thicknesses. *Biomaterials* **17**, 605-616.

LASNITZKI, I. (1994). Organ culture. *In:* "Animal cell culture: A practical approach" (R. I. Freshney, Ed.), pp. 213-261, Oxford University Press, Oxford.

LAUTENSCHLAGER, E. P., and MONAGHAN, P. (1993). Titanium and titanium alloys as dental materials. (Review). *Int Dent J* **43**, 245-253.

LEGEROS, R. Z., and CRAIG, R. G. (1993). Strategies to affect bone remodelling: Osteointegration. *J Bone Miner Res* **8**, S583-S596.

LEGEROS, R. Z., ORLY, I., GREGOIRE, M., and DACULSI, G. (1991). Substrate surface dissolution and interfacial biological mineralization. *In*: "The bone-biomaterial interface" (J. E. Davies, Ed.), pp. 76-88, University of Toronto Press, Toronto.

LEITÃO, J., and HEGDAHL, T. (1981). On the measuring of roughness. *Acta Odontol Scand* **39**, 379-384.

LEMONS, J. E. (1990). Dental implant biomaterials. *J Am Dent Assoc* **121**, 716-719.

LEMONS, J. E., and DIETSH-MISCH, F. (1999). Biomaterials for dental implants. *In*: "Contemporary implant dentistry" (C. E. Misch, Ed.), pp. 271-302, Mosby, St. Louis.

LEUNG, T. (1998). "Cellular and tissue responses to implant materials: Development of a novel organ culture model". [Ph.D. Thesis]. (University of London).

LEUNG, T., KAKAR, A., HOBKIRK, J. A., and THOROGOOD, P. (1994). Behaviour of fibroblasts during initial attachment to a glass-ceramic implant material *in vitro*: A time-lapse video micrographic study. *Biomaterials* **15**, 1001-1007.

LI, P., and DUCHEYNE, P. (1997). Quasi-biological apatite film induced by titanium in a simulated body fluid. *J Biomed Mater Res* **41**, 341-348.

LIAN, J. B., and STEIN, G. S. (1992). Concepts of osteoblast growth and differentiation: Basis for modulation of bone cell development and tissue formation. *Crit Rev Oral Biol Med* **3**, 269-305.

LINCKS, J., BOYAN, B. D., COCHRAN, D. L., LIU, Y., BLANCHARD, C., DEAN, D. D. and SCHWARTZ, Z. (1998a). MG63 cells discriminate between surface roughness and material composition. *J Dent Res* **77** (Special issue A), 246, Abstr. 1123.

LINCKS, J., BOYAN, B. D., COCHRAN, D. L., LIU, Y., BLANCHARD, C., DEAN, D. D. and SCHWARTZ, Z. (1998b). Cell type and maturation state determine cell response to surface roughness and composition. *J Dent Res* **77** (Special issue B), 966, Abstr. 2678.

LINCKS, J., BOYAN, B. D., BLANCHARD, C. R., LOHMANN, C. H., LIU, Y., COCHRAN, D. L., DEAN, D. D. and SCHWARTZ, Z. (1998c). Response of MG63 osteoblast-like cells to titanium and titanium alloy is dependent on surface roughness and composition. *Biomaterials* **19**, 2219-2232.

LINDER, L., ALBREKTSSON, T., BRÅNEMARK, P. I., HANSSON, H. A., IVARSSON, B., JÖNSSON, U., and LUNDSTRÖM, I. (1983). Electron microscopic analysis of the bone-titanium interface. *Acta Orthop Scand* **54**, 45-52.

LINDQUIST, L. W., CARLSSON, G. E., and JEMT, T. (1997). Association between marginal bone loss around osseointegrated mandibular implants and smoking habits: A 10-year follow-up study. *J Dent Res* **76**, 1667-1674.

LISTGARTEN, M. A., BUSER, D., STEINEMANN, S. G., DONATH, K., LANG, N. P., and WEBER, H. P. (1992). Light and transmission electron microscopy of the intact interfaces between non-submerged titanium-coated epoxy resin implants and bone or gingiva. *J Dent Res* **71**, 364-371.

LIU, F., MALAVAL, L., GUPTA, A. K., AUBIN, J. E. (1994). Simultaneous detection of multiple bone-related mRNAs and protein expression during osteoblast differentiation: Polymerase chain reaction and immunocytochemical studies at the single cell level. *Dev Biol* **166**, 220-234.

LOWENBERG, B., CHERNECKY, R., SHIGA, A., and DAVIES, J. E. (1991). Mineralized matrix production by osteoblasts on solid titanium in vitro. *Cells Mater* **1**, 177-187.

LUGOWSKI, S. J., SMITH, D. C., MCHUGH, A. D., and VAN LOON, J. C. (1991). Release of metal ions from dental implant materials *in vivo*: Determination of Al, Co, Cr, Mo, Ni, V, and Ti in organ tissue. *J Biomed Mater Res* **25**, 1443-1458.

MAH, C. (1990). The evolution of implants over the last fifty years. *Aust Prosthodont J* **4**, 47-52.

MAHONEN, A., PIRSKANEN, A., KEINÄNEN, R., and MÄENPÄÄ, P. H. (1990). Effect of 1,25 $(OH)_2D_3$ on its receptor mRNA levels and osteocalcin synthesis in human osteosarcoma cells. *Biochimica et Biophysica Acta* **1048**, 30-37.

MAJESKA, R. J., and RODAN, G. A. (1982). The effect of $1,25(OH)_2D_3$ on alkaline phosphatase in osteoblastic osteosarcoma cells. *J Biol Chem* **257**, 3362-3365.

MARTIN, J. Y., DEAN, D. D., COCHRAN, D. L., SIMPSON, J., BOYAN, B. D., and SCHWARTZ, Z. (1996). Proliferation, differentiation, and protein synthesis of human osteoblast-like cells (MG63) cultured on previously used titanium surfaces. *Clin Oral Implants Res* **7**, 27-37.

MARTIN, J. Y., SCHWARTZ, Z., HUMMERT, T. W., SCHRAUB, D. M., SIMPSON, J., LANKFORD, J., DEAN, D. D., COCHRAN, D. L., and BOYAN, B. D. (1995). Effect of titanium surface roughness on proliferation, differentiation, and protein synthesis of human osteoblast-like cells (MG63). *J Biomed Mater Res* **29**, 389-401.

MASSAS, R., PITARU, S., and WEINREB, M. M. (1993). The effects of titanium and hydroxyapatite on osteoblastic expression and proliferation in rat parietal bone cultures. *J Dent Res* **72**, 1005-1008.

MASUDA, T., SALVI, G. E., OFFENBACHER, S., FELTON D. A., and COOPER, L. F. (1997). Cell and matrix reactions at titanium implants in surgically prepared rat tibiae. *Int J Oral Maxillofac Implants* **12**, 472-485.

MATSUMOTO, K., ZIOBER, B. L., YAO, C. C., and KRAMER, R. H. (1995). Growth factor regulation of integrin-mediated cell motility (Review). *Cancer Metastasis Rev* **14**, 205-217.

MATTSSON, L., and WÅGBERG, P. (1993). Assessment of surface finish on bulk scattering materials: A comparison between optical laser stylus and mechanical stylus profilometers. *Precis Eng* **15**, 141-149.

MEENAGHAN, M. A., NATIELLA, J. R., MORESI, J. L., FLYNN, H. E., WIRTH, J. E., and BAIER, R. E. (1979). Tissue response to surface-treated tantalum implants: Preliminary observations in primates. *J Biomed Mater Res* **13**, 631-643.

MEFFERT, R. M., LANGER, B., and FRITZ, M. E. (1992). Dental implants: A review. *J Periodontol* **63**, 859-870.

MEYLE, J., WOLBURG, H., and VON RECUM, A. F. (1993). Surface micromorphology and cellular interactions. *J Biomaterials Applications* **7**, 362-374.

MEYLE, J., GULTIG, K., and NISCH, W. (1995). Variation in contact guidance by human cells on a microstructured surface. *J Biomed Mater Res* **29**, 81-88.

MICHAELS, C. M., KELLER, J. C., and STANFORD, C. M. (1991). *In vitro* periodontal ligament fibroblast attachment to plasma-cleaned titanium surfaces. *J Oral Implantol* **17**, 132-139.

MILLER, R. R., and MCDEVITT, C. A. (1991). A quantitative microwell assay for chondrocyte cell adhesion. *Anal Biochem* **192**, 380-383.

MIYAMOTO, S., AKIYAMA, S. K., and YAMADA, K. M. (1995). Synergistic roles for the receptor occupancy and aggregation in integrin transmembrane function. *Science* **267**, 883-885.

MOURSI, A. M., DAMSKY, C. H., LULL, J., ZIMMERMAN, D., DOTY, S. B., AOTA, S., and GLOBUS, R. (1996). Fibronectin regulates calvarial osteoblast differentiation. *J Cell Sci* **109**, 1369-1380.

MOURSI, A. M., GLOBUS, R. K., and DAMSKY, C. H. (1997). Interactions between integrin receptors and fibronectin are required for calvarial osteoblast differentiation *in vitro*. *J Cell Sci* **110**, 2187-2196.

MUSTAFA, K., LOPEZ, B. S., HULTENBY, K., WENNERBERG, A., and ARVIDSON, K. (1998). Attachment and proliferation of human oral fibroblasts to titanium surfaces blasted with TiO_2 particles - A scanning electron microscopic and histomorphometric analysis. *Clin Oral Implant Res* **9**, 195-207.

NAERT, I., QUIRYNEN, M., VAN STEENBERGHE, D., and DARIUS, P. (1992). A six-year prosthodontic study of 509 consecutively inserted implants for the treatment of partial edentulism. *J Prosthet Dent* **67**, 236-245.

NANCI, A., MCCARTHY, G. F., ZALZAL, S., CLOKIE, C. M. L., WARSHAWSKY, H., and MCKEE, M. D. (1994). Tissue response to titanium implants in the rat tibia: Ultrastructural, immunocytochemical and lectin-cytochemical characterization of the bone-titanium interface. *Cells Mater* **4**, 1-30.

NATIELLA, J. R. (1988). The use of animal models in research on dental implants. *J Dent Educ* **52**, 792-797.

NESBITT, S., NESBITT, A., HELFRICH, M., and HORTON, M. (1993). Biochemical characterization of human osteoclast integrins. Osteoclasts express $\alpha_v\beta_3$, $\alpha_2\beta_1$, and $\alpha_v\beta_1$ integrins. *J Biol Chem* **268**, 16737-16745.

NIEDERAUER, G. G., MCGEE, T. D., KELLER, J. C., and ZAHARIAS, R. S. (1994). Attachment of epithelial cells and fibroblasts to ceramic materials. *Biomaterials* **15**, 342-352.

NIIMI, A., UEDA, M., KELLER, E. E., and WORTHINGTON, P. (1998). Experience with osseointegrated implants placed in irradiated tissues in Japan and the United States. *Int J Oral Maxillofac Implants* **13**, 407-411.

NISHIMURA, N., and KAWAI, T. (1998). Effect of microstructure of titanium surface on the behaviour of osteogenic cell line MC3T3-E1. *J Mater Sci Mater Med* **9**, 99-102.

NISHIMURA, R. D., ROUMANAS, E., BEUMER, J., MOY, P. K., and SHIMIZU, K. T. (1998). Restoration of irradiated patients using osseointegrated implants: Current perspectives. *J Prosthet Dent* **79**, 641-647.

NORTON, M. R. (1998). Marginal bone loss levels at single tooth implants with a conical fixture design. The influence of surface macro- and microstructure. *Clin Oral Implants Res* **9**, 91-99.

OAKLEY, C., and BRUNETTE, D. M. (1993). The sequence of alignment of microtubules, focal contacts and actin filaments in fibroblasts spreading on smooth and grooved titanium substrata. *J Cell Sci* **106**, 343-354.

OGISO, M., YAMASHITA, M., and MATSUMOTO, T. (1998). The process of physical weakening and dissolution of the HA-coated implant in bone and soft tissue. *J Dent Res* 77, 1426-1434.

OKAMOTO, K., MATSUURA, T., HOSOKAWA, R., and AKAGAWA, Y. (1998). RGD peptides regulate the specific adhesion scheme of osteoblasts to hydroxyapatite but not to titanium. *J Dent Res* 77, 481-487.

O'NEAL, R. B., SAUK, J. J., and SOMERMAN, M. J. (1992). Biological requirements for material integration. (Review). *J Oral Implantol* **18**, 243-255.

ONG, J. L., PRINCE, C. W., RAIKAR, G. N., and LUCAS, L. C. (1996). Effect of surface topography of titanium on surface chemistry and cellular response. *Implant Dent* **5**, 83-88.

ORR, R. D., DE BRUIJN, J. D., and DAVIES, J. E. (1992). Scanning electron microscopy of the bone interface with titanium, titanium alloy and hydroxyapatite. *Cells Mater* **2**, 241-251.

OZAWA, S., and KASUGAI, S. (1996). Evaluation of implant materials (hydroxyapatite, glass-ceramics, titanium) in rat bone marrow stromal cell culture. *Biomaterials* **17**, 23-29.

PAREL, S. M., HOLT, R., BRÅNEMARK, P. I., TJELLSTRÕM, A. (1986). Osseointegration and facial prosthetics. *Int J Oral Maxillofac Implants* **1**, 27-29.

PIERSCHBACHER, M. D., and RUOSLAHTI, E. (1984). Cell attachment of fibronectin can be duplicated by small synthetic fragments of the molecule. *Nature* **309**, 30-33.

PILLIAR, R. M., DEPORTER, D. A., WATSON, P. A., PHAROAH, M., CHIPMAN, M., VALIQUETTE, N., CARTER, S., and DEGROOT, K. (1991). The effect of partial coating with hydroxyapatite on bone remodelling in relation to porous coated titanium alloy dental implants in the dog. *J Dent Res* **70**, 1338-1345.

PISTONE, M., SANGUINETI, C., FEDERICI, A., SANGUINETI, F., DEFILIPPI, P., SANTOLINI, F., QUERZE, G., MARCHISIO, P. C., and MANDUCA, P. (1996). Integrin synthesis and utilization in cultured human osteoblasts. *Cell Biol Int* **20**, 471-479.

PIZZOFERRATO, A., VESPUCCI, A., CIAPETTI, G., and STEA, S. (1985). Biocompatibility testing of prosthetic implant materials by cell cultures. *Biomaterials* **6**, 346-351.

PIZZOFERRATO, A., CIAPETTI, G., STEA, S., CENNI, E., ARCIOLA, C. R., GRANCHI, D., and SAVARINO, L. (1994). Cell culture methods for testing biocompatibility. *Clin Mater* **15**, 173-190.

PLANTEFABER, L. C., and HYNES, R. O. (1989). Changes in integrin receptors on oncogenically transformed cells. *Cell* **56**, 281-290.

PRICE, N., BENDALL, S. P., FRONDOZA, C., JINNAH, R. H., and HUNGERFORD, D. S. (1997). Human osteoblast-like cells (MG63) proliferate on a bioactive glass surface. *J Biomed Mater Res* **37**, 394-400.

PRIGENT, H., PELLEN-MUSSI, P., CATHELINEAU, G., and BONNAURE-MALLET, M. (1998). Evaluation of the biocompatibility of titanium-tantalum alloy versus titanium. *J Biomed Mater Res* **39**, 200-206.

PROSCAN 1000, USER MANUAL (1997). Scantron Industrial Products, Ltd., Taunton, England.

PULEO, D. A., and BIZIOS, R. (1992). Formation of focal contacts by osteoblasts cultured on orthopaedic materials. *J Biomed Mater Res* **26**, 291-301.

PULEO, D. A., HOLLERAN, L. A., DOREMUS, R. H., and BIZIOS, R. (1991). Osteoblast responses to orthopaedic implant materials *in vitro*. *J Biomed Mater Res* **25**, 711-723.

QU, J., CHEHROUDI, B., and BRUNETTE, D. M. (1996). The use of micromachined surfaces to investigate the cell behavioural factors essential to osseointegration. *Oral Dis* **2**, 102-115.

RAE, T. (1986). The biological response to titanium and titanium-aluminium-vanadium alloy particles. I. Tissue culture studies. *Biomaterials* **7**, 30-36.

RAHAL, M. D., BRÅNEMARK, P-I., and OSMOND, D. G. (1993). Response of bone marrow to titanium implants: Osseointegration and the establishment of a bone marrow-titanium interface in mice. *Int J Oral Maxillofac Implants* **8**, 573-579.

RANGERT, B., KROGH, P. H. J., LANGER, B., and VAN ROEKEL, N. (1995). Bending overload and implant fracture: A retrospective clinical analysis. *Int J Oral Maxillofac Implants* **10**, 326-334.

RANGERT, B. R., SULLIVAN, R. M., and JEMT, T. (1997). Load factor control for implants in the posterior partially edentulous patients. *Int J Oral Maxillofac Implants* **12**, 360-370.

RATNER, B. D. (1994). New ideas in biomaterial science - a path to engineered biomaterials. *J Biomed Mater Res* **27**, 837-850.

RATNER, B. D., JOHNSTON, A. B., and LENK, T. J. (1987). Biomaterial surfaces. *J Biomed Mater Res* **21** (A1 Suppl), 59-89.

RE, F., ZANETTI, A., SIRONI, M., POLENTARUTTI, N., LANFRANCONE, L., DEJANA, E., and COLOTTA, F. (1994). Inhibition of anchorage dependent cell spreading triggers apoptosis in cultured human endothelial cells. *J Cell Biol* **127**, 537-546.

REVEL, J. P., and WOLKEN, K. (1973). Electronmicroscope investigations of the underside of cells in culture. *Exp Cell Res* **78**, 1-14.

RICCIO, V., DELLA RAGIONE, F., MARRONE, G., PALUMBO, R., GUIDA, G., and OLIVA, A. (1994). Cultures of human embryonic osteoblasts. A new in vitro model for biocompatibility studies. *Clin Orthop* **308**, 73-78.

RICHARDS, R. G. (1996). The effect of surface roughness on fibroblast adhesion *in vitro*. *Injury* **27** Suppl 3, C38-C43.

RICHARDS, R. G., RAHN, B. A., and GWYNN I. A. (1995). Scanning electron microscopy of the undersurface of cell monolayers grown on metallic implants. *J Mater Sci Mater Med* **6**, 120-124.

RICHARDSON, A., and PARSONS, J. T. (1995). Signal transduction through integrins: A central role for focal adhesion kinase? (Review). *Bioessays* **17**, 229-236.

RIPAMONTI, U. (1991). The induction of bone in osteogenic composites of bone matrix and porous hydroxyapatite replicas: An experimental study on the baboon (*Papio ursinus*). *J Oral Maxillofac Surg* **49**, 817-830.

RODAN, G. A., and NODA, M. (1991). Gene expression in osteoblastic cells. *Crit Rev Eukaryot Gene Expr* **1**, 85-98.

RØYNESDAL, A., AMBJØRNSEN, E., STØVNE, S., and HAANÆS, H. R. (1998). A comparative clinical study of three different endosseous implants in edentulous mandibles. *Int J Oral Maxillofac Implants* **13**, 500-505.

RUOSLAHTI, E. (1996). RGD and other recognition sequences for integrins (Review). *Annu Rev Cell Dev Biol* **12,** 697-715.

SAITO, T., ALBELDA, S. M., and BRIGHTON, C. T. (1994). Identification of integrin receptors on cultured human bone cells. *J Orthop Res* **12**, 384-394.

SAUK, J. J., VAN KAMPEN, C. L., and SOMERMAN, M. J. (1991). Role of adhesive proteins and integrins in bone and ligament cell behaviour at the material surface. *In*: "The Bone Biomaterial Interface" (J. E. Davies, Ed.), pp. 111-119, University of Toronto Press, Toronto.

SCHNEIDER, G., and BURRIDGE, K. (1994a). Formation of focal adhesions by osteoblasts adhering to different substrata. *Exp Cell Res.* **214**, 264-269.

SCHNEIDER, G. B., and BURRIDGE, K. (1994b). Osteoblast focal adhesion formation and its role in osseointegration. *J Dent Res* **73**, 217, Abstr. 922.

SCHWARTZ, Z., MARTIN, J. Y., DEAN, D. D., SIMPSON, J., COCHRAN, D. L., and BOYAN, B. D. (1996). Effect of titanium surface roughness on chondrocyte proliferation, matrix production, and differentiation depends on the state of cell maturation. *J Biomed Mater Res* **30,** 145-155.

SCHWARTZ, Z., and BOYAN, B. D. (1994). Underlying mechanisms at the bone-biomaterial interface. *J Cell Biochem* **56**, 340-347.

SENNERBY, L., THOMSEN, P., and ERICSON, L. E. (1992). Ultrastructure of the bone-titanium interface in rabbits. *J Mater Sci Mater Med* **3**, 262-271.

SINGHVI, R., STEPHANOPOULOS, G., and WANG, D. I. C. (1994). Review: Effects of substratum morphology on cell physiology. *Biotech Bioeng* **43**, 764-771.

SINHA, R. K., and TUAN, R. S. (1996). Regulation of human osteoblast integrin expression by orthopaedic implant materials. *Bone* **18**, 451-457.

SINHA, R. K., MORRIS, F., SHAH, S. A., and TUAN, R. S. (1994). Surface composition of orthopaedic implant metals regulates cell attachment, spreading, and cytoskeletal organization of primary human osteoblasts in vitro. *Clin Orthop* **305**, 258-272.

SKALAK, R., and BRÅNEMARK, P. I. (1994). Definition of osseointegration. *In* "Osseointegration in skeletal reconstruction and joint replacement". (P-I. Brånemark, B. L. Rydevik, and R. Skalak, Eds.), pp. xi, Quintessence Publishing Co. Inc., Chicago.

SMITH, D. C., LUGOWSKI, S., MCHUGH, A., DEPORTER, D., WATSON, P. A., and CHIPMAN, M. (1997). Systemic metal ion levels in dental implant patients. *Int J Oral Maxillofac Implants* **12**, 828-834.

STANFORD, C. M., and KELLER, J. C. (1991). The concept of osseointegration and bone matrix expression. *Crit Rev Oral Biol Med* **2**, 83-101.

STANFORD, C. M., KELLER, J. C., and SOLURSH, M. (1990). Role of integrin receptors in osteoblast attachment to cpTi. *J Dent Res* **69**, 109, Abstr. 8.

STANFORD, C. M., KELLER, J. C., and SOLURSH, M. (1994). Bone cell expression on titanium surfaces is altered by sterilization treatments. *J Dent Res* **73**, 1061-1071.

STEELE, J. G., JOHNSON, G., and UNDERWOOD, P. A. (1992). Role of serum vitronectin and fibronectin in adhesion of fibroblasts following seeding onto tissue culture polystyrene. *J Biomed Mater Res* **26,** 861-864.

STEFLIK, D. E., CORPE, R. S., LAKE, F. T., SISK, A. L., PARR, G. R., HANES, P. J., and BUTTLE, K. (1997). Composite morphology of the bone and associated support-tissue interfaces to osseointegrated dental implants: TEM and HVEM analyses. *Int J Oral Maxillofac Implants* **12**, 443-453.

STEFLIK, D. E., HANES, P. J., SISK, A. L., PARR, G. R., SONG, M. J., LAKE, F. T., and MCKINNEY, R. V. (1992). Transmission electron microscopic and high voltage electron microscopic observations of the bone and osteocyte activity adjacent to unloaded dental implants placed in dogs. *J Periodontol* **63**, 443-452.

STEFLIK, D. E., PARR, G. R., SISK, A. L., LAKE, F. T., HANES, P. J., BERKERY, D. J., and BREWER, P. (1994). Osteoblast activity at the dental implant-bone interface: Transmission electron microscopic and high voltage electron microscopic observations. *J Periodontol* **65**, 404-413.

STEIN, G. S., LIAN, J. B., and OWEN, T. A. (1990). Relationship of cell growth to the regulation of tissue-specific gene expression during osteoblast differentiation. *FASEB J* **4**, 3111-3123.

STEINEMANN, S. G. (1998). Titanium - the material of choice? *Periodontology 2000* **17**, 7-21.

STOUT, K. J. (1981). Surface roughness - Measurement, interpretation and significance of data. Part I - Statistical parameters. *Materials in Engineering* **2**, 260-265.

STOUT, K. J., SULLIVAN, P. J., DONG, W. P., MAINSAH, E., LUO, N., MATHIA, T., and ZAHOUANI, H. (1993). The development of methods for the characterisation of roughness in three dimensions. EUR 15178 EN of commission of the European Communities, University of Birmingham, Birmingham.

SULLIVAN, D. Y. (1986). Prosthetic considerations for the utilization of osseointegrated fixtures in the partially edentulous arch. *Int J Oral Maxillofac Implants* **1**, 39-45.

SULLIVAN, D. Y., SHERWOOD, R. L., and MAI, T. N. (1997). Preliminary results of a multicentre study evaluating a chemically enhanced surface for machined commercially pure titanium implants. *J Prosthet Dent* **78**, 379-386.

SWART, K. M., KELLER, J. C., WIGHTMAN, J. P., DRAUGHN, R. A., STANFORD, C. M., and MICHAELS, C. M. (1992). Short-term plasma-cleaning treatments enhance *in vitro* osteoblast attachment to titanium. *J Oral Implantol* **18**, 130-137.

SZMUKLER-MONCLER, S., SALAMA, H., REINGEWIRTZ, Y., and DUBRUILLE, J. H. (1998). Timing of loading and effect of micromotion on bone-dental implant interface: Review of experimental literature. *J Biomed Mater Res* **43**, 192-203.

TAWIL, N., WILSON, P., and CARBONETTO, S. (1993). Integrins in point contacts mediate cell spreading: Factors that regulate integrin accumulation in point contacts vs. focal contacts. *J Cell Biol* **120**, 261-271.

TAYLOR, A. C. (1961). Attachment and spreading of cells in culture. *Exp Cell Res* Suppl **8**, 154-173.

TAYLOR, R. L., VERRAN, J., LEES, G. C., and WARD, A. J. P. (1998). The influence of substratum topography on bacterial adhesion to polymethyl methacrylate. *J Mater Sci Mater Med* **9**, 17-22.

THOMAS, T. R. (1981). Characterisation of surface roughness. *Precis Eng* **3**, 97-104.

THOMAS, T. R., and CHARLTON, G. (1981). Variation of roughness parameters on some typical manufactured surfaces. *Precis Eng* **3**, 91-96.

THOMPSON, G. J. and PULEO, D. A. (1996). Ti-6Al-4V ion solution inhibition of osteogenic cell phenotype as a function of differentiation timecourse *in vitro*. *Biomaterials* **17**, 1949-1954.

TOLMAN, D. E. (1995). Reconstructive procedures with endosseous implants in grafted bone: A review of the literature. *Int J Oral Maxillofac Implants* **10**, 275-294.

TOMÃS, H., CARVALHO, G. S., FERNANDES, M. H., FREIRE, A. P., and ABRANTES, L. M. (1997). The use of rat, rabbit or human bone marrow derived cells for cytocompatibility evaluation of metallic implants. *J Mater Sci Mater Med* **8**, 233-238.

UNGERSBÖCK, A., and RAHN, B. (1994). Methods to characterize the surface roughness of metallic implants. *J Mater Sci Mater Med* **5**, 434-440.

VAN BLITTERSWIJK, C. A., BAKKER, D., HESSELING, S. C. and KOERTEN, H. K. (1991). Reactions of cells at implant surfaces. *Biomaterials* **12**, 187-193.

VAN STEENBERGHE, D. (1989). A retrospective multicentre evaluation of the survival rate of osseointegrated fixtures supporting fixed partial prostheses in the treatment of partial edentulism. *J Prosthet Dent* **61**, 217-223.

VERCAIGNE, S., WOLKE, J. G. C., NAERT, I., and JANSEN, J. A. (1998). The effect of titanium plasma-sprayed implants on trabecular bone healing in the goat. *Biomaterials* **19**, 1093-1099.

VEZEAU, P. J., KOORBUSCH, G. F., DRAUGHN, R. A., and KELLER, J. C. (1996). Effects of multiple sterilization on surface characteristics and *in vitro* biologic responses to titanium. *J Oral Maxillofac Surg* **54**, 738-746.

VIHINEN, P., RIIKONEN, T., LAINE, A., and HEINO, J. (1996). Integrin $\alpha_2\beta_1$ in tumorigenic human osteosarcoma cell lines regulates cell adhesion, migration, and invasion by interaction with Type I collagen. *Cell Growth Differ* **7**, 439-447.

VON RECUM, A. F., and VAN KOOTEN, T. G. (1995). The influence of micro-topography on cellular response and the implications for silicone implants. *J Biomater Sci Polym Ed* **7**, 181-198.

WATAHA, J. C. (1996). Review: Materials for endosseous dental implants. *J Oral Rehabil* **23**, 79-90.

WAYNER, E. A., ORLANDO, R. A., and CHERESH, D. A. (1991). Integrins $\alpha_v\beta_3$ and $\alpha_v\beta_5$ contribute to cell attachment to vitronectin but differentially distribute on the cell surface. *J Cell Biol* **113**, 919-929.

WENNERBERG, A. (1996). "On surface roughness and implant incorporation" [Ph.D. Thesis]. (University of Gothenburg).

WENNERBERG, A., ALBREKTSSON, T., and ANDERSSON, B. (1993). Design and surface characteristics of 13 commercially available oral implant systems. *Int J Oral Maxillofac Implants* **8**, 622-633.

WENNERBERG, A., ALBREKTSSON, T., and ANDERSSON, B. (1996). Bone tissue response to commercially pure titanium implants blasted with fine and coarse particles of aluminium oxide. *Int J Oral Maxillofac Implants* **11**, 38-45.

WENNERBERG, A., ALBREKTSSON, T., ULRICH, H., and KROL, J. J. (1992). An optical three-dimensional technique for topographical descriptions of surgical implants. *J Biomed Eng* **14**, 412-418.

WENNERBERG, A., HALLGREN, C., JOHANSSON, C., and SAWASE, T. (1997). Surface characterization and biological evaluation of spark-eroded surfaces. *J Mater Sci Mater Med* **8**, 757-763.

WEYANT, R. J. (1994). Characteristics associated with the loss and peri-implant tissue health of endosseous dental implants. *Int J Oral Maxillofac Implants* **9**, 95-102.

WHEELER, S. L. (1996). Eight-year clinical retrospective study of titanium plasma-sprayed and hydroxyapatite-coated cylinder implants. *Int J Oral Maxillofac Implants* **11**, 340-350.

WHITEHEAD, S. A., SHEARER, A. C., WATTS, D. C., and WILSON, N. H. F. (1995). Comparison of methods for measuring surface roughness of ceramic. *J Oral Rehabil* **22,** 421-427.

WIDMARK, G., ANDERSSON, B., ANDRUP, B., CARLSSON, G. E., IVANOFF, C., and LINDVALL, A. M. (1998). Rehabilitation of patients with severely resorbed maxillae by means of implants with or without bone grafts. A 1-year follow-up study. *Int J Oral Maxillofac Implants* **13**, 474-482.

WILKE, A., ORTH, J., LOMB, M., FUHRMANN, R., KIENAPFEL, H., GRISS, P., and FRANKE, R. P. (1998). Biocompatibility analysis of different biomaterials in human bone marrow cell cultures. *J Biomed Mater Res* **40**, 301-306.

WILLIAMS, D. F. (1981). Implants in dental and maxillofacial surgery. *Biomaterials* **2**, 133-146.

WILLIAMS, D. F. (1990). Biocompatibility: An overview. *In*: "Concise encyclopaedia of medical and dental materials" (D. Williams, Ed.), pp. 51-59, Pergamon Press, Oxford.

WONG, M., EULENBERGER, J., SCHENK, R., and HUNZIKER, E. (1995). Effect of surface topology on the osseointegration of implant materials in trabecular bone. *J Biomed Mater Res* **29,** 1567-1575.

WYATT, C. C. L., and ZARB, G. A. (1998). Treatment outcomes of patients with implant-supported fixed partial prostheses. *Int J Oral Maxillofac Implants* **13**, 204-211.

YAN, W., NAKAMURA, T., KAWANABE, K., NISHIGOCHI, S., OKA, M., and KOKUBO, T. (1997). Apatite layer-coated titanium for use as bone bonding implants. *Biomaterials* **18**, 1185-1190.

YLIHEIKKILÄ, P. K., FELTON, D. A., WHITSON, S. W., AMBROSE, W. W., UOSHIMA, K., and COOPER, L. F. (1995). Correlative microscopic investigation of the interface between titanium alloy and the osteoblast-osteoblast matrix using mineralizing cultures of primary foetal bovine mandibular osteoblasts. *Int J Oral Maxillofac Implants* **10**, 655-665.

ZABLOTSKY, M. H. (1992). Hydroxyapatite coatings in implant dentistry (Review). *Implant Dent* **1**, 253-257.

ZARB, G. A., and ALBREKTSSON, T. (1991). Osseointegration: A requiem for the periodontal ligament? *Int J Periodontics Restorative Dent* **11**, 88-91.

ZARB, G. A., and ALBREKTSSON, T. (1998). Consensus report: Towards optimized treatment outcomes for dental implants. *J Prosthet Dent* **80**, 641.

Appendix I

Data for results in Chapter 2.

Table 1 Data for Table 2.1 and Figure 2.7 showing the surface roughness values obtained using the Proscan 1000 for the trial surfaces measured in the pilot study. Values are in μm. Measurements were made at 10 μm intervals for 150 sampling points. Area measured = 2.25 mm^2

Substrate	R_a	R_q	R_z	R_{max}	S	S_m	Area/mm^2
Ti as received 1	1.99	2.53	9.94	14.20	70.00	160.00	2.33
	2.13	2.71	11.70	15.40	50.00	150.00	2.33
	1.66	2.21	8.48	11.20	60.00	130.00	2.33
Ti as received 2	1.74	2.16	7.99	10.60	60.00	100.00	2.34
	1.88	2.29	8.86	11.90	50.00	110.00	2.34
	1.89	2.32	9.40	10.60	60.00	150.00	2.34
Ti as received 3	1.75	2.25	9.66	11.70	40.00	100.00	2.33
	1.91	2.26	8.30	10.50	50.00	100.00	2.33
	1.66	2.03	7.56	11.40	50.00	120.00	2.33
Ti as received 4	1.54	1.93	7.51	9.97	40.00	130.00	2.33
	1.94	2.47	8.40	13.20	60.00	90.00	2.33
	1.66	2.13	8.48	11.00	50.00	90.00	2.33
Ti as received 5	1.80	2.33	10.00	13.40	50.00	110.00	2.33
	1.97	2.46	9.77	13.60	70.00	120.00	2.33
	2.06	2.57	10.20	13.50	60.00	110.00	2.33
Polished Ti 1	0.70	0.89	3.78	4.59	30.00	60.00	2.26
	0.72	0.90	3.75	5.37	50.00	90.00	2.26
	0.70	0.84	3.55	4.77	40.00	70.00	2.26
Polished Ti 2	0.77	0.96	3.72	4.65	40.00	70.00	2.39
	0.65	0.81	3.06	3.45	40.00	60.00	2.26
	0.74	0.90	3.66	4.66	40.00	70.00	2.26
Polished Ti 3	0.76	0.92	3.27	4.40	50.00	70.00	2.26
	0.76	0.95	3.75	4.76	40.00	70.00	2.26
	0.77	0.96	3.44	4.77	40.00	90.00	2.26
Polished Ti 4	0.86	1.05	4.21	4.99	30.00	60.00	2.26
	0.73	0.89	3.60	4.95	30.00	60.00	2.26
	0.77	0.94	3.84	5.19	40.00	60.00	2.26
Polished Ti 5	0.80	1.04	4.62	6.53	40.00	60.00	2.27
	0.83	1.05	4.50	6.14	40.00	90.00	2.27
	0.87	1.09	4.40	5.60	40.00	80.00	2.27
Polished Zr 1	0.78	1.01	3.89	4.95	40.00	70.00	2.27
	0.77	0.97	3.87	4.69	40.00	70.00	2.27
	0.79	1.15	4.53	5.34	40.00	60.00	2.27
Polished Zr 2	0.79	0.98	3.87	4.53	40.00	70.00	2.26
	0.85	1.04	4.44	5.56	40.00	60.00	2.26
	0.79	0.95	3.79	5.05	40.00	60.00	2.26
Polished Zr 3	0.80	1.00	4.05	5.35	40.00	70.00	2.26
	0.77	0.98	4.06	4.91	40.00	80.00	2.26
	0.83	1.05	4.34	5.19	40.00	80.00	2.26
Polished Zr 4	0.84	1.01	3.89	4.95	40.00	70.00	2.27
	0.79	0.97	3.87	4.69	40.00	70.00	2.27
	0.95	1.15	4.53	5.34	40.00	60.00	2.27
Polished Zr 5	0.82	0.99	3.85	4.49	40.00	70.00	2.26

	0.75	0.93	3.76	4.80	40.00	100.00	2.26
	0.77	0.97	4.18	6.31	40.00	90.00	2.26
Zr as received 1	0.75	0.97	4.20	4.96	50.00	90.00	2.25
	0.83	1.05	4.27	5.61	40.00	90.00	2.25
	0.81	0.98	3.71	4.57	40.00	70.00	2.25
Zr as received 2	0.95	1.20	4.53	5.99	30.00	70.00	2.26
	0.94	1.14	4.32	5.11	40.00	70.00	2.26
	0.92	1.14	4.56	5.75	40.00	70.00	2.26
Zr as received 3	0.78	0.99	4.10	6.27	50.00	130.00	2.26
	0.99	1.28	5.62	7.82	40.00	80.00	2.26
	0.88	1.14	4.86	6.56	40.00	80.00	2.26
Zr as received 4	1.04	1.28	5.12	6.51	40.00	90.00	2.26
	0.94	1.16	4.40	5.92	40.00	90.00	2.26
	1.13	1.43	5.95	7.78	40.00	100.00	2.26
Zr as received 5	0.91	1.15	4.38	6.22	50.00	70.00	2.26
	0.84	1.06	4.25	5.62	40.00	70.00	2.26
	0.86	1.09	4.50	6.34	40.00	90.00	2.26
Zr blasted 1	1.15	1.46	6.30	7.84	40.00	100.00	2.30
	0.99	1.20	4.83	6.61	40.00	70.00	2.30
	1.28	1.61	6.89	11.00	40.00	90.00	2.30
Zr blasted 2	1.20	1.52	6.31	8.28	40.00	70.00	2.31
	1.34	1.67	6.20	7.63	40.00	80.00	2.31
	1.17	1.50	6.01	7.26	40.00	70.00	2.31
Zr blasted 3	1.31	1.66	7.00	9.02	40.00	90.00	2.31
	1.12	1.46	5.96	8.52	40.00	90.00	2.31
	1.32	1.71	7.16	10.20	50.00	90.00	2.31
Zr blasted 4	1.27	1.60	6.59	8.99	40.00	90.00	2.31
	1.46	1.86	8.01	11.40	40.00	100.00	2.31
	1.15	1.51	6.50	8.29	40.00	100.00	2.31
Zr blasted 5	1.29	1.57	6.36	8.64	40.00	80.00	2.30
	1.20	1.45	6.01	7.47	40.00	80.00	2.30
	1.20	1.47	5.58	7.69	40.00	70.00	2.30

Table I1 Data for Figure 2.8, showing the effect of different scanning intervals on the surface roughness parameter values for Ti as received. Values are in μm

No. of steps	Step size (μm)	R_a	R_z	R_{max}	S	S_m
400	1	1.91	6.49	10.44	21	64
		2.50	10.91	20.31	23	82
		2.56	9.85	17.69	27	213
		2.65	11.08	17.53	25	69
		2.13	9.37	20.61	29	72
		1.67	7.83	11.03	22	69
380	4	2.18	10.58	12.77	35	91
		2.12	12.59	20.43	38	136
		1.94	10.79	15.55	32	105
		1.85	11.21	15.45	34	92
		2.24	12.94	19.86	36	117
		2.38	14.21	22.72	35	120
		2.28	13.46	18.47	37	138
		2.14	11.93	18.38	32	107
		2.37	14.20	18.59	38	89
		2.02	11.16	14.29	34	103
		2.12	11.66	14.98	39	104

		2.00	11.02	14.81	29	97
300	5	2.25	14.05	19.37	49	151
		2.14	11.17	16.19	32	107
		2.42	13.34	16.15	37	77
		2.04	10.68	14.06	32	102
		2.17	11.87	16.27	44	142
		2.22	10.73	16.38	33	104
		2.05	12.05	18.51	47	105
		2.17	11.99	18.06	32	87
		2.42	13.34	16.15	37	77
		2.04	10.68	14.06	32	102
		2.17	11.87	16.27	44	142
		2.22	10.73	16.38	33	104
250	6	2.19	10.96	12.3	34	78
		2.06	10.68	16.51	37	155
		1.98	10.46	13.77	39	97
		2.15	11.66	14.96	33	97
		2.32	12.93	20.92	45	94
		2.31	13.40	19.50	35	109
		2.21	13.46	17.75	44	123
		2.13	10.86	16.12	32	81
		2.29	12.67	15.05	39	95
		2.03	11.01	14.16	38	152
		2.12	11.2	17.38	37	96
		2.01	10.39	14.73	35	96
190	8	2.18	10.08	12.38	41	101
		2.11	10.79	16.47	39	136
		2.05	10.63	13.57	47	90
		1.94	9.82	13.12	33	136
		2.25	11.82	17.22	55	110
		2.23	13.54	19.39	50	107
		2.28	11.82	15.98	43	108
		2.07	10.57	18.11	48	87
		2.40	12.48	15.01	47	83
		2.07	10.41	12.91	39	115
		2.12	11.03	18.09	54	110
		2.09	10.12	15.05	46	101
150	10	2.25	9.56	12.21	49	90
		2.20	11.27	17.85	51	207
		1.93	9.42	12.94	54	115
		1.95	9.69	12.27	41	107
		2.39	11.54	16.92	51	108
		2.36	13.96	21.58	50	113
		2.20	11.43	18.06	56	165
		2.11	10.45	15.41	43	81
		2.49	12.3	15.36	53	99
		1.96	9.55	11.58	45	103
		2.12	11.3	19.22	65	155
		2.25	10.24	15.35	45	127
75	20	1.95	7.56	10.62	81	125
		1.91	8.39	11.93	100	171
		1.95	8.79	15.61	90	186
		1.65	6.78	11.33	76	124
		2.26	9.66	15.52	106	166
		2.24	10.66	15.62	81	116
		2.27	8.83	11.86	82	186
		2.17	9.05	12.74	73	128
		2.30	10.37	15.31	89	228

		1.98	8.55	12.64	88	144
		2.24	10.67	14.53	78	130
		2.21	8.62	11.78	81	178
50	30	2.45	7.90	11.05	115	132
		2.03	7.43	11.38	118	252
		2.16	8.15	11.06	103	170
		1.61	6.70	9.97	113	160
		2.31	8.79	15.38	106	165
		2.44	10.31	15.96	126	216
		1.95	8.05	12.29	143	264
		1.94	6.51	9.50	108	110
		2.28	9.48	13.17	92	190
		1.84	7.02	9.92	125	129
		2.13	7.78	13.68	123	310
		2.22	6.28	9.45	125	192
38	40	2.47	7.92	13.70	142	176
		2.10	7.65	11.31	140	248
		1.89	6.64	8.51	151	166
		1.51	4.96	8.21	132	224
		2.03	7.42	11.11	165	224
		2.23	8.03	15.41	166	270
		2.40	10.31	23.38	171	420
		2.03	6.83	10.90	189	260
		2.27	7.71	10.37	136	193
		2.04	6.52	11.09	105	184
		1.75	7.65	10.32	138	240
		1.98	7.84	11.00	175	320
30	50	2.36	6.43	8.72	135	213
		2.25	6.55	10.43	156	350
		2.10	6.09	11.18	260	350
		1.70	6.02	9.72	225	267
		2.03	6.86	10.50	144	350
		1.89	6.76	8.19	225	238
		2.47	8.19	11.40	186	217
		2.05	6.95	10.63	144	158
		2.36	9.03	13.26	260	350
		1.56	4.92	6.33	163	210
		1.98	6.01	9.59	167	333
		2.01	6.29	10.64	169	417

Table III Data for Figure 2.9, showing the effect of different scanning intervals on the surface roughness parameter values for polished Ti. Values are in μm

No. of steps	Step size (μm)	R_a	R_z	R_{max}	S	S_m
400	1	0.82	4.11	5.85	10	18
		0.92	3.97	5.73	20	35
		0.94	4.91	5.99	12	21
		0.80	3.74	4.90	18	30
		0.87	4.35	4.96	11	23
		0.75	3.75	5.07	19	31
380	4	0.87	4.99	5.86	17	38
		0.83	4.40	5.73	21	40
		0.80	4.90	6.16	17	36
		0.90	4.85	5.91	21	42
		0.81	4.58	5.20	16	31

		0.75	4.71	5.67	21	37
		0.83	4.95	6.00	18	36
		0.84	4.51	5.60	21	33
		0.84	4.82	5.74	19	30
		0.85	4.73	5.33	22	36
		0.81	4.77	5.87	17	32
		0.77	4.56	6.13	22	40
300	5	0.88	4.89	5.60	20	35
		0.88	4.89	5.86	25	46
		0.85	4.95	5.51	20	40
		0.88	4.89	5.86	25	46
		0.92	5.04	6.20	20	40
		0.88	5.06	6.53	24	42
		0.87	4.75	6.08	19	38
		0.85	4.67	5.67	23	38
		0.81	4.63	5.38	19	34
		0.85	4.74	6.21	26	49
		0.86	5.17	6.37	22	41
		0.86	4.72	6.29	26	38
250	6	0.89	4.77	6.03	25	47
		0.80	4.29	5.35	25	43
		0.85	4.31	5.08	24	38
		0.78	4.00	5.08	25	40
		0.82	4.79	5.89	27	49
		0.78	4.23	5.09	21	45
		0.90	4.88	7.41	26	56
		0.84	4.47	5.17	24	42
		0.87	4.34	5.43	26	40
		0.83	4.44	5.18	23	49
		0.79	4.42	5.29	24	49
		0.80	3.92	5.04	23	39
190	8	0.79	4.11	4.85	30	49
		0.76	4.14	5.25	25	48
		0.77	4.24	6.84	33	56
		0.76	4.26	5.62	29	60
		0.81	4.01	4.97	29	56
		0.80	3.90	5.19	32	46
		0.84	4.08	4.63	29	51
		0.88	4.18	5.10	27	56
		0.84	4.53	5.18	31	53
		0.77	3.94	5.21	31	63
		0.91	4.58	5.39	30	53
		0.82	4.57	5.83	28	44
150	10	0.76	4.24	5.74	46	94
		0.79	4.04	5.11	33	76
		0.81	4.03	4.84	35	57
		0.74	4.02	5.37	34	71
		0.83	3.67	4.99	35	60
		0.82	4.34	5.26	35	65
		0.98	4.13	4.98	34	65
		0.81	4.15	5.24	35	64
		0.83	4.30	5.30	41	79
		0.91	4.55	6.19	34	49
		0.85	4.18	5.14	38	71
		0.91	4.39	5.92	36	48
75	20	0.82	3.72	4.96	76	113
		0.73	3.34	4.71	74	131
		0.89	3.51	5.68	96	120

		0.71	3.07	3.95	71	145
		0.90	3.91	5.08	79	124
		0.74	2.95	4.46	65	156
		1.06	4.34	5.36	73	100
		0.76	3.55	4.68	69	100
		0.93	4.37	5.69	81	127
		0.71	3.07	3.95	71	145
		0.92	4.14	5.00	84	105
		0.68	3.12	5.18	65	130
50	30	0.72	2.78	4.13	99	171
		0.68	2.33	3.79	106	163
		0.81	3.51	5.69	129	200
		0.76	2.76	3.55	103	203
		0.81	3.40	4.73	141	240
		0.76	2.80	3.28	103	154
		0.75	2.78	4.32	99	133
		0.83	3.12	4.93	112	150
		0.87	3.40	4.70	104	190
		0.62	2.24	3.05	92	147
		0.86	3.50	4.23	128	137
		0.72	2.59	3.49	101	252
38	40	0.82	2.91	4.38	107	280
		0.66	2.09	3.22	136	160
		0.71	2.50	3.33	147	216
		0.67	2.52	3.65	131	200
		0.92	3.00	4.82	138	173
		0.69	2.50	3.54	124	320
		0.91	2.77	3.76	140	200
		0.69	2.49	3.36	124	187
		0.85	2.95	3.53	170	171
		0.74	2.88	4.07	156	300
		0.74	2.71	4.12	151	207
		0.67	2.41	4.23	128	224
30	50	0.57	1.80	2.73	144	263
		0.68	2.14	3.43	179	350
		0.87	2.73	4.17	156	333
		0.72	2.05	3.14	150	425
		0.62	1.97	2.86	169	288
		0.69	2.09	2.67	186	210
		0.90	2.84	4.00	144	200
		0.74	2.35	4.55	150	288
		0.81	2.36	3.93	164	175
		0.73	2.25	2.92	208	383
		0.55	1.70	3.02	169	230
		0.63	2.10	4.22	171	375

Table IV Data for Figure 2.10, showing the effect of different scanning intervals on the surface roughness parameter values for polished Zr. Values are in μm

No. of steps	Step size (μm)	R_a	R_z	R_{max}	S	S_m
400	1	0.84	3.80	4.78	11	22
		0.84	3.38	5.23	23	53
		0.74	3.62	4.80	10	24
		1.00	3.90	5.41	23	33
		0.91	4.06	5.76	11	30
		0.89	3.58	4.99	27	48
380	4	0.85	4.53	5.63	18	37
		1.02	5.06	7.25	27	59
		0.80	4.50	5.07	16	33
		0.89	4.58	6.35	25	64
		0.93	4.69	5.15	17	32
		1.03	4.97	7.53	26	72
		0.85	4.55	5.34	17	29
		0.85	4.57	5.22	21	38
		0.82	4.59	5.13	17	31
		0.83	4.58	5.35	22	35
		0.87	4.89	5.35	16	30
		0.81	4.44	5.27	25	46
300	5	0.82	4.56	5.10	20	41
		0.85	4.59	5.54	26	42
		0.84	4.45	5.44	19	34
		0.85	4.34	5.71	24	39
		0.85	5.02	6.79	24	52
		0.76	4.11	5.08	26	45
		0.84	4.64	5.66	20	45
		0.89	4.55	5.30	25	41
		0.96	4.86	5.92	21	36
		0.79	4.45	5.70	24	39
		0.86	4.40	5.37	19	38
		0.77	4.45	5.60	25	54
250	6	0.87	4.52	5.32	26	49
		0.92	4.71	5.28	27	56
		0.88	4.73	6.37	24	46
		0.81	4.22	4.58	27	48
		0.92	4.48	5.18	21	41
		0.81	4.00	4.56	24	51
		0.84	4.14	4.98	24	44
		0.87	4.40	4.86	27	51
		0.75	3.88	5.04	24	39
		0.79	4.06	4.76	25	46
		0.86	4.43	5.68	23	44
		0.77	3.87	5.00	27	52
190	8	0.91	4.31	5.20	31	49
		0.87	4.41	5.28	32	51
		0.84	4.25	5.08	29	60
		0.82	4.12	4.77	33	65
		0.97	4.47	5.39	29	51
		0.79	3.78	4.45	29	58
		0.82	4.19	5.15	30	48
		0.86	4.49	5.70	32	65
		0.83	4.14	5.11	27	47
		0.84	4.35	5.02	28	47

		0.81	3.92	5.27	29	43
		0.76	4.05	5.41	33	57
150	10	0.92	4.12	5.03	36	63
		0.91	4.30	5.30	38	61
		0.82	4.21	5.14	35	50
		0.82	3.75	4.41	38	67
		0.96	4.77	6.17	37	62
		0.76	3.44	4.25	35	62
		0.73	3.83	4.45	37	75
		0.72	3.70	4.52	33	75
		0.72	4.05	5.12	43	82
		0.79	3.49	4.84	35	77
		0.75	3.50	4.28	34	60
		0.71	3.74	4.86	36	63
75	20	1.09	4.25	5.91	77	105
		0.85	3.43	4.91	68	97
		1.07	4.56	5.99	77	158
		0.78	3.30	4.46	64	93
		1.14	5.12	6.80	78	113
		0.80	3.15	4.19	61	107
		0.93	3.71	4.45	78	107
		0.90	3.53	4.94	60	78
		0.84	3.57	4.77	80	140
		0.82	3.42	4.08	64	95
		0.97	4.59	5.49	74	118
		0.67	2.63	3.76	78	112
50	30	0.82	2.94	4.94	141	168
		0.91	3.43	4.59	94	113
		0.68	3.23	4.54	141	159
		0.62	2.24	3.05	92	147
		0.98	3.72	4.88	111	174
		0.85	2.79	3.68	102	165
		0.86	2.97	3.91	88	159
		0.69	2.81	4.41	128	176
		0.68	2.61	3.48	110	143
		0.85	2.96	3.68	86	129
		0.74	2.65	3.93	104	171
		0.65	2.42	3.18	106	204
38	40	0.96	3.36	6.64	151	272
		0.72	2.47	4.12	142	260
		0.81	2.70	3.94	142	160
		0.82	2.62	3.69	128	160
		0.92	3.26	4.62	136	213
		0.95	3.25	4.25	151	320
		0.81	2.89	4.40	156	189
		0.82	3.03	4.09	147	232
		0.77	2.92	4.28	132	220
		0.65	2.23	3.77	194	187
		0.76	2.69	3.43	124	177
		0.66	2.52	3.61	124	207
30	50	0.83	3.09	4.89	163	288
		0.88	2.99	3.89	139	190
		0.85	2.74	4.29	175	150
		0.72	1.95	2.85	250	317
		0.80	2.71	6.00	288	700
		0.65	2.18	4.28	164	400
		0.87	2.91	3.78	144	171
		0.78	2.10	3.28	169	188

	0.73	2.29	3.94	192	263
	0.61	1.84	2.80	163	400
	0.73	2.54	3.32	156	186
	0.73	1.89	3.08	175	175

Table V Data for Figures 2.19 to 2.21, and Table 2.2, showing the roughness values of the final substrates used in the cell culture studies, obtained using the Proscan 1000. Values are in μm for three measurement areas made on 5 discs per substrate type. From the 15 Proscan images, roughness values for 3 different areas were obtained by moving the cursor positions to the desired locations along the x and y axes. This resulted in 45 measurements per roughness parameter in each x and y-axis. Measurements were made at 5 μm intervals for 300 sampling points (measurement area = 2.25 mm^2). Values shown are x-axis values (made across the lay for both polished Ti and Zr surfaces)

Substrate	R_a	R_q	R_z	R_{max}	S	S_m	Area/mm^2
Ti as received 1	2.19	2.84	11.92	20.36	41.00	133.00	2.543
	2.06	2.55	11.01	15.20	33.00	158.00	2.540
	2.25	2.92	13.03	19.00	39.00	144.00	2.540
	1.80	2.32	11.61	16.75	42.00	105.00	2.519
	2.30	2.94	13.11	16.66	45.00	119.00	2.519
	2.03	2.50	9.84	11.54	32.00	102.00	2.519
	2.02	2.58	12.40	17.81	39.00	87.00	2.553
	2.17	2.97	14.00	25.49	46.00	108.00	2.553
	2.17	3.07	14.51	25.12	46.00	179.00	2.553
Ti as received 2	1.77	2.17	9.49	13.30	36.00	100.00	2.544
	2.09	2.80	10.84	17.37	36.00	115.00	2.544
	1.97	2.50	11.31	15.23	32.00	113.00	2.544
	2.03	2.83	13.21	24.64	56.00	156.00	2.541
	1.91	2.48	11.88	15.75	39.00	108.00	2.541
	2.13	2.71	12.70	18.87	37.00	156.00	2.541
	1.73	2.15	9.85	11.55	32.00	58.00	2.534
	2.01	2.59	11.19	15.77	38.00	95.00	2.534
	2.06	2.58	12.00	14.47	31.00	72.00	2.534
Ti as received 3	2.27	3.05	14.94	29.28	58.00	164.00	2.578
	2.90	3.62	14.83	19.47	43.00	113.00	2.578
	1.92	2.43	10.34	14.81	33.00	137.00	2.578
	2.25	2.80	12.57	17.01	35.00	81.00	2.581
	1.84	2.42	11.83	20.49	42.00	151.00	2.581
	2.25	2.91	12.99	21.44	51.00	132.00	2.581
	2.16	2.74	12.74	22.16	46.00	92.00	2.590
	2.03	2.68	12.44	19.33	41.00	120.00	2.590
	2.49	3.31	13.26	21.46	44.00	153.00	2.590
Ti as received 4	2.39	2.91	11.06	13.99	39.00	110.00	2.539
	2.01	2.50	11.12	15.08	39.00	87.00	2.539
	2.19	2.70	10.86	13.39	39.00	82.00	2.539
	1.92	2.42	10.54	14.40	30.00	77.00	2.561
	1.87	2.34	9.56	11.82	31.00	73.00	2.561
	2.11	2.73	12.07	17.40	42.00	127.00	2.561
	2.24	2.76	11.76	14.93	29.00	103.00	2.543
	2.28	2.99	15.47	20.25	39.00	106.00	2.543
	2.21	2.83	12.34	16.63	37.00	97.00	2.543
Ti as received 5	2.07	2.73	13.16	20.82	41.00	122.00	2.551
	2.00	2.46	8.85	13.78	37.00	97.00	2.551
	2.09	2.72	12.22	16.44	38.00	94.00	2.551

	1.98	2.56	11.90	16.58	38.00	100.00	2.546
	1.96	2.61	10.98	17.11	40.00	103.00	2.546
	2.21	2.76	12.19	17.10	41.00	93.00	2.546
	2.29	2.82	12.09	16.44	40.00	89.00	2.562
	1.81	2.37	11.79	17.35	40.00	124.00	2.562
	2.06	2.61	11.16	15.10	35.00	106.00	2.562
Polished Ti 1	0.79	0.96	4.30	5.30	20.00	35.00	2.349
	0.81	0.99	4.36	4.91	20.00	37.00	2.349
	0.73	0.91	4.37	5.64	22.00	41.00	2.349
	0.78	0.97	4.30	5.46	21.00	48.00	2.351
	0.86	1.07	4.63	5.73	21.00	40.00	2.351
	0.79	0.98	4.48	5.95	22.00	40.00	2.351
	0.77	0.97	4.35	4.97	21.00	47.00	2.354
	0.83	1.02	4.82	5.53	19.00	43.00	2.354
	0.83	1.03	4.32	4.91	19.00	34.00	2.354
Polished Ti 2	0.91	1.13	4.63	5.38	20.00	41.00	2.361
	0.88	1.09	4.62	5.05	19.00	39.00	2.361
	0.82	1.04	4.76	5.88	23.00	40.00	2.361
	0.83	1.03	4.80	6.06	20.00	47.00	2.366
	0.87	1.10	4.91	5.99	20.00	41.00	2.366
	0.87	1.09	4.87	6.02	24.00	40.00	2.366
	0.87	1.08	4.64	5.63	22.00	37.00	2.360
	0.84	1.03	4.49	5.28	22.00	39.00	2.360
	0.88	1.10	5.26	6.23	22.00	41.00	2.360
Polished Ti 3	0.96	1.15	5.11	6.16	21.00	34.00	2.365
	0.86	1.09	5.17	6.10	19.00	45.00	2.365
	0.94	1.15	5.20	5.96	21.00	36.00	2.365
	0.89	1.11	4.68	5.50	19.00	45.00	2.376
	0.89	1.09	5.03	5.78	20.00	37.00	2.376
	0.90	1.11	4.92	5.83	23.00	41.00	2.376
	0.94	1.16	5.14	6.07	19.00	36.00	2.373
	0.95	1.15	4.64	6.40	21.00	46.00	2.373
	0.84	1.04	4.58	4.92	20.00	31.00	2.373
Polished Ti 4	0.82	1.00	4.24	5.33	21.00	44.00	2.355
	0.80	1.00	4.64	5.59	22.00	38.00	2.355
	0.74	0.94	4.43	5.27	20.00	49.00	2.355
	0.82	1.02	4.66	5.50	22.00	41.00	2.352
	0.85	1.05	4.65	5.28	20.00	48.00	2.352
	0.87	1.06	4.82	5.88	21.00	38.00	2.352
	0.90	1.08	4.50	4.75	18.00	32.00	2.361
	0.85	1.05	4.75	5.63	22.00	42.00	2.361
	0.84	1.02	4.29	5.49	21.00	34.00	2.361
Polished Ti 5	0.85	1.06	4.92	6.42	22.00	46.00	2.358
	0.88	1.08	4.49	5.70	21.00	42.00	2.358
	0.89	1.10	4.81	6.12	21.00	38.00	2.358
	0.84	1.03	4.57	5.46	21.00	38.00	2.354
	0.87	1.06	4.47	5.42	22.00	48.00	2.354
	0.90	1.09	4.69	5.58	24.00	39.00	2.354
	0.89	1.08	4.92	5.26	20.00	38.00	2.350
	0.88	1.09	4.71	5.62	22.00	35.00	2.350
	0.88	1.08	4.66	5.59	23.00	41.00	2.350
Polished Zr 1	0.82	1.00	4.30	4.98	23.00	38.00	2.325
	0.77	0.94	3.98	4.59	19.00	35.00	2.325
	0.75	0.93	4.17	4.66	21.00	40.00	2.325
	0.83	1.03	4.38	5.69	26.00	56.00	2.328
	0.83	1.07	5.07	6.73	22.00	47.00	2.328
	0.82	1.00	4.21	5.08	21.00	44.00	2.328
	0.82	0.99	4.27	4.68	21.00	38.00	2.330

	0.82	1.01	4.35	5.29	21.00	35.00	2.330
	0.74	0.91	3.83	4.57	21.00	42.00	2.330
Polished Zr 2	0.85	1.01	4.27	5.17	22.00	42.00	2.349
	0.86	1.03	4.15	4.96	23.00	41.00	2.349
	0.79	0.98	4.16	4.78	22.00	42.00	2.349
	0.86	1.04	4.50	5.12	22.00	41.00	2.350
	0.90	1.09	4.65	5.35	20.00	39.00	2.350
	0.90	1.09	4.43	5.07	19.00	33.00	2.350
	0.92	1.12	5.02	6.04	23.00	42.00	2.355
	0.94	1.14	4.96	5.59	21.00	37.00	2.355
	0.85	1.04	4.53	5.26	21.00	38.00	2.355
Polished Zr 3	0.80	0.97	4.24	4.97	21.00	35.00	2.333
	0.78	0.95	4.05	5.16	19.00	38.00	2.330
	0.85	1.01	4.15	4.86	20.00	36.00	2.330
	0.72	0.89	3.91	5.16	23.00	45.00	2.328
	0.72	0.90	4.02	4.97	23.00	46.00	2.328
	0.79	0.95	3.99	4.58	19.00	32.00	2.328
	0.67	0.83	3.51	4.13	24.00	51.00	2.294
	0.76	0.94	4.15	5.13	31.00	71.00	2.294
	0.65	0.81	3.75	4.66	27.00	50.00	2.294
Polished Zr 4	0.87	1.06	4.63	5.63	20.00	39.00	2.336
	0.77	0.96	3.99	4.83	21.00	43.00	2.336
	0.83	0.99	4.17	5.19	19.00	39.00	2.336
	0.78	0.98	4.54	5.55	22.00	44.00	2.340
	0.80	1.00	4.62	5.99	23.00	42.00	2.340
	0.89	1.06	4.64	5.01	20.00	39.00	2.340
	0.89	1.10	4.89	5.39	20.00	41.00	2.355
	0.87	1.08	4.95	6.74	22.00	41.00	2.355
	0.88	1.10	4.76	6.26	21.00	40.00	2.355
Polished Zr 5	0.87	1.08	4.81	5.70	20.00	35.00	2.349
	0.86	1.06	4.66	5.65	19.00	37.00	2.349
	0.88	1.08	4.90	5.68	22.00	39.00	2.349
	0.70	0.89	3.88	4.99	21.00	41.00	2.328
	0.77	0.94	4.22	5.19	20.00	45.00	2.328
	0.80	1.00	4.32	4.80	22.00	36.00	2.328
	0.86	1.03	4.46	5.55	22.00	36.00	2.342
	0.87	1.05	4.06	5.07	21.00	39.00	2.342
	0.83	1.01	4.39	4.93	19.00	35.00	2.342

Table VI Data for Figures 2.19 - 2.21 and Table 2.2, showing the roughness values of the substrates used in the main study obtained using the Proscan 1000. Values shown (in μm) are y-axis values (made along the lay for both polished Ti and Zr)

Substrate	R_a	R_q	R_z	R_{max}	S	S_m	Area/mm^2
Ti as received 1	1.96	2.58	11.85	18.83	33.00	105.00	2.540
	2.05	2.56	11.19	14.75	31.00	81.00	2.540
	1.99	2.49	10.79	14.55	33.00	78.00	2.540
	2.03	2.55	10.84	14.31	31.00	79.00	2.519
	1.81	2.28	10.57	15.43	31.00	83.00	2.519
	2.14	2.64	11.74	14.38	34.00	95.00	2.519
	1.74	2.18	10.43	12.57	30.00	75.00	2.553
	2.04	2.59	11.66	13.78	29.00	79.00	2.553
	2.02	2.58	10.77	14.87	30.00	102.00	2.553

Ti as received 2	1.96	2.43	10.81	13.37	32.00	74.00	2.544
	2.32	3.29	15.92	35.62	52.00	251.00	2.544
	1.93	2.39	9.93	13.73	31.00	104.00	2.544
	2.07	2.64	11.13	13.78	29.00	84.00	2.541
	2.01	2.53	11.23	14.20	29.00	89.00	2.541
	2.02	2.62	11.68	17.32	35.00	87.00	2.541
	1.79	2.23	10.17	12.16	29.00	66.00	2.534
	1.75	2.32	11.37	16.77	35.00	97.00	2.534
	1.77	2.32	11.01	16.70	33.00	95.00	2.534
Ti as received 3	2.41	3.05	13.34	20.63	36.00	129.00	2.578
	2.20	2.98	12.99	22.19	41.00	108.00	2.578
	2.20	3.05	13.71	26.18	42.00	214.00	2.578
	2.28	2.98	13.90	25.53	43.00	117.00	2.581
	2.38	3.02	13.65	20.45	40.00	103.00	2.581
	2.07	2.78	12.63	21.94	39.00	93.00	2.581
	2.23	2.81	12.69	18.97	30.00	108.00	2.590
	2.35	2.90	12.13	15.58	32.00	98.00	2.590
	2.28	2.97	12.64	20.09	31.00	126.00	2.590
Ti as received 4	1.84	2.35	11.65	14.92	33.00	100.00	2.539
	2.26	2.93	12.86	19.58	42.00	139.00	2.539
	1.90	2.40	10.63	14.54	30.00	77.00	2.539
	2.09	2.62	11.56	15.41	33.00	88.00	2.561
	2.09	2.58	10.54	13.28	28.00	87.00	2.561
	2.55	3.05	12.66	16.80	33.00	98.00	2.561
	2.25	2.83	12.73	16.16	35.00	131.00	2.543
	2.22	2.95	12.53	21.15	38.00	176.00	2.543
	2.24	3.44	14.78	36.33	66.00	200.00	2.543
Ti as received 5	2.13	2.90	13.79	22.08	43.00	118.00	2.551
	2.08	2.66	11.01	16.79	33.00	77.00	2.551
	2.15	2.92	12.82	20.18	40.00	120.00	2.551
	1.71	2.17	9.18	12.08	27.00	88.00	2.546
	1.98	2.58	13.16	19.52	36.00	98.00	2.546
	1.84	2.32	10.17	12.23	27.00	72.00	2.546
	2.33	3.20	12.75	20.78	36.00	84.00	2.562
	2.36	2.94	12.67	16.20	30.00	94.00	2.562
	2.01	2.56	10.43	16.07	32.00	108.00	2.562
Polished Ti 1	0.73	0.94	4.54	5.27	21.00	49.00	2.349
	0.75	0.91	3.82	4.56	24.00	38.00	2.349
	0.76	0.95	4.11	4.98	23.00	43.00	2.349
	0.82	0.99	4.12	5.48	20.00	34.00	2.351
	0.79	0.96	4.05	4.58	21.00	35.00	2.351
	0.82	1.01	4.15	5.58	22.00	41.00	2.351
	0.67	0.85	3.98	4.25	22.00	37.00	2.354
	0.73	0.90	3.91	4.38	21.00	35.00	2.354
	0.78	0.95	4.17	5.08	23.00	40.00	2.354
Polished Ti 2	0.77	0.95	4.56	6.20	24.00	47.00	2.361
	0.81	1.01	4.30	4.95	21.00	47.00	2.361
	0.83	1.02	4.61	5.43	21.00	49.00	2.361
	0.84	1.03	4.29	5.20	22.00	36.00	2.366
	0.79	1.00	4.70	5.49	22.00	41.00	2.366

	0.94	1.14	4.61	5.95	23.00	38.00	2.366
	0.89	1.12	4.66	6.60	26.00	55.00	2.360
	0.84	1.06	5.09	5.98	22.00	48.00	2.360
	0.85	1.02	4.29	4.71	23.00	37.00	2.360
Polished Ti 3	0.87	1.06	4.55	6.19	27.00	45.00	2.365
	0.87	1.07	4.54	5.44	22.00	48.00	2.365
	0.81	1.00	4.42	5.36	23.00	44.00	2.365
	0.90	1.11	4.84	5.87	24.00	48.00	2.376
	0.89	1.09	4.58	5.66	28.00	50.00	2.376
	0.89	1.11	4.85	5.74	24.00	46.00	2.376
	0.87	1.07	4.62	5.30	23.00	58.00	2.373
	0.96	1.18	5.16	5.83	23.00	47.00	2.373
	0.94	1.15	4.83	5.69	24.00	45.00	2.373
Polished Ti 4	0.79	0.98	4.45	5.32	22.00	48.00	2.355
	0.76	0.97	4.41	5.22	23.00	43.00	2.355
	0.75	0.95	4.51	5.68	23.00	55.00	2.355
	0.81	1.00	4.06	5.17	21.00	50.00	2.352
	0.79	0.99	4.44	6.11	25.00	49.00	2.352
	0.80	0.99	4.24	5.17	23.00	62.00	2.352
	0.81	0.99	4.13	4.68	21.00	44.00	2.361
	0.82	1.03	4.36	5.32	24.00	44.00	2.361
	0.76	0.96	4.52	4.91	22.00	43.00	2.361
Polished Ti 5	0.88	1.07	4.52	5.38	25.00	47.00	2.358
	0.82	1.02	4.66	6.17	23.00	46.00	2.358
	0.93	1.14	5.10	5.86	23.00	45.00	2.358
	0.80	1.00	4.44	5.52	25.00	52.00	2.354
	0.91	1.10	4.80	5.89	25.00	47.00	2.354
	0.85	1.06	4.90	6.42	25.00	51.00	2.354
	0.82	1.02	4.37	5.39	24.00	44.00	2.350
	0.79	0.97	4.32	5.36	24.00	43.00	2.350
	0.83	1.00	4.00	4.92	26.00	45.00	2.350
Polished Zr 1	0.68	0.85	3.97	5.40	29.00	66.00	2.325
	0.79	0.96	4.15	5.03	25.00	48.00	2.325
	0.76	0.94	4.09	4.96	28.00	58.00	2.325
	0.78	0.93	3.85	4.41	23.00	46.00	2.328
	0.77	0.95	4.10	4.85	26.00	49.00	2.328
	0.70	0.86	3.44	4.45	26.00	49.00	2.328
	0.79	0.98	4.09	4.42	28.00	48.00	2.330
	0.79	0.97	4.39	5.06	27.00	52.00	2.330
	0.79	0.97	3.77	4.66	26.00	52.00	2.330
Polished Zr 2	0.84	1.01	4.14	4.73	25.00	44.00	2.349
	0.83	0.99	4.07	5.02	23.00	41.00	2.349
	0.80	0.98	4.14	4.79	26.00	43.00	2.349
	0.86	1.07	4.71	5.57	26.00	43.00	2.350
	0.86	1.06	4.45	5.08	24.00	46.00	2.350
	0.79	0.97	3.96	4.60	24.00	49.00	2.350
	0.81	0.99	4.45	5.15	24.00	47.00	2.355
	0.86	1.04	4.25	5.05	24.00	40.00	2.355
	0.84	1.03	4.75	5.69	24.00	44.00	2.355
Polished Zr 3	0.85	1.06	4.36	5.50	24.00	53.00	2.333

	0.79	0.97	3.92	5.21	27.00	72.00	2.330
	0.83	1.02	3.76	4.95	25.00	62.00	2.330
	0.77	0.93	4.03	5.64	27.00	47.00	2.328
	0.83	1.01	4.30	5.12	28.00	47.00	2.328
	0.71	0.88	3.89	4.53	27.00	51.00	2.328
	0.66	0.80	3.31	3.82	28.00	49.00	2.294
	0.64	0.80	3.56	4.69	28.00	55.00	2.294
	0.74	0.90	3.95	4.91	32.00	50.00	2.294
Polished Zr 4	0.75	0.95	4.08	5.64	26.00	52.00	2.336
	0.70	0.86	3.82	4.39	25.00	47.00	2.336
	0.74	0.90	3.84	4.74	25.00	52.00	2.336
	0.76	0.96	4.17	5.20	27.00	55.00	2.340
	0.83	1.00	4.02	4.77	27.00	44.00	2.340
	0.89	1.07	4.07	4.71	26.00	58.00	2.340
	0.80	1.00	4.21	5.50	24.00	45.00	2.355
	0.81	1.00	4.14	5.22	26.00	51.00	2.355
	0.83	1.00	4.09	5.15	24.00	44.00	2.355
Polished Zr 5	0.79	1.01	4.42	5.06	25.00	51.00	2.349
	0.79	.96	4.01	4.67	25.00	49.00	2.349
	0.79	.99	4.02	5.53	27.00	49.00	2.349
	0.79	.96	4.01	4.42	25.00	50.00	2.328
	0.71	.87	3.77	4.47	25.00	46.00	2.328
	0.79	.96	4.09	4.96	27.00	56.00	2.328
	0.80	.99	4.29	4.91	27.00	59.00	2.342
	0.83	1.00	4.27	4.90	26.00	41.00	2.342
	0.87	1.04	4.23	5.24	25.00	40.00	2.342

Table VII Data for Table 2.3, showing the roughness values of the substrates used in the main study, obtained using the Surftest 4. n = 90 for Ti as received, and n = 45 for polished Ti and Zr. The evaluation length used was 4.8 mm, with a cut-off of 0.8 mm. Values are in μm. Measurements were not made in any particular direction for the Ti as received discs, while they were made across the surface lay for polished Ti and Zr discs

Substrate	R_a	R_q	R_z	R_{max}
Ti as received 1	1.67	1.86	9.64	11.35
	1.68	1.87	9.45	10.94
	1.66	1.85	9.44	11.34
	1.65	1.84	9.80	10.88
	1.65	1.83	10.69	14.11
	1.58	1.75	10.09	13.29
	1.55	1.72	9.56	11.62
	1.50	1.66	9.38	10.34
	1.46	1.62	9.30	10.62
Ti as received 2	1.56	1.74	9.76	11.47
	1.56	1.74	9.71	11.85
	1.60	1.78	10.09	13.43

	1.45	1.61	8.54	11.27
	1.40	1.55	8.16	11.16
	1.46	1.62	8.86	10.85
	1.34	1.48	8.10	9.37
	1.33	1.48	7.88	8.35
	1.30	1.45	8.36	8.79
Ti as received 3	1.71	1.90	10.03	11.48
	1.68	1.87	9.71	10.83
	1.66	1.85	10.12	11.57
	1.59	1.77	9.32	11.40
	1.64	1.82	9.29	11.40
	1.61	1.79	9.29	10.86
	1.56	1.74	10.54	11.51
	1.52	1.69	10.02	11.27
	1.50	1.67	9.82	10.69
Ti as received 4	1.56	1.74	10.54	11.51
	1.52	1.69	10.02	11.27
	1.50	1.67	9.82	10.69
	1.46	1.62	9.17	10.17
	1.46	1.62	9.25	10.10
	1.54	1.72	9.30	10.59
	1.39	1.54	8.31	10.28
	1.34	1.48	8.13	10.44
	1.37	1.52	9.31	11.00
Ti as received 5	1.45	1.61	8.92	10.24
	1.52	1.68	9.52	11.85
	1.48	1.65	9.11	11.28
	1.54	1.71	9.36	10.98
	1.53	1.70	9.34	10.86
	1.53	1.70	9.39	11.01
	1.31	1.46	8.69	10.37
	1.38	1.54	8.97	9.98
	1.37	1.52	8.74	10.40
Ti as received 6	1.65	1.84	10.34	12.54
	1.63	1.81	10.03	11.81
	1.61	1.79	10.03	12.04
	1.54	1.71	9.86	11.06
	1.50	1.67	9.32	10.90
	1.51	1.68	9.79	10.71
	1.59	1.77	9.24	9.53
	1.57	1.75	9.31	10.13
	1.56	1.74	9.27	9.53
Ti as received 7	1.52	1.69	8.94	9.55
	1.48	1.65	8.91	9.61
	1.49	1.65	8.85	10.12
	1.54	1.71	9.86	11.06
	1.50	1.67	9.32	10.90
	1.51	1.68	9.79	10.71
	1.59	1.77	9.24	9.53
	1.57	1.75	9.31	10.13

	1.56	1.74	9.27	9.53
Ti as received 8	1.59	1.76	9.39	10.85
	1.57	1.75	9.42	10.80
	1.56	1.73	9.25	11.15
	1.43	1.59	8.72	10.27
	1.52	1.69	9.48	11.50
	1.48	1.64	9.10	10.41
	1.51	1.68	9.29	10.65
	1.43	1.59	9.25	10.12
	1.43	1.59	9.19	9.95
Ti as received 9	1.27	1.41	7.92	9.01
	1.30	1.45	7.91	8.51
	1.28	1.42	7.88	8.84
	1.32	1.47	7.96	9.15
	1.33	1.47	7.59	8.86
	1.29	1.43	7.49	9.22
	1.34	1.49	8.93	12.03
	1.33	1.47	9.07	12.52
	1.32	1.46	9.11	12.91
Ti as received 10	1.30	1.44	7.33	8.52
	1.24	1.38	8.32	9.14
	1.21	1.35	8.40	9.30
	1.27	1.41	8.33	9.25
	1.25	1.39	8.18	8.95
	1.24	1.37	7.99	9.40
	1.33	1.48	8.55	9.82
	1.28	1.42	8.39	10.29
	1.28	1.42	8.10	8.33
Polished Ti 1	0.26	0.29	1.60	1.71
	0.28	0.31	1.73	2.02
	0.28	0.31	1.74	1.88
	0.28	0.31	1.82	2.30
	0.27	0.30	1.75	2.03
	0.26	0.29	1.71	1.95
	0.25	0.28	1.71	1.95
	0.25	0.28	1.81	2.51
	0.25	0.28	1.82	2.51
Polished Ti 2	0.28	0.31	1.90	2.01
	0.28	0.31	1.96	2.06
	0.28	0.31	1.89	2.08
	0.29	0.32	2.06	2.25
	0.28	0.31	2.05	2.29
	0.28	0.32	2.00	2.28
	0.27	0.30	1.80	1.93
	0.28	0.31	1.84	1.96
	0.27	0.30	1.79	1.87
Polished Ti 3	0.24	0.26	1.60	1.85
	0.24	0.26	1.63	1.77
	0.23	0.26	1.61	1.86

	0.22	0.25	1.49	1.54
	0.22	0.25	1.52	1.56
	0.22	0.24	1.53	1.65
	0.22	0.25	1.54	1.77
	0.24	0.26	1.61	2.10
	0.23	0.25	1.61	2.22
Polished Ti 4	0.28	0.31	1.95	2.42
	0.28	0.31	2.07	2.53
	0.28	0.31	2.05	2.52
	0.27	0.30	1.96	2.48
	0.27	0.30	1.96	2.30
	0.27	0.30	1.95	2.22
	0.31	0.34	1.97	2.37
	0.28	0.31	2.17	3.12
	0.27	0.30	2.12	3.14
Polished Ti 5	0.24	0.27	1.60	1.71
	0.24	0.27	1.56	1.67
	0.23	0.25	1.47	1.69
	0.24	0.27	1.72	1.88
	0.25	0.27	1.57	1.66
	0.25	0.28	1.67	1.79
	0.25	0.27	1.77	2.02
	0.25	0.27	1.87	2.15
	0.25	0.28	1.90	2.03
Polished Zr 1	0.17	0.19	1.29	1.38
	0.18	0.20	1.57	2.58
	0.17	0.19	1.33	1.44
	0.19	0.21	1.44	1.88
	0.19	0.21	1.38	1.80
	0.19	0.21	1.43	1.84
	0.19	0.22	1.36	1.83
	0.20	0.22	1.29	1.65
	0.21	0.24	1.37	1.85
Polished Zr 2	0.19	0.21	1.51	1.73
	0.17	0.19	1.45	1.67
	0.19	0.22	1.44	1.93
	0.18	0.20	1.51	1.99
	0.17	0.18	1.33	1.47
	0.20	0.22	1.56	2.20
	0.17	0.19	1.35	1.38
	0.16	0.18	1.34	1.54
	0.17	0.19	1.34	1.44
Polished Zr 3	0.14	0.16	1.25	1.41
	0.16	0.18	1.23	1.28
	0.16	0.18	1.37	1.76
	0.18	0.20	1.42	1.71
	0.19	0.21	1.53	2.23
	0.19	0.21	1.40	1.50
	0.15	0.17	1.20	1.46

	0.17	0.19	1.46	1.76
	0.17	0.19	1.37	1.52
Polished Zr 4	0.15	0.17	1.16	1.29
	0.16	0.18	1.31	1.51
	0.18	0.20	1.39	1.88
	0.17	0.18	1.24	1.73
	0.16	0.17	1.17	1.24
	0.16	0.18	1.15	1.35
	0.14	0.15	1.08	1.48
	0.15	0.17	1.26	1.51
	0.13	0.15	1.05	1.26
Polished Zr 5	0.16	0.18	1.29	1.88
	0.16	0.18	1.19	1.35
	0.15	0.17	1.25	1.65
	0.17	0.19	1.28	1.56
	0.17	0.19	1.31	1.79
	0.17	0.19	1.31	1.84
	0.17	0.19	1.36	1.56
	0.20	0.22	1.48	2.18
	0.17	0.19	1.36	1.65

Appendix II

Posters presented:

1). Adhesion of Human Osteosarcoma Cell Lines on Titanium.

- 45th Annual Conference of the British Society for the Study of Prosthetic Dentistry, 5-7th April, 1998, York.

- 15th International Conference on Oral Biology (ICOB), 28th June-1st July, 1998, Baveno, Italy.

2). Integrin expression of osteoblast-like cells attached to metallic implant materials.

- 46th Annual Conference of the British Society for the Study of Prosthetic Dentistry, 28-30th March, 1999, Liverpool.